Faculty of Medicine and Health Sciences

School of Biomedical Sciences

The University of Nottingham

# GPCRs in rat primary skeletal muscle cells

Mansour Emil Goerge Haddad

(Pharmacy.BCh, MSc)



This thesis is submitted to the University of Nottingham
For the degree of Doctor of Philosophy
July 2012

**Abstract**

GPCRs are the largest family of proteins in the human genome and a target for huge numbers of therapeutic drugs. However, the role of skeletal muscle in the action of these drugs is unclear. Given the unique importance of GPCR signalling in terms of glucose and fatty acid turnover in other tissues, it would be anticipated that GPCR identified to influence metabolism in these tissues might well be expressed in skeletal muscle.

This study investigated the expression of genes encoding GPCRs in skeletal muscle and in cultured preparations thereof. In particular, this study focussed on the expression and signalling of adenosine receptors, $\alpha_2$-adrenoceptor, P2Y receptors and $CB_1$ cannabinoid receptors and the impact of $CB_1$ receptor modulation upon insulin signalling in rat primary skeletal muscle cells.

All experiments in this work looked at GPCR expression and their signalling; with either tissues or cultured cells from rats. These experiments included:

1. Transcriptional profiling of skeletal muscle tissue in Wistar rats for GPCRs and proteins in associated signalling pathways.
2. Signalling of GPCRs (adenosine, $\alpha_{2A}$-adrenoceptor, P2Y) in rat primary skeletal muscle cells.
3. Cannabinoid signalling pathways and cross-talk with insulin signalling.
4. $CB_1$ cannabinoid receptor antagonist/inverse agonist/agonist treatment of rat primary skeletal muscle cells.

Expression of example members of the three major G protein coupling GPCR families was observed in rat skeletal muscle tissue. mRNA encoding $G_s$- ($A_{2A}$ adenosine receptor,

$\beta_2$-adrenoceptor), $G_i$- ($A_1$ adenosine receptor, $\alpha_{2A}$-adrenoceptor), and $G_q$-coupled ($P2Y_1$, $P2Y_2$ and $P2Y_6$ receptors) receptors were detected using gene microarray (Agilent, all ranked <10220 out of 41090). QRT-PCR (Taqman) identified $\alpha_{2A}$-adrenoceptor and $CB_1$ cannabinoid receptor mRNA expression at low level similar across myoblasts, myotubes and skeletal muscle tissue.

Functional responses to example members of the three major G protein coupling families of GPCR were also observed in rat primary skeletal muscle preparations. First, treatment of myotubes with the non-selective adenosine receptor agonist NECA elicited increases in cAMP, which were inhibited in the presence of the $A_{2B}$ adenosine receptor-selective antagonist, PSB603. In contrast, the $A_{2A}$-selective agonist, CGS21680 failed to evoke a significant cAMP elevation in myotubes. Second, neither basal nor forskolin–evoked elevation of cAMP was altered in the presence of the $A_1$-selective agonist, S-ENBA. Third, the $\alpha_2$-adrenoceptor agonist UK14304 inhibited forskolin–evoked cAMP levels, however, rauwolscine did not prevent this effect. Treatment with UK14304 also increased phosphorylation of ERK1/2; these responses, however, were inhibited by rauwolscine. In addition, rauwolscine in the absence of other ligands also inhibited ERK phosphorylation. Fourth, ATP and UTP, P2Y receptor agonists, elevated intracellular calcium ion levels in myoblasts.

Although expression of mRNA for $CB_1$ cannabinoid receptors was detected in myoblasts, myotubes and skeletal muscle tissue, forskolin–evoked elevation of cAMP was unaltered in the presence of the $CB_1$ receptor-selective agonist ACEA or the antagonist/inverse agonist rimonabant in cultured myotubes. AICAR-stimulated AMP-activated protein kinase activity was also unaltered by ACEA. However, treatment with ACEA increased activation of ERK1/2 and p38 mitogen-activated protein kinases; these responses were significantly inhibited by rimonabant.

Insulin treatment of myotubes increased the activation (phosphorylation) of AKT/protein kinase B, glycogen synthase kinase 3α and β, ERK1/2 and p38 MAP kinases; however, pre-treatment with ACEA for 24 hours failed to alter these responses.

In conclusion, these studies indicate expression and functional responses to select members of the three major G protein coupling families of GPCR in rat skeletal muscle preparations. These findings also provided evidence for expression of functionally active $CB_1$ cannabinoid receptors in skeletal muscle. However, they fail to support previous reports suggesting an interaction between insulin and $CB_1$ receptor signalling in these cells. The impact of $CB_1$ receptor function in skeletal muscle should be the subject of further investigation.

**Acknowledgements**

I would first like to thank my supervisors; Dr. Andrew Bennett, Dr. Stephen Alexander and Dr. Kostas Tsintzas for patient instruction, direction, support, help and guidance throughout my Ph.D. Without their help, wise advice and support, I could not finish this thesis.

I would also like to thank Dr. Richard Roberts for his helpful advice. I would like to thank the Frame Lab, the Graduate School and the School of Biomedical Sciences for providing me the opportunity to pursue my Ph.D at University of Nottingham.

I am deeply grateful to Philadelphia University in Jordan for its scholarship and financial support for the first three years of my Ph.D.

Finally, I would like to give my special thanks to my father, mother and family for their love, support and encouragement during the years of my Ph.D.

**Declaration**

I declare that the work presented in this thesis was carried out entirely by myself while I was a postgraduate student during the course of my Ph.D studies at the School of Biomedical Sciences, Medical School, University of Nottingham and has not been submitted for a degree at this or any other university.

Mansour Haddad

**Publications/Presentations**

**M. Haddad**, K. Tsintzas, S.P.H. Alexander and A.J. Bennett. (2011) Molecular characterization of G protein-coupled receptors (GPCRs) in rat skeletal muscle. British Pharmacology Society (BPS). London, UK.

**M. Haddad**, T. Kostas, S. Alexander and A. Bennett. (2011) Do $CB_1$ cannabinoid receptors regulate insulin signalling in rat primary skeletal muscle cells? The International Association for Cannabinoid Medicines ($IACM^{6th}$) and the European Workshop on Cannabinoids "Cannabinoid Conference" in Bonn, Germany.

**M. Haddad**, K. Tsintzas, S.P.H. Alexander and A.J. Bennett. (2010) Molecular characterization of G protein-coupled receptors (GPCRs). Faculty of Medicine and Health Sciences, University of Nottingham, Nottingham, UK. Oral Presentation-2010.

**M. Haddad**, K. Tsintzas, S.P.H. Alexander and A.J. Bennett. (2010) Molecular characterization of G protein-coupled receptors (GPCRs). Faculty of Medicine and Health Sciences, University of Nottingham, Postgraduate Research Forum Event, Nottingham, UK. Poster Presentation-2010.

**Table of Contents**

**List of Tables**

**List of Figures**

**List of Abbreviations**

**AA**: Arachidonic acid

**ACC**: Acetyl-CoA carboxylase

**ACEA**: Arachidonyl-2-chloroethylamide

**Actb**: Beta-actin

**AEA**: N-arachidonoylethanolamine (anandamide)

**AICAR**: 5-aminoimidazole-4-carboxyamide-1--D-ribofuranoside.

**2-AG**: 2-Arachidonoylglycerol

**AKT**: Serine threonine kinase/protein kinase B

**AM251**: 1-(2, 4-dichlorophenyl)-5-(4-iodophenyl)-4-methyl-N-(1-piperidyl) pyrazole - 3-carboxamide

**AMPK**: AMP-activated protein kinase

**ANOVA**: Analysis of variance

**APS**: Ammonium persulphate

**BMI**: Body mass index

**cAMP**: Cyclic-adenosine monophosphate

**CB1**: Cannabinoid receptor 1

**CB2**: Cannabinoid receptor 2

**cDNA**: Complementary DNA

**CGS21680**: 2-(4-[2-carboxyethyl]-phenethylamino) adenosine-5′-N-ethyluronamide

**CPT1**: Carnitine palmitoyl transferase 1

**CT**: Cycle threshold

**DAG**: Diacylglycerol

**DAGL**: Diacylglycerol lipase

**DGK**: Diacylglycerol kinase

**DMSO**: Dimethyl sulfoxide

**EC**: Endocannabinoids

**EPAC**: Exchange protein activated by cAMP

**FA**: Fatty acid

**FAAH**: Fatty acid amide hydrolase

**FAS/FASN**: Fatty acid synthase

**FFA**: Free fatty acid

**FOXO**: Forkhead box

**Fura-2AM**: L-[2-(carboxyloxazol-2-yl)-6-amino-benzofuran-5-oxy]-2-(2'-amino-5'methylphenoxy)ethane-N,N,N,N-tetraacetic acid pentaacetoxymethyl ester; fura 2-acetoxymethyl ester.

**GLUT4**: Glucose transporter-4

**GSK3**: Glycogen synthase kinase 3

**HFD**: High fat diet

**HSL**: Hormone sensitive lipase

**IBMX**: 3-isobutyl-1-methylxanthine

**IL-6**: Interleukin-6

**IPA**: Ingenuity Pathways Analysis

**IR**: Insulin receptor

**IRS**: Insulin receptor substrate

**LPC**: Lysophosphatidylcholine

**MAGL**: Monoacylglycerol lipase

**MAPK**: Mitogen activated protein kinase

**MCD**: Malonyl-CoA decarboxylase

**MGL**: Monoglyceride lipase

**MHC**: myosin heavy chain

**mRNA**: Messenger ribonucleic acid

**MRS2179**: 2'-Deoxy-N6-methyladenosine 3', 5'-bisphosphate

**NAPE**: N-arachidonoyl-phosphotidylethanolamine

**NECA**: 5'-N-ethylcarboxamidoadenosine

**OEA**: N-oleoylethanolamine

**pAKT**: Phospho-AKT

**PBS**: Phosphate buffered saline

**PCA**: Principle component analysis

**PCR**: Polymerase chain reaction

**PDK1**: 3′-phosphoinositide-dependent kinase 1

**PFA**: paraformaldehyde

**PGC-1**: Peroxisome proliferator-activated receptor γ coactivator 1α

**PH**: Pleckstrin-homology

**PI-3 kinase**: Phosphatidylinositol-3 kinase

**PKA**: cAMP-dependent protein kinase

**PKC**: Protein kinase C

**PLC**: Phospholipase C

**PLD**: Phospholipase D

**PPAR**: Peroxisome proliferator-activated receptor

**PSB603**: 8-[4-[4-(4-chlorophenzyl) piperazide-1-sulfonyl)phenyl]]-1-propylxanthine

**P-value**: Probability

**r**: Pearson correlation

**RIM**: 5-(4-Chlorophenyl)-1-(2, 4-dichloro-phenyl)-4-methyl-N-(piperidin-1-yl)-1H-pyrazole-3-carboxamide; rimonabant

**RT-PCR**: Reverse transcription polymerase chain reaction

**SDS-PAGE**: Sodium dodecyl sulfate polyacrylamide gel electrophoresis

**SEM**: Standard error of the mean

**S-ENBA**: (2S)-N6-(2-endonorbanyl) adenosine

**SHC**: Src homology 2 domain containing

**SREBPs**: Sterol regulatory element-binding proteins

**TAG**: Triacylglycerol

**TBE**: Tris/Borate/EDTA

**TBS**: Tri-Buffered saline

**TEMED**: (N,N,N',N'-Tetramethylethylenediamine)

**TG**: Triglyceride

**UCP3**: Uncoupling protein 3

**WHO**: World Health Organisation

**ZMP**: 5-aminutesoimidazole-4-carboxamide ribonucleoside

# Chapter 1

# Introduction

# 1 Chapter One: Introduction

## 1.1 GPCR

### 1.1.1 Definition

GPCRs constitute the largest family of proteins in the human genome consisting of approximately 1000 genes. GPCRs are the richest targets for pharmaceutical drugs on the market today, it is estimated that they are the targets of 30-50% of all medications due to their vast and varied roles in regulating the body and their involvement in key biological functions (Kobilka, 2007; Tilakaratne *et al.*, 2005).

### 1.1.2 GPCR structure

GPCRs are diverse in structure and sequence homology. However, they have common structural features including seven-transmembrane helices of 22-28 hydrophobic amino acids that reside in the cell membrane, three extracellular loops with N-terminus (with potential sites for glycosylation) and three intracellular loops with C-terminus (with potential sites for phosphorylation) as shown in Figure 1-1 (Fredriksson *et al.*, 2003; Perez *et al.*, 2005).

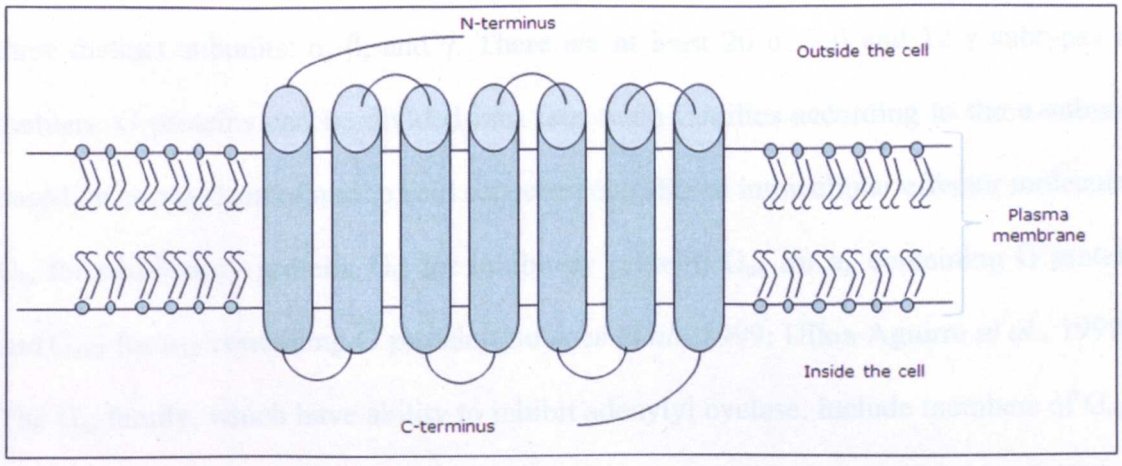


Figure 1-1: General features of GPCR structure. The common features are seven-transmembrane helices, three extracellular loops with N-terminus and three intracellular loops with C-terminus.

### 1.1.3 GPCR families

Based on sequence homology and functional similarity, GPCRs can be further separated into three major families or collections which are Class A (Rhodopsin family), Class B (Secretin-vasointestinal peptide (VIP) receptor family) and Class C (Metabotropic glutamate receptor family). The Class A family is by far the largest, recognizing a diverse array of ligands ranging from small biogenic amines (catecholamines and histamine) to peptides and complex glycoproteins. The Class B family binds several neuropeptides and peptide hormones. The Class C family binds glutamate, the major excitatory neurotransmitter as well as GABA, the major inhibitory neurotransmitter (Kristiansen, 2004).

### 1.1.4 Heterotrimeric G protein families

Heterotrimeric G proteins are considered as important signal transduction molecules (Kehrl, 1998). G proteins are a diverse class of heterotrimeric proteins composed of

three distinct subunits: α, β, and γ. There are at least 20 α, 7 β and 12 γ subtypes in humans. G proteins can be divided into four main families according to the α-subunit based on comparison of amino acid sequence and shared intracellular effector molecules: $G_{\alpha s}$ for stimulatory protein; $G_{\alpha i}$ for inhibitory protein; $G_{\alpha q}$ for $\alpha_q$ containing G protein and $G_{\alpha 12}$ for $\alpha_{12}$ containing G protein (Downes *et al.*, 1999; Ulloa-Aguirre *et al.*, 1999). The $G_{\alpha i}$ family, which have ability to inhibit adenylyl cyclase, include members of $G_{\alpha i1}$, $G_{\alpha i2}$, and $G_{\alpha i3}$. The α-subunits can be myristoylated or palmitoylated (Chen et al., 2001). This facilitates their association with membrane and seven-transmembrane receptors (Wedegaertner et al., 1995). Each family of α-subunits regulates a diverse cluster of effector proteins (for example; adenylyl cyclase, ion channels and phosphatidylinositol-specific phospholipase C), as illustrated in the Section 1.1.6. Moreover, the β and γ subunits might be as a dimer and a heterotrimer (Smrcka, 2008). The heterotrimer of heterotrimeric G proteins can function as a molecular switch for the receptor signalling, as illustrated in the Section 1.1.5.

### 1.1.5 G protein cycle

In their basal state, G proteins bind guanosine diphosphate (GDP). When a ligand binds to a GPCR, this activates the receptor, causing a conformational change in the receptor. This conformational change enhances its affinity for the G protein. The $G_\alpha$ protein then combines with the GPCR (the G protein is normally considered to be separate from the inactive receptor) and the $G_\alpha$ subunit is activated. GDP is exchanged for GTP at the α subunit and, as a result, the $G_{\beta\gamma}$ subunits dissociate from the GTP-bound α subunit to allow the activation of downstream effectors, as shown in Figure 1-2 (Rens-Domiano *et al.*, 1995). G protein signalling is terminated by the hydrolysis of GTP to GDP, conducted by the intrinsic GTPase activity of the $G_\alpha$ subunit, a step which may be

enhanced through an interaction with accessory proteins, like RGS (regulators of G protein signalling) proteins. This leads to re-association of the $G_{\alpha}$ and $G_{\beta\gamma}$ subunits and the GDP-bound G protein can then rebind a receptor to complete the cycle (Figure 1-2).

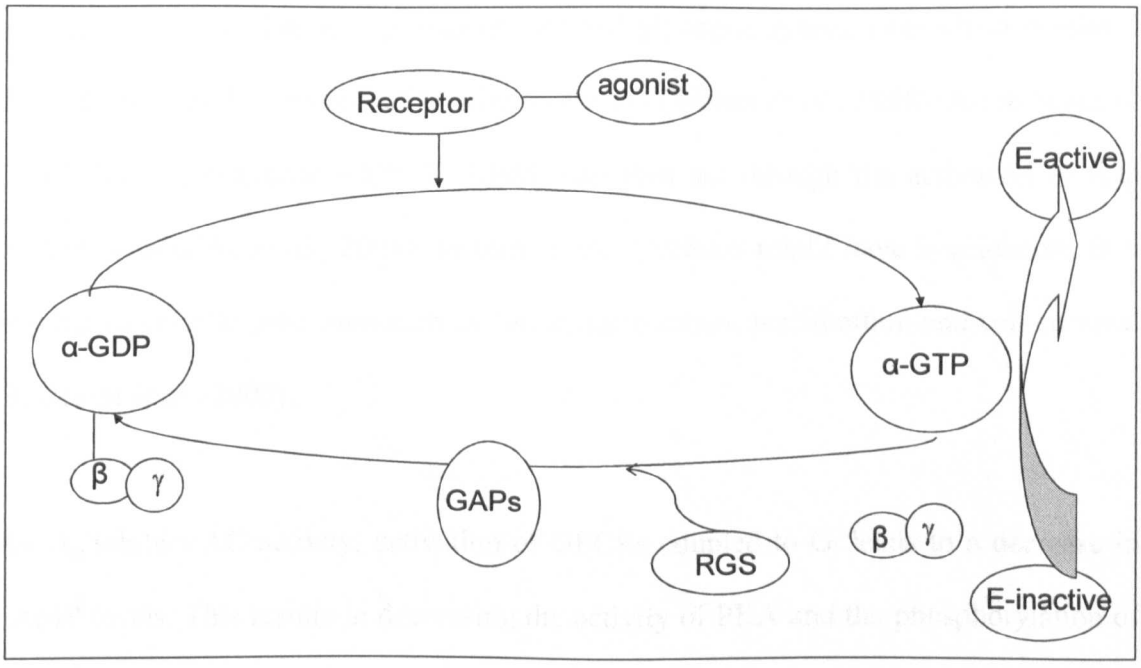


Figure 1-2: Schematic diagram showing the basic regulatory cycle of a G-protein, adapted from (Conklin *et al.*, 1993; Neer, 1995). E: Effector, GAPs: GTPase-activating proteins, GDP: Guanosine diphosphate, GTP: Guanosine triphosphate and RGS: Regulators of G protein signaling.

### 1.1.6 Main signalling mechanisms

The main signalling mechanisms are illustrated in Figure 1-3. $G_{\alpha s}$ stimulates adenylyl cyclase (AC) activity. This enzyme converts ATP to cAMP. Sufficient cAMP concentration can activate cAMP effector proteins, such as protein kinase A (PKA) or the exchange protein activated by cAMP (EPAC) (Qiao *et al.*, 2002). An increase of cAMP level activates protein kinase A (PKA) allowing the cellular response to take place. For example, release of adrenaline leads to increased cardiac muscle contractility through phosphorylation and activation of cardiac calcium channels (an effect mediated

through the initial activation of $\beta_1$-adrenoceptors) (Ochi *et al.*, 1986; Reuter, 1987), vasodilation of skeletal muscle vascular smooth muscle through phosphorylation and inhibition of myosin light chain kinase (an effect mediated through the initial activation of $\beta_2$-adrenoceptors) (Walter *et al.*, 1988) and mobilization of glucose in liver through glycogen phosphorylation of phosphorylase and glycogen synthase (an effect mediated through the initial activation of $\beta_2$-adrenoceptors) (Walter *et al.*, 1988). An increase of cAMP level also activates EPAC. EPAC can then act through the activation of Rap proteins (Enserink *et al.*, 2004). In turn, EPAC proteins might have implications in a number of cellular processes such as cell differentiation, proliferation and cell survival (Roscioni *et al.*, 2008).

As $G_{\alpha i}$ inhibits AC activity, activation of GPCRs coupled to $G_i$ leads to a decrease in cAMP levels. This results in decreasing the activity of PKA and the phosphorylation of proteins. $G_{\alpha i}$ protein-coupled receptors inhibit neurotransmitter release through stimulating $K^+$ efflux and inhibiting $Ca^{2+}$ channels in the nervous system (Pierce *et al.*, 2002). The mechanism behind this was suggested through $G_{\beta\gamma}$ subunit. The specific $G_{\beta\gamma}$ subunits from $G_{\alpha i}$-coupled receptors can directly modulate calcium channel fucntion. This was supported by the fact that transfection of cell lines expressing P/Q-type calcium channels with $G_{\beta\gamma}$ subunit was reported to cause modulation such that by the activation of GPCRs (Herlitze *et al.*, 1996), overexpression of $G_{\beta\gamma}$ in rat sympathetic neurons was also shown to reproduce the transmitter-induced calcium current inhibition (Ikeda et al., 1999), and P/Q type and N type channels were shown to be inhibited by pertussis toxin (PTX)-sensitive G proteins, $G_{\alpha i}$ (Shapiro *et al.*, 1994). Moreover, G-protein beta gamma complex was reported to directly bind to voltage-dependent calcium channels (De Waard *et al.*, 1997).

When a ligand binds to a $G_{\alpha q}$-protein coupled receptor, $G_{\alpha q}$ activates phospholipase C (PLC) β. The active PLC hydrolyses phosphatidylinositol 4,5-bisphosphate ($PIP_2$) to produce inositol 1,4,5-trisphosphate ($IP_3$) and 1,2-diacylglycerol (DAG). $IP_3$ is water-soluble, so it is able to migrate through the cytoplasm to the endoplasmic reticulum (ER). $IP_3$ can then bind to $IP_3$ receptors, which are tetrameric intracellular calcium channels, on ER. Consequently, $IP_3$ induces the channels ($IP_3$ receptors) to open by enhancing calcium binding to a stimulatory binding site on $IP_3$ receptors, where it allows calcium to be released from intracellular stores (Taylor *et al.*, 2002). An increase of $Ca^{2+}$ levels affects the activity of many enzymes and ion channels. DAG is hydrophobic, however, and it stays in the membrane to activate protein kinase C (PKC). This enzyme phosphorylates many proteins including smooth muscle myosin light chain kinase (MLCK), which leads to increased smooth muscle contractility, as well as phosphorylating selected isoforms of phospholipase $A_2$ leading to increased arachidonic acid production (Fuchs *et al.*, 1972; Gailly *et al.*, 1997).

When a ligand binds to a $G_{\alpha 12}$ protein-coupled receptor, Rho guanine nucleotide exchange factors are activated, leading to activation of the small G protein Rho. Rho-GTP activates many enzymes that regulate phosphorylation. For example, Rho kinases, JNK (a member of the mitogen-activated protein kinases), phosphatidylinositol 4-phosphate 5 kinase and phospholipase D. Rho kinase can lead to smooth muscle contraction through phosphorylation and inhibition of the function of myosin light chain phosphatase (Mizuno *et al.*, 2008).

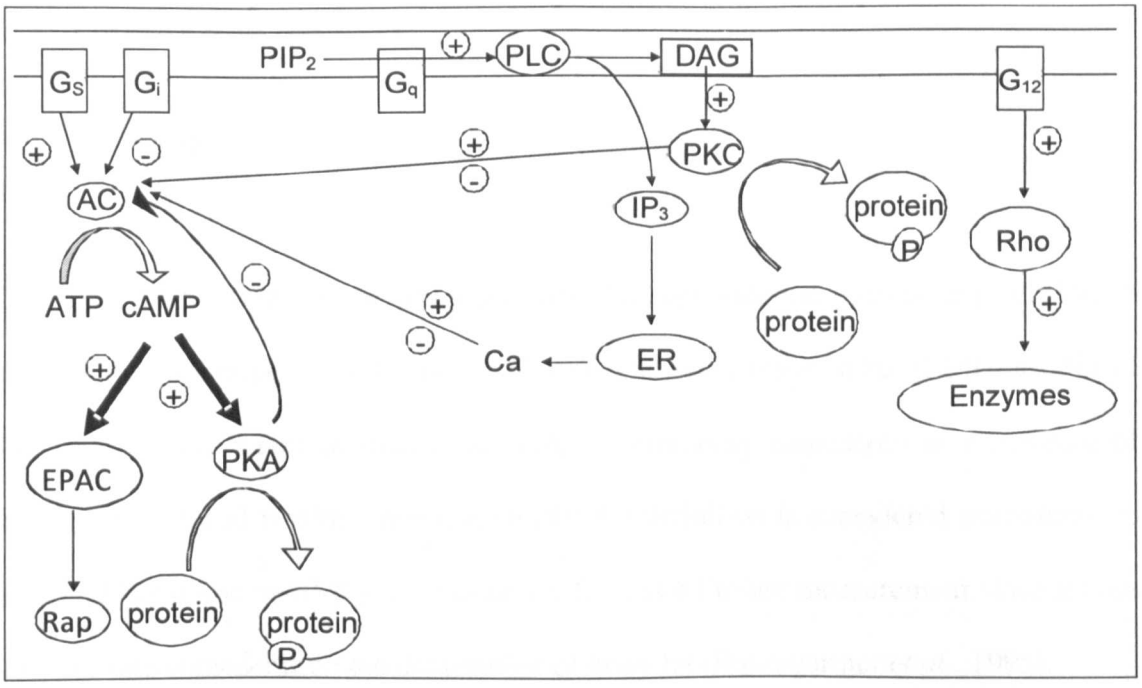


Figure 1-3: Schematic diagram showing the main four families of G-protein signalling mechanisms, adapted from (Jacoby *et al.*, 2006). P: phosphate, RGS: Regulators of G-protein signalling, ER: Endoplasmatic reticulum, PKC: protein kinase C, PKA: protein kinase A, and AC: adenylyl cyclase.

## 1.2 Obesity and diabetes

### 1.2.1 Obesity

Obesity can be defined as abnormal excessive fat accumulation (excess adiposity) to an extent that may impair health (James, 2004). The body mass index (BMI), a ratio of weight (kg) and height in meters squared, is commonly considered as a measure of obesity. The World Health Organization (WHO) definition is considered overweight as BMI $\geq$ 25 or obese as BMI $\geq$ 30. However, BMI is a limited measurement since it does not take into consideration the distribution of body fat (Baumgartner *et al.*, 1995).

Obesity is a growing health problem worldwide. Indeed, the epidemic of obesity poses a significant public health problem since it now afflicts millions globally. In fact, an unprecedented change in caloric availability during the mid 20$^{th}$ century has occurred in many western and developing countries. As a result, obesity results from the prolonged imbalance between energy intake and energy expenditure. Furthermore, obesity can be the result of programmed genetic susceptibility, a decrease in exercise and physical activity, and an increase in high-energy food in modern society (Astrup *et al.*, 1994; Astrup *et al.*, 2004). Lifestyle modifications such as diet and exercise have been shown to be successful for obesity (Hayes *et al.*, 2008; Markovic *et al.*, 1998; Thomas *et al.*, 2006), although, without pharmacological and surgical intervention, maintaining weight loss is difficult. In addition, the need to find effective pharmacological therapy is more essential as costs of health care rise with obesity rates (Wadden *et al.*, 2007).

Obesity leads to a range of secondary health problems including type 2 diabetes mellitus (Colditz *et al.*, 1995), hypertension (Witteman *et al.*, 1989), cardiovascular disease

(Rimm *et al.*, 1995), osteoarthritis, steatohepatitis and cancer (Calle *et al.*, 2004a; Calle *et al.*, 2003; Calle *et al.*, 2004b). In fact, obesity, especially visceral obesity, is a main independent risk factor for insulin resistance and has adverse metabolic effects for it, which leads to type 2 diabetes (Adams *et al.*, 2006; Allison *et al.*, 1999; Despres *et al.*, 2006; Reaven, 2005).

In obese individuals, body fat was found to be positively correlated with the percentage of type II fibres and negatively correlated with the percentage of type I fibres (Kriketos *et al.*, 1996; Storlien *et al.*, 1996) whereas endurance-trained male athletes were found to have a greater proportion of type I fibres (Andersson *et al.*, 2000). The use of histochemistry-based methods for determining fibre type proportion (Abou Mrad *et al.*, 1992; Warmington *et al.*, 2000) is possibly a limitation since such methods might not accurately identify mixed fibres. Therefore, it is recommended to examine the fibre composition of skeletal muscles using the single fibre level myosin heavy chain (MHC) isoform analysis in addition to histochemistry-based methods. Indeed, obesity was correlated with impaired oxidative metabolism in skeletal muscle (Kelley et al., 1999). Alterations in skeletal muscle fibre phenotype proportions may arise as a consequence of both lack of physical activity and obesity (imbalance between energy intake and energy expenditure). This possibly contributes to the complications associated with obesity (Berggren *et al.*, 2008; Perez-Martin *et al.*, 2001). This might be due to the fact that type I fibre-rich muscles have higher capacity for oxidation of fatty acid and glucose and higher capacity for insulin-stimulated glucose uptake (Daugaard *et al.*, 2000; Henriksen *et al.*, 1990; Song *et al.*, 1999). Therefore, a number of possible mechanisms for this effect were suggested, such as insulin resistance, increased stores of intramyocellular triglycerides and possibly the endocannabinoid system (Jeukendrup, 2002; Kelley, 2005).

Obesity is accompanied by an increase in plasma and tissue level of endocannabinoids due to a decrease in catabolism, an increase in production, or both (Engeli *et al.*, 2005; Sipe *et al.*, 2005). In addition, energy balance might also be regulated by endocannabinoids through peripheral effects on $CB_1$ receptor in the gastrointestinal tract, adipose tissue, liver, and skeletal muscle (Cavuoto *et al.*, 2007b; Liu *et al.*, 2005; Pagotto *et al.*, 2006).

### 1.2.2 Diabetes mellitus

Diabetes is a chronic metabolic disease characterized by persistently high blood glucose concentrations (≥7.0 mmol/l) in which either not enough insulin is produced from the body or insulin-target tissues do not respond to the insulin that is produced. There are three main categories of diabetes. The first is type 1 diabetes mellitus (also referred to as early-onset or insulin-dependent diabetes mellitus or juvenile diabetes), the second is type 2 diabetes mellitus (more rarely called late-onset, or non-insulin-dependent diabetes), and the third is gestational diabetes (Zimmet *et al.*, 1999).

Type 1 diabetes mellitus is caused by the inability of pancreatic β-cells to produce endogenous insulin. Successful treatment of type 1 diabetes requires the person to inject insulin. Type 2 diabetes mellitus is mainly caused by the failure of insulin to act on metabolic tissues, known as insulin resistance. In other words, insulin resistance is the reduced ability of insulin to stimulate glucose transport activity and metabolism effectively (Ferrannini *et al.*, 1991). As insulin is unable to clear out the high blood glucose level through GLUT4 in skeletal muscle and adipose tissues (insulin-dependent), hyperglycemia occurs. Consequently, hyperglycemia leads to many complications including kidney failure, neuropathy, retinopathy and infection since

these tissues including kidney, neurons and retina are unable to dispose the high glucose level, in particular of the glucose uptake in these tissues is controlled through an insulin-independent manner (Nathan, 1993).

There are multiple mediators suggested to facilitate insulin resistance. These mediators include an increase of the content of triglyceride in liver, pancreas, cardiac tissue and skeletal muscle (Despres *et al.*, 2006), visceral adipose tissue (Pan *et al.*, 1997), and an increase in inflammatory adipokines (interleukin-6 (IL-6) and tumor necrosis factor-alpha (TNFα)) from adipose tissue into circulation (Cote *et al.*, 2005). In addition, it has been suggested that endocannabinoids might also mediate skeletal muscle insulin resistance (Watt, 2009).

## 1.3 Skeletal muscle

Muscle tissues are divided into three types. These are cardiac, smooth and skeletal muscle. Cardiac muscle is striated and involuntarily controlled. Smooth muscle is non-striated and involuntarily controlled while skeletal muscle is striated and voluntarily controlled. Skeletal muscle has many functions in the body. These include producing skeletal movement, maintaining posture and body positions, storing nutrient reserves (proteins), producing heat to maintain body temperature and guarding the entrance and exit of the gastrointestinal tract (Allen, 2004).

### 1.3.1 Skeletal muscle contraction

Skeletal muscle is one of the most metabolically active tissues. It utilizes carbohydrate and fat as a source to generate fuel as adenosine triphosphate (ATP). This chemical energy can be processed to provide energy for the shortening and relaxation process of the cross-bridge between actin and myosin filament of striated muscle. This process is known as contraction.

A nerve action potential (AP) translates into muscle contraction through releasing acetylcholine (ACh) from the terminal ends of the motor axon to the neuromuscular junction (NMJ). ACh is released via exocytosis into the synaptic cleft. The nicotinic cholinergic receptor on the muscle membrane can then bind ACh. ACh actions are terminated by an enzyme called acetylcholinesterase (ACE) which is expressed in skeletal muscle (Herman *et al.*, 1985). Binding of ACh to these receptors changes its conformational shape and allows $Na^+$ to move down its concentration gradient into the

sarcoplasm. This causes depolarization of the muscle membrane. When another AP is generated, this signal (depolarization) is propagated to the transverse tubules. Membrane depolarization activates voltage sensitive L-type $Ca^{2+}$ channels, also known as "dihydropyridine receptors", this activates other calcium channels of the sarcoplasmic reticulum (SR) known as "Ryanodine receptors (RyR)". Indeed, ryanodine receptors can be activated by depolarisation via dihydropyridine receptors, cytosolic ATP, calmodulin kinase and PKA (Coronado et al., 1994; Fill et al., 2002). Moreover, the function of the ryanodine receptors can be influenced by proteins such as calmodulin (Yamaguchi et al., 2003). Furthermore, inorganic phosphate (Pi), accumulated during exercise, was found to potentiate the release of calcium from the ER through ryanodine receptors (Fruen et al., 1994). However, the potential role of cyclic ADP ribose to activate ryanodine receptors as an endogenous regulator is still controversial in skeletal muscle (Coronado et al., 1994). The skeletal muscle use of calcium is essential to mediate regulation of contraction. In response to AP, the SR triggers release of $Ca^{2+}$ through RyR. The $Ca^{2+}$ binds to troponin, which leads to a change in the position of troponin, pulling the tropomyosin to actin, and exposure of the active (myosin-binding) sites to actin. When myosin of the thick filaments is bound to actin of the thin filaments, they form cross-bridges. Consequently, this begins the contraction cycle.

The actin-myosin complex binds ATP, and then myosin breaks the cross-bridges. Myosin ATPase hydrolyzes ATP and this causes the myosin to revert to its original shape and to get ready for the next binding.

When the motor neuron stops sending AP, acetylcholinesterase (AChE) breaks down previously released ACh in the synaptic cleft and no new ACh is released at the

synaptic cleft. As a result, this leads to no new $Ca^{2+}$ being released from the SR and $Ca^{2+}$ being pumped back into the SR continuously. Then, the troponin-tropomyosin complex returns to its original state, hiding the myosin-binding sites on the thin filaments. Consequently, no cross-bridge is formed between actin and myosin. Then, the muscle stretches again to its resting state. Even with this simplified summary, it is clear that the contraction process is complicated (Berchtold *et al.*, 2000; Gillis, 1977; Lamb, 2000).

### 1.3.2 Skeletal muscle metabolism

Skeletal muscle is the largest tissue in the human body and represents ~40% of the human body mass and ~35-40% of the total body weight in the rat (Delbono *et al.*, 2007; James *et al.*, 1985; Pedersen, 2011). Occasionally, skeletal muscle is considered by some researchers as an endocrine organ, since it releases IL-6, which increases glucose metabolism in resting human skeletal muscle (Glund *et al.*, 2007). Skeletal muscle plays a crucial role in maintaining body glucose homeostasis; it clears the majority (70-80%) of ingested glucose, since it is the main site for insulin-dependent glucose uptake (Toft *et al.*, 1998). It is generally considered the most important site of insulin resistance. Indeed, skeletal muscle has the ability to oxidize fatty acid and glucose, and this may also play a crucial role in metabolic diseases (Cahova *et al.*, 2007). Therefore, it is generally considered as a main site of fatty acid and glucose metabolism (Zurlo *et al.*, 1990).

Skeletal muscle is the major site involved in energy balance and ~20% of energy expenditure occurs at rest in this tissue (Zurlo *et al.*, 1990). When skeletal muscle contraction occurs, ATP supports the energy for skeletal muscle. ATP is the only energy

source for contraction. Indeed, the skeletal muscle fuel metabolism needs ATP to be generated continuously in order to match ATP supply to ATP demand. Consequently, contractile activities are able to proceed. Skeletal muscle under normal physiological conditions depends on glucose and fat-based fuels for oxidative metabolism. Randle in the 1960s hypothesized the interaction, relationship and competition between glucose and fatty acids for oxidation, termed the glucose-fatty acid, or Randle cycle (Randle *et al.*, 1963). It described a nutrient-mediated regulation of metabolism and depended primarily on the free fatty acid (FFA) availability which was the main source to be oxidized. In Randle's study, biochemically, this occurred by β-oxidation through the accumulation of acetyl-CoA and citrate, an inhibitor of pyruvate dehydrogenase (PDH) and phosphofructokinase (PFK). Therefore, this reduced glycolysis and glucose oxidation by the accumulation of glucose-6-phosphate (G6P) and the inhibition of hexokinase (HK) activity. Consequently, according to the Randle cycle, this elevated the glucose concentration and inhibited glucose uptake. Moreover, the glucose-fatty acid cycle could also be reversed. When glucose concentrations were high, glycolysis occurred through metabolizing glucose into pyruvate (Randle *et al.*, 1963). This activated pyruvate dehydrogenase (PDH) which oxidized pyruvate to acetyl-CoA and finally led to the production of malonyl-CoA which inhibited carnitine palmitoyl transferase 1 (CPT-1), thus reducing β-oxidation rates (Sidossis *et al.*, 1996) (Figure 1-4).

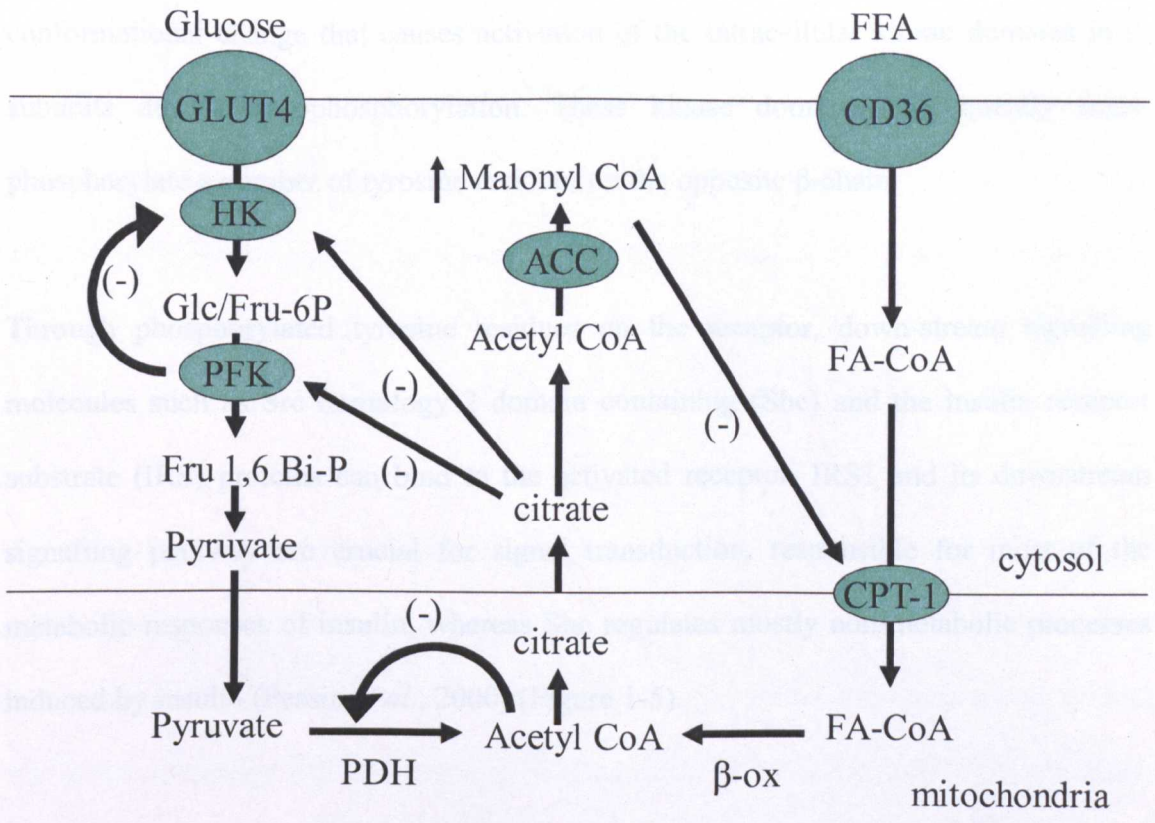


Figure 1-4: The mechanism of inhibition of fatty oxidation by glucose and inhibition of glucose metabolism by fatty acids, proposed by (Randle *et al.*, 1963). Pyruvate dehydrogenase (PDH), hexokinase (HK), phosphofructokinase (PFK), acetyl-CoA carboxylase (ACC), fatty acid translocase (FAT/CD36) and carnitine palmitoyl transferase 1 (CPT-1).

Skeletal muscle contains a fatty acid transporter, known as fatty acid translocase (FAT/CD36), and glucose transporters, such as GLUT1 and GLUT4. Once skeletal muscle is stimulated by hypoxia/contraction or insulin, GLUT4 are translocated to the plasma membrane to activate glucose uptake (Shepherd *et al.*, 1999).

The insulin receptor (IR) is a heterotetrameric transmembrane protein belonging to the tyrosine kinase receptor superfamily. The IR consists of four subunits, two extracellular insulin-binding α-peptides responsible for insulin binding, and two transmembrane β-peptides that contain intracellular tyrosine kinase domains. Insulin binds to the two α-chains of the IR on the outer surface of the plasma membrane. This binding leads to a

conformational change that causes activation of the intracellular kinase domains in β-subunits due to autophosphorylation. These kinase domains subsequently trans-phosphorylate a number of tyrosine residues on the opposite β-chain.

Through phosphorylated tyrosine residues on the receptor, down-stream signalling molecules such as Src homology 2 domain containing (Shc) and the insulin receptor substrate (IRS) proteins can bind to the activated receptor. IRS1 and its downstream signalling pathway are crucial for signal transduction, responsible for most of the metabolic responses of insulin, whereas Shc regulates mostly non-metabolic processes induced by insulin (Pessin *et al.*, 2000) (Figure 1-5).

The activated IR phosphorylates IRS1 and Shc on multiple tyrosine residues. The phosphorylated substrates (IRS and Shc) serve as docking sites for proteins containing Src homology 2 (SH2) domains such as class 1A phosphatidylinositol 3-kinase (PI-3K) and growth factor receptor-binding protein 2 (Grb2), respectively.

PI 3-kinase is composed of one regulatory subunit (p85) and one catalytic subunit (p110). The binding of the p85 subunit via its two SH2 domains to residues on IRS1 leads to a conformational change and activation of the catalytic p110 subunit and recruitment of PI-3K to the plasma membrane. The p110 subunit catalyses the phosphorylation of specific phospholipids, phosphoinositides, on the 3-position to produce phosphatidylinositol-3-phosphates. PI3,4P and PI3,4,5P are recognized by proteins that contain pleckstrin-homology (PH) domains including 3′-phosphoinositide-dependent kinase 1 (PDK1) and AKT.

AKT (also known as protein kinase B, PKB) relocates from the cytoplasm to the membrane to bind with phosphatidylinositol-3-phosphates. This induces a conformational change in AKT. At the membrane, PDK1 mediates phosphorylation of AKT. The activated AKT may then migrate to the cytosol or nucleus; where it can phosphorylate downstream targets and regulate a number of multiple intracellular substrates important for glucose, protein and fat metabolism (Shepherd *et al.*, 1998).

As mentioned above, the activated IR phosphorylates Shc on multiple tyrosine residues, which allows it to serve as a docking site for proteins SH2 domains such as Grb2. Grb2 is associated with the nucleotide exchange factor mammalian son-of-sevenless (mSos) via its Src homology 3 (SH3) domain. Binding of the Grb2-Sos complex induces mSos to activate Ras by exchanging Ras-bound GDP for GTP. Ras can activate multiple effectors such as PI-3K and RAF proto-oncogene serine/threonine-protein kinase. The active Raf kinase then triggers the phosphorylation of mitogen-activated protein (MAP) kinase kinase (MEK1/2) and subsequently, MEK1/2 activates the MAP kinases extracellular signal regulated kinase (ERK1/2, also known as p42/44 MAP kinases). Insulin signalling through this pathway can regulate transcription factors and thus gene expression and cell growth (Force *et al.*, 1998; Katz *et al.*, 2007).

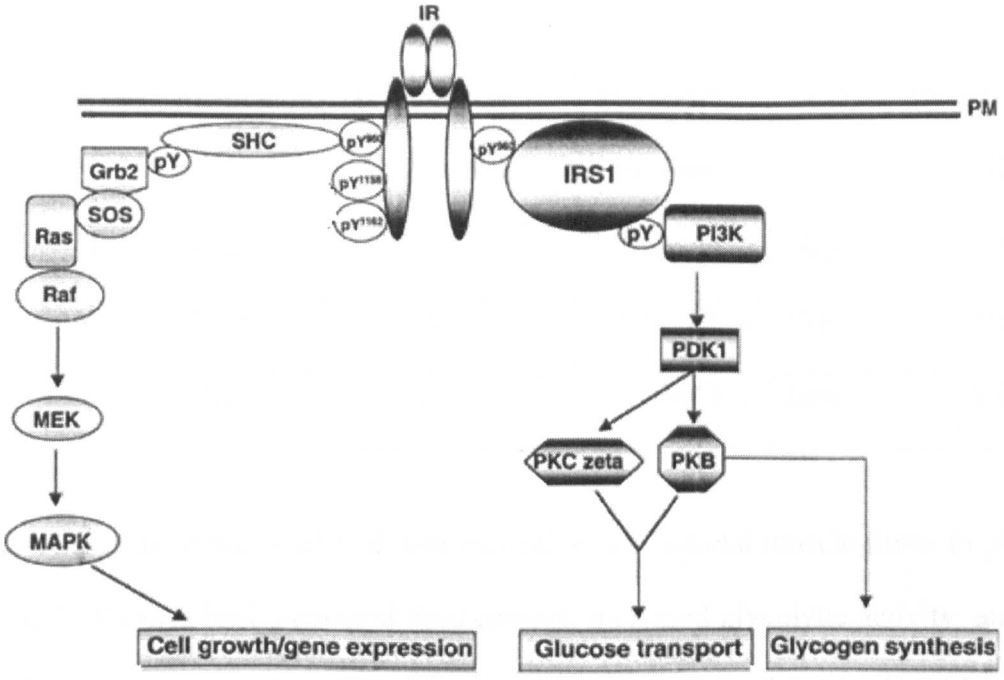


Figure 1-5: A scheme of insulin signalling pathways, adapted from (Le Marchand-Brustel *et al.*, 2003).

### 1.3.3 Skeletal muscle fibres

Skeletal muscle is a heterogeneous tissue, since it contains a variety of fibres that differ in contractile, functional, metabolic and molecular properties (Greenhaff, 1997). Human skeletal muscle is a mixed fibre-type composition. This is in contrast to other species, such as rat, in which some skeletal muscle mainly consists of a single fibre type (Fuentes *et al.*, 1998; Hamalainen *et al.*, 1995). There are three basic fibre types in both humans and rats depending on the expression of various isoforms of myosin light chains and myosin heavy chains; Fast-twitch oxidative-glycolytic (FOG), fast-twitch glycolytic (FG) and slow-twitch oxidative (SO) as shown in Table 1-1 (Close, 1972; Schiaffino *et al.*, 1994).

Table 1-1: Characteristics of human muscle fibre types.

| Fibre type | Mitochondrial density | Contractile function | Metabolic character | Enzyme activity | |
|---|---|---|---|---|---|
| | | | | Oxidative | Glycolytic |
| I (SO) | High | Slow | Oxidative | High | Low |
| IIa (FOG) | Medium | Fast | Intermediate | High | High |
| IIb (FG) | Low | Fast | Glycolytic | Low | High |

Currently, there is a wealth of data indicating that skeletal muscle fibres in obesity and type II diabetes have increased lipid content, increased glycolytic activity, and reduced oxidative enzyme activity. The lower oxidative enzyme activity in skeletal muscle was explained by either a reduced mitochondrial content or a reduced mitochondrial function (He *et al.*, 2001).

These metabolic characteristics including altered patterns of enzyme activity are related to insulin resistance of skeletal muscle. In addition, skeletal muscle fibre-type proportions was observed to have a relation to insulin resistance and obesity, specifically that the proportion of type IIb fibres was found to be higher and that of type I fibres was found to be lower (Berchtold *et al.*, 2000; He *et al.*, 2001; Kelley *et al.*, 2002; Kriketos *et al.*, 1996). Indeed, there is a correlation between insulin sensitivity and the proportion of type I fibres. Skeletal type I fibres have greater insulin-stimulated glucose transport (Daugaard *et al.*, 2000; Henriksen *et al.*, 1990; Song *et al.*, 1999). Type I fibres are known to be rich in mitochondria, so they have a relatively large capacity for oxidation (a high muscle capacity for fat utilization, higher oxidative capacity for carbohydrate). In addition, type I fibres have greater insulin sensitivity.

Little is known about GPCRs in skeletal muscle. One group of researchers mentioned that $CB_1$ receptors might have a role in the myoblast differentiation, proliferation and fibre phenotype (Hannon, 2010). However, this issue is still not yet well studied. Moreover, there are findings in the literature to suggest that $CB_1$ receptors may play a vital role in glucose uptake in skeletal muscle (Eckardt *et al.*, 2008b; Lindborg *et al.*, 2011). In addition, it was reported that $\beta_2$-adrenoceptors stimulated glucose uptake in rat skeletal muscle L6 cells and this uptake was inhibited by PI3K inhibitors; this implied that $\beta_2$-adrenoceptors stimulation might share insulin signalling pathways (Nevzorova *et al.*, 2006). Moreover, it was suggested that $\alpha_1$-adrenoceptors might affect key proteins such as AMPK which potentially might affect glucose uptake (Hutchinson *et al.*, 2006). In general, GPCRs in skeletal muscle might have a role in glucose uptake in the body, skeletal muscle differentiation and growth. However, these issues are still under investigation in skeletal muscle. Overall, there is a knowledge gap about potential functional impacts of GPCRs, especially for $CB_1$ receptors in skeletal muscle.

As obesity can lead to health problems including insulin resistance and type 2 diabetes mellitus (Colditz *et al.*, 1995), and skeletal muscle plays a crucial role in maintaining body glucose homeostasis in human body (Toft *et al.*, 1998), it is possible that the modulation of cannnabinoid receptors might play a role to improve glucose uptake and obesity. This is supported by the fact that 1) Endocannabinoid levels were found to be higher in several organs of obese animals, central and peripheral (Di Marzo *et al.*, 2001; Starowicz *et al.*, 2008). 2) Obese rodents compared to lean controls were found to be more sensitive to the anti-obesity effects of treatment with $CB_1$ receptor antagonists (Hildebrandt *et al.*, 2003). 3) RIM was found to reduce bodyweight and cause a clinically significant reduction in $HbA_{1c}$ levels in overweight or obese patients with type 2 diabetes (Scheen *et al.*, 2006). 4) During a glucose tolerance test, $CB_1$ receptor

agonism (AEA 10 mg/kg or ACEA 3 mg/kg) was found to lead to elevated circulating glucose levels in rats (Bermudez-Siva *et al.*, 2006).

## 1.4 Cannabinoids

Cannabinoids have been employed for religious ceremonies, as recreational drugs and as a medicine for thousands of years (Pacher *et al.*, 2006). Indeed, *Cannabis* plants are cultivated throughout the world. One of these plants is *Cannabis sativa* or hashish, known as marijuana. Marijuana use as medicine dates back to 2737 B.C; it was used for asthma, gynaecological disorders and migraines (Baker *et al.*, 2003; Kumar *et al.*, 2001; Lemberger, 1980).

At the end of the 19$^{th}$ century, cannabinol was first isolated as a phytocannabinoid and its chemical structure was identified in 1940. Later, $\Delta^9$-tetrahydrocannabinol (THC), a major constituent of *Cannabis* and the principal psychoactive phytocannabinoid, was isolated in 1964 (Gaoni Y, 1964) (Figure 1-6).

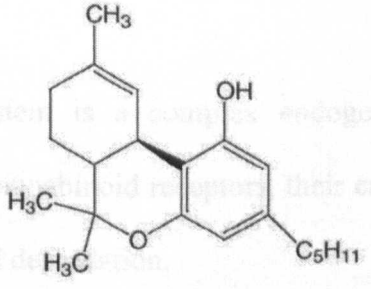


Figure 1-6: Chemical structure of THC.

Growing research in this field suggests medical benefits from exposure to THC; for example, appetite stimulation, anti-spasmodic activity, anti-nausea and analgesia. However, medical use has been limited since cannabis has psychological and physiological effects such as sedation, cognitive dysfunction, tachycardia and hypotension (Felder *et al.*, 2006).

25 years after the identification of THC, the first cannabinoid receptor was identified in rat brain (Devane *et al.*, 1988), and the $CB_1$ receptor was cloned in 1990 (Matsuda *et al.*, 1990). Consequently, this opened the way for researchers to detect the major endogenous cannabinoids (Devane *et al.*, 1988; Howlett *et al.*, 2002; Mechoulam *et al.*, 1995; Sugiura *et al.*, 1995) and to clone the $CB_2$ receptor in 1993 (Munro *et al.*, 1993).

The cannabinoid system was investigated for its actions in alteration of mood, feeding behaviour, vasorelatory effects, pain perception and regulation of metabolic factors in peripheral tissues (Randall *et al.*, 1996; Stein *et al.*, 1996). Indeed, the discovery of a selective $CB_1$ receptor antagonist (Perio *et al.*, 1996; Rinaldi-Carmona *et al.*, 1994) was notable for an influence on body metabolism. One of these $CB_1$ receptor antagonists is rimonabant (Acomplia) which was synthesized by Sanofi Recherche in France.

## 1.5 The endocannabinoid system

The endocannabinoid system is a complex endogenous signalling system, which consists of (at least) two cannabinoid receptors, their endogenous ligands, and enzymes for ligand biosynthesis and degradation.

### 1.5.1 $CB_1$ and $CB_2$ receptors

The $CB_1$ receptor is the major receptor responsible for the effects of the endocannabinoid system in metabolic functions. $CB_1$ receptors are the most common GPCRs expressed in the brain (Tsou *et al.*, 1998), but are also expressed in peripheral tissues such as adipose, liver, pancreas and skeletal muscle (Izzo *et al.*, 2010; Starowicz

*et al.*, 2008). On the other hand, $CB_2$ receptors were found to be predominantly abundant in immune system. Indeed, $CB_2$ receptors were expressed within the spleen, tonsils, and thymus (Brown *et al.*, 2002; Klein *et al.*, 2003; Liu *et al.*, 2009).

The $CB_1$ receptor is highly conserved among human, rat and mouse while the $CB_2$ is more diverse. The sequence analysis of rat $CB_1$ has 99.8% amino acid identity compared to mouse and 97% compared to human (Chakrabarti *et al.*, 1995). The sequence analysis of rat $CB_2$ has 93% amino acid identity compared to mouse and 81% compared to human (Griffin *et al.*, 2000; Reggio, 2003; Shire *et al.*, 1996). The homology between $CB_1$ and $CB_2$ is poor since they share only 44% amino acid identity. (Klein *et al.*, 1998; Munro *et al.*, 1993) (Figure 1-7).

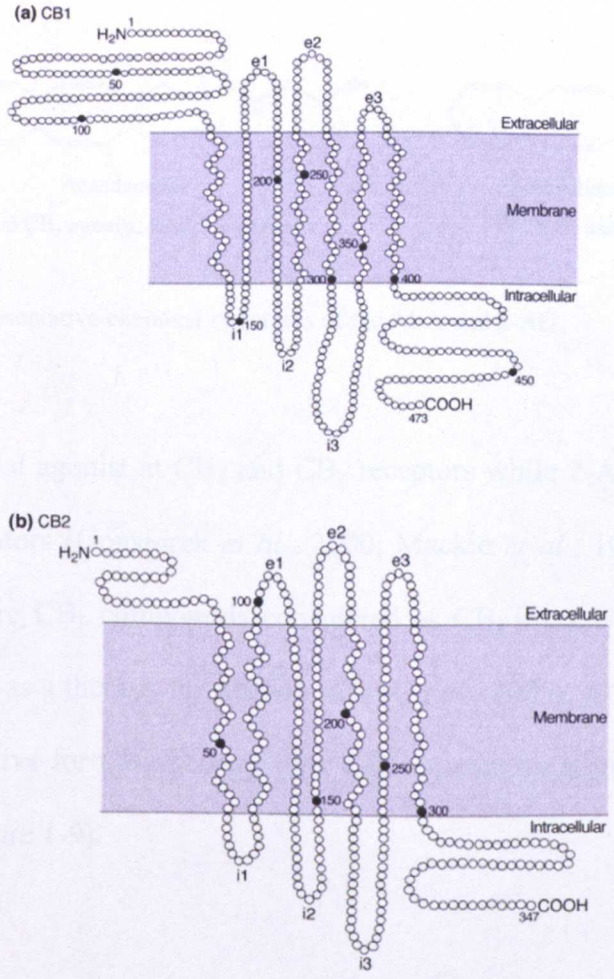


Figure 1-7: Representative structure of mouse cannabinoid receptors (Klein *et al.*, 1998).

## 1.5.2 Agonists and antagonists for $CB_1$ receptor

There are diverse groups of ligands for cannabinoid receptors including natural (herbal), synthetic, and endogenous compounds (Di Marzo *et al.*, 2006). The two major endocannabinoids are anandamide (AEA) and 2-arachidonoyl glycerol (2-AG), where AEA is an amide while 2-AG is an ester of arachidonic acid (Figure 1-8).

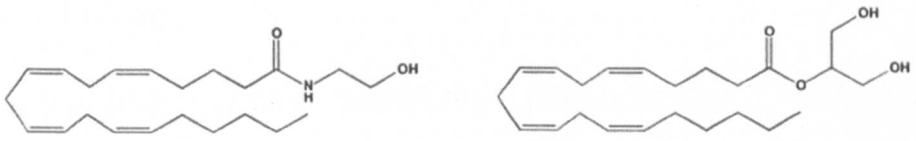

Anandamide

Partial $CB_1$ agonist, weak $CB_2$ agonist

2-Arachidonoyl-glycerol

Full $CB_1$ and $CB_2$ agonist

Figure 1-8: Representative chemical structures of the AEA and 2-AG.

AEA is a partial agonist at $CB_1$ and $CB_2$ receptors while 2-AG is a full agonist at $CB_1$ and $CB_2$ receptors (Gonsiorek *et al.*, 2000; Mackie *et al.*, 1993). Rimonabant (RIM) and AM251 are $CB_1$ compounds considered as $CB_1$ inverse agonists and antagonists. RIM was used as a therapy for obesity (Carai *et al.*, 2005). ACEA is a synthetic agonist which is selective for $CB_1$ receptor over $CB_2$ receptor by around 2000 times (Hillard *et al.*, 1999) (Figure 1-9).

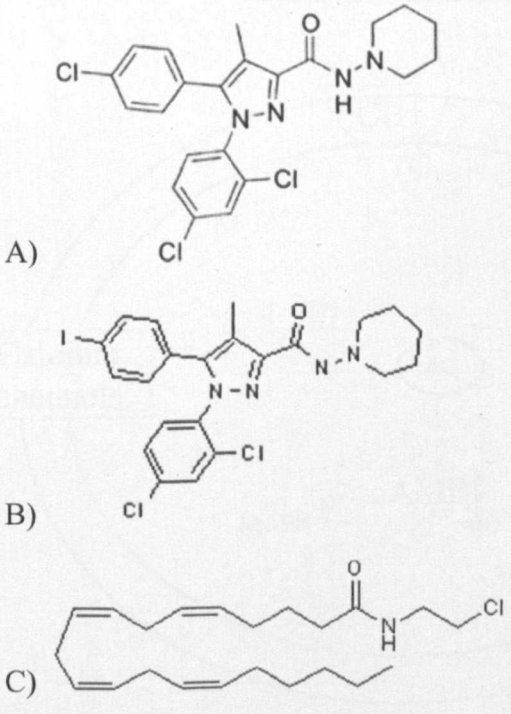

Figure 1-9: Structures of A) RIM, B) AM251 and C) ACEA.

### 1.5.3 $CB_1$ signalling

$CB_1$ receptor signalling is mediated through the G proteins of the $G_{i/o}$ family (Munro *et al.*, 1993). Indeed, the effect of activation of $CB_1$ receptor was inhibited by pertussis toxin (Felder *et al.*, 1998). $G_{i/o}$, in turn, inhibits adenylyl cyclase and consequently, inhibits cAMP accumulation. $G_{i/o}$ can directly regulate ion channels, inhibiting calcium channels (Caulfield *et al.*, 1992; Gebremedhin *et al.*, 1999; Mackie *et al.*, 1993) and activating potassium channels (Mackie *et al.*, 1995; McAllister *et al.*, 1999; Turu *et al.*). Activation of $CB_1$ receptor leads to phosphorylation of MAPK (Bosier *et al.*, 2010). A number of mechanisms may be involved in activation of MAPK such as activation of $G_{i/o}$ proteins, modulation with other GPCRs, insulin and growth factor receptors (Figure 1-10).

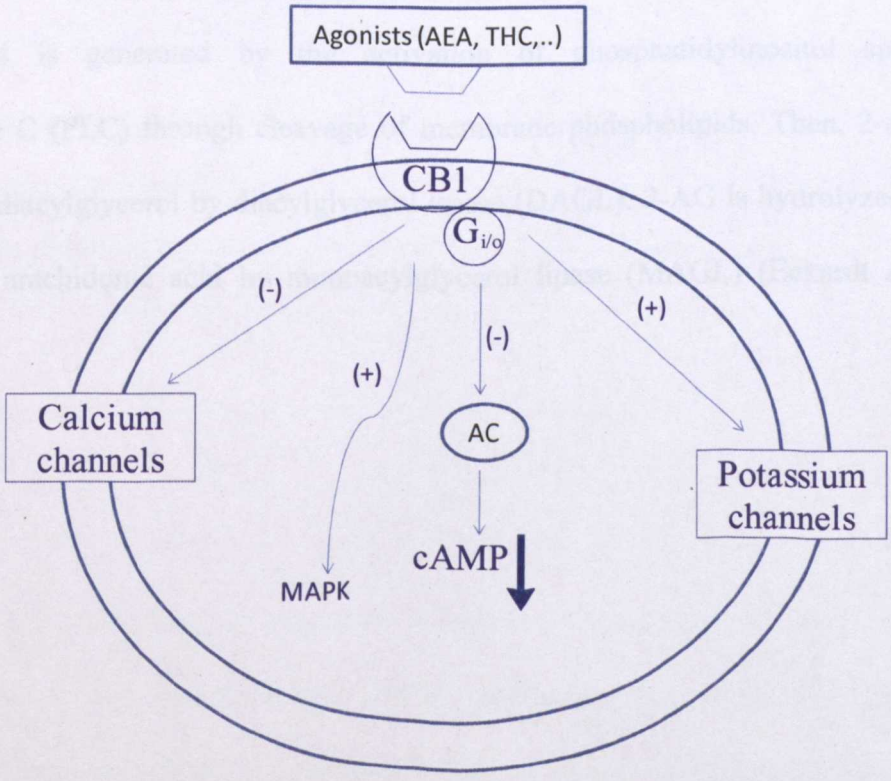


Figure 1-10: Main effects of $CB_1$ receptor on signal transduction pathways, adapted from (Pagotto *et al.*, 2006). $CB_1$ receptors couple through $G_{i/o}$ proteins which inhibit adenylate cyclase mediated conversion of ATP to cAMP, modulate Ca and K channels and activate MAPK.

### 1.5.4 Endocannabinoid synthesis and degradation

AEA and 2-AG were found to be derived from phospholipid in the cellular membranes incorporating long-chain polyunsaturated fatty acids (Fowler *et al.*, 2002). However, the exact mechanisms for cannabinoid synthesis have not yet been determined. One proposed mechanism is that AEA is synthesized from *N*-arachidonoyl-phosphatidylethanolamine (NAPE) which is enzymatically converted to AEA and phosphatidic acid by a specific phospholipase D, NAPE-PLD (Cadas *et al.*, 1996). The production of AEA is a calcium-dependent process (Di Marzo *et al.*, 1994; Mackie *et al.*, 2006). Once produced, AEA may be hydrolyzed into ethanolamine and arachidonic acid by fatty acid amide hydrolase (FAAH) (Eckardt *et al.*, 2008a). The production of 2-AG is also a calcium-dependent mechanism (Bisogno *et al.*, 1997; Di Marzo *et al.*, 1996). Diacylglycerol is generated by the activation of phosphatidylinositol specific phospholipase C (PLC) through cleavage of membrane phospholipids. Then, 2-AG is formed from diacylglycerol by diacylglycerol lipase (DAGL). 2-AG is hydrolyzed into glycerol and arachidonic acid by monoacylglycerol lipase (MAGL) (Eckardt *et al.*, 2008a).

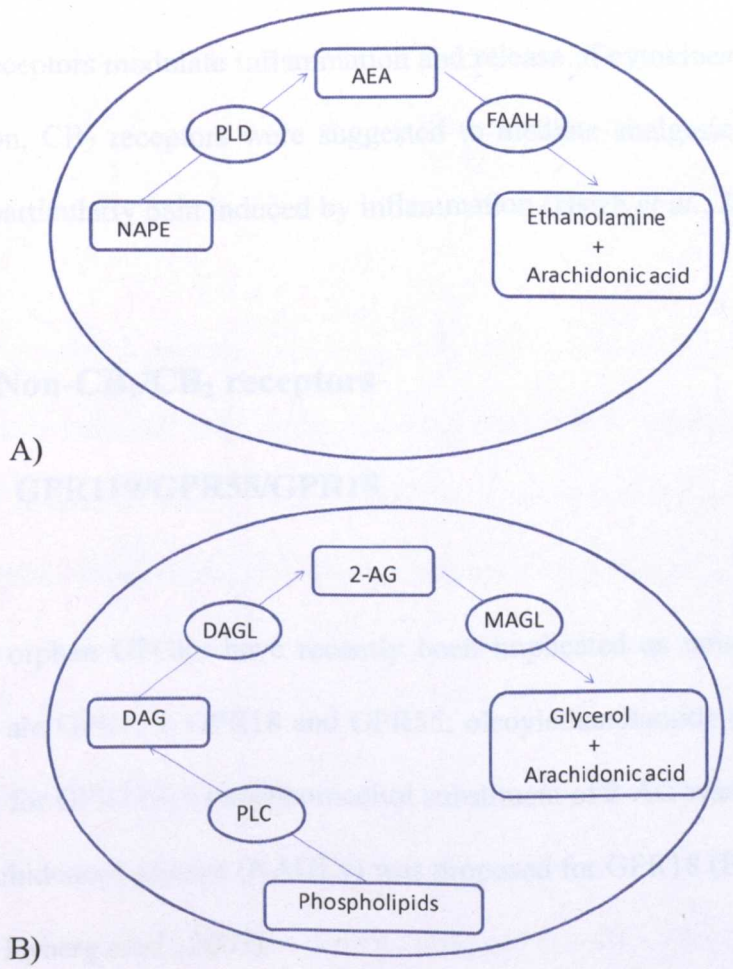


Figure 1-11: Representative biosynthesis and degradation pathways of AEA and 2-AG. A) AEA and B) 2-AG. N-arachidonoyl-phosphotidylethanolamine (NAPE), phospholipase D (PLD), fatty acid amide hydrolase (FAAH), phospholipase C (PLC), diacylglycerol lipase (DAGL) and monoacylglycerol lipase (MAGL), adapted from (Eckardt *et al.*, 2008a).

### 1.5.5 $CB_2$ receptors

$CB_2$ receptors are predominantly expressed in immune tissues and cells such as the spleen, thymus, monocytes, neutrophils, and B-lymphocytes (Liu *et al.*, 2009). $CB_2$ receptors were found recently to be expressed in brain also, in the brainstem, cerebellum, thalamic nuclei and cerebral cortex (Suarez *et al.*, 2009). Generally, the expression of $CB_2$ receptors in peripheral tissues such as adipose tissue, liver, pancreas and skeletal muscle is still under investigation.

$CB_2$ receptors modulate inflammation and release of cytokines (Pandey *et al.*, 2009). In addition, $CB_2$ receptors were suggested to mediate analgesic activity for neuropathic pain, particularly pain induced by inflammation (Hsieh *et al.*, 2011).

## 1.6 Non-$CB_1$/$CB_2$ receptors

### 1.6.1 GPR119/GPR55/GPR18

Three orphan GPCRs have recently been implicated as novel cannabinoid receptors. These are GPR119, GPR18 and GPR55; oleoylethanolamide (OEA) was proposed as a ligand for GPR119, a phosphoinositol substituent of 2-AG was proposed for GPR55 and N-arachidonoyl glycine (NAGLy) was proposed for GPR18 (Brown, 2007; Kohno *et al.*, 2006; Ryberg *et al.*, 2007).

There is a suggestion that AM251 or RIM, $CB_1$ antagonists, are GPR55 agonists (Kapur *et al.*, 2009; Oka *et al.*, 2009; Waldeck-Weiermair *et al.*, 2008; Yin *et al.*, 2009), although it is still controversial whether GPR55 is a true cannabinoid receptor (Oka *et al.*, 2007). GPR55 shares less than 15% sequence homology with $CB_1$ and $CB_2$ (Ross, 2003) and is expressed in adrenal glands, brain, small intestine (Lauckner *et al.*, 2008; Ryberg *et al.*, 2007; Sawzdargo *et al.*, 1999; Waldeck-Weiermair *et al.*, 2008; Whyte *et al.*, 2009).

GPR119, an oleoyl congener receptor, might be considered as free fatty acid (FFA) receptor or novel cannabinoid receptor since its natural ligands are fatty acid (FA) derivatives (Overton *et al.*, 2006). Of these, OEA, an analogue of the cannabinoid AEA, is one of the most active natural ligands. OEA is of particular interest since it was

observed to reduce food intake and body weight gain in rodents (Overton *et al.*, 2008). Since GPR119 is activated by OEA (Overton *et al.*, 2006), it has been suggested to play a role in obesity (Overton *et al.*, 2006).

GPR119 mRNA appears to be expressed only in a limited number of tissues, including pancreatic cells and enteroendocrine cells in the small intestine in man and rodent using RT-PCR (Lauffer *et al.*, 2009). GPR119 may raise intracellular cAMP concentrations in pancreatic β-cells through a $G_s$ mechanism (Overton *et al.*, 2008). GPR119 mRNA is also expressed in skeletal muscle from both rat and human (Soga *et al.*, 2005).

GPR18 mRNA was primarily found in leukocytes, thymus, spleen and testis (Alexander, 2012; Gantz *et al.*, 1997). AEA and THC were also reported as full agonists at GPR18 (McHugh *et al.*, 2012). Indeed, data suggested that GPR18 is a $G_i$ mechanism (Kohno *et al.*, 2006). However, the physiological role of GPR18 is still unknown.

### 1.6.2 PPARs

Recent studies indicate that cannabinoids act at a family of nuclear receptors called peroxisome proliferator-activated receptors (PPARs, with three sub-types α, β and γ). This family, which functions as transcription factors, is involved in lipid metabolism, inflammation and regulation of metabolism (Michalik *et al.*, 2006; O'Sullivan, 2007).

The endocannabinoids and related endogenous molecules such as AEA and OEA were shown to activate PPARα (Lo Verme *et al.*, 2005; Sun *et al.*, 2007). Briefly, the activation of PPARα induces the expression of genes required for the transport and β-oxidation of fatty acids in skeletal muscle (Ferre, 2004; Zhang *et al.*, 2004).

## 1.7 The endocannabinoid system effects

### 1.7.1 Central control of metabolic regulation

The $CB_1$ receptor was originally located in the central nervous system. The main role of endocannabinoids in brain is that they act as retrograde messengers (Maejima *et al.*, 2001), predominantly at GABAergic or glutamatergic synapses, although their retrograde signalling can inhibit the release of multiple neurotransmitters including serotonin, acetylcholine and neuropeptides (Maejima *et al.*, 2001; Straiker *et al.*, 2006). The physiological effects of endocannabinoids in the brain are to increase appetite and feeding, anxiety, neuroexcitability and pain perception (Bellocchio *et al.*, 2008; Di Marzo *et al.*, 2005) (Figure 1-12).

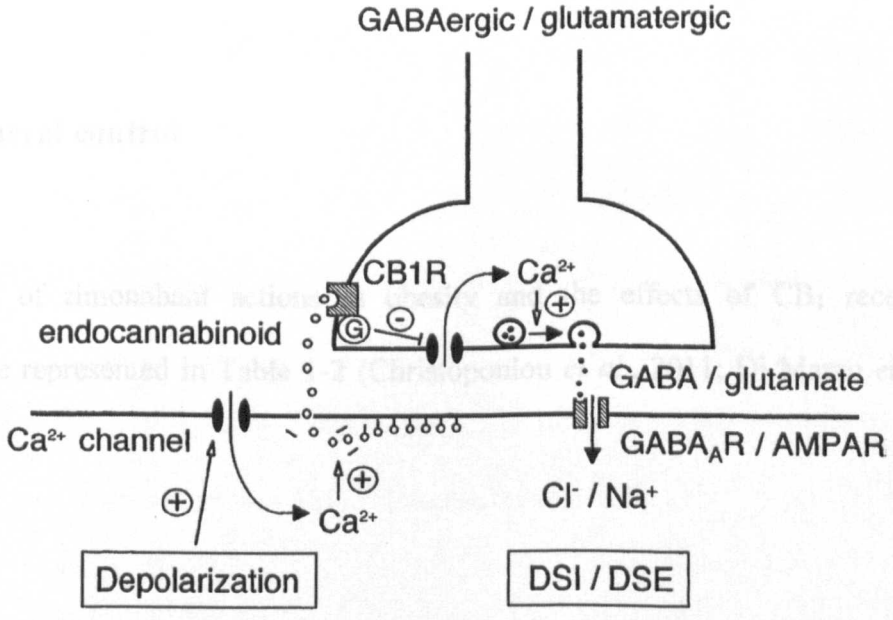


Figure 1-12: Representative retrograde inhibition of presynaptic neurotransmitter release by the cannabinoid system (Maejima *et al.*, 2001). Depolarization-induced suppression of inhibition (DSI) and depolarization-induced suppression of excitation (DSE).

The excitation of the neuron leads to depolarization and an influx of calcium ions. Then, postsynaptic calcium can activate enzymes that are responsible for endocannabinoid synthesis from lipid precursors in the postsynaptic cell. After that, endocannabinoids can leave the postsynaptic cell and bind to cannabinoid receptors on the presynaptic membrane of the neurons leading to an inhibition of presynaptic calcium influx (Christie *et al.*, 2001; Wilson *et al.*, 2002).

Endocannabinoids (ECs) are produced on demand (Hashimotodani *et al.*, 2007). They are highly lipophilic compounds and are not stored in vesicles for secretion. Originally, $CB_1$ antagonism was found to mediate a central hypophagic effect leading to weight loss (Di Marzo *et al.*, 2001; Vickers *et al.*, 2003). Furthermore, $CB_1$ knock-out mice were found to be resistant to diet-induced obesity (Osei-Hyiaman *et al.*, 2005; Ravinet Trillou *et al.*, 2004).

### 1.7.2 Peripheral control

The summary of rimonabant actions in obesity and the effects of $CB_1$ receptor activation were represented in Table 1-2 (Christopoulou *et al.*, 2011; Di Marzo *et al.*, 2005).

Table 1-2: Tissue-specific effects of RIM in obesity.

| Tissue | Mechanism |
|---|---|
| Hypothalamus | Decrease Appetite |
| Nucleus accumbens | Decrease Motivation to Eat |
| Skeletal Muscle | Increase Glucose Uptake |
| Adipose Tissue | Decrease adipogenesis |
| Liver | Decrease Lipogenesis |
| GI Tract | Increase Satiety signals and gastric emptying |

As previously stated, the skeletal muscle is the primary tissue for glucose uptake. $CB_1$ receptor mRNA and protein expression has been detected in skeletal muscle myotubes and tissues of rodents and humans (Cavuoto *et al.*, 2007b; Pagotto *et al.*, 2006). In addition, in mice fed a high fat diet (HFD), the expression of $CB_1$ in skeletal muscle was found to be up-regulated (Pagotto *et al.*, 2006). Chronic $CB_1$ receptor antagonism during euglycemic hyperinsulinemic clamp increased glucose uptake in diet-induced obese rats by several skeletal muscle groups (Nogueiras *et al.*, 2008).

Adipose tissue is a highly metabolically active tissue. mRNA expression of $CB_1$ receptors in rodent adipose tissues using RT-PCR (Cota *et al.*, 2003) and human adipose tissues using western blot (Roche *et al.*, 2006; Spoto *et al.*, 2006) have been described. It is worth mentioning that the expression of $CB_1$ in adipose tissue was up-regulated in rodent models of obesity (Bensaid *et al.*, 2003; Starowicz *et al.*, 2008; Yan *et al.*, 2007).

There is a strong indication that endocannabinoid system is present in the liver, specifically using mouse liver and *in situ* hybridization (Osei-Hyiaman *et al.*, 2005). The $CB_1$ receptor appears to influence the disease state of liver and whole body parameters as well. For example, treatment of obese (fa/fa) rats administered orally with 30 mg/kg RIM daily for 8 weeks was found to abolish hepatic steatosis. In parallel, it was also found to decrease total cholesterol, free fatty acids, and plasma levels of triglycerides and increase the high/low-density lipoprotein cholesterol (HDLc/LDLc) ratio (Gary-Bobo *et al.*, 2007).

There is conflicting data about the expression of $CB_1$ and $CB_2$ receptors in the pancreas (Starowicz *et al.*, 2008). $CB_1$ receptor mRNA expression was detected in pancreatic human islets (Bermudez-Silva *et al.*, 2008). However, further investigations found that $CB_1$ receptors were expressed in glucagon- and somatostatin-secreting α- and δ-cells and $CB_2$ receptor, not $CB_1$ receptor, was found to be colocalized in insulin-secreting β-cells and non β-cells from mouse using QRT-PCR and immunocytochemistry (Bermudez-Silva *et al.*, 2008; Juan-Pico *et al.*, 2006; Starowicz *et al.*, 2008; Tharp *et al.*, 2008).

Vagal $CB_1$ expression was found to be inhibited by gut peptides such as cholecystokinin (Burdyga *et al.*, 2004). Regarding $CB_1$ functions, activation of $CB_1$ receptor leads to reduce gastrointestinal motility in both rodents and humans (Coutts *et al.*, 1998; Esfandyari *et al.*, 2006; Izzo *et al.*, 1999). Furthermore, activation of $CB_1$ receptor decreases the rates of gastric emptying for HFD fed Mice (Di Marzo *et al.*, 2008).

These data suggest that the endocannabinoid system can at least play a role regarding glucose transport in skeletal muscle and abdominal obesity in adipose tissue and affect

whole body metabolic parameters in the liver (Mallat *et al.*, 2011).

## 1.8 Endocannabinoid system in obesity

AEA was found to increase food intake in rats, while the $CB_1$ antagonist RIM was found to inhibit food intake (Williams *et al.*, 1999). A key component in the development of diet-induced obesity for the effect of cannabinoids was found to be $CB_1$ receptor stimulation (Ravinet Trillou *et al.*, 2004). $CB_1$ receptors were found also to be involved in peripheral metabolic regulation.

There are several findings which support the belief that endocannabinoids might contribute to the development of obesity. First of all, a higher $CB_1$ receptor expression was shown in adipocytes of obese rats and elevated levels of endocannabinoids were found in animal models of diet-induced obesity (Bluher *et al.*, 2006). Secondly, $CB_1$ receptor knockout mice were resistant to diet-induced obesity (Ravinet Trillou *et al.*, 2004). Thirdly, obese rodents compared to lean controls were found to be more sensitive to the anti-obesity effects of treatment with $CB_1$ receptor antagonists (Hildebrandt *et al.*, 2003). Fourthly, FAAH activity in subcutaneous adipocytes was found be positively correlated with BMI in metabolically healthy humans (Cable *et al.*, 2011).

Finally, endocannabinoid levels were found to be higher in several organs of obese animals, central and peripheral (Di Marzo *et al.*, 2001; Starowicz *et al.*, 2008). This was also found in the circulation of obese human subjects (Engeli, 2008). 2-AG plasma concentration was found to be correlated with visceral adipose tissue mass (intra-

abdominal obesity) and markers of metabolic syndrome (FFA, TG, cholesterol and adiponectin) (Engeli, 2008).

## 1.9 Possible targets for $CB_1$ receptor

### 1.9.1 AKT

#### 1.9.1.1 Definition and structure

AKT is a family of serine/threonine-specific protein kinases. The AKT family comprises three different isoforms: AKT1 (also called PKB-alpha (PKBα)), AKT2 (PKB-beta (PKBβ)) and AKT3 (PKB-gamma (PKBγ)) (Manning *et al.*, 2007).

AKT isoforms are members of the AGC kinase family, which have extensive homology to protein kinases A, G, and C within their kinase domains. Although these AKT isoforms are coded by three different genes, those proteins are highly homologous, sharing a common structure which consists of an N-terminal regulatory domain (pleckstrin homology (PH) domain), a catalytic kinase domain, and a C-terminal region (Kumar *et al.*, 2005).

#### 1.9.1.2 AKT expression

AKT1 is more ubiquitously expressed, compared to AKT2 and AKT3; however, AKT2 is predominantly expressed in insulin-responsive tissues, such as skeletal muscle, adipose tissue and liver (Masure *et al.*, 1999) and AKT3 is expressed primarily in brain, lung, kidney and placenta (Masure *et al.*, 1999). Therefore, the main AKT isoforms which are expressed in the skeletal muscle are AKT1 and AKT2 (Cleasby *et al.*, 2007).

### 1.9.1.3 AKT targets

AKT2 activation leads to glucose transporter type 4 (GLUT4) translocation to the plasma membrane. GLUT4 translocation leads to increased glucose uptake in response to insulin (Calera *et al.*, 1998). However, the mechanism behind this process is still under investigation. AKT may play a role in glucose and lipid metabolism. In addition, AKT was shown to stimulate the association of hexokinase isoforms with the mitochondria. Hexokinases convert glucose to its active form, glucose 6-phosphate. However, the direct target of AKT responsible for this process is still under investigation (Majewski *et al.*, 2004). Furthermore, AKT mediates phosphorylation of the enzyme glycogen synthase kinase 3 (GSK-3) isoforms on a highly conserved N-terminal regulatory site (GSK-3α-S21, GSK-3β-S9). This inactivates GSK-3, thereby diminishing the repression of glycogen synthase (GS), which in turn results in stimulating glycogen synthesis (Brozinick *et al.*, 2003). GSK-3 was shown to induce degradation of the sterol regulatory element-binding proteins (SREBPs). SREBPs are transcription factors that switch on the expression of genes involved in cholesterol and fatty acid biosynthesis. AKT inactivates GSK-3 and helps SREBP stability and, thus, increases lipid production (Manning *et al.*, 2007).

AKT also regulates the expression of gluconeogenic and lipogenic enzymes by direct phosphorylation of S570 on peroxisome proliferator-activated receptor-γ coactivator-1α (PGC-1α) which is a coactivator that can control genes with several members of the forkhead box (FOXO) family of transcription factors. For example, FOXO1 promotes hepatic glucose production (Matsumoto *et al.*, 2007).

### 1.9.2 GSK-3

#### 1.9.2.1 Isoforms

Glycogen synthase kinase-3 (GSK-3) is a serine/threonine protein kinase. There are two GSK-3 isoforms (GSK-3α and GSK-3β) encoded by two distinct genes. GSK-3α has a molecular weight of 51 kDa and GSK-3β has a molecular weight of 47 kDa (Ciaraldi *et al.*, 2007; Woodgett, 1990).

#### 1.9.2.2 Signalling and importance

Insulin leads to phosphorylation of AKT. Consequently, AKT phosphorylates GSK-3 and inactivates it. However, GSK-3 inhibits IRS1 protein through phosphorylation. This leads to attenuated insulin signalling (Eldar-Finkelman, 2002). GSK-3 also diminished the repression of glycogen synthase through phosphorylation (Cross *et al.*, 1995). GSK-3 has been implicated in many disorders, such as cancer and diabetes (Eldar-Finkelman, 2002; Martinez *et al.*, 2002).

### 1.9.3 AMPK

#### 1.9.3.1 AMPK Structure and their functions

AMP-activated protein kinase (AMPK) is an αβγ heterotrimeric serine/threonine protein kinase composed of a catalytic ($\alpha_1$ or $\alpha_2$) subunit and regulatory ($\beta_1$ or $\beta_2$ and $\gamma_1$, $\gamma_2$ or $\gamma_3$) subunits encoded by different genes (Hardie, 2004). AMPK is a prime target of metabolic diseases such as type 2 diabetes, and the AMPK activator AICAR (5-amino-1-β-D-ribofuranosyl-imidazole-4-carboxamide) reverses many of the metabolic defects

in mouse models of obesity and insulin resistance (Fogarty *et al.*, 2010). The activation of AMPK can lead to an increase of fatty acid oxidation and glucose uptake into muscle, also increasing fatty acid oxidation, decreasing lipogenesis, cholesterol synthesis and gluconeogenesis in the liver. In addition, it also decreases lipolysis in adipose tissue. Furthermore, the activation of AMPK can lead to an increase in mitochondrial biogenesis (Gruzman *et al.*, 2009).

### 1.9.3.2 Functions in skeletal muscle

Activation of AMPK by AICAR in skeletal muscle enhances glucose uptake. In the rat skeletal muscle, AMPK activators including AICAR, were found to increase cell surface GLUT4 levels (Jessen *et al.*, 2003; Ju *et al.*, 2007).

Currently, there is evidence that AMPK activation stimulated glucose uptake in both contraction and hypoxia (Jessen *et al.*, 2005; Wright *et al.*, 2005). Acute muscle AMPK activation induces fatty acid oxidation by decreasing malonyl-CoA concentrations through phosphorylation and inhibition of acetyl-CoA carboxylase (ACC) and activation of malonyl-CoA decarboxylase (MCD). Malonyl-CoA is an inhibitor of carnitine palmitoyl transferase 1 (CPT1), the rate-limiting enzyme that transports long-chain fatty acids into mitochondria for β-oxidation. This effect leads to decreased lipid accumulation and increased muscle insulin sensitivity (Hardie *et al.*, 1997a; Hardie *et al.*, 1997b; Zhou *et al.*, 2009). Chronic AMPK activation by AICAR increases GLUT4, hexokinase activity and glycogen content, (Holmes *et al.*, 1999), as well as also increasing the levels of uncoupling protein 3 (UCP3) and PGC-1α in skeletal muscle (Jager *et al.*, 2007).

### 1.9.3.3 Mechanism of action for pharmacological AMPK activators

AICAR is a precursor for the monophosphorylated derivative 5-amino-1-β-D-ribofuranosyl-imidazole-4-carboxamide (ZMP), which mimics the effects of AMP for activation of AMPK. Consequently, ZMP causes allosteric activation and promotes the phosphorylation of AMPK by upstream kinases (Corton *et al.*, 1995) (Figure 1-4).

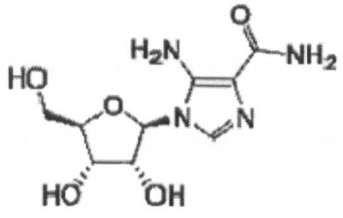


Figure 1-13: AICAR, a synthetic nucleotide analogue.

Metformin is a drug used for treatment of type 2 diabetes, where AMPK is a candidate target (Zhou *et al.*, 2001).

## 1.9.4 MAPKs

### 1.9.4.1 Definition, function and families

Mitogen-activated protein kinases (MAPKs) are serine/threonine protein kinases that regulate cellular activities including gene expression, cell proliferation, mitosis, differentiation, metabolism and programmed cell death. MAPK are divided into subfamilies which have several isoforms: extracellular signal-regulated kinase; ERK (ERK1 to ERK8), p38 (p38-α, -β, -γ), and c-Jun $NH_2$-terminal kinase; JNK (JNK1 to JNK3). MAPKs are targets of a phosphorylation cascade, composed of at least three components of kinases, including a MAPK kinase kinase (MAP3K), a MAPK kinase

(MAP2K), and a MAPK. These kinases are activated in series such that MAP3Ks (MAPK kinase kinase) phosphorylate and activate MAP2Ks (MAPK kinase). Consequently, MAP2Ks phosphorylate and activate MAPKs (Pearson *et al.*, 2001).

### 1.9.4.2 Structure of ERK1/2

ERK1 and ERK2 are a 43 and 41 kDa protein, respectively. Thr 183 and Tyr 185 residues on ERK1/2 are phosphorylated by the MAP2Ks MAPK/ERK kinase 1/2 (MEK1/2) (Pimienta *et al.*, 2007; Zhang *et al.*, 1994).

### 1.9.4.3 Pathways

The MAPK/ERK cascade starts when a variety of extracellular agents such as growth factors, hormones, and neurotransmitters bind to receptors on the cell surface. The best example for a description of the ERK pathway is the response after activation of tyrosine kinase family receptors.

As described above for the insulin receptors, signal transduction is initiated by ligand binding to the tyrosine kinase receptors, leading to phosphorylation of intracellular tyrosine residues, leading to recruitment of the Grb2-Sos complex which stimulates the GTPase Ras to exchange GDP for GTP, leading to activation of the Raf pathway. Raf kinase activates a series of three MAPK kinases, MAP kinase kinase (MEK) then phosphorylates ERK1/2 at both threonine and tyrosine residues (Force *et al.*, 1998; Katz *et al.*, 2007).

GPCR activation of ERK1/2 is complex, but can involve second messenger-dependent protein kinases (i.e. PKA and PKC). PKA activates the small GTPase, Rap1. Rap1 then interacts with B-Raf. Activated B-Raf then stimulates ERK. PKC directly phosphorylates Raf-1, and then Raf-1 can activate ERK (Force *et al.*, 1998; Katz *et al.*, 2007).

Another mechanism of GPCR activation of ERK1/2 is β-arrestin mediation. The phosphorylation of GPCR, in particular cytoplasmic serine and threonine residues, increases its affinity and binding to β-arrestin (Tobin, 2008). β-arrestin then act as scaffolding partner or adaptor protein which facilitates its coupling to alternative downstream signaling pathway such as MAPKs (JNK, ERK1/2 and p38) or facilitates its binding to endocytic proteins such as clathrin and adapter protein 2 (AP2) for endocytosis (Shenoy *et al.*, 2006; Shenoy *et al.*, 2003). The latter binding leads to internalization of GPCR as a mechanism of desensitization (Shenoy *et al.*, 2006; Shenoy *et al.*, 2003). Indeed, the MAPK is established to have roles in differentiation, proliferation and growth, although such roles are not yet described in skeletal muscle.

## 1.10 Aim of thesis

The field of pharmacogenomics has developed to investigate the questions surrounding the mRNA expression of genes, how a drug works and how a drug response may contribute to dissolve diseases or condition states. Experimental observation of GPCR gene expression and signalling pathway analysis offers a powerful way of understanding the presence of genes and how these genes affect function.

The aim of this thesis is to investigate GPCR gene expression and down-stream signalling, focussing on $CB_1$ receptors. The major themes of this thesis are;

1. To detect GPCR expression in skeletal muscle and their cognate down-stream signalling genes.
2. To investigate the signalling associated with these receptors, particularly $CB_1$ receptors, in rat primary skeletal muscle cells.
3. To examine cross-talk between cannabinoid and insulin signalling systems.
4. To examine the functionality of $CB_1$ receptor in rat primary skeletal muscle.

# Chapter 2

# Materials & Methods

# 2 Chapter Two: Materials and Methods

## 2.1 Reagents

ACEA, AEA, AM251 and AICAR were purchased from Tocris Company. Rimonabant was taken from the NIMH chemical Synthesis and Drug Supply Program. All other materials were purchased from Sigma unless otherwise mentioned.

## 2.2 Microarray

### 2.2.1 Materials

Whole genome rat 4*44K DNA microarrays were obtained from Agilent Technologies Inc. Agilent's One-Color Quick Amp Labeling kit, RNA Spike-In kit and Gene Expression Hybridization Kit were also purchased from Agilent Technologies Inc.

### 2.2.2 RNA isolation

RNA was extracted from skeletal muscle, liver, adipose tissues and primary rat skeletal muscle cells by homogenizing biopsy tissue in Trizol Reagent (2 mL for a 50 mg tissue) using the pro 200 homogenizer (Janke & Kunkel, Ultra-Turrrax T25). The samples were then incubated at room temperature for 5 minutes. 200 µl bromochloropropane (BCP) was added for each ml of Trizol Reagent used, the samples were then shaken vigorously. The homogenates were then centrifuged at 10,000 rpm (8960 g) at 4 C° for 15 minutes in a Beckman Allegra centrifuge. The upper, aqueous phase was transferred to a fresh tube. 0.7 ml isopropanol and 0.25 ml NaAcetate (2 M, pH 4) per ml of aqueous phase

were added and mixed well, and then the mixture was put in the freezer at –20 C° for one hour. The tube was then centrifuged at 10,000 rpm (8960 g) at 4 C° for 10 minutes. The supernatant was discarded and the pellet washed in 1 ml of 75% ethanol per 1 ml of Trizol Reagent. The supernatant was then discarded and the pellet left to air dry. After all the ethanol had evaporated, the pellet was dissolved in 50-100 µl RNase-free water.

### 2.2.3 RNA clean up

Cleaning up was done using the Qiagen RNeasy kit. This protocol can be used to further purify RNA. Buffer RLT (Lysis buffer) and ethanol were added to the sample to create conditions that promote selective binding of RNA to the RNeasy membrane. The sample was then applied to the RNeasy Mini spin column. Total RNA bound to the membrane. Contaminants were efficiently washed away and high-quality RNA was eluted in RNase-free water. RNA quantities and integrity values were determined using a ND-1000 Nanodrop spectrophotometer and Agilent bioanalyzer, respectively.

### 2.2.4 RNA quantity and quality

#### 2.2.4.1 Spectrophotometric detection of RNA

RNA was quantified using a spectrophotometer. The UV-absorbance at 230, 260 and 280 nm of the RNA samples was measured in a ND-1000 Nanodrop spectrophotometer. An OD260/OD280 ratio and OD260/OD230 between 1.8-2.0 were indicative of good purity RNA.

### 2.2.4.2 Agilent bioanalyzer

RNA quality is critical for microarray experiments. The integrity of the input template RNA was determined prior to labelling/amplification, using the Agilent 2100 bioanalyzer. For the assessment of total RNA quality, the Agilent bioanalyzer provides RNA Integrity Number (RIN). RIN provides a quantitative value for RNA integrity that facilitates the standardization of quality interpretation. Samples with a RIN below 7.5 were excluded from microarray experiment. Samples below this cut off point were not expected to give meaningful results (Kiewe *et al.*, 2009).

## 2.2.5 Agilent microarray

Sample preparation includes four steps: Preparing One-Color Spike-Mix; preparing labelling reaction; purifying the labelled/amplified RNA and quantifying the cRNA (Figure 2-1) and (Figure 2-2). One-Color Spike-Mix was prepared according to the protocol on Agilent One-Color RNA Spike-In Kit. The thawed Agilent One-Color Spike-Mix was heated at 37 C° for 5 minutes and vortexed again. Labelling was performed using the Agilent Gene Expression system according to protocol in Agilent Quick Amp Kit, One-Color. For the synthesis of cDNA, the low RNA input linear amplification kit (Agilent) was used to produce an initial RNA amplification of at least 100 folds. In brief, this strategy utilizes an adapter T7 primer for first-strand cDNA synthesis with MMLV reverse transcriptase, followed by in vitro transcription using T7 RNA Polymerase to simultaneously amplify target material and incorporate Cy3 labelled CTP (Perkin Elmer). The labelled/amplified RNA was then purified using Qiagen's RNeasy mini spin columns. The concentrations of cRNA (ng/μL) and cyanine 3 (pmol/μL) were measured using the NanoDrop ND-1000 spectrophotometer.

Labelling efficiency was determined using the yield and specific activity of each reaction. cRNA preparation must be repeated if the yield is less than 1.65 µg and the specific activity is less than 9.0 pmol Cy3 per µg cRNA.

Of each sample, 1.65 µg labelled cRNA was fragmented and hybridized on the Whole Rat Genome Expression Array (4x44K, Agilent). The samples were incubated at 60 C° for exactly 30 minutes in order to fragment RNA. Hybridization on microarrays slides (Agilent) was then carried out at 65 C° for 17 hours using an Agilent SureHyb chamber and an Agilent hybridization oven. Then, slides were washed in Gene Expression Wash. Afterwards, slides were dried and they were assembled into an appropriate slide holder for scanning. The TIFF images taken from the scanner were processed with Feature Extraction Software. See Appendix Section 9.1.5.

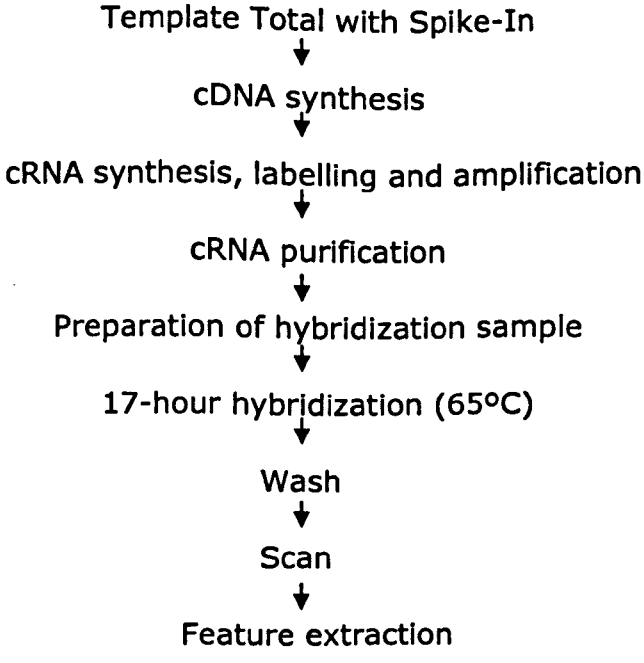


Figure 2-1: Workflow for sample preparation and array processing.

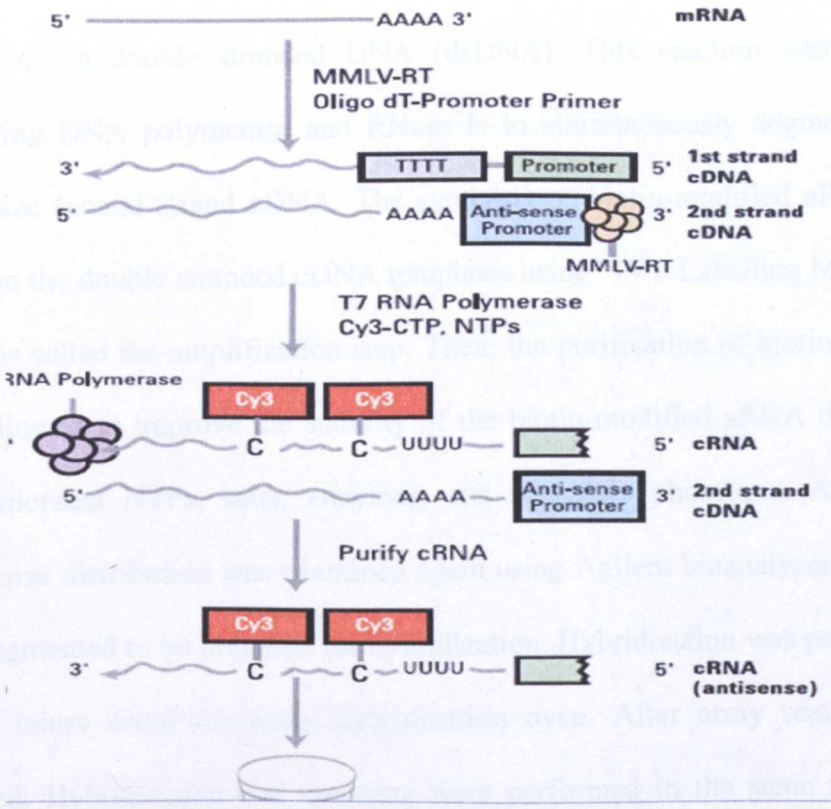


Figure 2-2: Schematic diagram of amplified and labelled cRNA procedure. Generation of cRNA for one-color microarray experiment is shown as stated in One–Color Microarray- Based Gene Expression Analysis (Quick Amp Labelling).

### 2.2.6 Affymetrix microarray

RNA was isolated from primary rat treated myotubes using the Trizol Reagent according to the manufacturer's instructions. The labelling, hybridization and scanning were performed by staff at the Nottingham Arabidopsis Stock Centre (NASC) (Figure 2-3).

Briefly, the isolated RNA was followed by purification with Qiagen RNeasy Kit. The synthesis first-strand cDNA was performed from RNA using T7 in vitro transcription technology. This technology used T7 oligo(dT) primer to synthesize cDNA. The synthesis second-strand cDNA was performed through converting the single-stranded

cDNA into a double stranded DNA (dsDNA). This reaction was carried out by employing DNA polymerase and RNase H to simultaneously degrade the RNA and synthesize second strand cDNA. The synthesis of biotin-modified aRNA was carried out from the double stranded cDNA templates using "IVT Labelling Master Mix". This step was called the amplification step. Then, the purification of biotin-modified aRNA was followed to improve the stability of the biotin-modified aRNA through removing unincorporated NTPs, salts, enzymes, and inorganic phosphate. After purification, aRNA size distribution was examined again using Agilent bioanalyzer. Labelled aRNA was fragmented to be prepared for hybridization. Hybridization was performed at 45 C° for 16 hours using the array hybridization oven. After array scanning, data were obtained. Hybridization and scanning were performed in the same instrument called GeneTitan. These data were analyzed using Affymetrix Operating Software. Finally, the output data were analyzed using the gene expression software called GeneSpring GX.

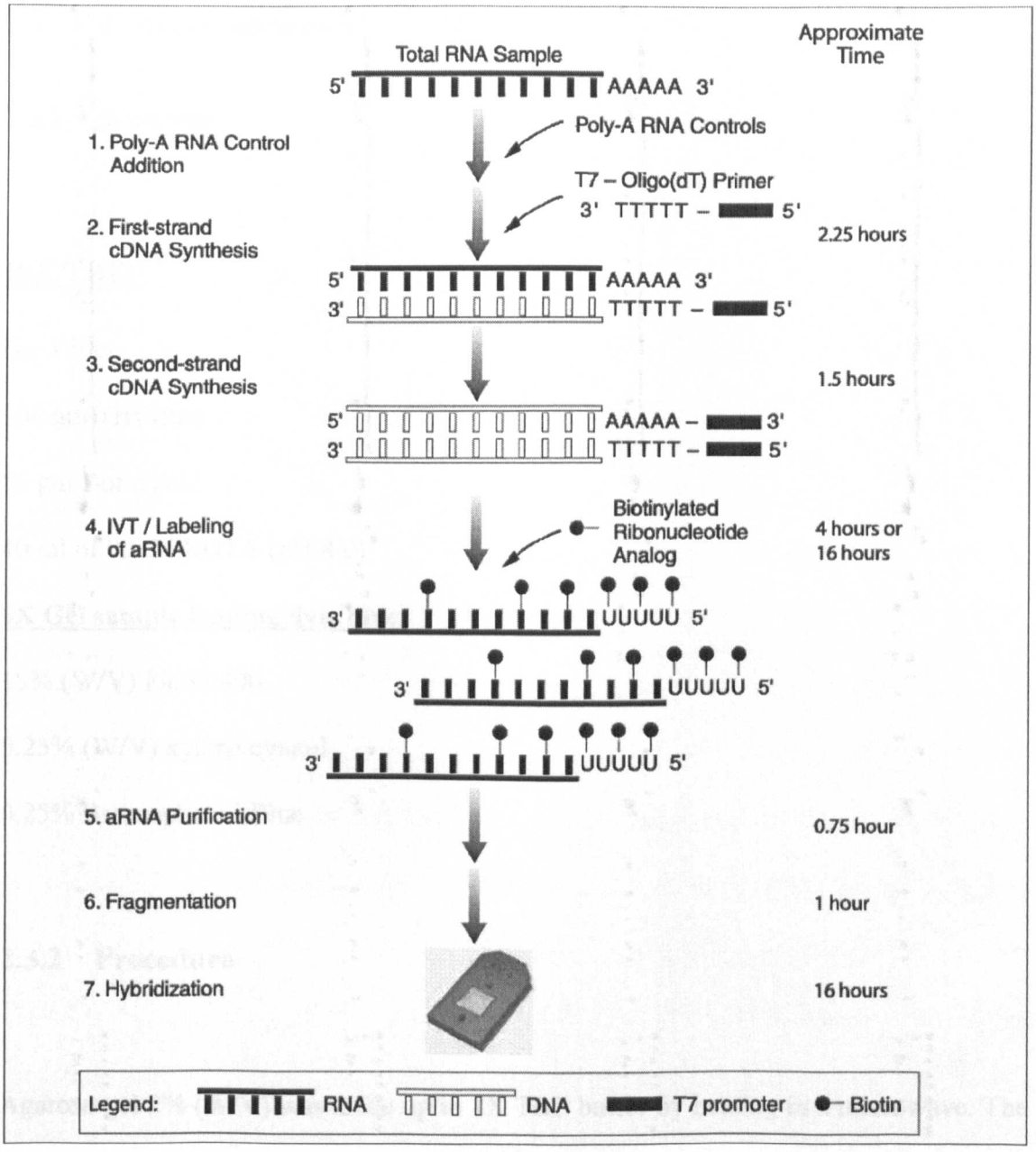


Figure 2-3: Overview of the array plate 3' IVT labelling assay, adapted from GeneChip® 3' IVT Express Kit.

## 2.3 Gel electrophoresis

### 2.3.1 Materials

**10X TBE:**

For 1 liter:

108 gm Tris Base

55 gm Boric acid

40 ml of 0.5 M EDTA (pH 8.0)

**6X Gel sample loading dye, blue:**

15% (W/V) Ficoll 400

0.25% (W/V) xylene cyanol

0.25% Bromophenol Blue

### 2.3.2 Procedure

Agarose gel 2% (W/V) was made up in 1X TBE buffer by heating in a microwave. The PCR product (10 µl of a 50 µl reaction) and 2 µl 6x loading dye were loaded onto the gel which was run for around one hour at a constant voltage of 100V. DNA marker (Fermentas; 100 bp DNA ladder) was used for determination of PCR product size. DNA was visualized and photographed with the GeneSnap programme using uv transillumination.

## 2.4 QRT-PCR (Taqman)

### 2.4.1 Materials

RNeasy Mini Total RNA Purification kits were purchased from Qiagen (West Sussex, UK). Reagents for reverse transcription of RNA to cDNA were purchased from Invitrogen (Paisley, UK). Taqman reagents were purchased from Applied Biosystems (CA, USA). Primers and probes were purchased from Eurofins MWG GmBH (Ebersberg, Germany).

### 2.4.2 First strand cDNA synthesis

Total RNA was reverse transcribed into cDNA using Superscript III First-Strand Synthesis System (Invitrogen). The following were added into 0.2 ml, RNase-free, PCR tubes: Total (500 ng) RNA, 1 µl random primers (100 ng/µl), 1 µl dNTPs (10 mM) and diethylpyrocarbonate (DEPC) water up to 13 µl. The tubes were vortexed and centrifuged briefly. Tubes were heated (MWG-Biotech Primus 96 Plus) to 65 C° for 5 minutes then placed on ice. Following brief centrifugation, master mix was prepared and added to each sample, by mixing 4 µl 5x RT buffer, 1 µl 0.1 M DTT, 1 µl RNaseOUT (40 U/µl) and 1 µl Superscript III (200 U/µl). The samples were vortexed, centrifuged and then incubated at 50 C° for 60 minutes, and the reaction was terminated at 70 C° for 15 minutes. Then, the cDNA was stored at – 20 C° until required.

### 2.4.3 Relative standard curve method QRT-PCR (Taqman)

RNA preparations and quantification: Total RNA was isolated from skeletal muscle,

liver, adipose tissues and primary rat skeletal muscle cells using Trizol (Invitrogen), and purified using RNeasy RNA clean up columns (Qiagen). RNA concentration was determined using a Nanodrop ND-1000.

RNA was reverse transcribed into cDNA using Superscript III reverse transcriptase (Invitrogen). The probes and primers were diluted to 10 mM, and 50 µl of probe and 75 µl of each primer were added to a 2.0 ml tubes. 1300 µl of Taqman Universal PCR Master Mix, Applied Biosystems (4304437), 500 µl of HPLC $H_2O$ were also added. The master mix was then vortexed and briefly centrifuged. A master mix for each target gene was produced according to the number of wells required (Table 2-1). 5 µl cDNA was pipetted into each well of the 96-well plates (StarPCR Raised Rim, Starlab), except for the NTC (no template control) where 5 µl of RNase-free $H_2O$ was used as a substitute. The Master Mix was then pipetted into each well giving a total volume of 20 µl in each well. An optical transparent adhesive film was then placed onto the plate (ABI Prism, 4311971) and a compressor pad placed on top. Quantification assays for each sample were carried out in triplicate. The mRNA levels were quantified using Real-time quantitative reverse transcriptase – polymerase chain reaction (qRT-PCR), performed in ABI StepOnePlus Real-Time PCR Systems using PCR thermal cycling programs as follows: 50 C° for 2 minutes, 95 C° for 10 minutes and 40 cycles of 95 C° for 15 seconds and 60 C° for one minute. The primers and probe were designed using Primer Express 3 software (ABI) and analyzed using Blast N (comparing the query sequence of the gene of interest with the database of sequences) to identify the query gene would be the primary target for amplification. The standard curve method was used, with slope between -3.2 and -3.6 and $R^2$ values of more than 99%, indicating that the amplification efficiency is almost 100%.

Table 2-1: PCR Master Mix components.

| | Volume per well |
|---|---|
| Taqman 2X Universal PCR Master mix | 13µl |
| Forward primer | 0.75µl |
| Reverse primer | 0.75µl |
| Probe | 0.5µl |
| HPLC Water | 5.0µl |
| Total volume | 20µl |

## 2.5 Sample preparation using Trizol reagent

### 2.5.1 Materials

Trizol reagent was purchased from Invitrogen.

### 2.5.2 Protein extraction

During RNA extraction procedure using Trizol reagent, after removing the aqueous phase, the protein was precipitated by adding 1.9 ml isopropanol to the organic bottom layer. Then, the samples were centrifuged at 5000 rpm (g=224) for 10 minutes at 4 C°. After that, the supernatant was removed and the pellet was then washed with 0.3 M guanidine HCl/ 95% ethanol. The tubes were centrifuged at 7200 rpm (g=465) for 5 minutes. The washing step was repeated three times. 2 ml of 100% ethanol was added and incubated at room temperature for 20 minutes followed by centrifugation at 7500 rpm (g=465). Finally, the supernatants were discarded; the pellets were dissolved in

SDS (sodium dodecyl sulfate)-urea sample buffer. To completely dissolve the pellets (proteins), sonication was performed for 15 seconds three times. The protein extracts were stored at -20 C° until required.

## 2.6 Delipidation of foetal bovine serum

Delipidation of foetal bovine serum was performed according to the method of Cham and Knowles with slight modification (Cham *et al.*, 1976). 125 ml FBS was mixed with 40:60 volume ratio of N-butanol (100 ml) and di-isopropyl ether (150 ml). The components were mixed thoroughly by end-over-end rotation on a daisy-wheel for 20 minutes followed by incubation on ice for 20 minutes. Centrifugation was done at 2500 rpm (g=56) for 5 minutes to separate the aqueous and organic phase. The aqueous phase was extracted carefully using a needle and syringe or pipette. Then, the serum was re-extracted again with 50 ml di-isopropyl ether, mixed, centrifuged and separated as before. Then, any trace of solvent was removed using a gentle stream of nitrogen gas for 1-2 hours. Delipidated serum was transferred to a wide mouthed beaker and then lyophilized using freeze dry for 24-48 hours and reconstituted with 50 ml of HPLC water. The serum was dialyzed overnight against PBS at 4 C°. The serum was filter sterilized using 0.2 μm crodisk syringe filters.

## 2.7 Western blot

### 2.7.1 Materials

30% Bis-acrylamide was purchased from Severn Biotech (Kidderminster, UK).

PageRuler Prestained Protein Ladder Plus or Seeblue Protein Ladder was purchased from Fermentas (York, UK). Nitrocellulose membrane was purchased from GE Healthcare (Amersham, UK).

**4x Separation Buffer, pH 8.8:**

1.5 M Tris.Cl

0.4% SDS

**4x Stacking Buffer, pH 6.8:**

0.5 M Tris.Cl

0.4% SDS

**SDS PAGE Separation Gel:**

30% Acrylamide solution: 8 ml

4x Separation buffer: 5 ml

Water: 6.8 ml

10% APS (ammonium persulphate): 200 µl

TEMED (N,N,N',N'-Tetramethylethylenediamine): 20 µl

**SDS PAGE Stacking Gel:**

30% Acrylamide solution: 1 ml

4x Separation buffer: 2.5 ml

Water: 6.5 ml

10% APS: 120 µl

TEMED: 12 µl

**5x SDS-UREA Buffer (store at 4 C°):**

90 mM Tris HCl pH 6.8 4.5 ml (from 1 M)

| | |
|---|---|
| 4% (W/V) SDS | 2 g |
| 5% (V/V) beta-mercaptoethanol | 2.5 ml |
| 7 M deionized urea | 35 ml (of 10 M) |

(Amberlite Monobed resin was used for 30 minutes to dissolve urea in deionised water).

0.1% (W/V) bromophenol blue make up with water to 50 ml.

**10x SDS PAGE Running Buffer:**

For 500 ml:

Tris base: 15 g (250 mM)

Glycine: 72 g (1.92 M)

SDS: 5 g (or 50 ml 10% SDS solution) (1%)

**10x Transfer Buffer (SDS free):**

For 500 ml:

| | |
|---|---|
| Tris base | 15 g |
| Glycine | 72 g |

**Stripping Buffer:**

25 mM glycine, (pH 2.0)

2% SDS

**Blocking buffer:**

3% fish gelatin in TBS-T

**10x TBS (Tri-Buffered saline) (TBS) pH 7.4:**

For 500 ml:

NaCl: 4.4 g

KCl: 1.0 g

Trisbase: 15.0 g

**TBS-T:**

Dilute 10X TBS 1:10 and add Tween-20 to 0.1% (V/V) final concentration.

**Ponceau Red:**

0.1% (W/V) Ponceau S (3-hydroxy-4[2-sulpho-4-(4-sulphophenylazo)-phenyl-azo]-2,7-napthalenedisulphoric acid) in 5% (V/V) acetic acid.

### 2.7.2 SDS-PAGE

The samples (20 µl) were loaded onto a 12% SDS polyacrylamide gel. 5 µl of seeblue marker (Invitrogen) was loaded with each gel as a molecular weight marker. The protein was separated by gel electrophoresis in a Bio-Rad gel apparatus (Mini-PROTEAN) filled with SDS-PAGE running buffer. A constant current of 150 volt was supplied for around one hour. The separated proteins from the gel were transferred to pre-soaked nitrocellulose membrane in transfer buffer. A constant current of 105 volt was supplied for around one hour. The protein was stained on the membrane with Ponceau S. Non-specific antibody binding was reduced by blocking the nitrocellulose membrane in blocking buffer (3% gelatin in 0.1% TBS.T) for one hour at room temperature with continuous gentle shaking. The nitrocellulose membrane was subsequently incubated with primary antibody overnight at 4 C° on a roller (Table 2-2). After overnight incubation, the membrane was washed with 1XTBST three times each 20 minutes. The membrane was then incubated with secondary antibody diluted 1:10,000 for one hour at room temperature. After washing three times for 5 minutes with 1XTBST, the membrane was rinsed with distilled water. Finally, the membrane was scanned using The Odyssey® Infrared Imaging System (LI-COR Biosciences, Lincoln, NE/USA), which equipped with two infrared channels. Using two detection channels, total and phosphorylated forms could be visualized and differentiated between on the same gel

(same experminet) using different secondary antibodies. Band intensities were quantified by densitometry, using Odyssey software version 3. For details of antibodies used in this study (Table 2-2).

### 2.7.3 Antibodies

Primary antibodies are summarized in (Table 2-2). Goat 680 anti-rabbit, goat 680 anti-mouse, goat 800 anti-rabbit and goat 800 anti-mouse secondary antibodies were purchased from Li-Cor Biosciences (Cambridge, UK). The secondary antibodies were raised in goat and they are anti-mouse or anti-rabbit.

Table 2-2: Details of primary and secondary antibodies used with Odyssey system.

| Antibody (Catalog number) | Company | Species raised in | Concentration | Condition | Secondary | Approx Weight (Bands) (kDa) |
|---|---|---|---|---|---|---|
| Monoclonal--phospho-p44/42 MAPK (ERK1/2)--(#4370) | Cell Signaling | rabbits | 1/1500 | Overnight incubation | 1/10000 | 44 |
| Monoclonal--p44/42 MAPK (ERK1/2)--(#9107) | Cell Signaling | mouse | 1/1500 | Overnight incubation | 1/10000 | 42 |
| Polyclonal -- Phospho-AMPKα--(#2531) | Cell Signaling | rabbits | 1/1000 | Overnight incubation | 1/10000 | 60 |
| Monoclonal--phospho-GSK-3α/β--(#9327) | Cell Signaling | rabbits | 1/1000 | Overnight incubation | 1/10000 | 51 α<br>46 β |
| Monoclonal -- GSK-3α/β--(sc-7291) | Santa Cruz Biotechnology | mouse | 1/1000 | Overnight incubation | 1/10000 | 51 α<br>47 β |
| Monoclonal -- phospho-AKT--(#4051) | Cell Signaling | mouse | 1/1000 | Overnight incubation—using bags | 1/10000 | 60 |
| Polyclonal – AKT--(#9272) | Cell Signaling | rabbits | 1/500 | Overnight incubation—using bags | 1/10000 | 60 |
| Monoclonal -- | Cell Signaling | mouse | 1/500 | Overnight | 1/10000 | 40 |

| | | | | | | |
|---|---|---|---|---|---|---|
| P38--(#9107) | | | | incubation | | |
| Monoclonal -- phospho-P38-- (9215) | Cell Signaling | rabbits | 1/500 | Overnight incubation | 1/10000 | 43 |
| Monoclonal-- cyclophilin-- (ab74173) | Abcam | mouse | 1/1500 | Overnight incubation | 1/10000 | 21 |

## 2.8 Quantification of protein samples

### 2.8.1 Materials

**Staining solution (Coomassie Blue):**

0.2% (W/V) Coomassie Brilliant Blue

20% (V/V) methanol

10% (V/V) acetic acid

**Destaining solution:**

20% (V/V) methanol

10% (V/V) acetic acid

**Storage solution:**

5% (V/V) acetic acid

### 2.8.2 Coomassie blue staining

After dissolving the pellet from protein extraction in SDS-urea buffer, the dissolved proteins were heated to 99 C° for 5 minutes, followed by centrifugation at 10,000 rpm

(g=896)for 5 minutes. 20 µl of SDS-urea samples were loaded onto SDS 12% polyacrylamide gels for electrophoresis. Coomassie Blue staining procedure was done to determine the relative quantity of proteins in the samples for western blot.

After electrophoresis, the apparatus was disassembled, and the gel was removed from the glass plates and transferred to a tray. The gel was soaked in staining solution for one hour with gentle shaking at room temperature. The staining solution was discarded, and the gel was destained using two-three changes of destaining solution on shaker overnight until bands were clearly visible. The blots were scanned using Odyssey (Infrared fluerescence). The relative quantity of proteins was determined through estimation of any sharp protein band stained by Coomassie Blue staining solution to ensure reliable comparisons of the protein quantities in different samples in which these quantities represent the total amount of protein loaded into each well.

## 2.9 3T3-L1 cell culture

### 2.9.1 Materials

3T3-L1 preadipocytes were obtained from American Type Collection (ATCC). FCS (foetal calf serum) was purchased from PAA Laboratories (Somerset, UK). NCS (newborn calf serum) was purchased from PAA Laboratories (Somerset, UK). Oil red O stain was purchased from British Drug Houses Ltd (Poole, England).

**Medium 1**

- Dulbecco's Modified Eagle Medium (DMEM) high glucose with 10% NCS

-2 mM glutamine

-1% of (10,000 units penicillin and 10 mg streptomycin/ml)

**Medium 2**

- DMEM high glucose with 10% FCS

-2 mM glutamine

-1% of (10,000 units penicillin and 10 mg streptomycin/ml)

-0.5 mM 1-methyl-3-isobutylxanthine

-0.25 μM dexamethasone

-166 nM insulin

**Medium 3**

- DMEM high glucose with 10% FCS

- 2 mM glutamine

- 1% of (10,000 units penicillin and 10 mg streptomycin/ml)

- 166 nM insulin

**Medium 4**

- DMEM high glucose with 10% FCS

- 2 mM glutamine

- 1% of (10,000 units penicillin and 10 mg streptomycin/ml)

### 2.9.2 3T3-L1 cell culture

#### 2.9.2.1 Thawing cells

The cryotube containing frozen cells in the $6^{th}$ passage was taken out of -80 C° freezer. Those cells were defrosted very quickly in 37 C° water bath for 1-2 minutes. Afterwards, the cryotube was removed from the water bath and the cells were quickly resuspended in 50 ml sterile conical tube with 10 ml of medium 1. The cells were incubated in 75 $cm^2$ tissue culture flasks at 37 C°, 5% $CO_2$ and 5% humidity with a media change every

48 hours.

### 2.9.2.2 Trypsinizing and passaging the cells

Once cells reached 75-80% confluency in 75 $cm^2$ flasks, the medium 1 was removed from the flasks and the cells were washed with PBS. After that, the cells were treated with the proteolytic enzyme trypsin (3 ml) to detach adherent cells from the surface of the flasks. After around 30 seconds-one minute, the trypsin was aspirated and the cells were then suspended in medium 1. Those cells from one culture flask were divided into 2-4 new culture flasks. The cells were incubated in 75 $cm^2$ tissue culture flasks at 37 C° and 5% $CO_2$, with a media change every 48 hours.

### 2.9.2.3 3T3-L1 cell culture

The cells were seeded at ~1 x $10^5$ cells in 35 mm dishes or 6 well plates. The cells were cultured until 100% confluent. After 2 days from reaching confluence, cells were induced to differentiate with medium 2. The cells were maintained in this media for 3 days. Then, the cells were incubated with medium 3 for 2 days. Differentiated cells were incubated with medium 4 for 2 days.

#### 2.9.2.4 Oil-Red O staining

This method was used to visualize lipid droplets after differentiation to adipocytes. After removing the media, cells were washed with PBS for three times. Then, the cells were fixed in 10% formalin at room temperature for 10 minutes. The cells were washed again with PBS for three times and then incubated for one hour at room temperature with Oil Red O stain. After that, the cells were washed again with PBS for three times and PBS was added to prevent dehydration. Images were taken for the cells using a digital camera connected to microscope (Nikon) at X40 magnification.

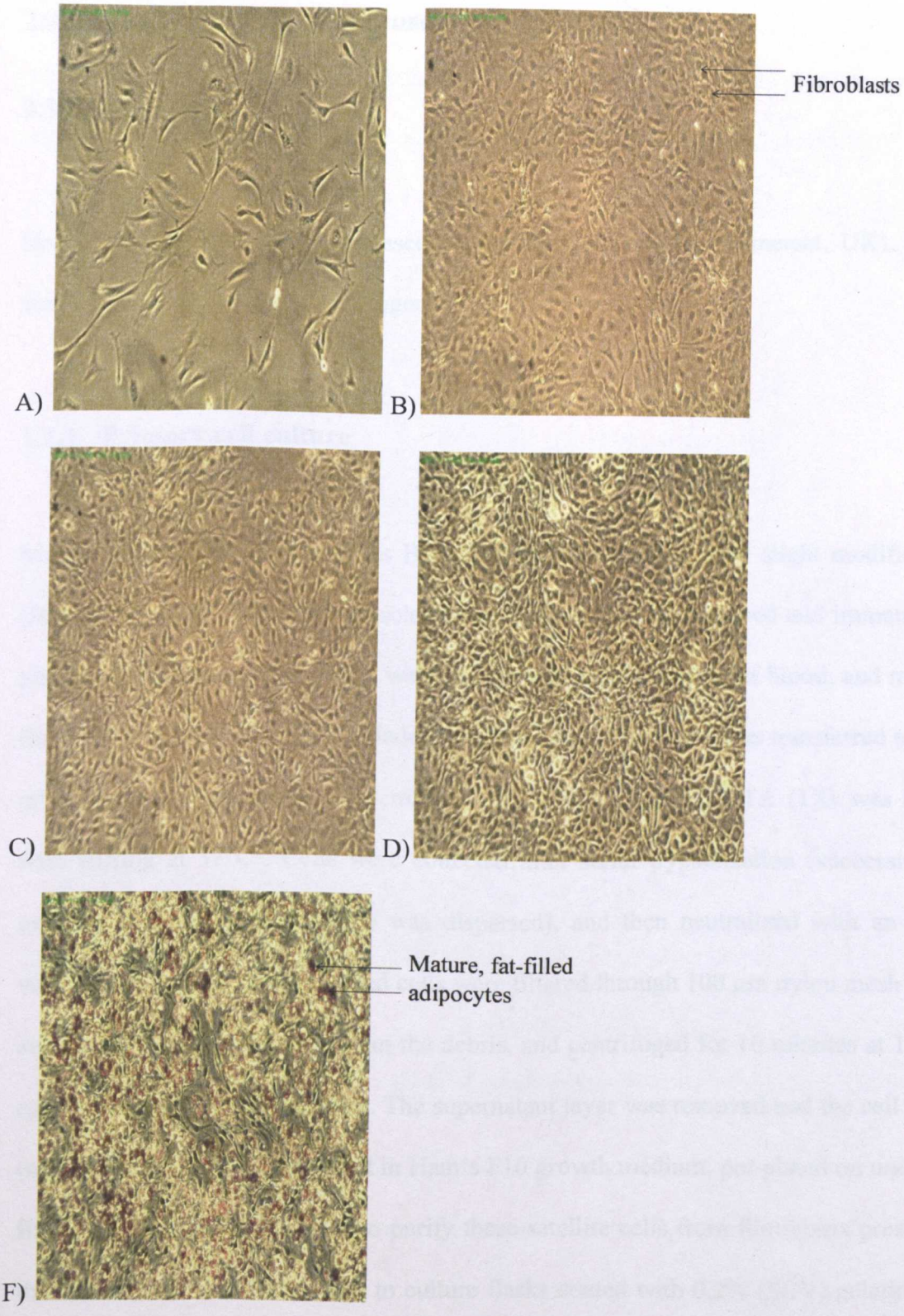


Figure 2-4: Representative photographs of 3T3-L1-fibroblast cells differentiating into 3T3-L1-adipocytes. A) 3T3-L1-fibroblast cells, B) confluent fibroblast fixed and stained with Oil Red O, C) fibroblast incubated in media 2, D) fibroblast incubated in media 3 and F) 3T3-L1 adipocytes were fixed and stained with Oil Red O.

## 2.10 Primary rat skeletal muscle cell culture

### 2.10.1 Materials

Ham-F 10 and FBS were purchased from PAA Laboratories (Somerset, UK). Horse serum was purchased from Invitrogen.

### 1.1.1 Primary cell culture

Muscle culture was performed as Blau and Webster method with slight modification (Blau *et al.*, 1981). Hindlimb muscles from Wistar rats were removed and immersed in phosphate buffered saline (PBS), washed to remove the remnants of blood, and minced finely with scissors and scalpel blades on a Petri dish. The tissue was transferred to a 50 ml flask for trypsinization: 5-10 ml of 0.25% (W/V) trypsin/EDTA (1X) was added with stirring at 37 C°. Cells were collected after serial trypsinization (successive 15 minutes periods; until all tissue was dispersed), and then neutralized with an equal volume of medium. The collected cells were filtered through 100 μm nylon mesh ("cell strainers") to purify the cells from the debris, and centrifuged for 10 minutes at 17,000 rpm (g=26) at room temperature. The supernatant layer was removed and the cell pellet (satellite cells) was re-suspended in Ham's F10 growth medium, pre-plated on uncoated flasks for 10 minutes at 37 C° to purify these satellite cells from fibroblasts present in the extract, and then transferred to culture flasks coated with 0.2% (W/V) gelatin. The satellite cells were then grown to confluent myoblasts and differentiated into myotubes in growth medium. 20% (V/V) fetal bovine serum (FBS) and 5 ml of penicillin and streptomycin (10,000 units penicillin and 10 mg streptomycin/ml in 0.9% NaCl) were added to Ham's F10.

After one day, the cells were fed with fresh medium, cells require fresh medium every 48 hours. The cells were fed with 20% (V/V) FBS fresh medium for three weeks, then reduced to 10% (V/V) FBS fresh medium for two weeks and then changed to 6% horse serum and 10 mM glucose Ham's F for two to three days.

A)

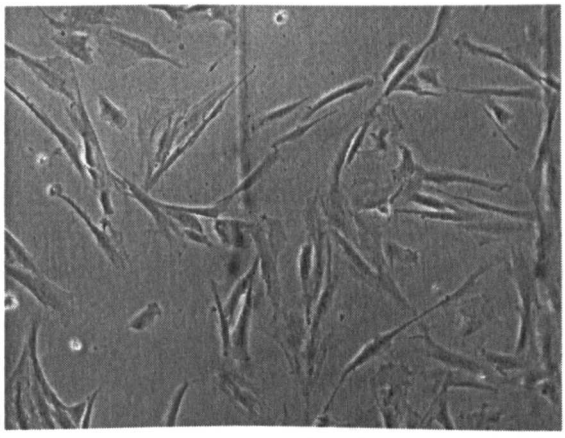

B)

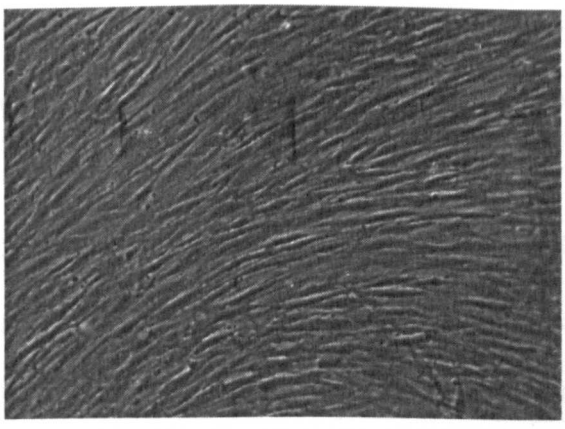

Figure 2-5: Representative myoblasts and myotubes derived from Wistar rat skeletal muscle. A) myoblasts taken during the third week of tissue culture and B) myotubes taken during sixth week of tissue culture.

## 2.11 cAMP assay

### 2.11.1 Materials

cAMP Kit was obtained from Cayman Chemical (Europe).

### 2.11.2 cAMP assay/ cAMP EIA

Accumulated cAMP in the myotube cells was measured by a competitive enzyme immunoassay (EIA) kit (Cayman Chemical). Cells were cultured in 6-well cell culture dishes and then cells were pretreated. At the end of the exposure period, 40 µl 5 M HCl was added to each well (2 ml media 6% horse serum). The plates were stored at -20 C° until assayed in duplicate for cAMP using an EIA kit according to the manufacturer's instructions for cAMP measurement with acetylation (Cayman Chemical).

Then, the experimental well plates were thawed in 0.1 M HCl and media (6% horse serum) at room temperature for 20 minutes and scraped to ensure total cell lysis and release of cAMP into the HCl. The lysates of the samples were collected into 1.5 ml microcentrifuge tubes and centrifuged under 10,000 g for 10 minutes at 4 C°. The supernatants were transferred to new tubes. 500 µl of the supernatants were transferred to new tubes for acetylation process. Standards and samples were acetylated in 1.5 tubes. 0.05 ml of samples or standard solutions was added in duplicate to mouse monoclonal anti-rabbit IgG coated wells of a 96-well plate. cAMP linked to acetylcholinesterase (Tracer) and cAMP antiserum were added to the appropriate wells. Then, the plate was incubated 18-24 hours at 4 C°.

After washing 5 times using a plate washer (Skatron Instruments), the plate was incubated with 200 µl Ellman's solution (the acetylcholinesterase (AChE) substrate) for 90-120 minutes at room temperature with gentle shaking (400-600 rpm). The plate was read at a wavelength of 405 nm to measure the intensity of the colour (yellow) that developed. The measurement was inversely proportional to the amount of free cAMP present. The concentration was calculated by the 4-parameter logistic equation obtained

from the standard curve using GraphPad Prism, version 5.03 (GraphPad Software Inc). The cAMP concentration of samples was determined and given as pmol/well. Each sample was performed in duplicate.

## 2.12 Calcium imaging

### 2.12.1 Materials

Fura-2AM (L-[2-(carboxyloxazol-2-yl)-6-amino-benzofuran-5-oxy]-2-(2'-amino-5'methyl phenoxy)ethane-N,N,N,N-tetraacetic acid pentaacetoxymethyl ester)) was bought from Calbiochem company.

### 2.12.2 Glass coverslip preparation

Satellite cells were grown on 19 mm glass coverslips and differentiated into myoblasts over around 14-21 days as described in the methods (Section 2.8.2).

### 2.12.3 Fura-2AM cell loading

The intracellular $[Ca^{2+}]_i$ was quantified in single cells within myoblast clusters with the $Ca^{2+}$-sensitive fluorescent dye fura-2AM using Andors IQ imaging system.

Cells were washed with $Ca^{2+}$ buffer, then were incubated with 5 µl 1 mM fura 2-acetoxymethyl ester (fura-2 AM) dissolved in 895µl buffer (NaCl, 145 mM; KCl, 5 mM; CaCl2, 2 mM; MgSO4.7H2O, 1 mM; HEPES, 10 mM; glucose, 10 mM) with 100 µl FCS for one hour and 15 minutes at 37 C°.

After loading with the fluorescent calcium indicator fura-2 AM, the cells were washed three times with buffer to remove the extracellular fura-2AM and incubated in the $Ca^{2+}$ buffer for 15 minutes before using cells in imaging (Figure 2-6 and Figure 4-14).

When fura2-AM enters the cell membrane, it is then cleaved by cytoplasmic esterases into impermeable fura2 and AM component. Indeed, fura2 is a UV light excitable dye which binds to free intracellular $Ca^{2+}$ more selectively over other cations such as $Mg^{2+}$ (Grynkiewicz *et al.*, 1985). Fura2 is excited at 340nm and 380nm wavelengths of light. The excitation spectrum of fura2 peaks at 380nm in the absence of $Ca^{2+}$, while the peak shifts to 340nm without a significant change in the emission peak when $Ca^{2+}$ is bound to fura2, for example after $Ca^{2+}$release from the sarcoplasmic reticulum.

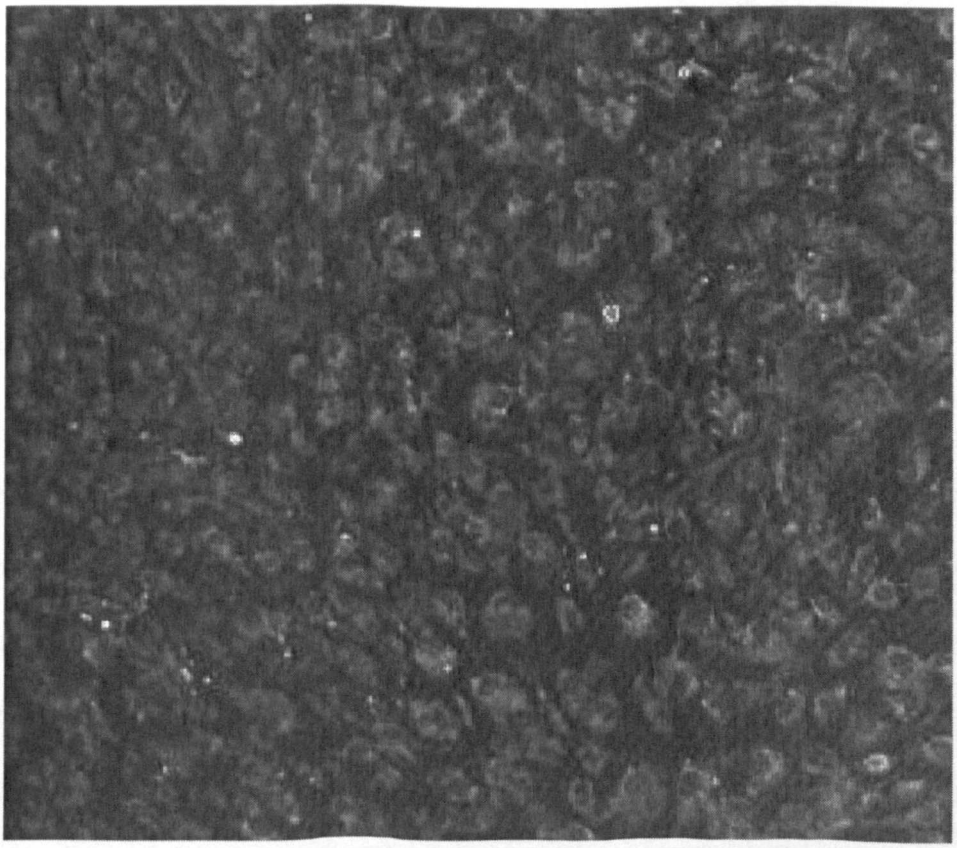

Figure 2-6: Myoblasts after loading with fura-2AM. For colour image, see (Figure 4-14).

### 2.12.4 Calcium imaging studies of myoblasts

Coverslips were fixed to a Perspex chamber using vacuum grease. A coverslip with adherent cells was positioned on the stage of a inverted fluorescence microscope and examined using Retiga chilled digital intensified charge-coupled device (CCD) camera. Cells were suprafused with $Ca^{2+}$ buffer. Changes in $[Ca^{2+}]_i$ were measured as the ratio of peak fluorescence emission intensities (measured at 500 nm) at excitation wavelengths of 340nm and 380nm, respectively. $[Ca^{2+}]_i$ was calculated from fluorescence emission, monitored by Retiga chilled digital intensified charge-coupled device (CCD) camera, using a standard curve created with solutions containing known concentrations of $Ca^{2+}$.

After around one minute of measuring basal responses, a standard protocol was followed in which myoblast cells were exposed to 10 μM of UTP for around one minute then 20 minutes as a washout period. After that cells were exposed to ATP (1 mM) for one minute followed by 20 minutes washout period. Finally, cells were exposed to 4 μM of ionomycin for one minute.

Images were taken at a rate of one image per 5 seconds. UTP and ATP produce a robust calcium signal which reach the peak after approximately 30 seconds and take about 3 minutes to go back to basal. So, one image per 5 seconds interval is sufficient to trace the calcium signal in primary rat skeletal muscle cells. Besides that, there are technical limitations in the Andors IQ imaging system which could not capture images in a rate faster than one image per 5 seconds. The intensity measurements were then collected in Microsoft Excel. Excel and Prism software was used to calculate each cell's intensity change and the mean intensity of all cells over time.

Increases in $[Ca^{2+}]_i$ were measured by subtracting mean basal $[Ca^{2+}]_i$ from the peak $[Ca^{2+}]_i$ measurement. The percentage of cells that responded to drug was also determined. Cells were also identified by responsiveness to drug. Myoblasts displaying an increase in ratio (from basal) < ~0.08 (standard deviation of basal period) following suprafusion with the buffer were considered as non-responsive and therefore excluded from the study.

## 2.13 Glucose uptake assays

### 2.13.1 Materials

3H 2-Deoxy-D-glucose (2-DOG) (specific activity 0.74 TBq/mmole) was purchased from PerkinElmer. DMEM zero glucose and 1 g/L glucose was purchased from Invitrogen.

**Reaction buffer:**

-138 mM NaCl,

-1.85 mM $CaCl_2$,

-1.3 mM $MgSO_4$,

-4.8 mM KCl,

-0.2% (W/V) BSA,

-50 mM HEPES pH 7.4

### 2.13.2 Glucose uptake in 3T3-L1 cells

24 hours before the experiment, the differentiated 3T3-L1 adipocytes in 6 well plates were serum-starved using 12.5 mM glucose, serum free DMEM. After the starving period, the cells were washed three times with PBS at 37 C° and incubated with 2 ml reaction buffer for 45 minutes at 37 C°. Then, the cells were treated with insulin (200 nM) in reaction buffer for 10 minutes, followed by the addition of 250 µl of 27.8kBq 3H 2-DOG and 1.5 mM of cold 2-DOG for 10 minutes. Glucose uptake was terminated by washing the cells with ice cold PBS containing 10 mM glucose three times. Then, the cells were solubilised in 500 µl 0.5 M NaOH and 0.1% SDS. 300 µl of lysate was

transferred to a scintillation vial and 5 ml liquid scintillant was added. Radioactivity was measured using a scintillation counter (LKB Instruments, Maryland, USA). Samples were assayed for 2-DOG uptake as disintegrations/minute/well.

### 2.13.3 Glucose uptake in skeletal muscle myotubes

The procedure is identical to that described for 3T3-L1 cells with the exception that the myotubes were starved for 2-5 hours in Ham-F containing 6 mM glucose. In order to examine whether the glucose uptake could be changed in primary rat skeletal muscle myotubes, insulin dose-response curve was examined first.

### 2.13.4 Glucose uptake in 3T3-L1 cells/skeletal muscle myotubes (adjusted protocol).

The procedure is identical to that described for original protocol with the exception that DMEM ((0% serum and 6 mM glucose) or (0% serum and 0% glucose)) were used instead of Ham-F 10.

## 2.14 Immunocytochemistry

### 2.14.1 Materials

0.1 M PBS

Triton X-100

Serum/BSA

Primary antibody (rabbit polyclonal to glucose transporter GLUT4 (ab33780))

TTBS (Triton + Tris buffered saline)

Secondary antibody (Alexa Flouro® 488 goat anti-rabbit IgG (H+L)*2mg/ml)

Shaker table

Dark box

### 2.14.2 Procedure

The myotube cells on glass coverslips were fixed in 4% PFA (paraformaldehyde) for thirty minutes at room temperature. After PFA was aspirated, the cells were incubated at room temperature with ice-cold 0.1 M PBS for 10 minutes. Then, the cells were washed with 0.1 M PBS three times. The coverslips were blocked with 50 µl goat serum, 6 µl Triton 100%, 1 ml 0.1 M PBS for one hour at room temperature. Then, the coverslips were incubated with the indicated primary antibody, raised in rabbit, (GLUT4; 1:1000 dilution) overnight at 4 C°, followed by washing for five times with 0.1 M PBS for 10 minutes. After that, secondary antibody (Alexa Flouro® 488 goat anti-rabbit IgG (H+L)*2mg/ml; 1:500 (2 µl per ml TTBS)) was added for one hour and followed by washing with 0.1 M PBS for five times for 10 minutes. Then, the coverslips were kept dry overnight, the coverslips were then mounted onto microscope slides using mounting medium with DAPI. Cells were viewed and photographed with fluorescent microscope 1X40. Image on fluorescent microscope on green channel for antibody and blue for DAPI (nuclear stain) were used. Cells were taken with an oil immersion lens at 40x magnification.

# Chapter 3

# GPCRs Expression

# 3 Chapter Three: mRNA expression of GPCRs and associated signalling partners in skeletal muscle tissues

## 3.1 Introduction

G protein coupled receptors (GPCRs) are the largest family of proteins in the human genome. Indeed, GPCRs are the richest targets for pharmaceutical drugs on the market today; it is estimated that they are the targets of 30-50% of all medications due to their vast and varied roles in regulating the body processes, metabolism and signal transduction and their involvement in key biological functions (Kobilka, 2007; Tilakaratne *et al.*, 2005). GPCRs are expressed in every tissue and play a major role in many diseases.

G proteins are a diverse class of heterotrimeric proteins composed of three distinct subunits: α, β, and γ. G proteins can be divided into four main families: $G_{\alpha s}$; $G_{\alpha i}$; $G_{\alpha q}$ and $G_{\alpha 12}$ (Downes *et al.*, 1999; Ulloa-Aguirre *et al.*, 1999). The main signalling mechanisms are illustrated in Chapter One (Figure 1-3).

$G_{\alpha s}$ stimulates adenylyl cyclase (AC) activity. This enzyme converts ATP to cAMP. An increase of cAMP level activates protein kinase A (PKA). As $G_{\alpha i}$ inhibits AC activity, activation of GPCRs coupled to $G_i$ leads to a decrease in cAMP levels. This results in decreasing the activity of PKA. When an agonist binds to a $G_{\alpha q}$ protein-coupled receptor, $G_{\alpha q}$ activates phospholipase C (PLC). The active PLC hydrolyses phosphatidylinositol 4,5-bisphosphate ($PIP_2$) to produce inositol 1,4,5-trisphosphate ($IP_3$) and 1,2-diacylglycerol (DAG). $IP_3$ is water-soluble, so it is able to diffuse through the cytoplasm to the endoplasmic reticulum, where it allows $Ca^{2+}$ to be released from

enzymes and ion channels. DAG is hydrophobic, however, and it stays in the membrane to activate protein kinase C (PKC). This enzyme phosphorylates many proteins such as the insulin receptor substrate-1 in skeletal muscle (Schmitz-Peiffer *et al.*, 2008; Waraich *et al.*, 2008). When a ligand binds to a $G_{\alpha 12}$ protein-coupled receptor, Rho guanine nucleotide exchange factors are activated, leading to activation of the small G protein Rho. Rho-GTP activates many enzymes, such as Rho kinases that regulate phosphorylation.

Skeletal muscle is a heterogeneous tissue since it contains a variety of fibres that differ in contractile, functional, metabolic and molecular characteristics (Pette *et al.*, 1997; Staron *et al.*, 1999). Moreover, skeletal muscle is the largest organ in the human body and represents ~40% of the human body mass and 35-40% of the total body weight in the rat (Delbono *et al.*, 2007; Pedersen, 2011). Indeed, skeletal muscle utilizes the majority (70-80%) of ingested glucose since it is the main site for insulin-dependent glucose uptake (Toft *et al.*, 1998). Therefore, it is generally considered the most important site of insulin resistance.

By virtue of their large number, widespread expression and important mechanistic and regulatory roles in cell physiology and biochemistry, GPCRs play multiple well-recognized roles in clinical medicine. Therefore, GPCRs might be important in maintaining homeostasis in skeletal muscle though mediating responses to neurotransmitters and hormones. Finding the most highly expressed GPCRs will be hopefully helpful to define and characterize vital potential in terms of identifying novel targets related to clinical disorders. For most of those targets, it remains an open question whether the expression of these GPCRs in skeletal muscle is an important contributor to potential functional and metabolic roles in this tissue.

Identifying those receptors could be performed by assessing the binding of radioligands (i.e. radiolabelled agonists or antagonists), antisense approaches, expression studies (protein and mRNA level) and signalling pathways responses to such GPCRs. However, there are several challenges for some of these techniques. Indeed, the expression of receptor at protein level and radioligand binding assays can be difficult as limited validated antibodies to detect receptor protein and limited radioligands to bind to particular receptors are commercially available. Moreover, the availability of such agonists and antagonists to examine the signalling of GPCRs, in particular for orphan GPCRs, may be limited.

There are, however, very few studies about the expression of GPCRs and their signalling and the diversity and roles of these receptors in skeletal muscle. There has yet been no comprehensive analysis carried out of GPCRs and GPCRs signalling pathways in skeletal muscle published in the literature. This study utilized microarray technology to identify the identity and relative levels of GPCRs expressed in skeletal muscle.

## 3.2 Aims

The purpose of the investigations in this chapter was to characterize the mRNA expression of GPCRs and their ancillary signalling proteins in rat mixed fibre-type skeletal muscles using DNA microarray and QRT- PCR (Taqman) techniques.

## 3.3 Experiment design and methods

### 3.3.1 Tissue collection

Two male adolescent Wistar rats (180-200 g, 4-6 weeks old) were killed by cervical dislocation without anesthesia. This method was approved by the University of Nottingham Ethics Committee and the Animals Scientific Procedures Act (ASPA). Liver, adipose (mixed from subcutaneous, epididymal and omental) and skeletal muscle were obtained. Skeletal muscle (mixed fibre-type from hindlimb) tissues were separated bilaterally: tissue was immediately frozen in liquid nitrogen and stored at -80 °C with liver and adipose tissue, muscle tissue was cultured after the isolation of satellite cells in gelatine-coated flasks. The fibre type distributions for rat skeletal muscle used in this study was represented in Table 3-1 (Staron *et al.*, 1999).

Table 3-1: Fibre type expression (%) in different muscles from the rat, adapted from (Staron *et al.*, 1999).

| **Muscle** | **Fibre type (%)** | | | | |
|---|---|---|---|---|---|
| | **I** | **IIA** | **IIB** | **IC** | **(IIC, IIAD, IIDB and IID)** |
| Soleus | 82 | 9.3 | - | 1.8 | 6.9 |
| Tibialis Anterior | 2.4 | 12.2 | 49 | 0.2 | 36.2 |
| Extensor Digitorum Longus | 4.0 | 15.5 | 30 | 0.8 | 49.7 |
| White Gastrocnemius | 0.1 | 0.8 | 77 | - | 22.1 |
| Red Gastrocnemius | 22 | 18 | 5.1 | 1.9 | 53 |

Due to the cost implications, the microarray experiments were performed from two rats in this chapter. However, it is recommended to perform more repeats to support the

results deduced in this chapter, in particular it is hard to depend on 2 repeats due to variations in species or technical work. Indeed, more repeats will solidate the data statistically.

### 3.3.2 Tissue culture

Tissue culture was performed as described in Chapter 2, Section 2.8.

### 3.3.3 Microarray procedure

Agilent 4*44K DNA one color whole genome microarrays were used to measure the expression of 41090 genes in liver, adipose tissue and mixed fibre-type of skeletal muscle from rat hindlimb. The microarray experiment was carried out as described in the Methods; Chapter 2, Section 2.2.5.

After assessing the quality control criteria (Appendix 9.1.6) generated from feature extraction software, extracted data were further processed with GeneSpring GX 11.

### 3.3.4 Normalization

Normalization is necessary in microarray experiments since the absolute amounts of RNA cannot be determined, due to variations in labelling and hybridization. Expression intensities resulting from the same amount of RNA can differ when comparing two microarrays. Therefore, comparison of data from multiple arrays or multiple samples on a single array requires the data to be normalized. Data values below 1.0 were omitted and then set to 1.0. The raw data were then transformed by taking the log to base 2.

Then, the 75$^{th}$ percentile value was subtracted from each measurement in that array.

Summary:

Step 1: $Log_2$ transformation.

Step2: Percentile Shift. 75th percentile was calculated for each array and this value was subtracted from each value on the array. 75th percentile value was determined after ranking the values from the highest to lowest relative intensity values.

Calculations:

Figure 3-4-A was taken as an example to explain how the data were arrived at.

Skeletal muscle:

Glut4 has a raw data (relative intensity value) =32326 and the 75th percentile of this array =252.

Step1:

$Log_2$ for the raw data of Glut4=14.9 and $Log_2$ for the raw date of 75th percentile=7.9.

Step2:

$Log_2$ for the raw data of Glut4 - $Log_2$ for the raw data of 75th percentile=14.9-7.9=7 (Table 3-2 ).

Table 3-2: Explanation of normalization calculations for Glut4 in skeletal muscle, liver and adipose tissues.

| | Raw/Glut4 | Raw (75th percentile) | $Log_2$Glut4 | $Log_2$ (75th percentile) | Difference |
|---|---|---|---|---|---|
| Skeletal muscle | 32326 | 252 | 14.9 | 7.9 | 7 |
| Liver | 11.76 | 220.95 | 3.5 | 7.8 | -4.3 |
| Adipose | 21858 | 294.94 | 14.4 | 8.2 | 5.2 |

### 3.3.5 Reproducibility

The reproducibility of microarray was determined by calculating Pearson correlations using Graphpad Prism, version 5.03 (GraphPad Software Inc) on normalized data for all pair combinations of microarrays among biological replicate tissues (two animals, with 3 technical sites for skeletal muscle and one technical site for adipose and liver) (Table 3-3).

Table 3-3: The two biological skeletal muscle, liver and adipose replicates. Site A is a mixture of extensor digitorum longus and tibialis anterior, site B is a mixture of soleus and plantaris, and site C is a mixture of red and white gastronemius muscle with roughly equal amounts of each muscle.

| Rat A | Rat B |
|---|---|
| Skeletal muscle-Site A | Skeletal muscle-Site A |
| Skeletal muscle-Site B | Skeletal muscle-Site B |
| Skeletal muscle-Site C | Skeletal muscle-Site C |
| Liver | Liver |
| Adipose | Adipose |

### 3.3.6 Concordance

Concordance is defined as an agreement in the types of data (entities) that occurs among the pairs (biological or technical replicates) which reflects their degree of similarity in terms of entity expression.

Concordance was calculated by dividing entities classified as "present" in all replicates by entities classified as "present" in at least one of them (Figure 3-1).

Concordance=B/(A+B+C).

A: number of entities available only in first repeat.

B: number of entities available in both first and second repeat.

C: number of entities available only in second repeat.

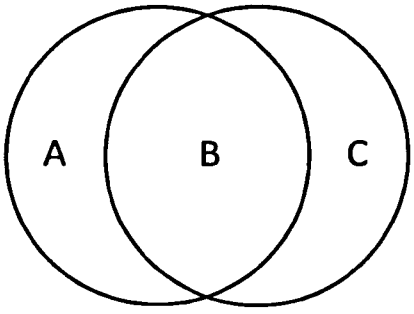


Figure 3-1: A Venn diagram for calculating concordance.

The term entities "genes" were used throughout this study to designate the transcripts that are identified by these probes "features".

Entities were considered "present" only if the output was uniform, not saturated and above the background. Entities were also considered "marginal" only if the output was not above or equal to background. However, entities were considered "absent" only if the output was not uniform and saturated.

A feature is non-uniform if the pixel noise of the feature exceeds a threshold established for a "uniform" feature. A feature is saturated if 50% of the pixels in a feature are above the saturation threshold which equal 65000.

"Present", "marginal" or "absent" are terms defining the nature of the hybridization (binding of probe to gene) signals on each microarray. However, the terms "expressed transcripts", "weakly transcripts" and "not expressed transcripts" are different. The latter are terms defined by comparing the results obtained among different conditions (disease vs normal) and should not be confused with "present", "marginal" and "absent" (Rimbault *et al.*, 2009). Therefore, not all GPCR entities classified as "present" are expressed and some GPCR entities classified as "marginal" might be expressed.

The use of the threshold (present detection) will eliminate the entities that are likely to be unreliable and will keep the entities classified as "present". These entities, which are classified as "present", might be expressed or not. Consequently, the use of the threshold will increase true positive to false negative.

Filtering by signal will remove the entities with a signal close to background. However, the choice of how to determine the background is arbitrary (Background subtraction method was applied through identifying the position of the probe on the microarray and calculating the background signal and subtracting it from the hybridization signal of the probe (Figure 3-2)). However, many systematic sources may still remain to contribute to the background signal component, including any non-specifically-bound fluorescent signal or contaminants on the glass, fluorescent signal that is non- specifically associated with the DNA probes themselves and any artifacts from washing, hybridization and labelling.

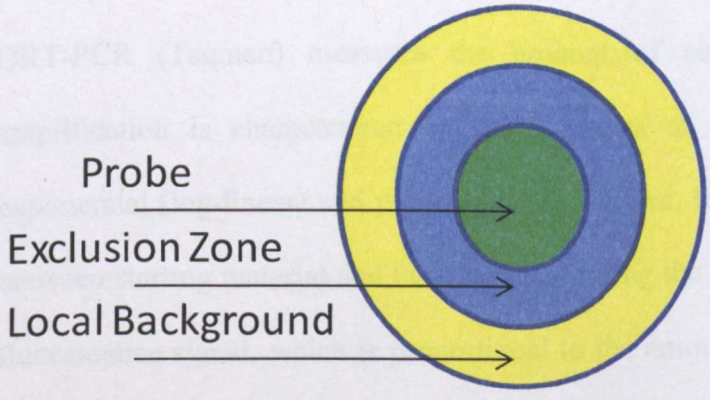


Figure 3-2: Background substraction method.

This method (Agilent microarray) was used in this study to eliminate the entities that are likely to be unreliable (entities are not classified as "present" in all replicates).

### 3.3.7 QRT-PCR (Taqman)

Myoblast and myotube cells were grown and differentiated as described in Chapter 2. The cells were collected in TriReagent, and processed as described in Chapter 2, Section 2.2.2. RNA was reverse transcribed into cDNA using Superscript III reverse transcriptase (Invitrogen). Then, QRT-PCR (Taqman) was performed as described in Chapter 2, Section 2.4.

Gene expression levels (in arbitrary units) were determined from the mean of triplicate determinants of each sample. As stated in Chapter 2, Section 2.4, data from Taqman were only used if the slope of the standard curve for each plate was between -3.2 and -3.6 and $R^2$ values of more than 0.99. In addition, Ct values of triplicate readings for an individual sample, which were more than 0.5 Ct apart, were excluded. The following primers and probes (Eurofins) were used (Table 3-4).

QRT-PCR (Taqman) measures the amount of accumulated PCR product. PCR amplification is characterized by three phases of the amplification reaction; lag, exponential (log-linear) and plateau phases. Indeed, there is a quantitative relationship between starting material and PCR product during the exponential phase of PCR. When fluorescence signal, which is proportional to the amount of accumulated PCR product, increases during PCR cycles, it reaches the threshold cycle (Ct value) at which the fluorescent signal is first recorded during the exponential phase. The threshold is usually detected when $10^{11}$-$10^{12}$ PCR product molecules are present. This enables an accurate quantification of starting material using QRT-PCR (Taqman). The fewer the number of cycles required to reach the log amplification phase for a particular gene, the greater the amount of the target gene detected. The standard curve was then performed by plotting the Ct values against the logarithm of the initial cDNA serial dilution.

Usually, reference genes were used as the non-variant normalizing genes.

The mRNA expression levels of specific genes were not normalized to the mean of the mRNA expression level of β-actin and 18S in this study. The reason behind that was explained by variant cycles in different stage of differentiation in skeletal muscle (myoblast, myotube and tissue) for β-actin and 18S.

Table 3-4: Oligonucleotide sequences for probes and primers.

| Gene | Sequences (5' → 3') | Amplicon size (bp) | Gene Bank Accession No. |
|---|---|---|---|
| *18s* | FWD CGGCTACCACATCCAAGGAA<br>PROBE TGCTGGCACCAGACTTGCCCTC<br>REV GCTGGAATTACCGCGGCT | 188 | M10098 |
| *Actb* | FWD GAGCGTGGCTACTCCTTCGT<br>PROBEACCACAGCTGAGCGCGAGATCGT<br>REVGTAGCACAGCTTCTCCTTGATGTC | 72 | NM_001100 |
| *Cnr1* | FWD CCAAAAGTGGAGAGCGACAAC<br>PROBE ATCCAGATCACCATGCCGTTCACA<br>REV CGTCTCGAAGGTCCCAATGT | 68 | NM_012784.4 |
| *Gpr40* | FWD CCTGCCCGACTCAGTTTCTC<br>REV CGGAGGCAGCCCACATAG<br>PROBE TTCTGCTCTTCTTTCTGCCCTTGGTTATCA | 80 | NM_153304.1 |
| *Adra2a* | FWD GGCCTCAGCGGACATCCT<br>PROBE TGGCCACGCTGGTCATTCCCTT<br>REV CATAACCTCGTTGGCCAAAGA | 64 | NM_012739.3 |
| *Gpr119* | FWD TCCATATTCCAGCAGACCACCTA<br>PROBE CATGGGCCCTGCACCTTCTTTGC<br>REV GCACAAACCTTGGGTGAAACA | 70 | NM_181770.1 |

## 3.4 Statistical analysis

Analysis was performed using GraphPad Prism, version 5.03 (GraphPad Software Inc). Data were represented as means ± standard error of mean (SEM).

## 3.5 Results

### 3.5.1 Reproducibility

In order to examine the reproducibility between replicates, Pearson correlation was performed. Correlations on normalized data among skeletal muscles and among liver replicates were above 0.97 (Pearson correlation), indicating high reproducibility. Similarly, correlation between adipose replicates was slightly lower at ~ 0.96. Adipose tissue samples were taken from three different parts with different proportions of

subcutaneous, epididymal and omental adipose tissue (Figure 3-3 and Table 3-5).

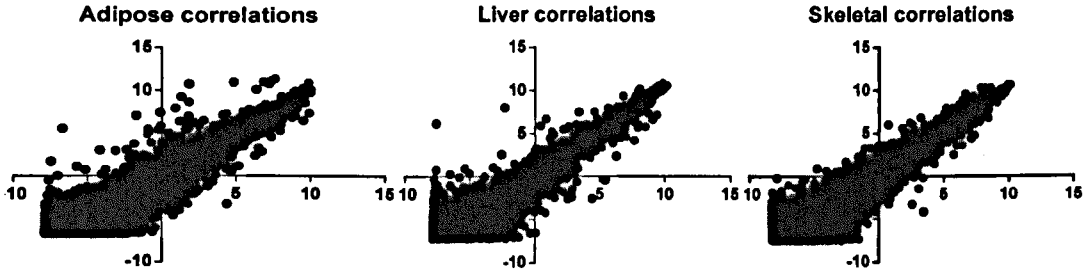


Figure 3-3: The correlation between two biological replicates; from liver (0.97) (Pearson score), adipose tissue (0.95) and mixed fibre-type skeletal muscle (0.97) taken from hindlimb from two rats. The axes represent the relative intensity values for gene expressions.

Table 3-5: Correlation between two biological replicates from mixed fibre-type hindlimb skeletal muscle (0.97) taken from two rats. Site A was a mixture of extensor digitorum longus and tibialis anterior, site B was a mixture of soleus and plantaris, and site C was a mixture of red and white gastrocnemius muscle with roughly equal amount of each muscle.

| Correlation | | | Rat A | | | Rat B | | |
|---|---|---|---|---|---|---|---|---|
| | | | Site | | | Site | | |
| | | | A | B | C | A | B | C |
| Rat A | Site | A | | 0.98 | 0.95 | 0.97 | 0.98 | 0.97 |
| | | B | 0.98 | | 0.95 | 0.96 | 0.97 | 0.96 |
| | | C | 0.95 | 0.95 | | 0.96 | 0.96 | 0.95 |
| Rat B | Site | A | 0.97 | 0.96 | 0.96 | | 0.98 | 0.98 |
| | | B | 0.98 | 0.97 | 0.96 | 0.98 | | 0.98 |
| | | C | 0.97 | 0.96 | 0.95 | 0.98 | 0.98 | |

## 3.5.2 Concordance

In order to examine the similarity of relative expression among entities classified as "present", concordance was calculated.

Entities (22839, 26199, 28466, 29476, 24574 and 23610) classified as "present" were observed in six mixed fibre-type skeletal muscles (Table 3-6). The concordance among skeletal muscle replicates was 79–90% for these entities. The concordance for all

skeletal muscle replicates is 79% for the entities classified as "present".

GPCR entities (133, 119, 215, 161, 191 and 115) classified as "present" were observed in six mixed fibre-type skeletal muscles (Table 3-6). The concordance among the skeletal muscle replicates was 51–82% for the GPCR entities classified as "present". The concordance for all skeletal muscle replicates is 51% for the GPCR entities classified as "present".

Table 3-6: The number of whole genome entities and GPCR entities classified as "present" in each individual muscle tissue from two biological replicates.

| | | | whole genome entities | GPCR entities |
|---|---|---|---|---|
| Rat A | Site | A | 22839 | 133 |
| | | B | 28466 | 215 |
| | | C | 24574 | 161 |
| Rat B | Site | A | 26199 | 119 |
| | | B | 29476 | 191 |
| | | C | 23610 | 115 |

The differences in concordance among replicates might be ascribed to differences in biological or technical issues, labelling, hybridization or washing issues. The concordance rate for entities classified as "present" for all skeletal muscle replicates (79%) from rat whole genome microarray was higher than the concordance rate for GPCR entities (51%). The possible reasons for this observation are that a large percentage of GPCRs may be detected at marginal levels relative to the background of those entities on the microarray slides (background level). Another reason is that the expression levels for GPCR entities possibly are usually lower than overall genome entities that contain structural proteins. In other words, the variation in the numbers of GPCR entities classified as "present" among different replicates is explained by GPCR entities might be located in low ranking as "present" and high ranking as "marginal".

### 3.5.3 Confirmatory expression

*Glut4, fabp3, ppara and pparg* were selected as confirmatory genes to define skeletal muscle, liver and adipose tissue for the microarray experiments in order to reflect the microarray reliable data in a tissue specific manner.

The present study revealed that the *glut4*/muscle-fat glucose transporter was highly expressed in skeletal muscle and adipose tissue while low expression was observed in liver tissue (Figure 3-3A). Fatty acid binding protein 3 (*fabp3*) was also highly expressed in skeletal muscle while low expression was observed in liver and adipose tissues (Figure 3-3B). *Ppara* was highly expressed in liver and skeletal muscle tissue while low expression was observed in adipose tissue (Figure 3-3C). *Pparg* was highly expressed in adipose tissue while low expression was observed in liver and skeletal muscle tissues (Figure 3-4D).

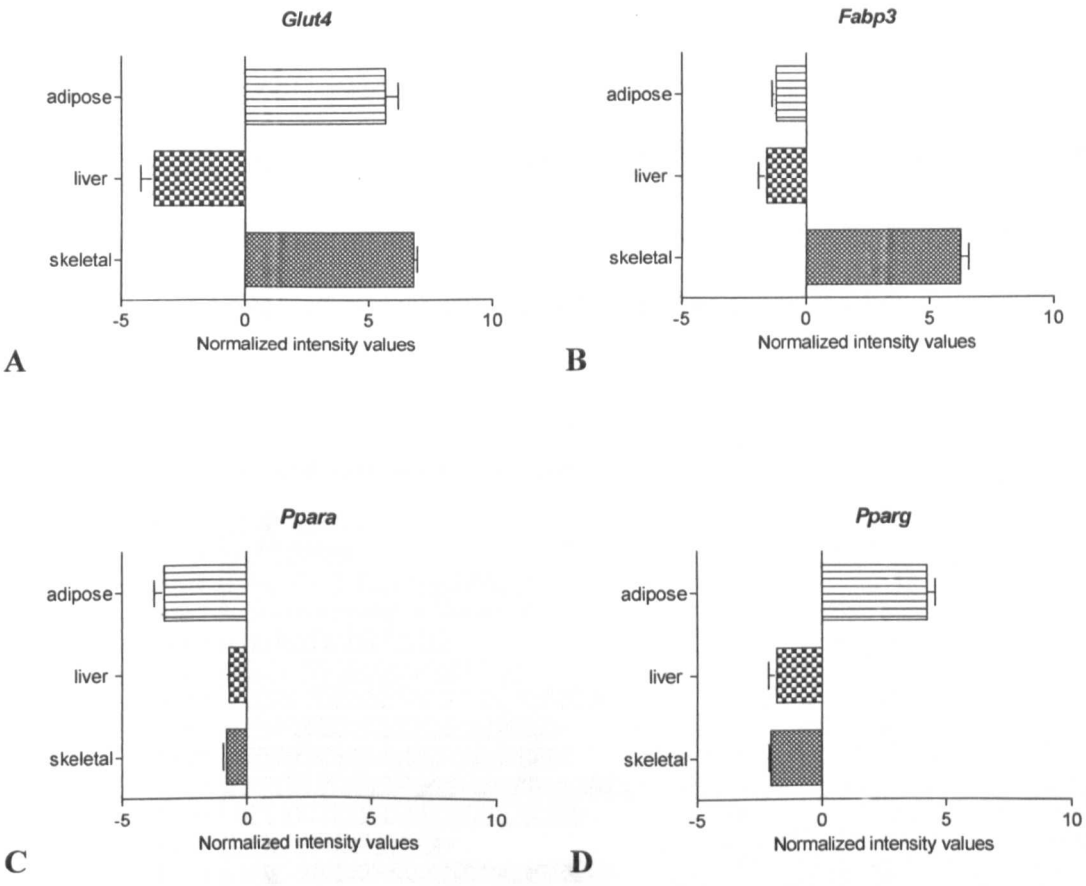


Figure 3-4: RNA transcript levels for (A) *glut4,* (B) *fabp3*, (C) *ppara* and (D) *pparg* in mixed skeletal muscle, liver and adipose from two male Wistar rats. (As number per group is not equal, statistics was not performed).

### 3.5.4 Skeletal muscle type definition

In order to determine the type of skeletal muscle fibres, the relative intensity values of the rat fast and slow fibre type specific structural subunits were determined (Figure 3-5); Troponin I (*tnni1*), troponin T 1 (*tnnt1*), tropomyosin 3 (*tpm3*), myosin light chain 2 (*myl2*), and, myosin heavy chain 7 (*myh7)* are markers for slow twitch muscle (Barton *et al.*, 1999; Gahlmann *et al.*, 1988; Pieples *et al.*, 2000; Smerdu *et al.*, 1994; Tajsharghi, 2008). Troponin I 2 (*tnni2*), troponin T 3 (*tnnt3*), troponin C 2 (*tnnc2*) tropomyosin 1 (*tpm1*), myosin light chain 1 (*myl1*) and myosin light chain 3 (*myl3*)

myosin heavy chain 1 (*myh1)* myosin heavy chain 2 (*myh2)* are markers for fast twitch muscle (Periasamy *et al.*, 1984; Pieples *et al.*, 2000; Schreier *et al.*, 1990; Smerdu *et al.*, 1994; Tajsharghi, 2008). Slow twitch muscle structural subunits (*tnni1, tnnt1, tpm3, myl2* and *myh7*) and fast twitch muscle structural subunits (*tnni2, tnnt3, tnnc2, tpm1, myl1, myl3, myh1* and *myh2*) were detected (419 ranking out of 41090).

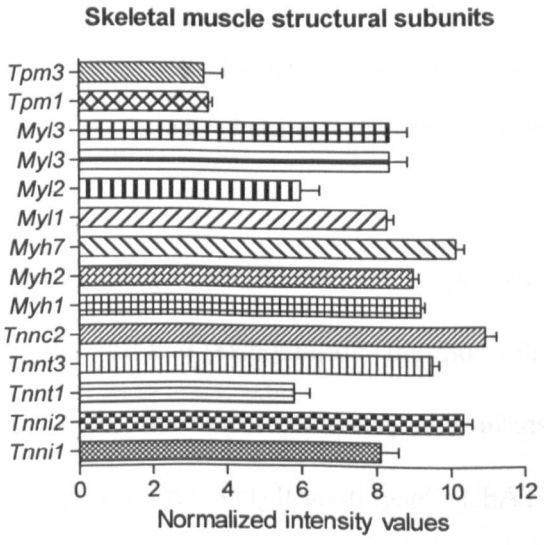


Figure 3-5: RNA transcript levels for muscle structural subunits classified as "present" in mixed skeletal muscle tissue for three replicates from two independent repeats (male Wistar rats).

### 3.5.5 mRNA expression for skeletal muscle-defining receptors

In order to define skeletal muscle, the relative expression of ryanodine receptors was investigated. *Ryr1* and *ryr3* were classified as "present". However, *ryr2* was classified as "marginal" in all skeletal muscle replicates (38038 ranking out of 41090). *Ryr1* was highly detected compared to *ryr3* in skeletal muscle (269 and 20718, respectively ranking out of 41090) and above reference gene (TATA box binding protein (Tbp)) (Figure 3-6). In other words, *ryr1* was highly expressed in skeletal muscle compared to others (Figure 3-6).

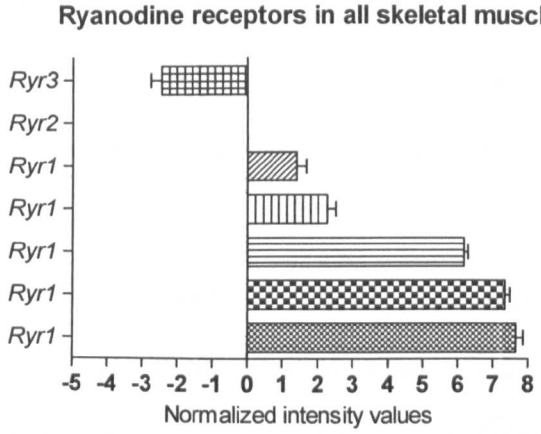


Figure 3-6: RNA transcript levels for ryanodine receptors classified as "present" in mixed skeletal muscle tissue for three replicates from two independent repeats (male Wistar rats).

Neuromuscular junctions (NMJs) consists of presynaptic (the axon terminal of a motor neuron), synaptic cleft and postsynaptic (the motor end plate of a muscle fibre) elements. Acetylcholine (ACh), the major excitatory neurotransmitter at neuromuscular junctions, is synthesized by "choline acetyltransferase" (ChAT), and ACh is loaded into synaptic vesicles by "the vesicular acetylcholine transporter" (VAChT) (de Castro *et al.*, 2009). ACh diffuses into the synaptic cleft and activates the nicotinic acetylcholine receptors which are expressed in skeletal muscle (Kues *et al.*, 1995). ACh actions are terminated by acetylcholinesterase (AChE) which is also expressed in skeletal muscle (Herman *et al.*, 1985). It is worth noting that there are synaptic-vesicle-associated proteins such as synaptophysin and synaptotagmin (Fox *et al.*, 2007; Juzans *et al.*, 1996), and axonal proteins (neurofilaments) to support normal axonal growth, are expressed in neurons (Hoffman *et al.*, 1987).

In order to define skeletal muscle and also to examine any contamination from the nerve terminal, the relative mRNA expression of nicotinic acetylcholine receptor subunits α, β, ε, δ and γ genes (*chrnα, chrnβ, chrnγ, chrnδ, chrnε*), acetylcholinesterase gene (*ache*),

choline acetyltransferase (*chat*) and vesicular acetylcholine transporter (*slc18a3*), neurofilaments (light (*nefl*), medium (*nefm*) and heavy (*nefh*)), synaptotagmin I and II (*syt1 and syt2*) and synatophysin (*syp*) were investigated using the microarray.

Nicotinic acetylcholine receptor subunits α1, β1, ε, δ and γ genes were detected (high intensity values (ranking ~ 8000 out of 41090)) compared to muscarinic receptor 3 gene (*chrm3*) (ranking for chrm3 was ~ 14547 out of 41090). Other muscarinic receptors were classified as "marginal" in all skeletal muscle repilcates (ranking ~ 30000 out of 41090). Acetylcholinesterase (*ache*) was detected (high intensity values) compared to synaptotagmin I and II (*syt1 and syt2*). Moreover, choline acetyltransferase (*chat*) and vesicular acetylcholine transporter (*slc18a3*), neurofilaments (light (*nefl*), medium (*nefh*) and heavy (*nefh*)) were not detected in skeletal muscle tissues (Figure 3-7).

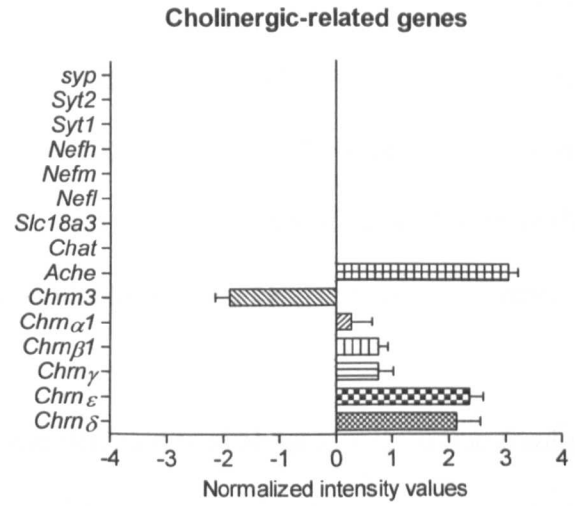


Figure 3-7: RNA transcript levels for nicotinic receptor subunits, muscarinic receptor 3 and acetylcholinesterase classified as "present" in mixed skeletal muscle tissue for 3 replicates from two independent repeats (male Wistar rats).

### 3.5.6 mRNA expression of GPCRs

The mRNA relative intensity values of GPCR entities classified as "present" in all skeletal muscle replicates using microarray is shown in Table 9-12 in Appendix.

88 GPCRs out of 329 (taken from "The International Union of Basic and Clinical Pharmacology") in all skeletal muscle samples were classified as "present" using Agilent microarray. From 88 GPCRs, a number of different receptors coupled to different G proteins were selected for further investigation in the next chapters based on the following criteria:

1) Any of the signals for the GPCR entities is above the lowest signal of reference gene (*tbp*) of any skeletal muscle replicates (-0.2) or above the lowest signal from any of the nicotinic cholinergic subunits (chrnα1) of any skeletal muscle

replicates (-0.72=~-1). *Tbp* is used as a reference gene to normalize the gene expression in tissues that display structural reorganization and architectural changes (Yuzbasioglu *et al.*, 2010). Moreover, it is well-known that nicotinic cholinergic receptors are expressed in skeletal muscle (Kues *et al.*, 1995).

2) Known and available ligands, local expertise and cost.

38 GPCR entities were detected in skeletal muscle tissue (ranked higher (higher relative intensity values) than either nicotinic cholinergic alpha subunit (*chrnα1*) or reference gene (*tbp*) (12526 and 10220 ranking out of 41090, respectively)), see (Table 9-12) in Appendix. From these 38 GPCR entities, $\beta_2$-adrenoceptors, $P2Y_1$, $P2Y_2$ and $P2Y_6$ receptors, $A_1$ and $A_{2A}$-adenosine receptors, NPY Y1 receptor and $\alpha_2$-adrenoceptors were selected as shown in Table 3-7. These GPCR entities include three main families that coupled to different G proteins ($G_s$, $G_i$ and $G_q$) in this study. Examples of $G_s$-GPCRs are $\beta_2$-adrenoceptor, $A_{2A}$-adenosine receptor, $G_i$-GPCRs are $A_1$ adenosine receptor and NPY Y1 receptor, and $G_q$-GPCRs are $P2Y_1$, $P2Y_2$ and $P2Y_6$ receptors. These examples of detected GPCR entities will be investigated in the next chapter to examine the possible different signalling in skeletal muscle cells. Indeed, investigation of the different families ($G_s$, $G_i$ and $G_q$) of GPCRs might help to confirm the expression and understand the expected signalling and functional role of these receptors and to investigate the possible cross-talk between GPCRs signalling and their signalling partners' genes.

Table 3-7: Relative intensity values for selected detected GPCRs (comprising three major families of G protein signalling) in all skeletal muscle replicates. Site A is a mixture of extensor digitorum longus and tibialis anterior, site B is a mixture of soleus and plantaris, and site C is a mixture of red and white gastrocnemius muscle with roughly equal amounts of each muscle. The GPCRs was selected depending on known and available ligands local expertise, cost and above either cholinergic subunit (*chrnα1*) or *tbp* relative intensity values. NA: Not Applicable.

| Rat A | | | Rat B | | | | GPCR (gene name) [gene id] |
|---|---|---|---|---|---|---|---|
| Site | | | | | | | |
| A | B | C | A | B | C | Principal G protein | |
| 1.7 | 1.2 | 0.9 | 1.4 | 1.6 | 1.7 | $G_q$ | purinergic receptor P2Y, G-protein coupled 2 (P2ry2), mRNA [NM_017255] |
| 1.2 | 0.8 | 1.2 | 1.1 | 1.1 | 0.9 | $G_s$ | adrenergic receptor, β 2 (Adrb2), mRNA [NM_012492] |
| 0.0 | -0.2 | 0.5 | 0.7 | 0.5 | 0.3 | $G_s$ | adenosine A2a receptor (Adora2a), mRNA [NM_053294] |
| -0.3 | -0.7 | 0.1 | 0.0 | 1.0 | 0.0 | $G_q$ | pyrimidinergic receptor P2Y, G-protein coupled, 6 (P2ry6), mRNA [NM_057124] |
| -0.6 | -1.3 | -0.7 | -0.5 | -0.4 | -0.6 | $G_i$ | adenosine A1 receptor. [Source:Uniprot/SWISSPROT;Acc:P25099] |
| 0.2 | 0.1 | -1.2 | -0.5 | -1.2 | -1.5 | $G_i$ | adrenergic receptor, alpha 2a (Adra2a), mRNA [NM_012739] |
| -1.2 | -1.2 | -1.9 | -1.8 | -1.7 | -0.9 | $G_q$ | purinergic receptor P2Y, G-protein coupled 1 (P2ry1), mRNA [NM_012800] |
| -1.2 | -1.1 | -2.8 | -1.8 | -1.0 | -1.7 | $G_i$ | neuropeptide Y receptor Y1 (Npy1r), mRNA [NM_001013032] |
| -0.2 | 0.0 | 0.3 | 0.3 | 0.8 | -0.2 | NA | TATA box binding protein (Tbp), mRNA [NM_001004198] |
| 0.1 | -0.6 | -0.7 | 1.1 | 1.5 | 0.3 | NA | cholinergic receptor, nicotinic, alpha 1 (muscle) (Chrna1), mRNA [NM_024485] |

### 3.5.7 mRNA expression of GPCRs using QRT-PCR (Taqman)

Some entities were selected to be examined by QRT-PCR (Taqman). The criteria was to cover different ranking areas from the microarray entities list and to select GPCR entities that possibly have some expected roles in skeletal muscle glucose metabolism (Eckardt *et al.*, 2008b; Lindborg *et al.*, 2011; Overton *et al.*, 2008; Ravinet Trillou *et al.*, 2004; Swaminath, 2008).

Examining mRNA expression of these receptors ($CB_1$ receptor, GPR119, $\alpha_2$-adrenoceptors and GPR40) in skeletal muscle will be helpful in this study for further investigation. This is due to the fact that $CB_1$ receptors have been implicated to possibly play a role in the development of insulin resistance in obese as well as diabetic patients with elevated levels of endocannabinoids (Ravinet Trillou *et al.*, 2004). Moreover, a relationship between GPR40 or GPR119 and diabetes has been suggested. However, the mechanisms behind these issues are still unclear (Overton *et al.*, 2008; Swaminath, 2008). In order to examine the expression of these receptors and validate the mRNA expression of GPCRs, QRT-PCR (Taqman) was performed.

mRNA of *actb* and *18S* were detected in QRT-PCR (Taqman) at Ct values of ~ 19 and 22, respectively (ranking in the microarray; 8 and 275, respectively, out of 41090). mRNA for *adra2a* and *cnr1* were detected in rat skeletal muscle tissues at Ct ~ 32 and 27, respectively (ranking in the microarray; 14208 and 34463/35034 out of 41090, respectively). There was no significant difference in the expression of *adra2a* and *cnr1* between skeletal muscle and adipose tissues using QRT-PCR (Taqman). *Gpr40* was not detected using QRT-PCR (Taqman) (ranking in the microarray; 40809 out of 41090). *Gpr119* was detected at Ct ~ 33 (ranking in the microarray; 25255 out of 41090-

marginal in 4 skeletal muscle replicates out of 6 replicates) (Figure 3-6)). Overall, *actb*, *18S*, *cnr1*, *gpr119* and *adra2a* were detected in skeletal muscle tissues.

Table 3-8: Ct values for QRT-PCR (Taqman) for GPCR entities and reference genes for skeletal muscle cells and tissues and for liver and adipose tissues from two replicates from two rat repeats.

| Gene/Ct value | Skeletal | Myotube | Myoblast | Liver | Adipose |
|---|---|---|---|---|---|
| *Actb* | 19.5 | 16.5-17.5 | 16.5-17.9 | 20.0 | 17.6 |
| *18S* | 21.5-23.0 | 21.5 | 22.5 | 22.5 | 22.5 |
| *Gpr40* | Undetermined | Undetermined | Undetermined | Undetermined | Undetermined |
| *Cnr1* | 26.5-27.0 | 27.5 | 27.5 | 31.0 | 27.5 |
| *Adra2a* | 31.0-32.0 | 30.0 | 28.0 | 37.0 | 30.0 |
| *Gpr119* | 32.0-33.0 | 35.0-36.0 | 35.0 | 31.0 | 31.5 |

### 3.5.8 mRNA expression of GPCR protein signalling partners

To measure the mRNA levels of a comprehensive profile of GPCR signalling-related gene products, microarray was used.

mRNA of four main G protein α subunits *(gnas, gnai (gnai2 and 3), gnaq, gna11* and *gna12)* were classified as "present" in all skeletal muscle replicates. However, *gnas* was found be highly detected (553 ranking out of 41090) compared to others and above *tbp* reference gene (Figure 3-8-A).

The mRNA sequence for the *gnai2* isoform was validated compared to the provisional mRNA sequence of *gnai1* and *gnai3* in rat. All G-protein β and γ isoforms were classified as "present" in all skeletal muscle replicates. *Gnb1, gnb2, gnb5, gng5, gng10* and *gng12* were highly detected compared to the others (3351, 2562, 6308 and 8247

ranking out of 41090) and above *tbp* reference gene (Figure 3-8-B,-C).

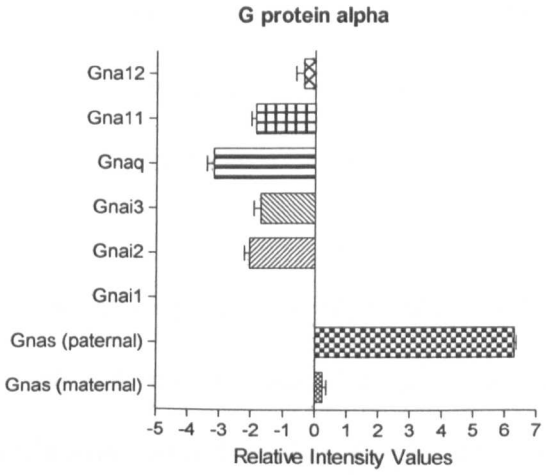


A)

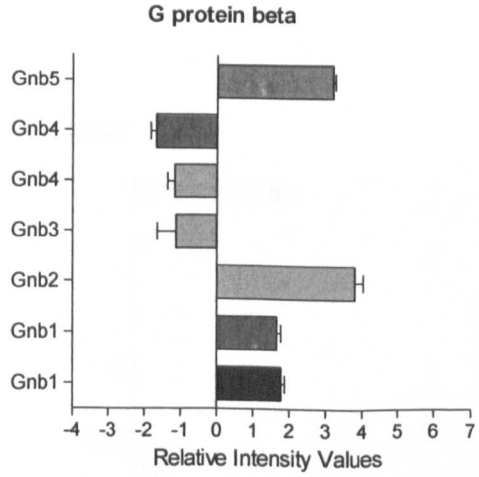


B)

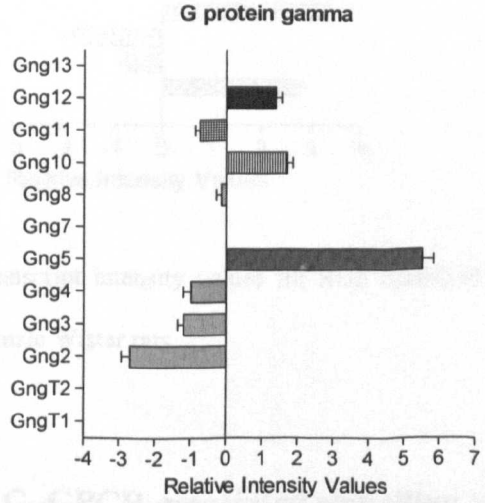


C)

Figure 3-8: RNA transcript intensity values for G protein-α (A), G protein-β (B) and G protein-γ (C) subunits classified as "present" in mixed skeletal muscle generated from two male Wistar rats.

GPCR signalling pathways are modulated by ancillary proteins including regulator of G protein signalling (RGS). RGS are proteins that act as GTPase accelerating proteins for alpha subunit (De Vries *et al.*, 2000; Sierra *et al.*, 2000). To investigate the relative expression of these genes, microarray was used.

mRNA encoding *rgs2, rgs3, rgs4, rgs5, rgs10, rgs11, rgs14, rgs19* and *Axin1* were classified as "present" in all skeletal muscle replicates. *Rgs2, rgs5 and Axin1* were highly detected compared to the others (3366, 4414 and 3094 ranking out of 41090) and above *tbp* reference gene (Figure 3-9).

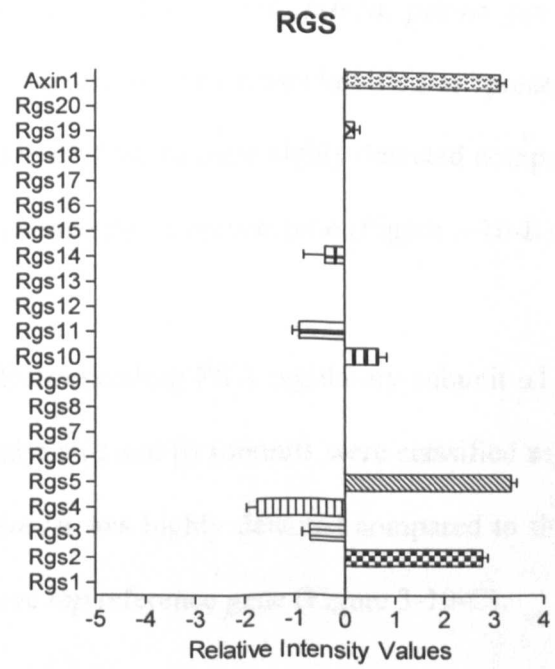


Figure 3-9: RNA transcript intensity values for RGS classified as "present" in mixed skeletal muscle generated from two male Wistar rats.

### 3.5.8.1 $G_s$ and $G_i$-GPCR-associated signalling proteins

$G_{\alpha s}$ and $G_{\alpha i}$ modulate adenylyl cyclase (AC) activity. This enzyme converts ATP to

cAMP. Phosphodiesterase (PDE) is an enzyme that terminates cAMP signalling. The cAMP level modulates protein kinase A (PKA) activity. There are different isoforms of AC, PKA and PDE. To investigate the relative expression of these genes, microarray was used.

mRNA encoding *adcy2, adcy4, adcy5, adcy6, adcy7 and adcy10* were classified as "present" in all skeletal muscle replicates. *Adcy2* and *adcy6* were highly detected compared to the others (1061 and 2631, respectively ranking out of 41090) and above *tbp* reference gene (Figure 3-10-A).

mRNA encoding *pde1b, pde2a, pde4a, pde4b, pde4d, pde7a, pde7b, pde8a, pde9a, pde10a* and *pde11a* were classified as "present" in all skeletal muscle replicates. *Pde4a, pde4b and pde4d* were highly detected compared to others (8480 ranking out of 410990) and above *tbp* reference gene (Figure 3-10-B).

mRNA encoding PKA regulatory subunit α1 and α2 (*Prkar1a* and *Prkar2a*) as well as catalytic (α and β) subunits were classified as "present" in all skeletal muscle replicates. *Prkar1a* was highly detected compared to the others (6759 ranking out of 41090) and above *tbp* reference gene (Figure 3-10-C).

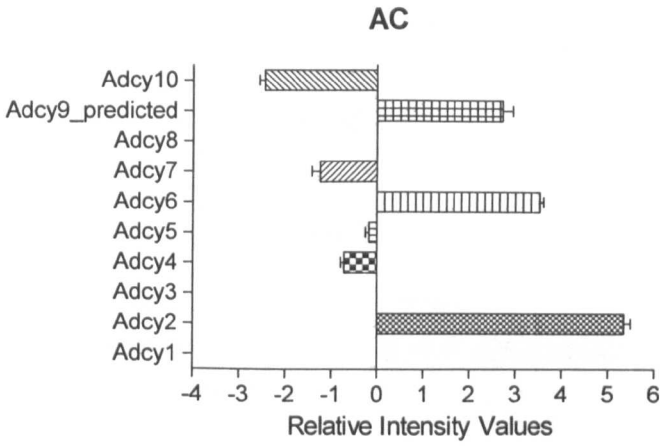
AC
Adcy10
Adcy9_predicted
Adcy8
Adcy7
Adcy6
Adcy5
Adcy4
Adcy3
Adcy2
Adcy1
-4 -3 -2 -1 0 1 2 3 4 5 6
Relative Intensity Values

A)

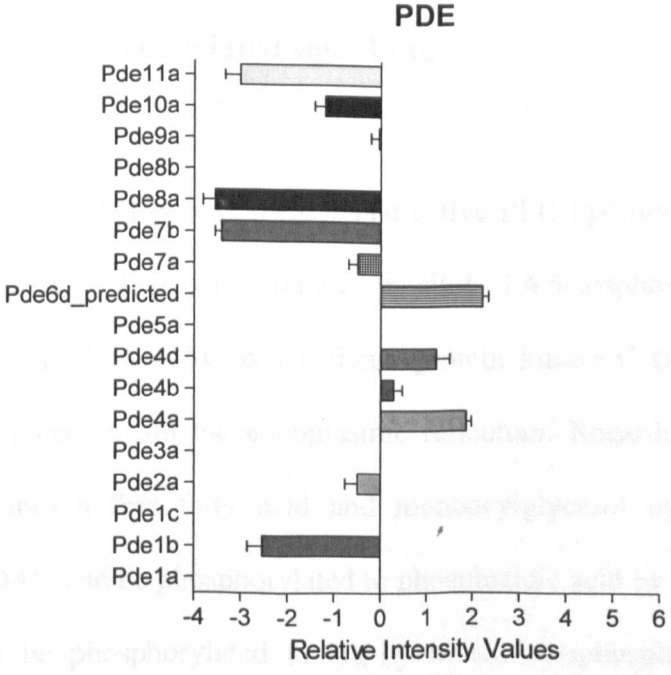
PDE
Pde11a
Pde10a
Pde9a
Pde8b
Pde8a
Pde7b
Pde7a
Pde6d_predicted
Pde5a
Pde4d
Pde4b
Pde4a
Pde3a
Pde2a
Pde1c
Pde1b
Pde1a
-4 -3 -2 -1 0 1 2 3 4 5 6
Relative Intensity Values

B)

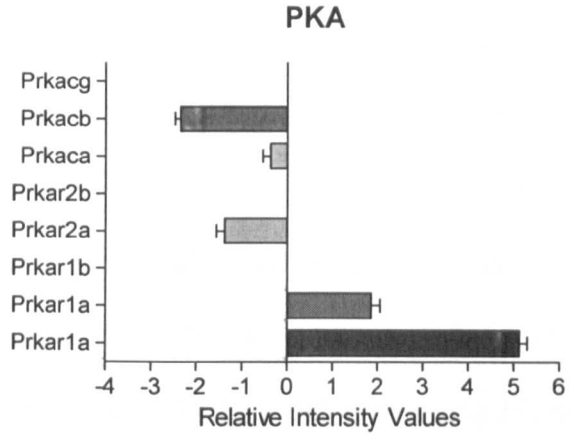


C)

Figure 3-10: RNA transcript intensity values for AC (A), PDE (B) and PKA subunits (C) and classified as "present" in mixed skeletal muscle generated from two male Wistar rats.

### 3.5.8.2 $G_q$-protein-associated signalling

$G_{\alpha q}$ activates phospholipase C (PLC). The active PLC hydrolyses phosphatidylinositol 4,5-bisphosphate ($PIP_2$) to produce inositol 1,4,5-trisphosphate ($IP_3$) and 1,2-diacylglycerol (DAG). DAG can activate protein kinase C (PKC), and $IP_3$ can also activate $IP_3$ receptors on the endoplasmic reticulum. Regarding DAG, DAG can be hydrolyzed into a free fatty acid and monoacylglycerol by diacylglycerol lipase. Moreover, DAG can be phosphorylated to phosphatidic acid by DAG kinase. Regarding $IP_3$, $IP_3$ can be phosphorylated to $IP_4$ by inositol-trisphosphate kinase (*itpk*) while inositol phosphate can be dephosphorylated to inositol by inositol monophosphatase (*impa*). To investigate the relative expression of these genes, microarray was used.

mRNA encoding *plcb3, plcb4, plcd1, plcd3, plcd4, plce1* and *plcl1* were classified as "present" in all skeletal muscle replicates. *Plcd1* and *plcd4* were highly detected compared to the others (7286 ranking out of 41090) and above *tbp* reference gene

(Figure 3-11-A). mRNA encoding *dagla, daglb, dgka, dgkg and dgkz* were classified as "present" in all skeletal muscle replicates. *Daglb and dgkz* were highly detected compared to the others (7018 ranking out of 41090) and above *tbp* reference gene (Figure 3-11-B). mRNA encoding *prkca, prkcb, prkcd, prkce, prkcg, prkch, prkcq* and *prkcz* were classified as "present" in all skeletal muscle replicates. *Prkcd and prkcq* were highly detected compared to the others and above *tbp* reference gene (10220 ranking out of 41090) (Figure 3-11-C). mRNA encoding $IP_3$ receptors (*itpr1, itpr2* and *itpr3*), $IP_3$ kinase b and c (*itpkc* and *itpkb*), *impa1* and *impa2* were classified as "present" in all skeletal muscle replicates. *Impa1* and *impa2* were detected in skeletal muscle compared to *tbp* reference gene (Figure 3-11-D).

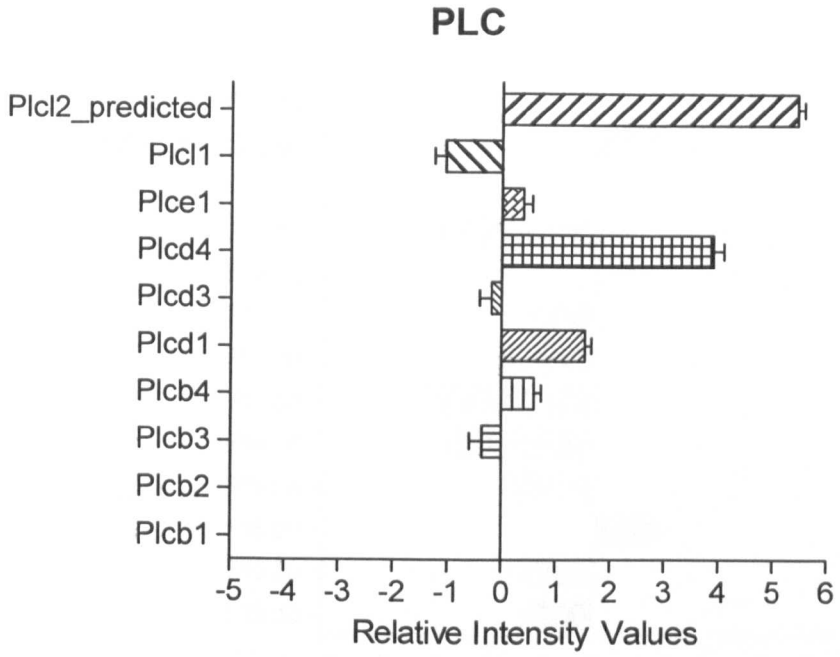
PLC
Plcl2_predicted
Plcl1
Plce1
Plcd4
Plcd3
Plcd1
Plcb4
Plcb3
Plcb2
Plcb1
-5 -4 -3 -2 -1 0 1 2 3 4 5 6
Relative Intensity Values

A)

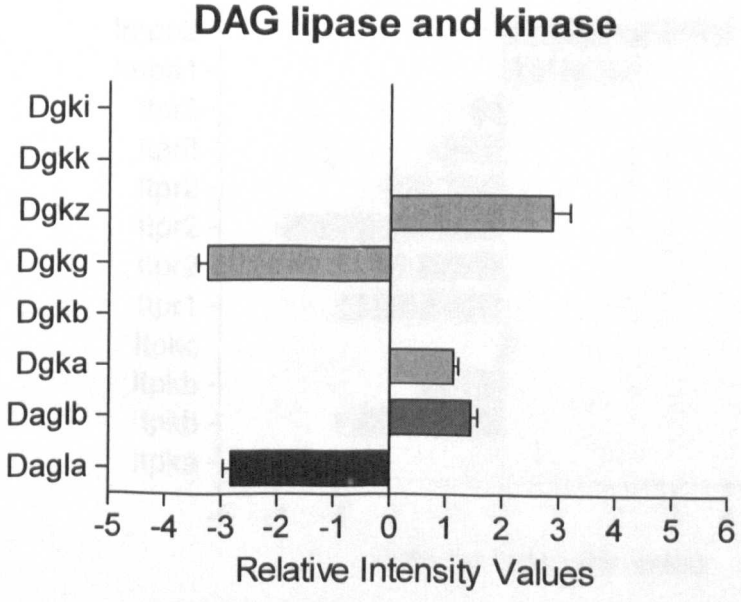
DAG lipase and kinase
Dgki
Dgkk
Dgkz
Dgkg
Dgkb
Dgka
Daglb
Dagla
-5 -4 -3 -2 -1 0 1 2 3 4 5 6
Relative Intensity Values

B)

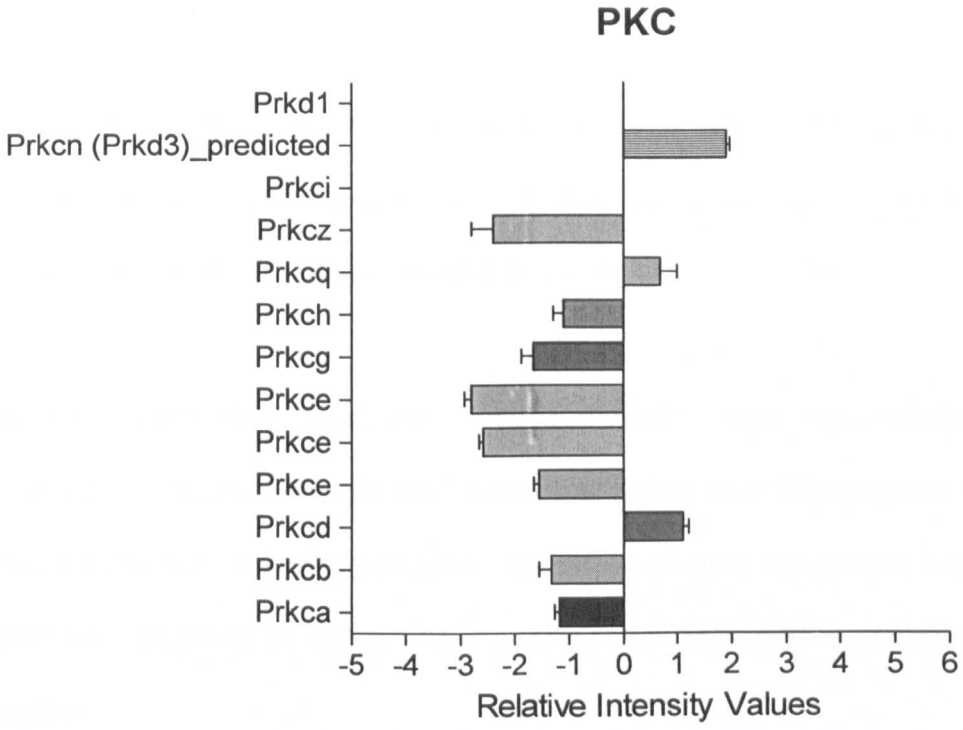


C)

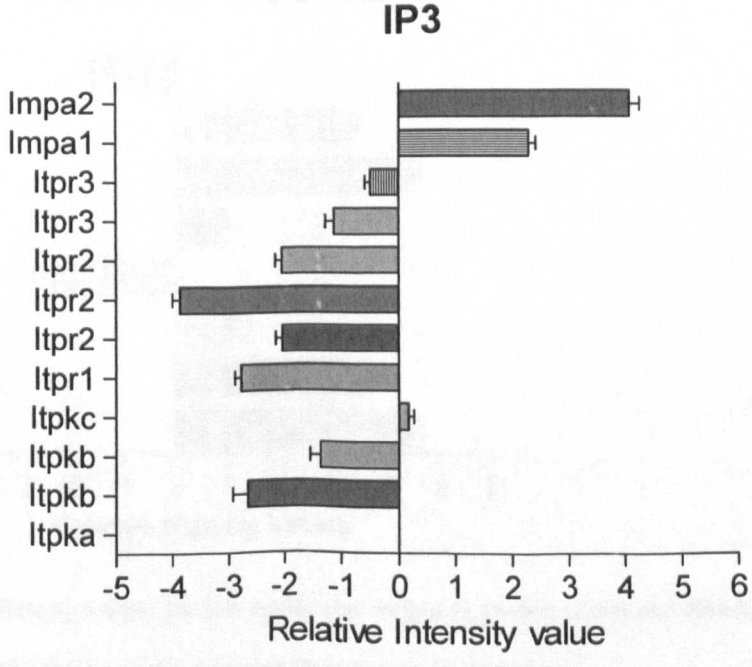


D)

Figure 3-11: RNA transcript intensity values for PLC (A), DAG related genes (B), PKC (C), and $IP_3$-related genes (D) classified as "present" in mixed skeletal muscle generated from two male Wistar rats.

### 3.5.8.3 $G_{12}$-protein signalling

$G_{\alpha 12}$ activates Rho guanine nucleotide exchange factors for the small G protein Rho. Consequently, Rho-GTP activates many enzymes such as Rho kinases. To investigate the relative expression of these genes, microarray was used.

mRNA encoding *rhoa, rhob, rhod, rhog, rhoq* and *rock1, rock2* were classified as "present" in all skeletal muscle replicates. *Rock1* was highly detected compared to the other (3412 ranking out of 41090) and above *tbp* reference gene. *Rhoa and rhoq* were highly detected compared to others (3188 ranking out of 41090) and above *tbp* reference gene.

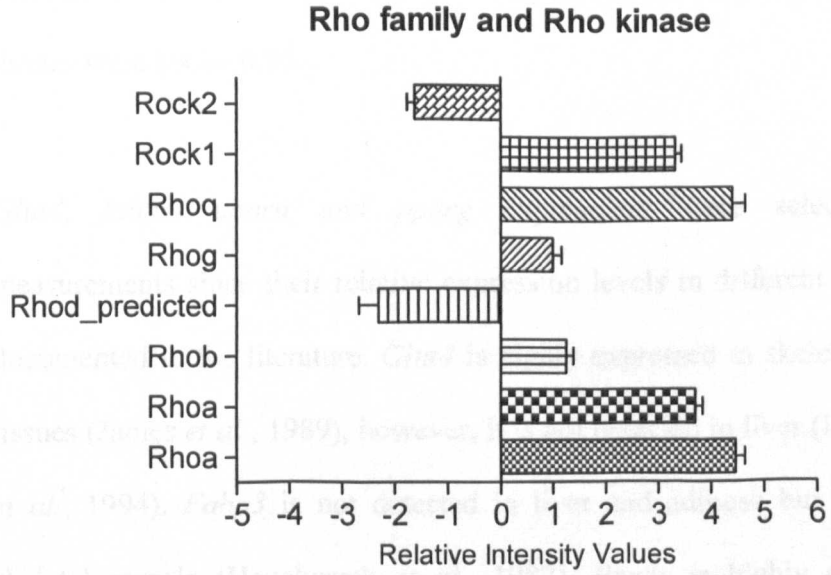


Figure 3-12: RNA transcript intensity values for low molecular weight G protein (Rho) and Rho-kinase classified as "present" in mixed skeletal muscle generated from two male Wistar rats.

## 3.6 Discussion

Traditional methods for the quantification of gene expression, such as RT-PCR or Northern blot analysis, focus on a single gene at a time. Therefore, these techniques are not suitable to determine the relative mRNA expression of GPCRs, G proteins and their target enzymes in skeletal muscle. Microarrays can be used to study simultaneously the relative expression of many genes.

### 3.6.1 Validation of the microarray

The two biological replicates were found to be reproducible since the Pearson correlations for normalized data for all pair combinations among biological replicate tissues were above 0.96.

*Glut4, fabp3, ppara and pparg* expressions were selected as confirmatory measurements since their relative expression levels in different tissues have been well documented in the literature. *Glut4* is highly expressed in skeletal muscle and adipose tissues (James *et al.*, 1989), however, it is not detected in liver (Liu *et al.*, 1992; Rayner *et al.*, 1994). *Fabp3* is not detected in liver and adipose but is highly expressed in skeletal muscle (Heuckeroth *et al.*, 1987). *Ppara* is highly expressed in liver and skeletal muscle with low expression in adipose tissue (Braissant *et al.*, 1996; Lemberger *et al.*, 1996). *Pparg* is expressed predominantly in adipose tissue with low expression seen in liver and muscle (Kiec-Wilk *et al.*, 2005; Vidal-Puig *et al.*, 1997). The findings of the present study confirmed that: a) *glut4* is highly expressed in skeletal muscle and adipose tissue relative to liver; b) *fabp3* is highly expressed in skeletal muscle and

negligibly expressed in liver and adipose; c) *ppara* is highly expressed in liver and skeletal muscle; and d) *pparg* is highly expressed in adipose tissue with low expression seen in liver and skeletal muscle tissue. This gave the microarray data to be valid and reliable to detect relative mRNA expression of genes in a tissue specific manner.

Slow and fast twitch muscle structural subunit genes mRNA were expressed in skeletal muscle. This reflects that the dissection has been covered both fast and slow skeletal muscle fibres. This also indicates that the detected GPCR entities will cover different types of fibres.

Contraction is one of the primary functions of skeletal muscle, involving cell-surface acetylcholine receptors and intracellular ryanodine receptors. Release of acetylcholine at the neuromuscular junction activates nicotinic acetylcholine receptors to cause skeletal muscle depolarization and contraction. Indeed, ryanodine receptors induce $Ca^{2+}$ release into the cytoplasm to prolong the contraction.

Nicotinic acetylcholine receptor subunits α1, β, ε, δ and γ genes and *ache* were detected in skeletal muscle tissue compared to choline acetyltransferase (*chat*), vesicular acetylcholine transporter (*slc18a3*), synaptotagmin I and II (*syt1* and *syt2*), synatophysin (*syp*) and neurofilaments (light (*nefl*), medium (*nefm*) and heavy (*nefh*)). This gave evidence for skeletal muscle specific receptor expression and also gave evidence that less contamination occurred to skeletal muscle from the nerve terminal during the dissection itself.

In this study, *ryr1* was highly expressed in skeletal muscle (269 ranking out of 41090) (Table 3-8). This is in line with what was shown in human and murine skeletal muscle

(Giannini *et al.*, 1995; Lanner *et al.*, 2010; Sei *et al.*, 1999). Moreover, *ryr2* was predominantely expressed in murine heart muscle and almost all over in the brain (Giannini *et al.*, 1995). *Ryr3* was universally expressed in murine tissues (Giannini *et al.*, 1995).

It was shown that RyR1 is responsible for sarcoplasmic reticulum (SR) depolarization-induced calcium release. This is supported by the fact that when RyR1 deficient skeletal muscle cells were used, calcium release was mostly eliminated in skinned skeletal muscle fibres of mice (Ikemoto *et al.*, 1997). However, RyR3 gave a weak SR depolarization-induced calcium release in skinned skeletal muscle fibres of RyR1 knock-out mice (Endo, 2009; Ikemoto *et al.*, 1997). Therefore, targeting RyR1 selectively might have implications for the contraction of skeletal muscle. The implication of this is that RyR1 might have a role in skeletal muscle contraction, consequently, it should be recommended to be also investigated as a therapeutic target for glucose uptake in skeletal muscle.

### 3.6.2 GPCR expression in skeletal muscle

GPCRs expression was examined in this study using two different techniques, Agilent microarray and QRT-PCR (Taqman). Using Agilent microarray, 38 GPCR entities were found to be expressed in skeletal muscle in this study. These include $LPA_1$ lysophosphatidic acid receptors (endothelial differentiation, lysophosphatidic acid G protein-coupled receptor, 2 (Edg2)), chemokine receptors 4 (CXCR4), glucagon receptor 2, platelet-activating factor receptors, $GABA_{B1}$ receptors, $S1P_2$ sphingosine-1-phosphate receptors (endothelial differentiation, sphingolipid G protein-coupled receptor, 5 (Edg5)), parathyroid hormone receptors, $mGlu_2$ and $mGlu_3$ metabotropic

glutamate receptors, dopamine $D_5$ receptors, neurotensin receptor 2, opioid receptor delta 1, calcitonin receptors 1, arginine vasopressin receptors 1A, bradykinin $B_2$ receptors and $C5a_1$ complement peptide receptors. However, other GPCR entities can not be excluded for being expressed in skeletal muscle.

These GPCRs are somewhat less well-known in terms of their activity in the skeletal muscle system. Relatively little information in the literature is reported in both normal and disease state about the role of these GPCRs in functional activities and in signal transduction of skeletal muscle tissues.

The importance of such GPCR patterns detected in skeletal muscle tissue might be approved in the regulation of several intracellular functions. These functions in skeletal muscle might include contractile responses, glucose uptake, regulation of metabolism and skeletal muscle proliferation, differentiation and growth. To date, virtually no information is available regarding physiological functions, pathophysiological roles, regulation and gene expression patterns of such GPCRs in skeletal muscle tissues.

As a large number of GPCR entities were discussed in this study, these GPCR entities were divided in their groups (class A, class B and class C) as described in Chapter One:

## G PROTEIN-COUPLED RECEPTORS CLASS A

$LPA_1$ lysophosphatidic acid receptors gene mRNA was found to be expressed in a wide range of different human and mouse tissues including skeletal muscle, heart, brain, stomach, kidney, spleen, thymus, testis and lung (An *et al.*, 1998; Choi *et al.*, 2010; Ye, 2008). $LPA_1$ lysophosphatidic acid receptors were also shown to couple to $G_{\alpha i}$, $G_{\alpha q}$, and $G_{\alpha 12/13}$ (Fukushima *et al.*, 1998; Ishii *et al.*, 2000). As skeletal muscle expressed *lpar1* in

this study, it is possible that the activation of $LPA_1$ lysophosphatidic acid receptors affect proliferation and differentiation in skeletal muscle. Therefore, $LPA_1$ lysophosphatidic acid receptor agonists might be considered as a therapeutic target to improve skeletal muscle mass. This is supported by the fact that 1) The activation of $LPA_1$ lysophosphatidic acid receptors by LPA was shown to stimulate proliferation, migration, and invasion in human colon cancer cell lines (DLD1) which expressed *lpar1* (Shida *et al.*, 2003). 2) *Lpar1−/−* mice were also found to have a higher adiposity than wild-type mice (Simon *et al.*, 2005). 3) $LPA_1$ lysophosphatidic acid receptor activation reduced the differentiation of mouse 3T3F442A preadipocytes (Simon *et al.*, 2005). Apart from that potential role, $LPA_1$ lysophosphatidic acid receptors might have a role in glucose uptake. As skeletal muscle expressed *lpar1* in this study, it is also possible that $LPA_1$ lysophosphatidic acid receptors play a role in glucose uptake in skeletal muscle, and it might be, therefore, considered as a therapeutic option for diabetes. The implication of this is that $LPA_1$ lysophosphatidic acid receptor agonists should be recommended to be investigated as a therapy to treat diabetes. This is probably due to the fact that LPA was shown to stimulate GLUT4 translocation and glucose uptake in 3T3-L1 adipocytes and L6 GLUT4myc myotubes which expressed $LPA_1$ lysophosphatidic acid receptors (Yea *et al.*, 2008), and acute administration of LPA in mice was also shown to cause a fall in blood glucose level (Yea *et al.*, 2008).

Regarding another GPCR, GPCR activators such as chemokines, a large family of 8 to 10-kd cytokines or proteins, act as chemoattractants (Luster, 1998). The activation of chemokine receptors by chemokines lead to activation of phospholipases through G proteins which yield to an increase in $IP_3$, the release of calcium and the activation of protein kinase C (Luster, 1998). Moreover, chemokines were also shown to activate the Ras and Rho families (Laudanna *et al.*, 1996). Chemokines such as SDF1α, stromal

cell-derived factor-1 alpha, can bind to specific GPCRs such as CXCR4 (Gi or Gq coupled). Indeed, *cxcr4* was detected in skeletal muscle in this study. This is consistent with *cxcr4* was expressed in skeletal muscle satellite cell lines (Ratajczak *et al.*, 2003). As skeletal muscle expressed *cxcr4* and *sdf1a* (1277 ranking out of 41090) in this study, it is possible that CXCR4 in skeletal muscle plays a role in migration during myogenesis which is essential for skeletal muscle growth and regeneration. This is suggested due to the fact that it was shown that SDF1α enhances migration and proliferation of the immortalized C2C12 muscle cell line (Odemis *et al.*, 2007), and chemokines were also suggested to be important for muscle precursor cells in the migration during myogenesis (Vasyutina *et al.*, 2005). Therefore, CXCR4 agonists might be recommended to be examined as a therapeutic option to improve skeletal muscle myogenesis, growth and to treat skeletal muscle regeneration disorders.

Platelet activating factor (PAF) receptors are thought to couple via $G_q$ protein and activate PLC which leads to calcium release and increase in DAG (Deo *et al.*, 2004; Izumi *et al.*, 1995; Shimizu *et al.*, 1992). PAF is a phospholipid activator with several physiological functions such as being a mediator of inflammation. Moreover, PAF is released from cells such as macrophages, basophils, monocytes and polymorphonuclear neutrophils. PAF response might be mediated through PAF receptors. As it was suggested that binding of PAF to its PAF receptors will be involved in its biological function such as inflammation, and PAF receptors gene mRNA was expressed in skeletal muscle in this study, it is possible that PAF receptors might have an inflammatory role in skeletal muscle. Therefore, therapeutic intervention by PAF receptor antagonists might be useful to decrease inflammation in skeletal muscle.

Apart from that potential role, PAF receptors might have a role in proliferation. As skeletal muscle expressed *ptafr* in this study, it is possible that PAF receptors might have a role in proliferation and differentiation in skeletal muscle through modulation mitogen-activated protein (MAP) kinase activity. This is supported by the fact that it was shown that stably transfected cells (Chinese Hamster Ovary Cells) with PAF receptors activate MAP kinase and MAP kinase kinase when these cells were exposed to PAF (Honda *et al.*, 1994), and it was also shown that PAF induced growth stimulation and inhibition in a dual manner in rat fibroblasts over-expressing PAF receptors (Kume *et al.*, 1997). The implication of this is that PAF receptors should be recommended to be investigated as a therapeutic option for skeletal muscle growth.

$S1P_2$ sphingosine-1-phosphate receptors (*s1pr2* (*edg5*)) gene mRNA was expressed in C2C12 myoblast and myotubes (Meacci *et al.*, 2003). $S1P_2$ sphingosine-1-phosphate receptors were also shown to couple to $G_{\alpha i}$, $G_{\alpha q}$, and $G_{\alpha 12/13}$ (Jiang *et al.*, 2007). As skeletal muscle expressed *s1pr2* in this study, and S1P was also shown to inhibit C2C12 proliferation and stimulate myogenic differentiation through activation of ERK1/ERK2 and p38 MAPK via $S1P_2$ sphingosine-1-phosphate receptors (Donati *et al.*, 2005), it is possible that $S1P_2$ sphingosine-1-phosphate receptors affect proliferation and differentiation in skeletal muscle. The implication of this is that $S1P_2$ sphingosine-1-phosphate receptor agonists should be examined as a potential therapeutic option to stimulate skeletal muscle growth and lean weight gain.

Another GPCR that needs attention is dopamine $D_5$ receptor (*drd5*). Dopamine receptors are classified into two groups, namely $D_1$-like and $D_2$-like receptors; the $D_1$ receptor/$D_5$ receptor group ($D_1$-like) and the $D_2$ receptor/$D_3$ receptor/D4 receptor group ($D_2$-like) are based on their molecular structures, physiological functions and

pharmacological activities. $D_1$-like receptors are positively coupled to adenylyl cyclase via heterotrimeric $G_s$ protein activation and the formation of cAMP while the $D_2$-like receptors are mainly coupled to $G_i$ which negatively modulates cAMP generation by inhibiting the activity of adenylyl cyclase (Herve *et al.*, 1993; Strange, 1993). Indeed, it was shown that the dopamine $D_1$ and dopamine $D_5$ receptors mediate the anti-atrophy effects of the dopamine 1/5 receptor after the treatment of skeletal muscle with selective dopamine $D_1/D_5$ receptor agonist, SKF 81297, through an increase in skeletal muscle cAMP (Reichart *et al.*, 2011). Moreover, levodopa with carbidopa ((L-3,4-dihydroxyphenylalanine (L-DOPA), the precursor to the dopamine)), was also shown to diminish glycogen synthase activity, glycogen concentration and insulin-stimulated glucose transport in rat skeletal muscle, possibly through intervening insulin-stimulated tyrosine phosphorylation of insulin receptor substrate (IRS)-1 (Smith *et al.*, 2004). Furthermore, *drd5* was detected in skeletal muscle in this study. In sum, it is possible that dopamine $D_5$ receptor might have multiple roles in skeletal muscle including glucose uptake and skeletal muscle growth. Further investigation should be recommended to examine dopamine $D_5$ receptor agonists as a therapeutic target to treat skeletal muscle regeneration disorders and to examine dopamine $D_5$ receptor antagonists as a therapeutic target to treat diabetes.

Neurotensin (nts) receptor 2 *(Ntsr2)* gene mRNA was expressed in mouse and rat brain (Chalon *et al.*, 1996; Sarret *et al.*, 1998; Walker *et al.*, 1998). Nts-stimulated ERK1/2 was shown in rat cultured cerebellar granule cells expressing nts receptor 2 (Gendron *et al.*, 2004; Sarret *et al.*, 2002). Neurotensin is a 13 amino acid neuropeptide released from the brain. The activation of nts receptors 2 with SR48692 and SR142948A, nts receptor 1 antagonist and nts receptor 2 agonist respectively, was found to stimulate the MAP kinase activity and trigger inositol phosphate accumulation and calcium

mobilization in Chinese hamster ovary cells (CHO) expressing human nts receptor 2 (Vita *et al.*, 1998). Indeed, skeletal muscle expressed *ntsr2* in skeletal muscle in this study. It is possible that nts receptors 2 might play a role in proliferation, differentiation and contraction in skeletal muscle. Therefore, it is recommended to investigate the nts receptor 2 agonists as a pharmacological option to stimulate lean weight gain and skeletal muscle growth.

Opioid receptors couple to $G_i$ protein (Law *et al.*, 2000). Activation of opioid receptors delta 1 was also shown to increase intracellular calcium levels in neuroblastoma x glioma hybrid NG108-15 cells (Jin *et al.*, 1992), and to stimulate ERK1/2 activity in rat fibroblasts and human embryonic kidney (HEK) cells, expressing opioid receptors delta 1 (Burt *et al.*, 1996; Schulz *et al.*, 2004; Tso *et al.*, 2000). Indeed, skeletal muscle expressed opioid receptors delta 1 (*oprd1*) in this study. It was also reported that the density of opioid receptors delta 1 was found to be higher in muscles from obese diabetic mice compared to normal mice using autoradiography (Evans *et al.*, 1995; Evans *et al.*, 1996). It was also shown that beta-endorphin, a non-selective endogenous opioid receptors ligand, increased the glucose uptake in soleus muscles taken from lean male mice via opioid receptor delta 1 (Evans *et al.*, 2001), and increased glucose uptake in resting and contracting skeletal muscle (Evans *et al.*, 1997). Indeed, beta-endorphin was found to be released into the circulation during exercise (Carr *et al.*, 1981; Goldfarb *et al.*, 1997). Taken together, it is possible, therefore, that these opioid receptors delta 1 might be important for maintaining muscle function during exercise through beta-endorphin, and might also be involved in glucose uptake, differentiation and growth in skeletal muscle. Therefore, it is possible that the opioid receptors delta 1 agonists might be considered as a therapeutic option for diabetes and skeletal muscle regeneration disorders.

Arginine vasopressin (AVP) receptor 1A (*avpr1a*) gene mRNA was expressed in skeletal muscle in this study. This is consistent with *avpr1a* was shown to be expressed in human skeletal muscle tissue, and was also shown to be expressed significantly higher in proliferating myoblasts than in differentiated myotubes in rat L6C5 myogenic cells (Alvisi *et al.*, 2008; Thibonnier *et al.*, 1996).

AVP was shown to induce myogenic differentiation of rat L6 cells and mouse satellite cells (Nervi *et al.*, 1995). Moreover, the effects of AVP could be mediated through the Arginine vasopressin receptors 1A which were found to couple to $G_q$ in CHO cells (Briley *et al.*, 1994). Arginine vasopressin receptors 1A overexpressed in mouse skeletal muscle in mice was also shown to exhibit significantly increased expression of differentiation markers such as Pax7, embryonic-MHC and myogenin and to accelerate the activation of satellite cells compared to mock-transfected mice (Toschi *et al.*, 2011). Taken together, these data suggest a potential role of this receptor in induction of myogenic differentiation and that could be involved in the regulation of myogenesis in skeletal muscle. Therefore, further investigation is recommended to examine this receptor as a potential therapeutic target for diseases characterized by altered muscle regeneration.

Another GPCR that needs attention is bradykinin $B_2$ receptor, bradykinin exerts its effect on two subtypes of $G_q$-GPCR, namely bradykinin $B_1$ and $B_2$ receptors (Leeb-Lundberg *et al.*, 2005). Bradykinin $B_2$ receptor (*bdkrb2*) mRNA was detected in skeletal muscle in this study. This is consistent with the bradykinin $B_2$ receptor was found to be detected on the plasma membrane of skeletal muscle cells of the rat hindlimb (Figueroa *et al.*, 1996), and it was also reported that bradykinin $B_2$ receptors were expressed in guinea pig skeletal muscle tissue (Rabito *et al.*, 1996).

As *bdkrb2* was detected in skeletal muscle in this study, it is possible that bradykinin $B_2$ receptors might play a role of insulin resistance and glucose uptake in skeletal muscle, and therefore bradykinin $B_2$ receptor agonists be recommended to be investigated as a therapeutic target for diabetic patients. This is supported by the fact that chronic *in vivo* administration of bradykinin was shown to significantly improve whole body glucose tolerance in the severely insulin resistant obese Zucker rat which was suggested to be a result of the enhanced insulin-stimulated skeletal muscle glucose uptake (Henriksen *et al.*, 1998), and bradykinin $B_2$ receptor knockout mice was also shown to have impaired insulin-dependent glucose transport (Duka *et al.*, 2001). Apart from that potential role, bradykinin $B_2$ receptor might have an inflammatory role. Bradykinin, a nine amino acid polypeptide, is one of various inflammatory mediators released from inflamed tissues after tissue injury to mediate the inflammatory process (Dray *et al.*, 1993). As inflammatory muscle pain was shown to be associated with the up-regulation of both bradykinin $B_1$ and $B_2$ receptors which contributed to mechanical hyperalgesia in inflammatory muscle pain in male Swiss mice (Meotti *et al.*, 2012), and *bdkrb2* was also detected in skeletal muscle in this study, it is possible that bradykinin $B_2$ receptors might play a role in inflammatory skeletal muscle pain. Therefore, antagonizing bradykinin $B_2$ receptors in skeletal muscle might be considered as a therapeutic target for pain management.

With regard to another GPCR, $C5a_1$ complement peptide receptors gene mRNA was reported to be expressed in monocytes, neutrophils, esinophils and basophils, and it was also shown that c*5ar1* was expressed in human liver and HepG2, lung cells, astrocytes and microglia cells (Haviland *et al.*, 1995; Lacy *et al.*, 1995). It was also shown that c*5ar1* was up-regulated in injured human skin and rat burn injury (Greco *et al.*, 2010; Yang *et al.*, 2007) and up-regulated in casting and tenotomy-induced muscle atrophy in

male mice (Bialek *et al.*, 2011). Indeed, skeletal muscle expressed c*5ar1* in this study. Taken together, it is possible, therefore, that the $C5a_1$ complement peptide receptors play a role in skeletal muscle injury, wound pathophysiology and growth. However, little information in the literature was reported about the role of $C5a_1$ complement peptide receptors in skeletal muscle. Apart from that potential role, $C5a_1$ complement peptide receptors might have a role in obesity. It was also reported that c*5ar1* was up-regulated from omental adipose in obese human being compared to normal human being using gene expression microarray (Gomez-Ambrosi *et al.*, 2004). It is possible, therefore, that $C5a_1$ complement peptide receptors in skeletal muscle might be investigated as a therapeutic target for obesity. The implication of this is that $C5a_1$ complement peptide receptor antagonists should be investigated to decrease weight, to improve skeletal muscle growth and wound healing.

## G PROTEIN-COUPLED RECEPTORS CLASS B

Glucagon receptor (*Gcgr*) gene mRNA were expressed in multiple tissues at relatively high levels such as liver, kidney, heart, adipose tissue and at relatively low level in rat skeletal muscle tissue (Hansen *et al.*, 1995). Glucagon, which is secreted from the alpha cells of the pancreas, exerts its effects by binding to the glucagon receptors. Glucagon receptors are known to couple to $G_s$, $G_i$ and $G_q$ (Jiang *et al.*, 2003a; Mayo *et al.*, 2003). Coupling to $G_s$ will activate AC and increase cAMP level, and then the elevation of cAMP level will activate PKA which lead to the phosphorylation of many proteins in the liver involved in glycogenolysis (such as glycogen phosphorylase kinase, glucose-6-phosphatase and glycogen synthase), gluconeogenesis (such as phosphoenolpyruvate carboxykinase (PEPCK) and glucose-6-phosphatase) and glycolysis (such as pyruvate kinase) (Jiang *et al.*, 2003a). The two splice variant glucagon receptor transcripts has been reported in rat tissues, however the physiological significance of these transcripts

remain unclear. Little is known about the glucagon receptors in skeletal muscle. However, antagonizing glucagon action through the glucagon receptors, which was expressed in skeletal muscle in this study, might provide avenue for a therapeutic option for diabetes.

Apart from that potential role, glucagon receptors might activate ERK in skeletal muscle. As *Gcgr* was expressed in skeletal muscle in this study, it is possible, therefore, that glucagon receptors might affect proliferation and differentiation through ERK activation or contraction through calcium release in skeletal muscle. This is probably due to the fact that glucagon was also shown to activate ERK1/2 in Human Embryonic Kidney (HEK) cells expressing human glucagon receptor (Jiang *et al.*, 2001) and glucagon was also shown to mediate calcium rise in baby hamster kidney cells (BHK) expressing human glucagon receptor (Hansen *et al.*, 1998). The implication of this is that glucagon receptors might be recommended to be investigated as a therapeutic target for skeletal muscle growth and contraction.

It is worth noting that glucagon receptor might preferentially couple to $G_{\alpha s}$, but it also couples to other G-proteins. Although most GPCRs can activate more than one $G_{\alpha}$-subtype, each GPCR shows preferential coupling to one subtype over another such as $G_s$, $G_i$ and $G_q$. Consequently, the defined $G_{\alpha}$-subtype activates specific downstream signalling pathway (Alexander *et al.*, 2012). This phenomenon might be defined by ligands under experimental or physiological conditions since the ligands induce conformational changes in the receptor. However, there is no evidence in the literature weather the overexpression is related to this phenomenon.

Parathyroid hormone (PTH) receptors 1 (*pthr1*) gene mRNA was abundantly expressed in rat kidney and bone tissues, and it was also expressed in many other rat tissues

including skeletal muscle, ovary, placenta, aorta, adrenal gland, bladder, brain, cerebellum, breast, heart, ileum, liver, lung, placenta, skin, spleen, stomach, uterus, and testes (Lee *et al.*, 1996; Tian *et al.*, 1993; Urena *et al.*, 1993). Moreover, PTH receptors 1 are thought to couple to $G_s$, $G_q$, $G_i$ and $G_{12}$ (Mahon *et al.*, 2006; Plati *et al.*, 2007; Singh *et al.*, 2005). Indeed, skeletal muscle expressed *Pthr1* in this study. Overall, it is possible that PTH receptors 1 modulate cAMP and calcium release in skeletal muscle tissue which might be important for muscle growth and contraction as discussed previously. The implication of this is that PTH receptors 1 might be recommended to be investigated to improve contraction-stimulated glucose uptake, consequently the PTH receptors 1 agonist might be used to treat diabetes.

Calcitonin receptor (*Calcr*) was shown to be linked to adenylyl cyclase and phospholipase C (Poyner *et al.*, 2002). Calcitonin is released from the parathyroid glands and its inhibitory effect on bone resorption is caused by the activation of calcitonin receptors in mature osteoclasts (Poyner *et al.*, 2002). *Calcr* was shown to be expressed in mature rat and human osteoclasts (Chen *et al.*, 2004; Nicholson *et al.*, 1986). However, this receptor was not detected in osteoclast progenitor cells, but the expression of this receptor increased during mouse and rat osteoclast differentiation (Quinn *et al.*, 1999). *Calcr* was also found to be expressed in mice and human satellite cells (Fukada *et al.*, 2007; Gnocchi *et al.*, 2009; Yamaguchi *et al.*, 2012). As *calcr* was expressed in skeletal muscle in this study, it is possible that calcitonin receptor might play a role in proliferation in skeletal muscle which might be important for skeletal muscle growth. This is supported by the fact that the activation of the calcitonin receptors was shown to increase ERK1/2 activity in HEK cells expressing calcitonin receptors (Chen *et al.*, 1998), and it was also reported that calcitonin receptor protein expression was down-regulated on activated satellite cells (Fukada *et al.*, 2007).

Therefore, calcitonin receptor agonists should be recommended to be investigated as a therapeutic option to improve skeletal muscle growth.

With regards to another GPCR, $GABA_{B1}$ receptors (*Gabbr1*) gene mRNA was expressed in human and rat brain (Berthele *et al.*, 2001; Bischoff *et al.*, 1999). It was also reported to be expressed in peripheral rat tissues including testis, ovary, urinary bladder, heart, spleen, liver, small intestine, large intestine, lung, kidney and stomach (Castelli *et al.*, 1999). Indeed, $GABA_{B1}$ reeceptors were found to inhibit and activate adenylyl cyclase activity via the $G_i$ and $G_{\beta\gamma}$ subunits (Hashimoto *et al.*, 1997). Moreover, *Gabbr1* was also expressed in skeletal muscle in this study. Taken together, it is possible that $GABA_{B1}$ reeceptors decrease cAMP level which might be important for skeletal muscle growth. This is supported by the fact that it was demonstrated that modulation of skeletal muscle cAMP levels by inhibition of phosphodiesterases (PDEs) or activation of $\beta_2$-adrenoceptors increase rodent skeletal muscle mass (Hinkle *et al.*, 2005; Hinkle *et al.*, 2002). However, the mechanism behind this is still unclear. Therefore, $GABA_{B1}$ receptor agonists might be considered to be investigated to improve skeletal muscle growth in rats.

Metabotropic glutamate receptors are classified into group I ($mGlu_1$ and $mGlu_5$ metabotropic glutamate receptors), group II ($mGlu_2$ and $mGlu_3$ metabotropic glutamate receptors) and group III ($mGlu_4$, $mGlu_6$, $mGlu_7$ and $mGlu_8$ metabotropic glutamate receptors) based on signal transduction and sequence homology. $mGlu_2$ and $mGlu_3$ metabotropic glutamate receptors (*grm2* and *grm3*) gene mRNA was expressed in rat neurons (Parmentier *et al.*, 1996; Tanabe *et al.*, 1992; Tanabe *et al.*, 1993). The action of glutamate can also exert through $mGlu_2$ and $mGlu_3$ metabotropic glutamate receptors. As skeletal muscle expressed *grm2* and *grm2* in this study, and $mGlu_2$ and $mGlu_3$ metabotropic glutamate receptors were also found to couple predominantly to $G_i$

proteins (Niswender *et al.*, 2010; Parmentier *et al.*, 1996), and $mGlu_2$ metabotropic glutamate receptors was also found to inhibit adenylyl cyclase in CHO cells, it is possible that $mGlu_2$ and $mGlu_3$ metabotropic glutamate receptor decrease cAMP level in skeletal muscle which might be important, as discussed previously, for skeletal muscle growth.

Regarding 38 CPCRs detected in skeletal muscle in this study, three main families of GPCRs ($G_s$, $G_i$ and $G_q$) were detected in skeletal muscle tissue using the microarray. Examples include $G_s$-GPCR (β-adrenoceptor, $A_{2A}$ adenosine receptors), $G_i$-GPCR ($A_1$ adenosine receptor and NPY $Y_1$ receptor) and $G_q$-GPCR ($P2Y_1$ and $P2Y_2$ receptors). These GPCRs will be investigated in this study for further signalling and functional roles in skeletal muscle. The discussion of these receptors will be found in the next chapter.

Regarding the other GPCRs which were detected in skeletal muscle using QRT-PCR, *adra2a* mRNA were detected in QRT-PCR (Taqman) and these agreed with the microarray. GPR40 mRNA was not detected in QRT-PCR (Taqman) and this agreed with the microarray. $CB_1$ mRNA was also detected using QRT-PCR (Taqman). However, it was classified as "marginal" in the microarray. This did not contradict with the reliability of the microarray data since it was reported that the validation did not often result in agreement between microarray and QRT-PCR data (Morey *et al.*, 2006). Moreover, GPR119 was detected using QRT-PCR (Taqman) at high Ct values (Ct~32-35, low expression). It also agreed with the microarray that detected GPR119 at ranking ~25000. So, in general, the intensity values from the microarray agreed with Ct values from QRT-PCR (Taqman) except with *cnr1*. Finally, *cnr1*, *gpr119* and *adra2a* were detected in skeletal muscle tissue and will be investigated in this study for further

signalling and functional roles in skeletal muscle. The discussion of these receptors will be also found in the next chapters.

With the recognition of detected GPCRs mRNA relative expression and their downstream associated signalling partner genes, it is possible to understand the signalling of GPCRs in skeletal muscle tissues. GPCRs, in general, can be linked to ubiquitous downstream effectors. Such receptor signalling systems can also offer alternative therapeutic approaches. Therefore, the expression of these GPCR signaling partners will be discussed in the following section.

### 3.6.3 GPCR signalling partners

GPCR responses can be controlled through signalling proteins such as G proteins, protein kinases, phospholipases, etc. When ligands bind to GPCRs, GPCRs transduce a specific signal through a second messenger inside the cells. This raises the question of how the specific signal can be produced.

One possible way to raise the specificity of the response is by determining specific isoforms of signalling protein expressed in that tissue. GPCR signalling partner protein gene expression was examined in skeletal muscle. Little has been reported about mRNA expression of GPCR signalling partner genes in skeletal muscle.

All of the main G protein alpha subunits (*gnas*, *gnai* and *gnaq*) genes were classified as "present" in skeletal muscle at different intensity values in this study. *Gnas* was found to be high expressed compared to *gnai*, *gnaq*, *gna11* and *gna12*. However, the microarray data can not exclude or include the mRNA expression of $G_i$, $G_q$, $G_{11}$ and $G_{12}$

genes, as described in Section 1.3.6. Indeed, this is in line with another study that showed that mouse skeletal muscle expressed *gnas*, *gnai2* and *gnai3* (Suzuki *et al.*, 1998).

As *gnas* was expressed in skeletal muscle in this study (Figure 3-8-A), it is possible that the $G_s$ signalling cascade affects skeletal muscle phenotypes. This is suggested due to the fact that $G_{\alpha i2}$ overexpression was shown to cause a switch to slow fibre phenotypes (Minetti *et al.*), and $G_s$ knockout mice were found to have more slow-twitch fibres than littermate controls (Chen *et al.*, 2009). However, the mechanism is still unclear. The implication of this is that antagonizing $G_s$ protein should be recommended to be investigated to increase slow fibre phenotype which is useful in insulin resistance in skeletal muscle as described previously in Chapter one.

*Gnb1, gnb2, gnb5, gng5, gng10* and *gng12* were expressed in skeletal muscle in this study (Figure 3-8-B, C). mRNA encoding beta and gamma G protein subunits including *gnb1, gnb2, gnb5, gng10* and *gng12* were expressed in different areas in rat brain (Betty *et al.*, 1998). Indeed, it is possible that different isoforms expressions might bind to G alpha subunit which might give a specificity of G protein signalling, G protein-receptor interaction or different cross-talk with other signalling. However, little in the literature is reported about the roles of these specific isoforms.

GPCR signalling can be regulated by a further class of proteins, RGS proteins. RGS are proteins that act as GTPase accelerating proteins for G alpha subunit (De Vries *et al.*, 2000; Sierra *et al.*, 2000). One mechanism through which RGS control the signalling of G protein is substrate specificity. The specificity for RGS could also regulate certain GPCRs pathways. For example, RGS2 seems to act on $G_q$ over $G_i$ preferentially

(Hubbard *et al.*, 2006). Indeed, the recognition of tissue-specific distribution for RGS is of great importance.

*Rgs2, rgs5 and axin1* were expressed in skeletal muscle in this study (Figure 3-9). *Rgs5* agrees with studies in the literature in human skeletal muscle and heart using northern blot (Chen *et al.*, 1997a; Seki *et al.*, 1998). This is in line with a previous study that reported that *rgs2* mRNA was detected in rat skeletal muscle, liver, kidney, heart, spleen and testis (Miles *et al.*, 2000). *Axin1* was also reported to be expressed in mouse tissues including testis, lung, heart, kidney, brain, ovary, spleen and liver (Zeng *et al.*, 1997). Moreover, it was reported that *rgs3, rgs5, rgs9, rgs11, rgs12* and *rgs16* were detected in human skeletal muscle (Larminie *et al.*, 2004).

As *rgs2* was expressed in skeletal muscle in this study (Figure 3-9), and the specificity for RGS2 seems to act on $G_q$ over $G_i$ preferentially (Hubbard *et al.*, 2006; Ingi *et al.*, 1998), it is possible that RGS2 affect GPCR ($G_q$ protein family), such as P2Y receptors which were expressed in skeletal muscle (Table 3-7), and consequently, the signalling of $G_q$-GPCRs might affect $IP_3$ concentration, calcium level in the skeletal muscle and finally affect contraction.

**$G_s$ and $G_i$-GPCRs associated signalling partner genes**

Major signalling genes for $G_s$ and $G_i$-GPCRs were detected at different intensity values. $G_s$ and $G_i$ modulate adenylyl cyclase, which are important in catalyzing the conversion of ATP to cAMP. *Adcy2 and adcy6* were expressed in skeletal muscle (Figure 3-10-A). This is in line with that *adcy2* and *adcy6* mRNA expression were detected in mouse

skeletal muscle (Suzuki *et al.*, 1998). Deletion of AC6 was performed in mouse, nothing was reported about obvious skeletal muscle phenotypes (Tang *et al.*, 2008).

As *adcy2* and *adcy6* were expressed in skeletal muscle (Figure 3-10-A), it is possible that AC2 and AC6 were activated by GPCRs signalling pathways from $G_s$, $G_i$, and $G_q$ through uncoventional mechanism. Furthermore, the response for GPCRs might also be determined by specific isoforms of AC expressed in skeletal muscle. This is supported by the fact that 1) Purification of recombinant AC2 from Sf9 cell membranes was activated by Gβγ (Taussig *et al.*, 1993) and AC2 was also activated by PKC in HEK-293 cells transfected with recombinant AC2 (Lustig *et al.*, 1993). 2) Recombinant AC6 expressed in insect cells (Hi-5 cells) was inhibited by PKA (Chen *et al.*, 1997c), and recombinant AC6 expressed in Sf21 cells was also inhibited by PKC (Lai *et al.*, 1999). 3) $G_{\beta\gamma}$ subunit increased AC2 activity while it decreased AC1 activity in membranes from Sf9 cells infected with AC1 or AC2 (Tang *et al.*, 1991).

cAMP production can be stopped through inhibition of AC or activation of the GTPase function of the $G_s$ protein. Termination of cyclic nucleotide signalling is mediated by a family of enzymes, called PDEs. This family can hydrolyze 3'5'-cyclic guanosine monophosphate (cGMP) and/or cAMP, depending on the particular subfamily. Knowing the isoform expression in skeletal muscle could allow selective enhancement of cyclic nucleotide levels through the use of PDE isoform-selective inhibitors. PDE2, PDE4, PDE7 and PDE8 selectively hydrolyze cAMP, PDE9 selectively hydrolyzes cGMP and PDE1 hydrolyzes both cGMP and cAMP (Lewis *et al.*, 2006). *Pde4a, Pde4b and Pde4d* were expressed in skeletal muscle in this study (Figure 3-10-B). Indeed, high mRNA expression of PDE4B was found in human skeletal muscle using microarray (Bingham *et al.*, 2006). It was also reported that PDE4 subtypes were all inhibited by

rolipram, PDE4 inhibitors (Wang *et al.*, 1997).

As *pde4* is expressed in skeletal muscle in this study (Figure 3-10-B), and PDE4 inhibitors such as roflumilast have recently been approved for chronic obstructive pulmonary disorder, it is possible that PDE4 inhibitors may reduce skeletal muscle atrophy in a manner similar to G-protein–coupled receptor activation ($\beta_2$-adrenoceptor). Indeed, PDE4 might have implications in muscular disorders such as muscular dystrophy (Hinkle *et al.*, 2005). Indeed, rolipram, a selective PDE4 inhibitor, was found to prevent the mouse skeletal muscle weakness and wasting with limb casting and sciatic nerve resection (Hinkle *et al.*, 2005). Furthermore, PDE activity was observed to be higher in skeletal muscle of dystrophic mice (Bloom, 2005; Lin *et al.*, 1976). Indeed, PDE4 was reported to contribute to the major cAMP hydrolyzing activity in mouse skeletal muscle (Bloom, 2002). Overall, this suggests that imbalance between cAMP degradation and production in skeletal muscle might cause harmful effects on the signalling cascades related to skeletal muscle fibre atrophy. Therefore, PDE4 should be recommended as a therapeutic option for skeletal muscle growth. The implication of this is that PDE4 inhibitors should be investigated to treat skeletal muscle dystrophy.

cAMP exerts the majority of its effects through the protein kinase PKA, which is made up of regulatory and catalytic subunits. Regulatory subunits include RIα, RIβ, RIIα and RIIβ subunits, while catalytic subunits comprise Cα, Cβ, and Cγ. Each subunit is encoded by a unique gene. In this study, PKA regulatory (subunit α1) subunit is expressed in skeletal muscle (Figure 3-9-B).

The expression of regulatory subunit α1 and α2 agrees with the literature regarding the expression of these genes in rat and mouse skeletal muscle (Burton *et al.*, 1997; Morita

*et al.*, 1995). The beta and gamma isoforms were also reported to be expressed in brain, testis and adipose (Brandon *et al.*, 1997). Moreover, mRNA and protein expression of both RIα and Cα were found to be detected in mouse embryonic skeletal muscle (Imaizumi-Scherrer *et al.*, 1996) and RIα mRNA was also expressed in soleus muscle (Hoover *et al.*, 2001).

RIα was suggested to functionally compensate the RIIα in mouse skeletal muscle deficient RIIα through the analysis of L-type calcium channel regulation (Burton *et al.*, 1997). There is no PKA subunit knockout reported in animals. However, mutant Prkar1α in embryonic stem cells and in liver tissue was shown to produce a dominant negative RIα regulatory subunit (RIα) which leads to decrease in PKA activity (Willis *et al.*, 2011). Indeed, further investigation should be recommended to examine whether Prkar1α is the main subunit responsible for the PKA activity in skeletal muscle.

Since *pde4* and *adcy6* were expressed in skeletal muscle, it is possible that PKA might be an important regulator of cAMP concentration in this tissue. This is supported by the fact that PKA was found to phosphorylate and activate human PDE4D in COS1-cells (Hoffmann *et al.*, 1998; Houslay *et al.*, 2003), and recombinant AC6 expressed was inhibited by PKA (Chen *et al.*, 1997c). Therefore, PKA might be considered as a therapeutic option to modulate cAMP in skeletal muscle, consequently PKA should be recommended to be investigated as a therapeutic option for skeletal muscle growth as discussed previously.

**$G_q$-GPCRs associated signalling partner genes**

Major signalling genes associated with $G_q$-GPCRs were expressed at different relative

intensity values. PLC isozymes, depending on the structure, are classified into six families (β, γ, δ, ε, ζ, η), where the β family are the primary targets for $G_q$.

*Plcd1 and plcd4* were expressed in skeletal muscle (Figure 3-10-A). Regarding *plcd1* expression, this is in line with *plcd1* was expressed in mouse, rat and human skeletal muscle tissue (Cheng *et al.*, 1995; Homma *et al.*, 1989; Lee *et al.*, 1999). Moreover, the nuclear accumulation of PLCδ1 was reported to be affected by calcium in Madin Darby canine kidney (MDCK) cells stably expressing GFP-PLCδ1 (Fujii *et al.*, 1999; Okada *et al.*, 2005; Yagisawa, 2006). However, the mechanism behind this issue is not known yet. PLCδ1 activity, purified from the cytosolic fraction of bovine brain, was also shown to be stimulated by bovine brain $G_{\beta\gamma}$ (Park *et al.*, 1993). Therefore, PLCdδ1 might cross-talk to other conventional GPCR signallings. *Plcd4* was expressed in skeletal muscle in this study. This is consistent with that *plcd4* was detected in normal human tissues, including skeletal muscle and kidney tissues using northern blot analysis (Leung *et al.*, 2004). *Plcd1* and *plcd4* were also shown to be expressed in proliferating hepatoma cells (Santi *et al.*, 2003). As *plcd4* was expressed in skeletal muscle (Figure 3-10-A), and overexpression of PLCδ4 was shown to activate ERK1/2 in breast cancer cell line (MCF-7 cells) (Leung *et al.*, 2004), it is possible that PLCδ4 in skeletal muscle will activate ERK which possibly affects proliferation in skeletal muscle cells. Therefore, the implication of this is that PLCδ4 should be recommended to be investigated as a therapeutic option for skeletal muscle regeneration. To examine this issue, knockout mice should be recommended to investigate the effects of PlCδ1 and PlCδ4. Overall, major regulation of GPCRs might be directed depending on PLC isoforms expressed in tissues. Little in the literature is reported about the role of these isoforms.

Regarding PLC signalling, the active PLC hydrolyzes phosphatidylinositol 4,5-

bisphosphate ($PIP_2$) to produce inositol 1,4,5-trisphosphate ($IP_3$) and 1,2-diacylglycerol (DAG). Indeed, DAG activates protein kinase C (PKC).

DAG levels can be regulated by phosphorylating DAG by Diacylglycerol kinase (DGK) to form phosphatidic acid, then allowing the recycling of phosphatidic acid into membrane phospholipid. It was suggested that DGK isoforms might have substrate specificity *in vivo* through subcellular location (van Blitterswijk *et al.*, 2000). *Dgkz* was expressed in skeletal muscle (Figure 3-10-B). This agrees with the literature regarding *dgkz* mRNA expression in mouse skeletal muscle (Chibalin *et al.*, 2008). Indeed, endogenous and green fluorescent protein-tagged overexpressed DGKζ was found to be localized mostly to the nucleus compared to overexpressed DGKα, DGKβ, and DGKI in mouse C2C12 cells (Evangelisti *et al.*, 2006). Down-regulation of *Dgkz* by siRNA in C2C12 was shown to markedly impair differentiation (Evangelisti *et al.*, 2006). Taken together, this isoform (DGKζ) might have a different signalling pathway and substrate specificity from the other isoforms in skeletal muscle. Moreover, it is possible that DGKζ might play a role in skeletal muscle growth. Further work is recommended to investigate subcellular location of DGKζ in skeletal muscle using tagged overexpressed protein and immunofluorescent imaging and to investigate its role in differentiation and proliferation process.

DAG can be hydrolyzed into a free fatty acid and monoacylglycerol by diacylglycerol lipase. Indeed, diacylglycerol (DAG) lipase is a key enzyme in the biosynthesis of the endocannabinoid, 2-AG. It is worth noting that two DAG lipase isozymes were cloned; DAGLα and DAGLβ (Bisogno *et al.*, 2003). *Daglb* was expressed in skeletal muscle (Figure 3-10-B). Moreover, protein expression of DAGLα and DAGLβ have been reported to be expressed in mouse brain (Bisogno *et al.*, 2003). However, little in the

literature is reported about the roles of these proteins.

Regarding PKC, mRNA expression for each gene isoform usually differs among tissues. *Prkcd and prkcq* were expressed in skeletal muscle (Figure 3-10-B). This is consistent with *Prkcd* was expressed in rat primary skeletal muscle and differentiated rat L6 cells at the level of RNA and protein (Horovitz-Fried *et al.*, 2006). Moreover, *prkcq* was reported to be the most abundantly expressed PKC isoform in mouse skeletal muscle (Osada *et al.*, 1992).

As *prkcq* was expressed in skeletal muscle (Figure 3-11-C), it is possible that activation of PKCθ by GPCR expressed in skeletal muscle plays a role in insulin resistance and glucose metabolism. This is probably due to the fact that PKCθ protein expression was shown to be higher in insulin-resistant fast muscle fibres than slow muscle fibres (Donnelly *et al.*, 1994) and transgenic mice with dominant negative PKCθ in skeletal muscle were found to have hyperglycemia, hyperinsulinemia and gain weight (Serra *et al.*, 2003). The implication of this is that PKCθ might be investigated as a therapeutic option for diabetes and obesity.

Regarding $G_q$-GPCR signalling, inositol phosphate can be dephosphorylated to inositol by an enzyme called inositol monophosphatase (IMPA). $IP_3$ receptors (*itpr1, itpr2* and *itpr3*), $IP_3$ kinase b and c (*itpkc* and *itpkb*), *impa1* and *impa2* were classified as "present" in all skeletal muscle replicates. However, no obvious differential relative expression was observed among different types of $IP_3$ receptors, $IP_3$ kinases and IMPA isoforms. It is worth mentioning that $IP_3$ receptors sequences are provisional in rats. Further investigation should be recommended to examine these $IP_3$ receptors using DNA sequencing, QRT-PCR (Taqman) and immunoblotting. *Imap1* and *imap2* were expressed in skeletal muscle in this study (Figure 3-10-D). mRNA and protein

expressions of both IMPA1 and IMPA2 were shown at different levels in different areas in mouse brain (Sjoholt *et al.*, 2000; Willsky *et al.*, 2006). However, little in the literature was reported about the different roles of these isoforms.

**$G_{12}$-GPCRs associated signalling partner genes**

Major signalling genes for $G_{12}$-GPCRs were detected at different intensity values in this study. *Rock1*, *rhoa and rhoq* were expressed (Figure 3-11). This is consistent with *rock1* was reported to be expressed in rat tissue such as skeletal muscle, liver, heart, lung, kidney and pancreas while *rock2* was reported to be expressed mainly in the brain (Amano *et al.*, 2000; Ishizaki *et al.*, 1996; Matsui *et al.*, 1996; Meyer *et al.*, 2006). mRNA expression of *rhoa* and *rhob* was reported to be expressed in CNS and the peripheral nervous system of chicken embryos (Malosio *et al.*, 1997). ROCK1 deficient mice were shown to induce insulin resistance by impairing insulin signalling in skeletal muscle (Lee *et al.*, 2009). Therefore, the activation of ROCK1 in skeletal muscle might be recommended to be investigated as a therapeutic option for treatment of diabetes.

In summary, this chapter showed that $LPA_1$ lysophosphatidic acid receptors (endothelial differentiation, lysophosphatidic acid G protein-coupled receptor, 2 (Edg2)), CXCR4, glucagon receptor 2, platelet-activating factors receptors, $GABA_{B1}$ receptors, $S1P_2$ sphingosine-1-phosphate receptors (endothelial differentiation, sphingolipid G-protein-coupled receptor, 5 (Edg5)), parathyroid hormone receptors, $mGlu_2$ and $mGlu_3$ glutamate receptors, dopamine $D_5$ receptors, neurotensin receptor 2, opioid receptor delta 1, calcitonin receptors 1, arginine vasopressin receptor 1A, bradykinin $B_2$ receptors, C5a1 complement peptide receptors, $CB_1$ receptor, GPR119, $\alpha_2$-adrenoceptor, $\beta_2$-adrenoceptor, $A_1$ and $A_{2A}$-adenosine receptors, NPY Y1 receptor, $P2Y_1$, $P2Y_2$ and

$P2Y_6$ receptors genes mRNA were detected in skeletal muscle. Moreover, $G_s$, $G_{\beta 1}$, $G_{\beta 2}$, $G_{\beta 5}$, $G_{\gamma 10}$, $G_{\gamma 12}$, RGS2, RGS5, Axin1, AC2, AC6, PDE4a, PDE4d, PKA RIα, PLCδ4, PLCδ1, DAGIβ, DGKζ, DGKα, PKCδ, PKCθ, IMPA1, IMPA2, ROCK1, RhoA and RhoQ genes mRNA were also highly detected in skeletal muscle tissue compared to other isoforms. However, the other GPCR entities cannot be excluded. These entities which are expressed in skeletal muscle in this study might be therapeutic options to improve contraction, glucose uptake, proliferation, differentiation, myogenesis and growth in skeletal muscle. The implication of this is that these targets should be recommended to be investigated for diabetes, obesity and muscle regeneration disorders.

This chapter gave a picture and guide for the some GPCRs detected in skeletal muscle, their signaling protein genes in skeletal muscle, which has not previously been reported, in order to be investigated in this study. In the next chapter, signalling will be investigated for these GPCRs representative of the different families.

# Chapter 4

# GPCR Signalling

# 4 Chapter Four: GPCR Signalling in Skeletal Muscle Cells *in vitro*

## 4.1 Introduction

GPCRs expressed in adult skeletal muscle would be anticipated to mediate the effect of a variety of endogenous substances on physiological roles on skeletal muscle, such as muscle contraction, glucose uptake, control of muscle mass and expression of synaptic proteins. However, there have been very few studies directly focusing on the function of GPCRs in skeletal muscle.

Myotubes are primary skeletal muscle cells sharing the morphological, metabolic and biomedical characteristics and properties of adult skeletal muscle (Henry *et al.*, 1995; Raymond *et al.*, 2010). Our study showed that mRNA for many GPCRs were expressed in skeletal muscle tissues; notably $A_1$ and $A_{2A}$ adenosine receptors, $\beta_2$-adrenoceptors, NPY Y1 receptor, GPR119 receptor, $CB_1$ receptor, $P2Y_1$, $P2Y_2$ and $P2Y_6$ receptors, $\alpha_{2A}$-adrenoceptors (see Chapter 3). Since there has been little evaluation of GPCR signalling in myotubes, and it was not possible to investigate all the GPCR apparently expressed in skeletal muscle, some examples were chosen. This selection was based on an attempt to examine signalling through the three main groups of G protein, $G_s$, $G_i$ and $G_q$, as well as receptor targets previously examined in the laboratories at Nottingham.

From the top 38 highly ranked GPCRs list detected using the microarray and GPCRs detected using the QRT-PCR (Taqman) in skeletal muscle, $A_{2A}$ adenosine receptors, GPR119 and $\beta_2$-adrenoceptors were selected as $G_s$-coupled, while $\alpha_{2A}$-adrenoceptors and $A_1$ adenosine, NPY Y1 and $CB_1$ cannabinoid receptors were selected as $G_i$-coupled.

This group ($G_s$ and $G_i$-GPCRs) were tested by quantifying levels of cAMP. However, $P2Y_1$, $P2Y_2$ and $P2Y_6$ receptor were selected as $G_q$-coupled and were tested by assessment of levels of intracellular calcium ions.

## 4.2 Aims

To assess the downstream signalling of GPCRs in rat primary skeletal muscle cells using cAMP assay, calcium imaging and immunoblotting.

## 4.3 Experimental design and methods

### 4.3.1 cAMP assay

Accumulated cAMP in the myotube cells was measured by a competitive Enzyme Immunoassay (EIA) kit (Cayman Chemical). Cells were prepared as discussed in Chapter 2, Section 2.10. Where indicated, cells were pre-incubated with the phosphodiesterase inhibitor, 3-isobutyl-1-methylxanthine (IBMX) (30 μM) 20 minutes prior to agonist addition. Similarly, where indicated, antagonists were added 20 minutes prior to agonist addition. In some instances, cells were co-exposed to the adenylyl cyclase activator forskolin simultaneously with agonists. At the end of the exposure period for the drugs, 40 μl 5 M HCl was added to each well (2 ml media (Ham-F10), 6% horse serum), before assessment of cAMP levels as described in the Methods (Section 2.11).

### 4.3.2 Calcium imaging

Cells were assessed by imaging for intracellular calcium ion levels as described above (see Chapter 2, Section 2.12). Myoblast cells on the coverslips were exposed to UTP, ATP and ionomycin, as indicated, for one minute. In some instances, MRS2179 was perfused over the cells for 3 minutes prior to agonist addition. Peak ratios were calculated by subtracting the baseline fluorescence ratio (excitation at 340/380 and emission at 500 nm) from the fluorescence ratio obtained during drug superfusion (ΔFR). The results are presented as means ± standard error of mean (SEM) in change in fluorescence ratio units (ΔFR) and mean ± SEM of the area under the curve (AUC) in arbitrary units.

### 4.3.3 Western blot of ERK activation

Wistar rat (5 weeks old) primary vastus lateralis 90% myotubes in 6 well plates were serum-starved (Ham-F 10 medium in the absence of further additives) for 3 hours. Antagonists were applied for 30 minutes before agonists (incubated for the indicated periods). After treatment, cells were washed with ice-cold PBS, and then scraped with Trizol (800 μl per well). After separation on SDS-PAGE gels and blotting, each blot was analyzed for p-ERK to ERK ratios to assess ERK activation.

## 4.4 Statistical analysis

Data were analyzed using one way ANOVA and Bonferroni post-hoc test. Analysis was performed using GraphPad Prism, version 5.03 (GraphPad Software Inc). Differences

were considered significant at $P< 0.05$. Data are reported as means ± SEM of triplicate or quadruplicate wells generated from two animals (n=2), except where indicated.

Statistics was performed from low number of repeats (n=2 rats) (no statistical difference was observed among the replicates within the same treatment) for cAMP and western blot experiments in this chapter due to cost implications. Indeed, it is recommended to perform more repeats to support the results deduced in this chapter, in particular it is hard to depend on statistical analysis from 2 repeats due to variations in species or technical work. Indeed, more repeats will solidate the data statistically.

Due to the limitations of time and cost, a complete concentration response curve or time response curve were not performed for every drug. Instead, a single concentration and a single time point were used based on the previous literature. Different concentrations and time points are required to have a clear comprehensive image about the nature of the response.

## 4.5 Results

### 4.5.1 Effect of GPR119 agonists on cAMP levels

Treatment of myotube cells with the endogenous GPR119 agonist OEA (10 μM) for 10 minutes did not result in a significant increase in cAMP compared to vehicle (0.01% DMSO). Treatment of myotube cells with forskolin (100 nM) and OEA (10 μM) in combination also did not lead to any increase in cAMP levels (Figure 4-1).

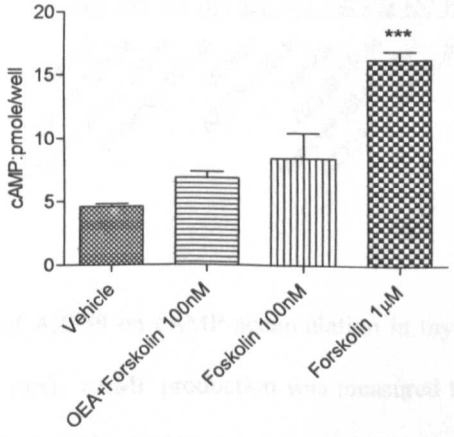


Figure 4-1: Effect of OEA on cAMP accumulation in myotubes (n=2 rats). cAMP production was measured following incubation of cells for 10 minutes with vehicle (0.01% DMSO), forskolin (100 nM, 1 μM), OEA (10 μM) and forskolin after 10 minutes incubation. (***) $p < 0.001$ versus vehicle. Data were analyzed using one way ANOVA test followed by Bonferroni post-hoc.

Treatment of myotube cells with the synthetic GPR119 agonist AZ359 (25 and 100 nM) for 10 minutes failed to evoke a significant increase in cAMP levels compared to vehicle (0.01% DMSO). Similarly, treatment of myotube cells in the presence of either 100 nM forskolin or 30 μM IBMX, a nonselective phosphodiesterease inhibitor, did not increase cAMP levels compared with IBMX or forskolin alone (Figure 4-2).

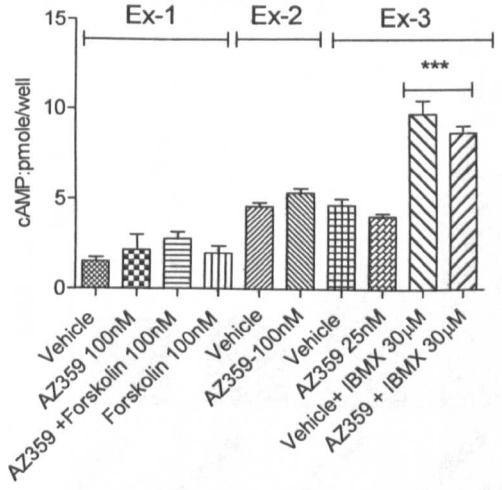


Figure 4-2: Effect of AZ359 on cAMP accumulation in myotubes in three different experiments (three different rats) (n=2 rats). cAMP production was measured following incubation of cells for 10 minutes with vehicle (0.01% DMSO), AZ359 (25 nM and 100 nM), forskolin, AZ359+IBMX and IBMX, Ex1; experiment 1; Ex2; experiment 2; Ex3; experiment 3. (***) $p < 0.001$ versus vehicle or AZ359. Data were analyzed using one way ANOVA test followed by Bonferroni post-hoc.

In order to confirm the activity of the novel GPR119 agonist, its effect on cAMP levels in 3T3-L1 mouse adipocytes was examined. Treatment of cells with AZ359 (100 nM) for 10 minutes did not show a significant increase in cAMP compared to vehicle (0.01% DMSO). Interestingly, treatment of 3T3-L1 adipocyte cells with forskolin (100 nM) and AZ359 (100 nM) resulted in a significant inhibition of cAMP accumulation compared to forskolin alone ($p < 0.01$) (Figure 4-3).

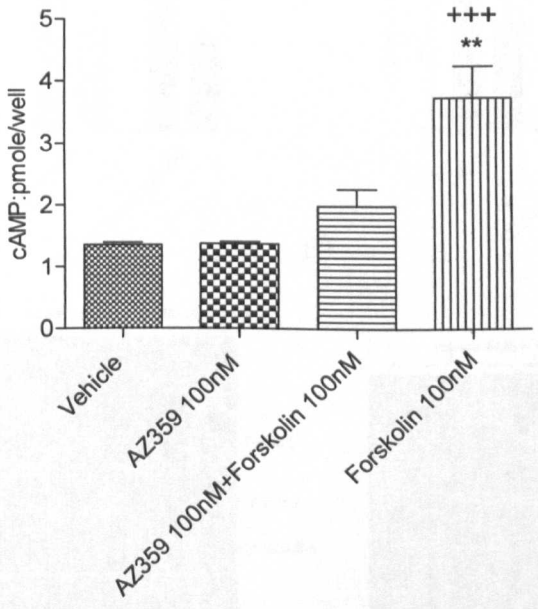


Figure 4-3: Effect of AZ359 on cAMP accumulation in 3T3-L1 adipocytes (n=2 experiments). cAMP production was measured following incubation of cells for 10 minutes with vehicle (0.01% DMSO), AZ359 (100 nM) and forskolin (100 nM). (**) $p < 0.01$; ** forskolin ± AZ359, (+++) $p < 0.001$; +++ forskolin versus vehicle. Data were analyzed using one way ANOVA test followed by Bonferroni post-hoc.

### 4.5.2 Effect of the GPR119 agonist AZ359 on ERK phosphorylation

Treatment of myotube cells with AZ359 (25 nM) failed to show a significant increase in P-ERK1/ERK1 and P-ERK2/ERK2 ratios at 5, 10 and 15 minutes compared to vehicle (0.01% DMSO) (Figure 4-4). The molecular weight of the bands for P-ERK1/ERK1 and P-ERK2/ERK2 was detected at 44 kDa and 42 kDa, respectively, as expected.

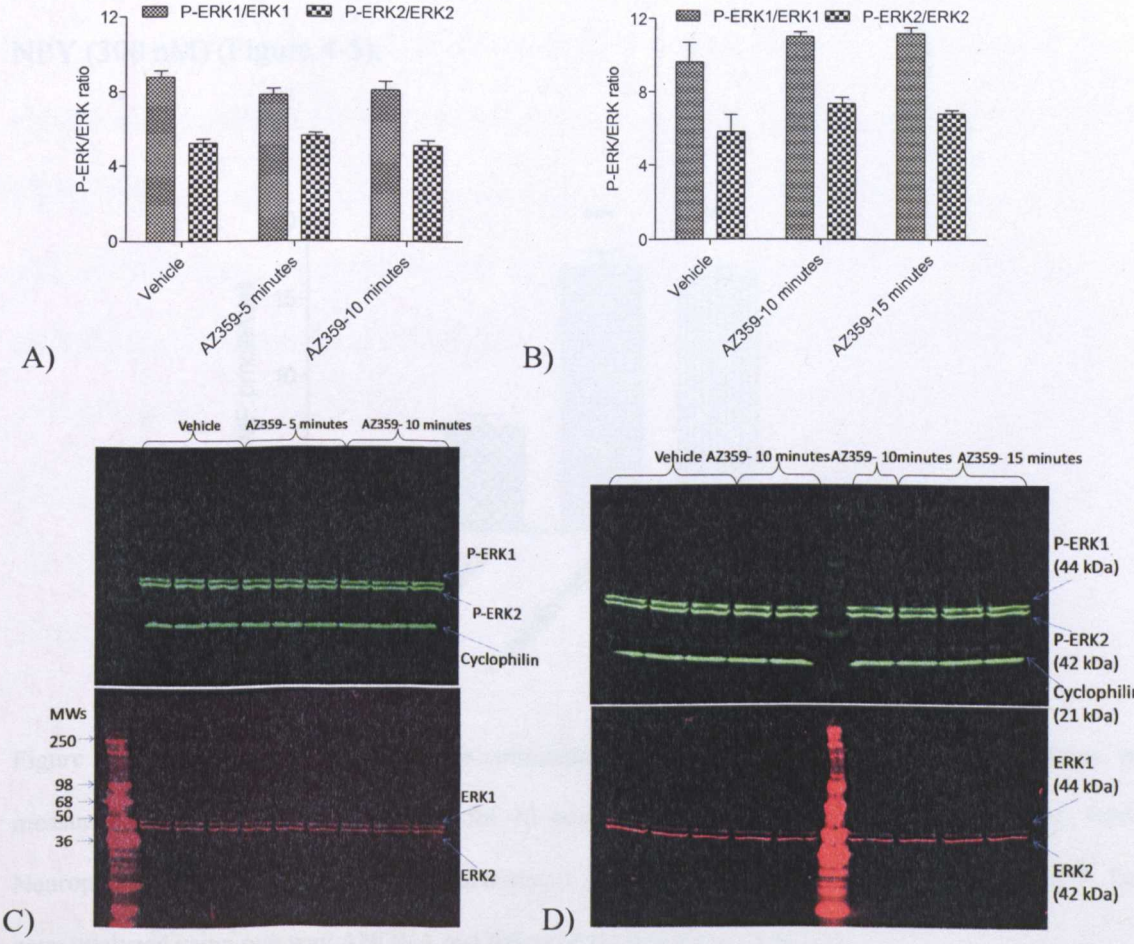


Figure 4-4: Effect of AZ359 on phosphorylation of ERK in rat primary skeletal muscle cells (n=2 rats). A) Myotubes were treated with vehicle (0.01% DMSO), AZ359 (25 nM) for 5 and 10 minutes. B) Myotubes were treated with vehicle (0.01% DMSO), AZ359 (25 nM) for 10 and 15 minutes. C) Representative blots showing myotubes treated with vehicle (0.01% DMSO), AZ359 (25 nM) for 5 and 10 minutes, phospho-ERK 1/2 (green bands), ERK 1/2 (red bands). D) Representative blots showing myotubes treated with vehicle (0.01% DMSO), AZ359 (25 nM) for 10 and 15 minutes, phospho-ERK 1/2 (green bands), ERK 1/2 (red bands). Data were analyzed using one way ANOVA test followed by Bonferroni post-hoc.

### 4.5.3 Effect of a NPY Y1 receptor ligand on cAMP levels

As mRNA encoding the NPY Y1 receptor was detected in skeletal muscle in this study, the potential inhibitory effect of NPY on cAMP levels was assessed. Neither basal levels of cAMP nor forskolin (1 μM)-stimulated cAMP were altered in the presence of NPY (300 nM) (Figure 4-5).

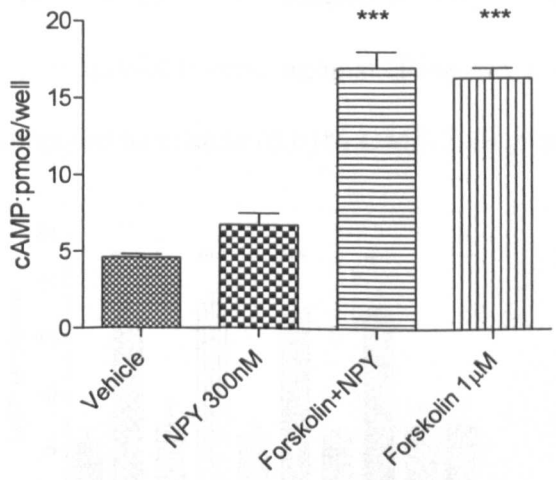


Figure 4-5: Effect of NPY on cAMP accumulation in myotubes (n=2 rats). cAMP production was measured following incubation of cells for 10 minutes with vehicle (0.01% DMSO), [Leu31, Pro34] Neuropeptide Y (NPY) (300 nM) and forskolin (1 μM). (***) $p < 0.001$ versus vehicle or NPY. Data were analyzed using one way ANOVA test followed by Bonferroni post-hoc.

### 4.5.4 Effect of cannabinoid receptor ligands on cAMP levels

Since $CB_1$ receptor mRNA was detected using QRT-PCR (Taqman) in this study, the potential inhibitory effect of $CB_1$ agonists on cAMP levels was assessed.

In myotubes, neither basal nor forskolin (1 μM)–evoked elevation of cAMP was altered significantly in the presence of ACEA, the selective $CB_1$ receptor agonist (Hillard *et al.*, 1999), (10 nM), AEA, endogenous cannabinoid receptor agonist (Lin *et al.*, 1998), (10 μM) or RIM, $CB_1$ antagonist/inverse agonist (Rinaldi-Carmona *et al.*, 1994), (100 nM) for 10 minutes compared to vehicle (0.01% DMSO) (Figure 4-6).

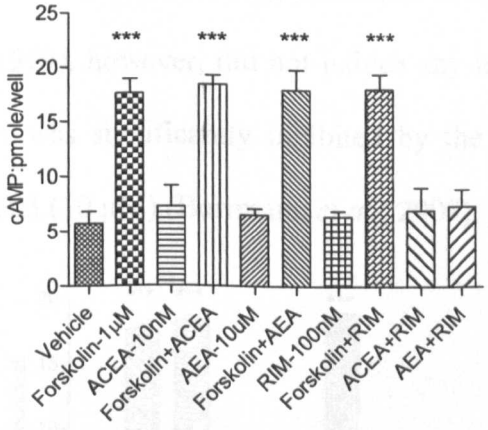


Figure 4-6: Effect of ACEA, AEA and RIM on cAMP accumulation in myotubes (n=2 rats). cAMP production was measured following incubation of cells for 10 minutes with vehicle (0.01% DMSO), cannabinoids and forskolin, ACEA (10 nM), AEA (10 μM), forskolin (1 μM) or RIM (100 nM) 30 minutes prior. (***) $p < 0.001$ versus vehicle, ACEA, AEA or RIM. Data were analyzed using one way ANOVA test followed by Bonferroni post-hoc.

### 4.5.5 Effect of adenosine receptor ligands on cAMP levels

mRNA encoding $A_{2A}$ and $A_1$ adenosine receptors was detected in skeletal muscle in this study, where $A_{2A}$ adenosine receptors were anticipated to elevate cAMP levels and $A_1$ adenosine receptors would likely inhibit cAMP production.

Treatment of myotube cells with the non-selective adenosine receptor agonist NECA (Castanon *et al.*, 1994; Klotz *et al.*, 1998) at concentrations anticipated to activate $A_{2A}$ and $A_{2B}$ adenosine receptors (100 nM and 10 μM, respectively) for 10 minutes showed significant increases in cAMP compared to vehicle (0.01% DMSO). Treatment of myotube cells with the selective $A_{2A}$ adenosine receptor agonist CGS21680 (100 nM) (Ongini *et al.*, 1999), however, did not induce any increase in cAMP. The stimulatory effect of NECA was significantly inhibited by the selective $A_{2B}$ adenosine receptor antagonist PSB603 (10 μM) (Borrmann *et al.*, 2009), $p < 0.001$ (Figure 4-7).

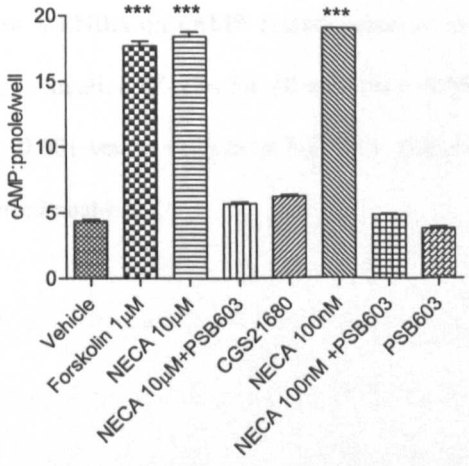


Figure 4-7: Effect of NECA, CGS21680 and PSB603 on cAMP accumulation in myotubes (n=2 rats). cAMP production was measured following incubation of cells for 10 minutes with vehicle (0.01% DMSO), NECA (100 nM and 10 μM), PSB603 (10 μM), CGS21680 (100 nM) and forskolin. (***) $p <$ 0.001 versus vehicle or NECA+PSB603. Data were analyzed using one way ANOVA test followed by Bonferroni post-hoc.

The potential coupling of $A_1$ adenosine receptors to inhibition of cAMP was investigated using the $A_1$ receptor-selective agonist S-ENBA (Haynes *et al.*, 1998; Hussain *et al.*, 1995). However, neither basal nor forskolin (1 μM)–evoked elevation of cAMP in myotube cells was altered in the presence of S-ENBA (100 nM) (Figure 4-8).

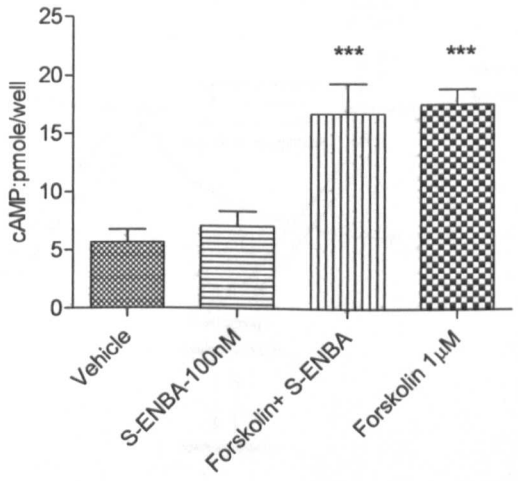


Figure 4-8: Effect of S-ENBA on cAMP accumulation in myotubes (n=2 rats). cAMP production was measured following incubation of cells for 10 minutes vehicle (0.01% DMSO), S-ENBA (100 nM) and forskolin. (***) $p < 0.001$ versus vehicle or S-ENBA. Data were analyzed using one way ANOVA test followed by Bonferroni post-hoc.

In order to investigate the presence of other components of the adenosine system (Figure 4-9), the expression for the enzymes and transporters required for adenosine cycling was assessed.

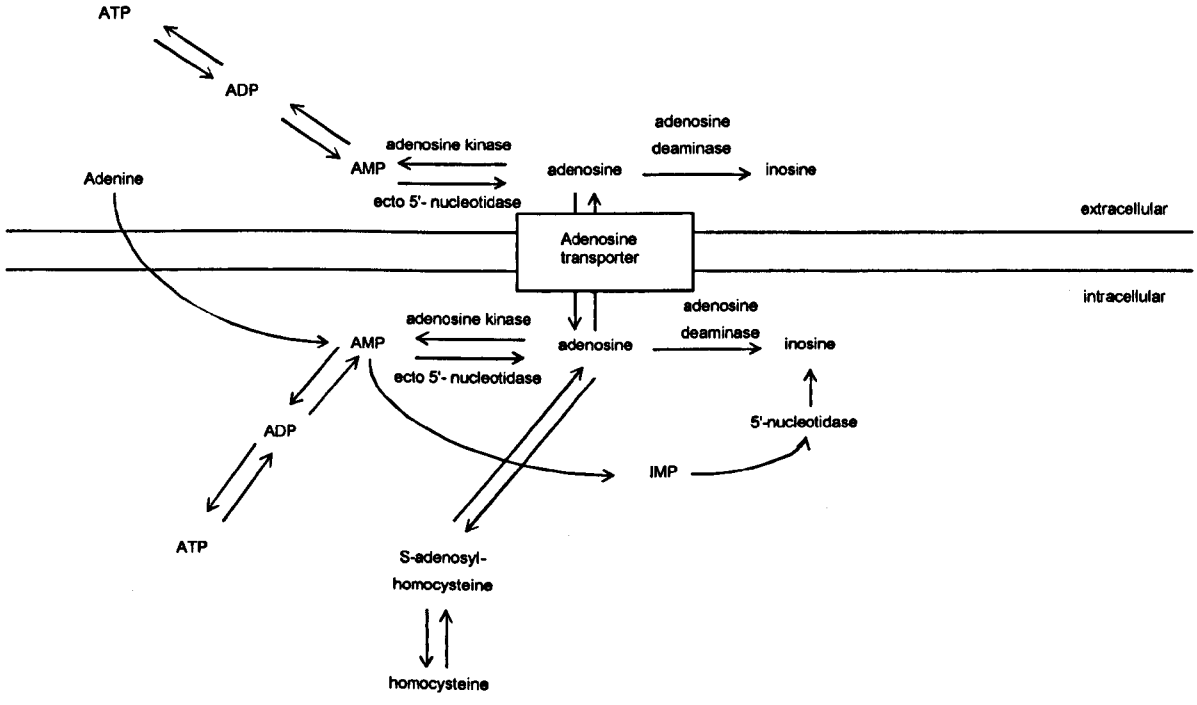


Figure 4-9: Schematic summary of the regulation of extra- and intracellular adenosine and inosine concentrations. ATP: adenosine tri-(di-, mono-) phosphate; ADP; adenosine diphosphate; AMP; adenosine monophosphate. IMP; inosine monophosphate (Marshall, 2000; Spielman *et al.*, 1991).

Adenosine deaminase, adenosine kinase and S-adenosylhomocysteine hydrolase mRNA expression were detected in the skeletal muscle tissue in this study. In addition, ecto-5' nucleotidase and ectonucleotide pyrophosphatase/phosphodiesterase 1, 2 and 3 mRNA were also detected in the skeletal muscle. Nucleoside transporters mRNA were detected as well (Table 4-1).

Table 4-1: RNA transcript intensity values for genes related to adenosine machinery in mixed skeletal muscle from 3 replicates generated from two male Wistar rats. The number represents the relative intensity values for these genes which are all above *tbp* (TATA box binding protein) reference gene.

| Gene | Gene name | Rat A | | | Rat B | | |
|---|---|---|---|---|---|---|---|
| | | A | B | C | A | B | C |
| Ada | Adenosine deaminase | 2.1 | 1.7 | 1.8 | 1.6 | 1.7 | 2.0 |
| Adk | Adenosine kinase | 2.7 | 3.8 | 3.1 | 3.3 | 3.4 | 3.1 |
| Ahcy | S-adenosylhomocysteine hydrolase | 3 | 2.8 | 2.3 | 4.1 | 3.7 | 4.1 |
| Slc28a1 | Solute carrier family 28 (nucleoside transporters) 1 | -1 | -1.2 | -1.2 | -2.7 | -3.1 | -2.5 |
| Slc28a2 | Solute carrier family 28 (nucleoside transporters) 2 | 3.2 | 3 | 3.5 | 0.5 | 0.2 | 0.8 |
| Slc29a1 | Solute carrier family 29 (nucleoside transporters) 1 | 5 | 4.2 | 5.4 | 4.9 | 5 | 4.9 |
| Nt5e | 5' nucleotidase, ecto | -0.7 | -0.7 | -0.9 | -0.5 | -0.3 | -0.7 |
| Enpp1 | Ectonucleotide pyrophosphatase/phosphodiestera se 1 | 1.7 | 1.2 | 1.2 | 1.7 | 1.7 | 2 |
| Enpp2 | Ectonucleotide pyrophosphatase/phosphodiestera se 2 | 0.6 | 0.3 | 0.7 | 0.6 | 1.1 | 0.9 |
| Enpp3 | Ectonucleotide pyrophosphatase/phosphodiestera se 3 | 1.4 | 1.2 | 2.1 | 1.6 | 2.3 | 2.3 |

### 4.5.6 Effect of $\alpha_2$-adrenoceptor ligands on cAMP levels

Adra2a expression was detected using QRT-PCR (Taqman) and microarray in this study. Functional expression of the $\alpha_{2A}$-adrenoceptor as a $G_i$-coupled receptor was assessed by quantifying cAMP levels. Treatment of myotube cells with UK14304, an $\alpha_2$-adrenenoceptor agonist (Jasper *et al.*, 1998), inhibited forskolin (1 μM)-evoked elevation of cAMP significantly. However, rauwolscine, the selective $\alpha_2$-adrenoceptor antagonist (Convents *et al.*, 1989; Uhlen *et al.*, 1994), did not prevent this effect (Figure 4-10).

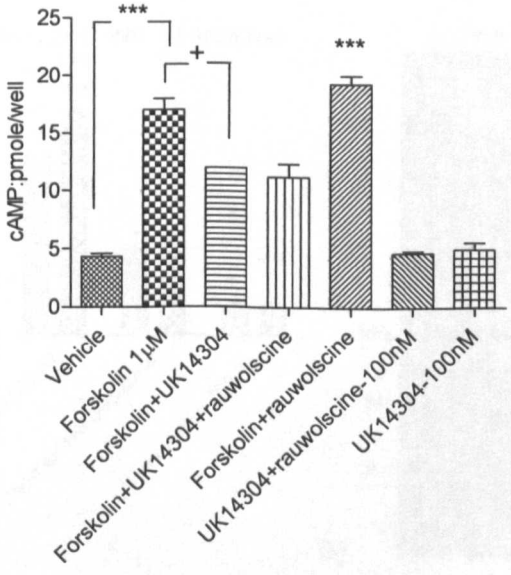


Figure 4-10: Effect of UK14304 and rauwolscine on cAMP accumulation in myotubes (n=2 rats). cAMP production was measured following incubation of cells for 10 minutes with vehicle (0.01% ethanol), UK14304 (100 nM) and rauwolscine (100 nM). * vs basal. + vs forskolin. Data were analyzed using one way ANOVA test followed by Bonferroni post-hoc.

### 4.5.7 Effect of $\alpha_2$-adrenoceptor ligands on ERK phosphorylation

$\alpha_2$-adrenoceptor coupling to ERK phosphorylation was investigated as an alternative coupling mechanism. Treatment of myotube cells with UK14304 for 10 minutes showed a significant increase in P-ERK1/ERK1 and P-ERK2/ERK2 ratios compared to vehicle (0.01% ethanol). The molecular weight of the bands for P-ERK1/ERK1 and P-ERK2/ERK2 was detected at 44 kDa and 42 kDa, respectively as expected. Interestingly, treatment of myotube cells with rauwolscine (100 nM), 30 minutes prior to the addition of UK14304 inhibited the effect of UK14304 significantly for both P-ERK1/ERK1 and P-ERK2/ERK2 ratio. However, rauwolscine showed a significant inhibition of basal levels of ERK phosphorylation as well (Figure 4-11).

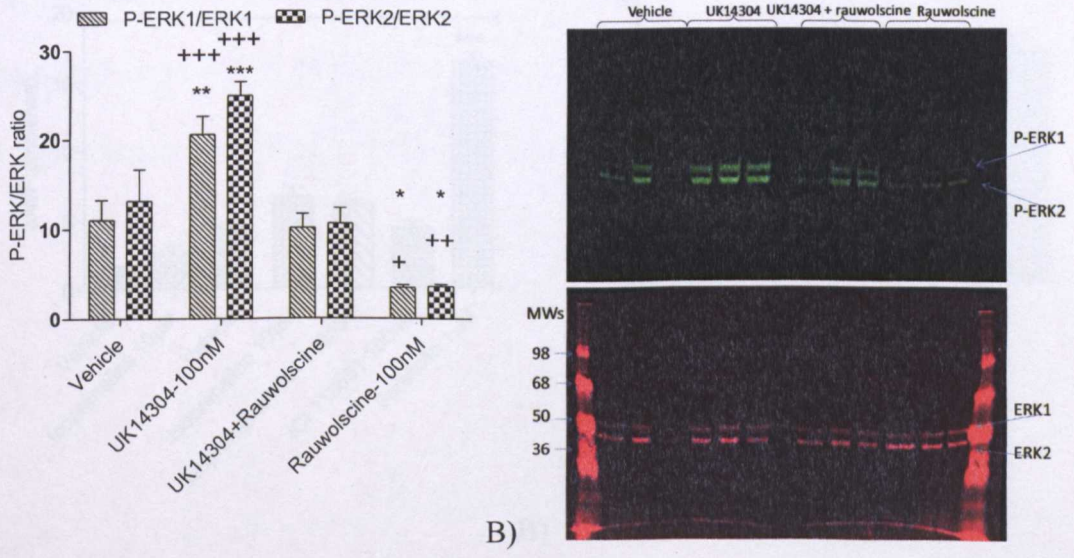


Figure 4-11: Effect of UK14304 and rauwolscine on phosphorylation of ERK in rat primary skeletal muscle cells (n=2 rats). A) Myotubes were treated with vehicle (0.01% ethanol), UK14304 (100 nM) for 10 minutes, UK14304 for 10 minutes + rauwolscine (100 nM) 30 minutes prior. * ± UK14304. + ± rauwolscine. B) Representative blots showing myotubes treated with vehicle (0.01% ethanol), UK14304 (100 nM) for 10 minutes + rauwolscine (100 nM) 30 minutes prior, phospho-ERK 1/2 (green bands), ERK 1/2 (red bands). Data were analyzed using one way ANOVA test followed by Bonferroni post-hoc.

### 4.5.8 Effect of β-adrenoceptor ligands on cAMP levels

The potential coupling of $\beta_2$-adrenoceptors to elevation of cAMP levels was assessed, since mRNA encoding $\beta_2$-adrenoceptor was detected using microarray in this study.

Isoprenaline, a non-selective β-adrenoceptor agonist (Bylund *et al.*, 1994), failed to increase cAMP levels in myotube cells, as did the $\beta_2$-adrenoceptor-selective antagonist ICI118551 (Bilski *et al.*, 1983) (Figure 4-12-A). In contrast, isoprenaline evoked a significant elevation of cAMP levels in 3T3-L1 adipocytes (Figure 4-12-B).

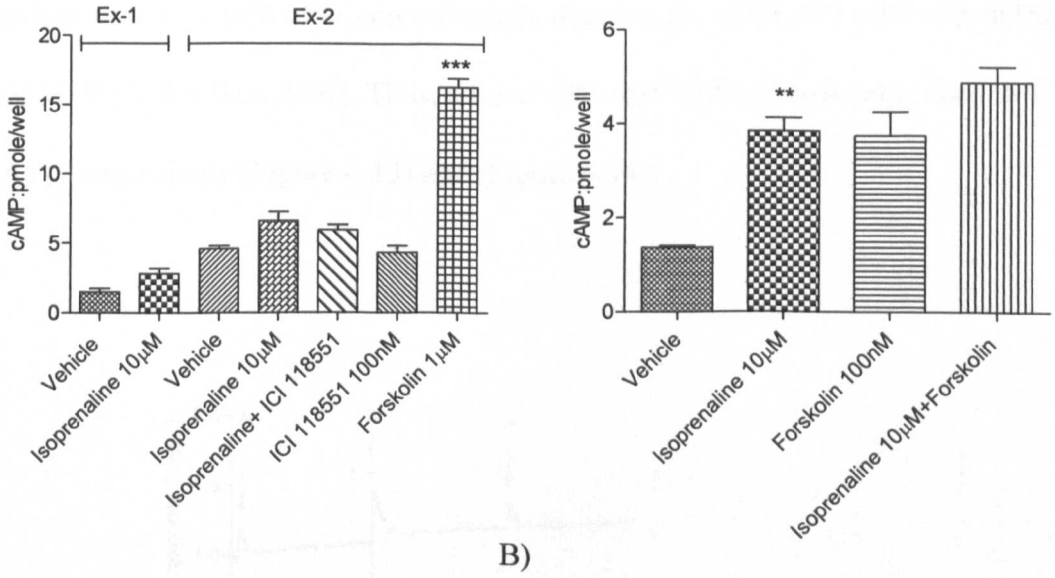


A) B)

Figure 4-12: Effect of isoprenaline on cAMP accumulation in myotubes and 3T3-L1 adipocytes (n=2 rats and n=2 experimets, respectively). A) Effect of isoprenaline on cAMP accumulation in myotubes. cAMP production was measured following incubation of cells for 10 minutes with vehicle (0.01% DMSO), isoprenaline (10 μM), ICI118551 (100 nM) and forskolin (1 μM). Ex-1; experiment 1, Ex-2; experiment 2 (***) $p < 0.001$ versus vehicle. B) Effect of isoprenaline on cAMP accumulation in 3T3-L1 adipocytes. cAMP production was measured following incubation of cells for 10 minutes with vehicle (0.01% DMSO), isoprenaline (10 μM) and forskolin (100 nM). (**) $p < 0.01$ versus vehicle. Data were analyzed using one way ANOVA test followed by Bonferroni post-hoc.

### 4.5.9 Elevation of intracellular calcium ion levels in myotubes

mRNA encoding $P2Y_1$, $P2Y_2$ and $P2Y_6$ receptors was detected using the microarray in this study. As the majority of P2Y receptors are $G_q$-coupled, $Ca^{2+}$-imaging techniques were employed to investigate their functional coupling.

748 myoblast cells were imaged from four animals. ATP (1 mM) elevated intracellular calcium ion levels in all 748 myoblast cells (imaged from four animals; 150-250 cells/animal), with a peak increase in fluorescence ratio (ΔFR; Fura-2 340/380 nm excitation) of 0.33 ± 0.06 after approximately one minute, while 575 cells responded to 10 μM UTP (0.18 ± 0.08 ΔFR). Thus, around 77% and 100% of cells responded to UTP and ATP, respectively (Figure 4-13) and (Figure 4-14).

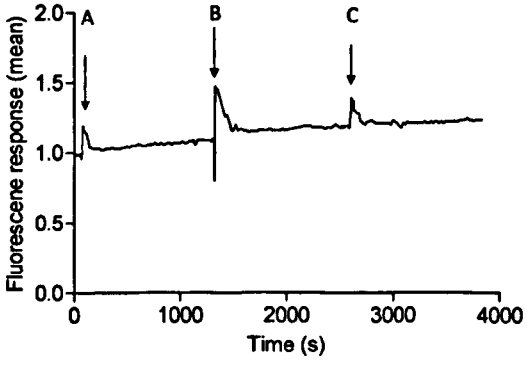


Figure 4-13: A representative trace showing changes in 340:380 nm excitation wavelength ratios in myoblast cells, in response to UTP, ATP and ionomycin. Recording of 340:380 ratio were made at various time points, where at point A, the cells were exposed to UTP (10 μM) for one minute, twenty minutes later, at point B, the cells were exposed to ATP (1 mM), twenty minutes later, at point C, the cells were exposed to ionomycin (4 μM); (imaged from four animals; 150-250 cells/animal).

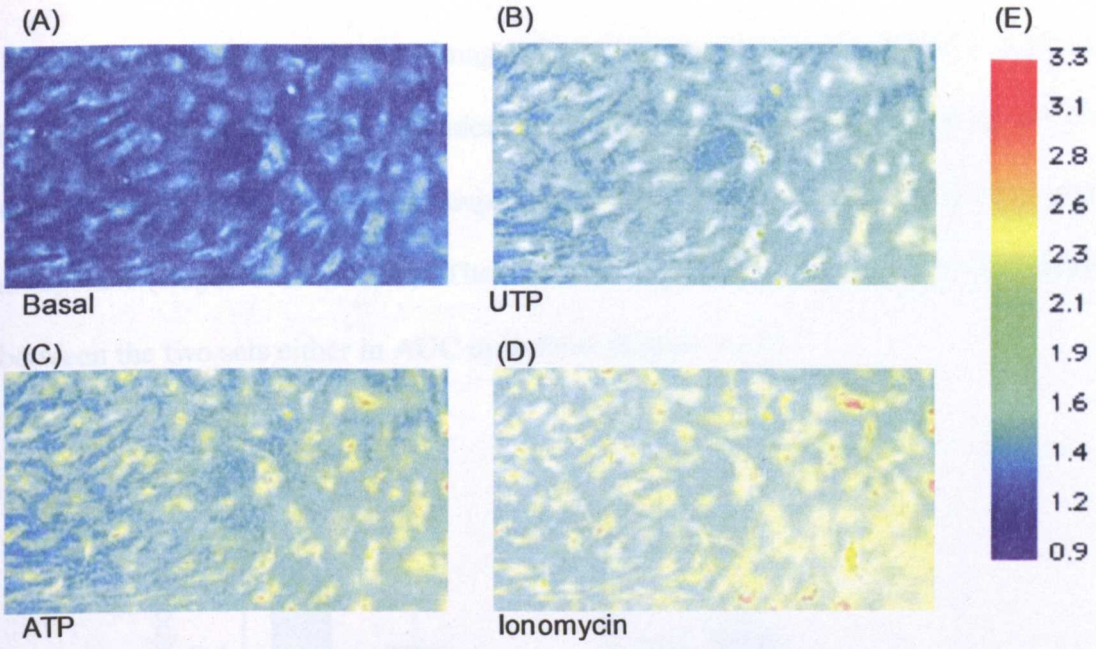


Figure 4-14: Ratiometric pseudocolour images of myoblast cells. A; basal, B, myoblast cells following exposure to 10 μM UTP; C, myoblast cells following exposure to 1 mM ATP; D, myoblast cells following 4 μM ionomycin; E, colour scale, arbitrary numbers representing 340:380 ratios.

Two sets of myoblast cells were imaged from 4 different rats. One set (713 cells) were investigated for responses to ATP alone, while ATP responses in the other set (815 cells) were assessed after 3 minutes exposure to MRS2179, a selective $P2Y_1$ receptor antagonist (Boyer *et al.*, 1998). There was no significant difference in the response between the two sets either in AUC or in Peak (Figure 4-15).

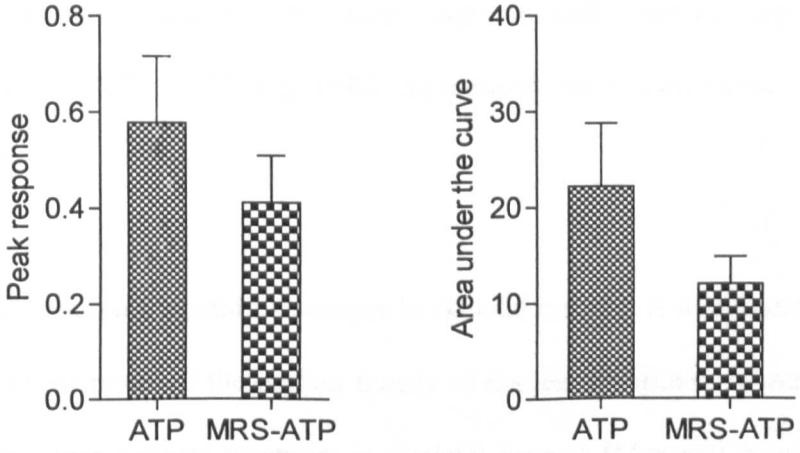


Figure 4-15: Pre-exposure of myoblast cells to the $P2Y_1$ receptor antagonist (MRS2179) (10 μM, for 3 minutes) on the effects of ATP (1 mM)-evoked peak response (A) and AUC (in arbitrary units) (B) in the whole population of cells. Myoblast cells showed an elevation in intracellular calcium levels in response to 1 mM ATP; imaged from four animals; 150-250 cells/animal.Data were analyzed using Paired t test.

## 4.6 Discussion

A number of GPCRs were observed to be expressed in skeletal muscle tissue using the microarray and QRT-PCR (Taqman), as mentioned in Chapter Three. The signalling (functionality) associated with these receptors has not previously been investigated in detail in skeletal muscle. Therefore, conventional second messenger studies (investigating cAMP, $Ca^{2+}$ and ERK activation) were conducted to assess their functionality.

cAMP is an important second messenger in skeletal muscle. It was found to increase the expression of members of the orphan family of nuclear receptors, subfamily 4 (NR4A), compared to other nuclear receptors in skeletal muscle (Maxwell *et al.*, 2005). These transcription factors regulate the gene expression of proteins responsible for fat and glucose metabolism through up-regulating the mRNA expression of pyruvate dehydrogenase kinase 4 (PDK4), forkhead box protein O1 (FOXO1), peroxisome proliferator-activated receptor-γ coactivator (PGC-1α), phosphatidate phosphatase LPIN1 (lipin-1α), GLUT4 and muscle phosphofructokinase (Pfkm) (Chao *et al.*, 2007; Kanzleiter *et al.*, 2010; Lessard *et al.*, 2009). The implication of this is that activation of NR4A receptors might improve glucose glycolysis, glucose transport and lipid oxidation in skeletal muscle, and consequently NR4A receptors might be a therapeutic target for diabetes and obesity. Another critical second messenger is calcium, which transduces extracellular signals into numerous intracellular events in many cell types. Indeed, the functions of calcium range from short-term responses, such as contraction and activation of some enzymes (such as adenylyl cyclase), to longer-term responses such as gene expression (Berridge, 1997). In skeletal muscle, calcium has a crucial role for contraction (Berchtold *et al.*, 2000). When calcium is released from sarcoplasmic

reticulum, it binds to troponin and pulls tropomyosin allowing the myosin to bind to the actin, consequently, contraction occurs (Berchtold *et al.*, 2000). Calcium might also improve contraction-stimulated glucose uptake through activating GLUT4 translocation, calmodulin-dependent protein kinases, calmodulin and protein kinase Cs (Ihlemann *et al.*, 1999; Jessen *et al.*, 2005; Wright *et al.*, 2004; Youn *et al.*, 1991). However, the mechanism is still unclear.

One family of GPCRs, called adrenoceptors, was investigated using the cAMP assay. The adrenoceptors are divided into two major types: α and β-adrenoceptors.

In terms of $\alpha_2$–adrenoceptors, *adra2a* expression was found in rat skeletal muscle using northern blot analysis (Lorenz *et al.*, 1990). Consistent with this report, $\alpha_{2A}$-adrenoceptors were also detected using the microarray and QRT-PCR (Taqman) in this study. The accepted roles for $\alpha_{2A}$-adrenoceptors include acting as the major feedback regulator of noradrenaline release at nerve terminals and the regulation of insulin secretion through noradrenaline in pancreatic islets through reducing the cAMP formation (Ahren, 2000; Nakaki *et al.*, 1981). It is noteworthy that a mutation of $\alpha_{2A}$-adrenoceptors has been shown to be associated with obesity and metabolic alterations (Lima *et al.*, 2007). However, there is a lack of possible roles of the $\alpha_{2A}$-adrenoceptors in skeletal muscle in the literature. Therefore, a cAMP assay was performed to test the functionality of this receptor.

UK14304 was found to inhibit cAMP elevation evoked by forskolin. However, rauwolscine did not prevent this effect. The concentration which was used in this study for UK14304 is in line with that (100 nM) shown to inhibit forskolin-evoked cAMP level in rat primary superior cervical ganglionic (SCG) cells (Shivachar et al., 1999),

and the concentration which was used in this study for rauwolscine is also in line with that (100 nM) shown to reverse the effect of UK14304 inhibition of secretin-stimulated cAMP level in purified rat bile duct-ligated (BDL) cholangiocytes via $\alpha_2$-adrenoceptors (Francis et al., 2007). This suggests that the effect of UK14304 regarding cAMP might not function through $\alpha_{2A}$-adrenoceptors since this effect was not blocked by rauwolscine or it is also possible that the concentration used for rauwolscine did not block the effect of UK14304 in these primary skeletal muscle cells. In other words, the concentration used for rauwolscine might not overcome the effect of UK14304 regarding the cAMP, in particular of the similar relative affinities for UK14304 and rauwolscine to $\alpha_{2A}$-adrenoceptors (Kd=10 nM and Ki=3.5 nM, respectively) (Neubig *et al.*, 1988; Wainscott *et al.*, 1998). Different concentration points of rauwolscine and concentration-response curve for UK14304 are required to have a clear comprehensive image of the response in these primary skeletal muscle cells regarding cAMP.

Interestingly, UK14304 evoked a significant elevation of phosphorylated ERK1/2; an effect blocked by rauwolscine. Furthermore, the inhibitory effect of rauwolscine on basal levels of cAMP could be interpreted to mean that $\alpha_2$-adrenoceptors in this tissue exhibit constitutive activity. Rauwolscine has been reported to be an inverse agonist in stable Chinese hamster ovary cell lines expressing constitutively activated porcine $\alpha_{2A}$-adrenoceptors in which the suppression of cAMP production in these cells is reversed by rauwolscine (Wade *et al.*, 2001). However, nothing in the literature is reported about constitutively activated rat $\alpha_{2A}$-adrenoceptors. It is also possible that the influence of rauwolscine on ERK activation, but not for cAMP inhibition in this study, might be ascribed to an antagonist bias (i.e. affecting one pathway and not affecting another) (Kenakin, 2010; Urban *et al.*, 2007). It is also possible that $\alpha_2$-adrenoceptors mediate the ERK phosphorylation through an adenylyl cyclase-independent cascade in this study.

ERK phosphorylation might be mediated through $G_{\beta\gamma}$ subunit. This is in line with that overexpressed $G_{\beta\gamma}$ subunit in CHO cells was shown to activate MAP kinase (van Biesen *et al.*, 1995). As activation of $\alpha_2$-adrenoceptors was shown in this study to stimulate ERK, and ERK signal transduction was traditionally suggested to growth related process (Bennett *et al.*, 1997; Jones *et al.*, 2001; Lopez-Ilasaca, 1998), it is possible that $\alpha_2$-adrenoceptors have a role in skeletal muscle growth. The implication of this is that long-term treatment of rats with $\alpha_2$-adrenoceptor agonists should stimulate skeletal muscle growth and lean weight gain.

For $\beta_2$-adrenoceptors, in this study, the microarray experiment showed that the mRNA encoding $\beta_2$-adrenoceptors was detected. This agrees with reports of the expression of β–adrenoceptor mRNA in rat skeletal muscle tissues and with expression of $\beta_2$–adrenoceptors in rat L6 cells using RT-PCR (Nagase *et al.*, 2001; Sato *et al.*, 2010). However, treatment of myotube cells with isoprenaline, a non selective β–adrenoceptor agonist (Bylund *et al.*, 1994), did not increase cAMP levels. The concentration which was used in this study for isoprenaline is in line with that (10 μM) shown to increase cAMP production in rat L6 cell membranes (Coppock *et al.*, 1996). Moreover, the concentration which was used in this study for ICI118551 is also in line with that (100 nM) shown to inhibit the isoprenaline-evoked cAMP level in rat primary SCG cells (Shivachar *et al.*, 1999). However, it is worth noting that the concentration used for ICI118551 might not block the effect of isoprenaline (10 μM). In other words, the high concentration of isoprenaline might not be antagonized by the concentration used for ICI118551. Therefore, it is suggested to try another concentration for ICI118551 and isoprenaline. Indeed, the concentration ratio between the isoprenaline and ICI118551 is an important issue to consider in this case as the relative affinity of ICI118551 and

isoprenaline to the receptor, Ki=1.2 nM and Ki=904 nM, respectively (Kikkawa *et al.*, 1997; Kostka *et al.*, 1989).

The explanation behind the lack of response to isoprenaline in myotubes may be due to the fact that mRNA expression levels might not reflect protein expression levels in rat primary skeletal muscle cells. Moreover, skeletal muscle tissue contains multiple cell types (satellites, myoblasts and myotubes) and receptor expression might be restricted to a specific cell type. Further investigations should focus on $\beta_2$-adrenoceptor protein expression using immunoblotting, immunocytochemistry or radioligand binding and should examine any possible potentiation of the effect of isoprenaline in the presence of cholera toxin in skeletal muscle cells indicating that $\beta_2$-adrenoceptor is $G_s$-coupled. Indeed, it should be expected to increase cAMP level in response to isoprenaline and cholera toxin. The rationale behind the use of cholera toxin is also to potentiate the cAMP in myotubes, in particular the cholera toxin induces irreversible potentiation to adenylyl cyclase through ADP-ribosylation for $G_s$-subunit (Kahn *et al.*, 1984).

Another family, which was investigated, was adenosine receptors, which are divided into $A_1$, $A_{2A}$, $A_{2B}$ and $A_3$ adenosine receptors based on pharmacology and coupling to cAMP production. $A_1$ and $A_3$ adenosine receptors are coupled to inhibitory $G_i$-proteins, whereas the $A_{2A}$ and $A_{2B}$ adenosine receptors are coupled to stimulatory $G_s$ proteins.

In this study, $A_1$ and $A_{2A}$ adenosine receptor mRNA was detected in skeletal muscle tissue using the microarray. This is consistent with a previous study that showed that mRNA encoding for adenosine $A_1$ and $A_{2A}$ receptors was detected in rat primary skeletal muscle cells and tissues using northern blot (Lynge *et al.*, 2003).

In order to examine the signalling of adenosine receptors and particularly to investigate the $G_s$-coupling GPCRs, we examined cAMP accumulation in primary rat skeletal muscle cells. NECA, a non-selective adenosine receptor agonist (Castanon *et al.*, 1994; Klotz *et al.*, 1998), was used to examine activation of the $A_{2A}$ or $A_{2B}$ adenosine receptor, while S-ENBA was used to examine activation of the $A_1$ adenosine receptor. S-ENBA did not show any inhibition of cAMP, although the concentration of S-ENBA chosen is consistent with that (100 nM) shown to increase whole cell currents of both inner-wall and cannula-derived human Schlemm's canal cells through $A_1$ adenosine receptors (Karl *et al.*, 2005). However, little in the literature is reported about rats. The lack of response to $A_1$ adenosine receptor stimulation in this study is in line with a previous study that showed forskolin-evoked cAMP was not suppressed by the $A_1$ adenosine receptor agonist, R-PIA in rat primary skeletal muscle (Lynge *et al.*, 2003).

However, NECA, a non-selective agonist for adenosine receptors (Castanon *et al.*, 1994; Klotz *et al.*, 1998), stimulated cAMP accumulation at both 100 nM and 10 μM. The concentration of NECA which was used in this study is in line with that (100 nM) shown to increase cAMP levels in rat coronary endothelial cells (Bindewald *et al.*, 2004). To examine which adenosine receptor ($A_{2A}$ or $A_{2B}$) leads to increases in cAMP levels, CGS21680, an $A_{2A}$ adenosine receptor-selective agonist (Ongini *et al.*, 1999) and PSB603, an $A_{2B}$ adenosine receptor-selective antagonist (Borrmann *et al.*, 2009), were employed. CGS21680 did not alter cAMP levels. However, PSB603 blocked the effect of NECA. This is consistent with a previous study which showed that the stimulation of $A_{2B}$ adenosine receptors by NECA activates adenylyl cyclase and increased cAMP selectively, and not the $A_{2A}$ adenosine receptors which were not stimulated by CGS21680 in rat primary skeletal muscle cells (Lynge *et al.*, 2003). The concentration which was used in this study for PSB603 is in line with that (10 μM) shown to inhibit

adenosine-induced bicarbonate ion secretion in duodenal rats through $A_{2B}$ adenosine receptors (Ham *et al.*, 2010). Similarly, the concentration of CGS21680 used in this study is also in line with that (100 nM) shown to elevate rabbit carotid body cAMP content (Chen *et al.*, 1997b), and (100 nM) shown to enhance cAMP accumulation in hippocampal nerve terminals of aged rats (Rebola *et al.*, 2003). Therefore, the $A_{2B}$ adenosine receptor is an active receptor with regards to cAMP modulation. Regarding $A_{2A}$ adenosine receptor, the lack of response for $A_{2A}$ adenosine receptors might indicate that the number of $A_{2A}$ adenosine receptors might be too small to elicit adenylyl cyclase activation. As indicated above for the β-adrenoceptors, another explanation for the lack of effect of $A_{2A}$ adenosine receptor activation is the mismatch between mRNA and protein expression. Also as suggested above, since skeletal muscle contains multiple cell types (satellites, myoblasts and myotubes), receptor expression might be restricted to a specific cell type. Further work to assess $A_{2A}$ adenosine receptor expression might involve immunoblotting, immunocytochemistry or radioligand binding assay.

The mRNA expression of adenosine receptors, together with the functional coupling of the $A_{2B}$ adenosine receptor, suggests a role for adenosine in skeletal muscle function (Figure 4-9).

$A_{2B}$ adenosine receptor activation was found to increase NR4A expression in smooth muscle (Mayer *et al.*, 2011), it is possible, therefore, that $A_{2B}$ adenosine receptors affect NR4A through the cAMP pathway in skeletal muscle, and consequently, $A_{2B}$ receptors might modulate fat and glucose metabolism in skeletal muscle tissue. This is supported by the fact that 1) NR4A mRNA was found to be expressed in skeletal muscle using microarray in this study. 2) cAMP was found to be involved in increase of expression of NR4A in skeletal muscle (Kawasaki *et al.*, 2011; Pearen *et al.*, 2008; Pearen *et al.*,

2006). 3) NR4A was shown to be reduced in skeletal muscle of diabetic animals (Fu *et al.*, 2007). 4) NR4A was associated with genes related to glucose and fatty acid utilization through up-regulating the mRNA expression of PDK4, FOXO1, PGC-1α and lipin-1α (Pearen *et al.*, 2008). 5) NR4A null mice after high-fat feeding compared with wild-type animals was shown to exhibit decreased mRNA expression of GLUT4 and PDK4 and Lipin 1α and impaired insulin receptor substrate 1 (IRS-1) phosphorylation and insulin resistance in skeletal muscle, and slower blood glucose clearance and increased body weight and decreased energy usage (Chao *et al.*, 2009). 6) In C2C12 cells, C2C12 siRNA-NR4A cells were shown to decrease mRNA expression of fatty acid translocase (CD36/fat), uncoupling protein-3 (UCP3) and GLUT4 compared to wild type native C2C12 cells (Maxwell *et al.*, 2005). 7) In C2C12 cells transfected with adenovirus-mediated NR4A expression, non-insulin glucose uptake was shown to be increased significantly compared to normal C2C12 cells (Chao *et al.*, 2007). Taken together, modulation of $A_{2B}$ adenosine receptor by ligands might affect glucose and fatty acid utilization in skeletal muscle. Therefore, the implication of this is that $A_{2B}$ adenosine receptor agonists should be recommended to be investigated as a therapeutic option in diabetes or obesity.

Adenosine could reach skeletal muscle either from the bloodstream, the motor neuron innervations or the skeletal muscle itself. As skeletal muscle expressed ecto-5'-nucleotidase (ecto-5'-NT) and ecto-phosphodiesterases in this study (Table 4-1), it is possible that skeletal muscle mediates adenosine generation through the extracellular cAMP-adenosine pathway. This is supported by the fact that interstitial accumulation of 5'-AMP (intermediary metabolite of adenosine synthesis) and adenosine was observed after incubation newborn rat skeletal muscle cells with exogenous cAMP (Chiavegatti *et al.*, 2008). This effect was inhibited by using the ecto-phosphodiesterase (1, 3-

dipropyl-8-sulfophenylxanthine (DPSPX)) and ecto-5'-NT (alpha, beta-methylene adenosine 5'-diphosphate (AMPCP)) inhibitors (Chiavegatti *et al.*, 2008; Tofovic *et al.*, 1991; Zimmermann, 1992) in which ecto-phosphodiesterase inhibitors inhibit the conversion of cAMP to 5'-AMP and ecto-5'-NT inhibitors inhibit the conversion of 5'-AMP to adenosine.

Furthermore, adenosine could be also transported into or out of the rat primary skeletal muscle cells through an equilibrative nucleoside transporter, ENT1 (SLC29A1) transporter. This may be due to the fact that when incubation rat primary skeletal muscle cells with the adenosine transporter inhibitor nitrobenzylthioinosine, the ENT1 transporter inhibitor (Ackley *et al.*, 2003; Geiger *et al.*, 1985), the rate of extracellular adenosine accumulation in the electro-stimulated muscle cells was larger compared with control cells (Lynge *et al.*, 2001).

In addition, adenosine can be metabolized in skeletal muscle through adenosine kinase and adenosine deaminase, producing adenosine monophosphate (AMP) and inosine, respectively. Inosine was shown to be implicated in cellular proinflammatory responses to ischemia in mice skeletal muscle and was also reported to activate $A_3$ adenosine receptor in mast cells (Jin *et al.*, 1997; Wakai *et al.*, 2001). However, this issue is not understood yet. AMP generated by the action of adenosine kinase, can be used to regenerate ATP in skeletal muscle. However, intracellular adenosine and homocysteine can be produced from S-adenosylhomocysteine (AdoHcy) through S-adenosylhomocysteine hydrolase (*ahcy*). Homocysteine could be then recycled into cysteine. Indeed, low plasma cysteine level was reported to be associated with progressive loss of human skeletal muscle mass (Droge *et al.*, 1998).

Another family of receptors, the P2Y receptors, was investigated using $Ca^{2+}$-imaging. P2Y receptors are a family of plasma membrane GPCRs involved in several cellular functions and are divided into $P2Y_1$, $P2Y_2$, $P2Y_4$, $P2Y_6$, $P2Y_{11}$, $P2Y_{12}$, $P2Y_{13}$ and $P2Y_{14}$.

In this study, mRNA for $P2Y_1$, $P2Y_2$, and $P2Y_6$ receptors were detected in skeletal muscle using the microarray. This is consistent with a previous study that these receptors were also expressed in mouse C2C12 myoblast and myotubes (Banachewicz *et al.*, 2005). However, in one study in the literature, the expression of $P2Y_1$ and $P2Y_2$ was not detected in human skeletal muscle fibre using immunoblotting and immunohistochemistry. Nevertheless, these receptors were expressed in the vasculature (Borno *et al.*, 2011). This might be ascribed to the difference in physiology between human and rat species or the disconnect between mRNA and protein levels, as suggested previously.

The vasodilatatory effect of the purinergic system was shown to be ~50% lower in diabetic patients compared to control subjects, although the distribution and mRNA expression of receptors were similar in both groups (Borno *et al.*, 2011). Moreover, ATP, localized at the nerve terminal, may be released after stimulation of the prejunctional neurones, leading to activation of P2Y receptors. ATP was also shown to activate glucose uptake in mouse C2C12 skeletal muscle cells through P2 receptors (Kim *et al.*, 2002). Taken together, P2Y receptors might have a therapeutic role in skeletal muscle and diabetes. It is possible, therefore, that the activation of $P2Y_1$, $P2Y_2$ and $P2Y_6$ receptors by agonists in skeletal muscle might be therapeutic targets for diabetic patients.

Little is known about the effects of P2Y receptor activation on skeletal muscle. The

effects of P2Y agonists (ATP and UTP) were tested on levels of intracellular calcium. Intracellular calcium concentration was increased by UTP, which was mainly attributed to P2Y receptors, since UTP is a selective agonist for $P2Y_2$ receptors (El-Tayeb *et al.*, 2006). The explanation behind the fewer number of cells (77%) responding to UTP is possibly due to the fact that the $P2Y_2$ receptors expression might be different during the stage of differentiation for the cells or relative RNA expression level might not reflect the protein expression level in all cells population. Ionomycin was used as a positive control. Ionomycin is supposed to produce a maximum calcium response. However, in the protocol I followed, in which I used ionomycin at the end of the protocol, it is possible that the small response of ionomycin and the differences in the background colour (Figure 4-14) are due to issues regarding the loading of the fura-2 dye. Further work is suggested to be performed regarding identification of $P2Y_2$ receptors expression in skeletal muscle cells using siRNA- $P2Y_2$ receptors or $P2Y_2$ receptor antagonists.

As UTP was shown to increase calcium level in skeletal muscle cells in this study, and UTP was shown to activate ERK dependant on calcium in mouse C2C12 myoblasts (Banachewicz *et al.*, 2005), and ERK was shown to have a role in myoblast proliferation (Bennett *et al.*, 1997; Jones *et al.*, 2001), it is possible that UTP through $P2Y_2$ receptor play a role in skeletal muscle growth. Moreover, as $P2Y_1$, $P2Y_2$ and $P2Y_6$ receptors mRNA was detected in skeletal muscle in this study, and it was also shown that at least UTP as a selective $P2Y_2$ receptor increase calcium level in skeletal muscle cells in this study, it is possible that P2Y receptor might play a role in contraction in skeletal muscle. The implication of this is that P2Y receptors might improve contraction-stimulated glucose uptake. Therefore, P2Y receptor agonists should be recommended to be investigated for diabetes.

The response for ATP was found to be higher than the response for UTP. This possibly suggests that ATP might work through the $P2Y_1$ receptor, not through the $P2Y_2$, and that UTP might work through the $P2Y_2$. MRS2179, the $P2Y_1$ receptor-selective antagonist (Boyer *et al.*, 1998) was investigated to block the effect of ATP. MRS2179 did not inhibit the effect of ATP.

The concentration which was used in this study for MRS2179 is consistent with that (10 μM) shown to prevent ERK activation induced by oxygen and glucose deprivation in rat hippocampal slices (Traini *et al.*, 2011), and is also consistent with that observed to block $P2Y_1$ receptors associated with endogenous calcium activity in mouse astrocytic processes (Di Castro *et al.*, 2011). It might be that other receptors contributed to the response of ATP, such as $P2Y_2$, $P2Y_6$ and $P2X_5$. The concentration used in this study for ATP (1 mM) was possibly too high relative to concentration used for MRS2179 (10 μM), in particular ATP and MRS2179 has similar relative affinity for $P2Y_1$ receptors, Ki=48 nM and Ki=84 nM, respectively (Waldo *et al.*, 2002; Webb *et al.*, 1996). In other words, the concentration used for MRS2179 did not block the effect of ATP. Therefore, it is suggested to take the concentration used for ATP into consideration and perform concentration response curve for ATP or try different concentrations of both ATP and MRS2179. Further selective antagonists for $P2Y_1$ receptors, such as MRS2500 (Cattaneo *et al.*, 2004; Hechler *et al.*, 2006) could be also used to clarify the involvement of $P2Y_1$ receptors. Alternatively, siRNA investigations might allow definition of the role of particular P2 receptors in ATP- and UTP-evoked calcium responses. Further experimental work is also recommended to support the P2Y signalling and exclude the $P2X_5$ signalling such as repeating the same experiments using buffer without calcium ions to ascertain the source of calcium.

As ATP increase calcium level in skeletal muscle in this study, and ATP was shown to

stimulate the proliferation of cancer cells (Deli *et al.*, 2008), and to stimulate the proliferation of astrocytes via P2Y receptors (Neary *et al.*, 2009), it is possible that P2Y receptors play a role in skeletal muscle growth.

A series of investigations of cAMP levels was performed for $CB_1$, GPR119 and NPY Y1 receptors. It is well known that the $CB_1$ receptor is coupled to $G_i$ in many tissues (Demuth *et al.*, 2006). In this study, the mRNA expression of $CB_1$ was detected in rat skeletal muscle culture and tissue using QRT-PCR (Taqman) (see Chapter 3). The $CB_1$ receptor is very highly expressed in the brain (Tsou *et al.*, 1998), but also many studies have found that the $CB_1$ receptor is expressed in peripheral tissues, including adipose and skeletal muscle tissues. However, to date, no specific role(s) of $CB_1$ in the skeletal muscle has been fully understood.

Neither basal nor forskolin (1 μM)–evoked elevation of cAMP was altered significantly in myotube cells in the presence of ACEA (10 nM), AEA (10 μM) or RIM (100 nM) for 10 minutes. Indeed, the concentration which was used for ACEA and AEA in this study is in line with that (10 nM) and (10 μM), respectively shown to activate ERK in rat myotube cells (Chapter 5, Figure 5-3), and the concentration which was used for RIM in this study is also in line with that (100 nM) shown to block ERK phosphorylation (Chapter 5, Figure 5-3). However, it was shown that cannabinoid receptor ligands produce a $CB_1$ receptor-dependent reduction in cAMP levels in transfected CHO cells (Hillard *et al.*, 1999) and different rat brain regions (Bidaut-Russell *et al.*, 1990), and treatment of rat L6 myotube cells with 100 nM RIM for 24 hour was also shown to increase intracellular cAMP production (Esposito *et al.*, 2008). The Esposito *et al* study is not consistent with the present study. This is due to the fact that rat L6 cells are different from rat primary skeletal muscle cells, and the exposure time of RIM is also

different between two studies. It is worth noting that $CB_1$ receptor is functionally-active receptor depending on *cnr1* was detected in skeletal muscle tissue using QRT-PCR (Taqman), and the activation of $CB_1$ receptor by ACEA phosphorylates ERK1/2 in $CB_1$ dependent manner (data was presented in Chapter 5 (Figure 5-3) for convenience).

NPY Y1 receptors are expressed throughout the central and peripheral nervous systems, where the receptor mediates a variety of responses such as the regulation of metabolism and food intake (Gerald *et al.*, 1996; Larsen *et al.*, 1999). Several NPY Y1 receptor antagonists were developed as potential anti-obesity agents (MacNeil, 2007). NPY Y1 receptor mRNA is also expressed primarily in kidney, heart and skeletal muscle and vascular smooth muscle (Nakamura *et al.*, 1995). Activation of NPY Y1 receptors mainly inhibits adenylyl cyclase via $G_i$ proteins (Kassis *et al.*, 1987).

Nothing is known in the literature about possible roles for the NPY Y1 receptor in skeletal muscle. However, neither basal nor forskolin-evoked elevation of cAMP concentration was altered after treatment of myotubes with the selective NPY Y1 receptor agonist [$Leu^{31}$, $Pro^{34}$] Neuropeptide Y (Fuhlendorff *et al.*, 1990) . The concentration which was used in this study for NPY is in line with that (300 nM) shown to inhibit cAMP accumulation in rat slices of the dorsomedial medulla (Fuxe *et al.*, 1987; Harfstrand *et al.*, 1987).

GPR119 is of particular interest since its activation leads to reduced food intake and body weight gain in rodents (Overton *et al.*, 2006). Little is known about GPR119 downstream signalling. However, it is coupled to the $G_s$-protein (Ning *et al.*, 2008; Soga *et al.*, 2005). In the literature, GPR119 was found to raise intracellular cAMP concentrations through $G_s$-coupled in which increase cAMP levels would be expected to

potentiate glucose-stimulated insulin secretion (GSIS) in pancreatic β-cells (Furman *et al.*, 2010; Overton *et al.*, 2008; Soga *et al.*, 2005).

GPR119 was previously found to be expressed in skeletal muscle from both rats and humans using RT-PCR (Soga *et al.*, 2005). In this study, it was also detected in skeletal muscle tissue using QRT-PCR (Taqman). Therefore, GPR119 signalling was investigated using the cAMP assay. Neither AZ359 nor OEA affected cAMP accumulation in rat primary skeletal muscle cells. Moreover, AZ359 did not increase cAMP in the presence of IBMX. The concentration of IBMX which was used in this study is in line with (30 μM) shown to increase cAMP levels in cultured human breast cancer cells (Eilon *et al.*, 1983). Moreover, IBMX was used as a control for the assay and as a potentiating agent for AZ359. The concentration of OEA which was used in this study is in line with that (10 μM) shown to increase cAMP levels in the murine GLUTag intestinal L-cell line. In these cells, GPR119-specific siRNA was shown to reduce OEA-induced cAMP levels (Lauffer *et al.*, 2009).

However, somewhat unexpectedly, AZ359 was shown to inhibit the forskolin-evoked elevation of cAMP concentration in the adipocyte cell line, 3T3-L1. Therefore, GPR119 might couple with the $G_i$ since it showed an inhibition for forskolin in 3T3-L1 adipocytes. To investigate that, further work is suggested to test if GPR119 is $G_i$-coupled in 3T3-L1 using pertussis toxin. Indeed, pertussis toxin should be expected to inhibit AZ359-induced inhibition of forskolin-stimulated cAMP level, indicating that GPR119 is $G_i$-coupled in 3T3-L1.

As GPR119 was detected in adipose tissue in this study, and AZ359 was also found to decrease cAMP level induced by forskolin (Figure 4-3), it is expected that OEA should

inhibit cAMP level induced by forskolin via GPR119. The implication of this is that GPR119 agonists might be a therapeutic option for obesity due to the fact that OEA is a hypophagic agent (Overton *et al.*, 2006).

GPR119 was also investigated for ERK signalling in rat primary skeletal muscle cells using immunoblotting. However, no phosphorylation was observed following GPR119 activation at any time point. It is possible that GPR119 did not couple to $G_s$ in rat primary skeletal muscle culture. It is also possible that mRNA might not reflect the proteins level in skeletal muscle. Further investigation is suggested to examine the protein expression level for this receptor such as immunoblotting or immunocytochemistry.

Regarding signalling via $G_i$-GPCRs (including $\alpha_{2A}$-adrenoceptors, $A_1$ adenosine receptor, $CB_1$ receptor and NPY Y1 receptor), the activation of these GPCRs did not inhibit forskolin-evoked cAMP. The different explanations behind the lack of response for the activation of $G_i$-GPCRs might be due to: 1) As skeletal muscle expressed *adcy2 and adcy6*, it is possible that decrease in cAMP level by inhibition of AC2 and AC6 through $G_i$ protein might be neutralized by activation of AC through $G_{\beta\gamma}$ subunit. This is supported by the fact that $G_{\beta\gamma}$ subunit was found to increase AC2 activity in insect ovarian Sf9 cells infected with recombinant baculovirsus (B-rACII) (Tang *et al.*, 1991), and coexpressed $G_i$ protein in Sf9 cells was also found to inhibit AC2 and AC6 activity (Taussig *et al.*, 1994). 2) The receptors might not couple to $G_i$ protein subunit, therefore, no effect was observed for ligands. 3) $G_i$ protein might not be expressed in skeletal muscle; a potential significant influence is that the conditions for culturing myotubes are different from those *in vivo,* including intermittent innervation and variable (time, concentration, etc.) exposure to hormones. 4) The mismatch between mRNA and

protein expression of these receptors, as suggested previously. As activation of any of the identified $G_i$ GPCRs failed to decrease cAMP levels, it is strongly supported that these GPCRs did not couple to $G_i$ subunit. However, further investigation is suggested to examine the protein expression of these receptors and $G_i$ subunit using immunoblotting and immunocytochemistry. Moreover, investigation is recommended to test the signalling of these receptors using cAMP assay in presence of electrode to mimic the *in vivo* conditions for this primary cell culture. Further investigation is also suggested to examine the coupling of these receptors to $G_i$ protein using pertusis toxin, for example, the effect $\alpha_{2A}$-adrenoceptors of ERK phosphorlyation can be examined if ERK phosphorlyation occurred through coupling to $G_i$ protein. Indeed, inhibition of ERK phosphorlyation should be observed in the presence of pertusis toxin. Furthermore, siRNA for $G_{\beta\gamma}$ subunit is suggested to examine the effect of these GPCRs activation on the cAMP level.

These findings provided evidence for functionally-active $A_{2B}$ adenosine receptors, $CB_1$ receptors and (potentially) $\alpha_2$-adrenoceptors in skeletal muscle which might be important for skeletal muscle fat and glucose metabolism and skeletal muscle growth. These findings also provide evidence for $G_s$-coupling for the $A_{2B}$ adenosine receptor and $G_q$-coupling for $P2Y_1/P2Y_2/P2Y_6$ receptors. However, these findings did not provide direct evidence for $G_i$-coupling for any $G_i$-GPCR tested, including the $CB_1$ receptor (Table 4-2). The impact of the $CB_1$ receptor in skeletal muscle will be the subject of further investigation in the following chapter.

Table 4-2: Summary of findings for Chapter 4.

| Receptors | cAMP level | ERK phosphorylation | Calcium level |
|---|---|---|---|
| $CB_1$ | no effect | increase (↑) | |
| $A_{2B}$ | increase (↑) | | |
| $A_{2A}$ | no effect | | |
| $A_1$ | no effect | | |
| $\alpha_{2A}$ | no effect | increase (↑) | |
| P2Y | | | increase (↑) |
| GPR119 | no effect | | |
| NPY | no effect | | |

# Chapter 5

# Cannabinoid Signalling

# 5 Chapter Five: Cannabinoids and insulin signalling in rat primary skeletal muscle cells

## 5.1 Introduction

Obesity has grown in the United States and throughout the world at an unprecedented rate in recent decades (Ogden *et al.*, 2006; Singh *et al.*, 2011). Obesity, especially fat accumulation in the intra-abdominal region is linked to disease states such as: type 2 diabetes mellitus (Colditz *et al.*, 1995), hypertension (Witteman *et al.*, 1989), cardiovascular disease (Rimm *et al.*, 1995), osteoarthritis, steatohepatitis, and cancer (Calle *et al.*, 2004a; Calle *et al.*, 2003; Calle *et al.*, 2004b). Indeed, obesity has been linked to the development of insulin resistance and other metabolic abnormalities underlying the pathology of Type 2 diabetes mellitus. The pathogenesis of Type 2 diabetes mellitus is the failure of insulin action on metabolic tissues – known as insulin resistance. In other words, insulin resistance is the reduced ability of insulin to effectively stimulate glucose transport due to alteration of insulin receptor expression or insulin release in response to food ingestion (Del Prato *et al.*, 2002; Ferrannini, 1998; Mosthaf *et al.*, 1991). Moreover, insulin resistance can be associated with altered insulin receptor sensitivity which might be modulated by potential pharmacological agents such as RIM (Kahn, 1978).

Skeletal muscle is the largest tissue in the human body and represents ~40% of the human body mass and 35-40% of the total body weight in the rat (Delbono *et al.*, 2007; Pedersen, 2011). Indeed, it plays a crucial role in maintaining body glucose homeostasis (James *et al.*, 1985) and it clears out the majority (70-80%) of ingested glucose since it is the main site for insulin-dependent and non-insulin-dependent or contraction-

mediated glucose uptake (Baron *et al.*, 1988; Ferrannini *et al.*, 1983; Toft *et al.*, 1998). Therefore, skeletal muscle is generally considered as the most important site of insulin resistance. Insulin resistance in skeletal muscle participates in glucose intolerance and consequently in compensatory hyperinsulinemia (Nistala *et al.*, 2006).

Because of the crucial role of skeletal muscle in the etiology of glucose transport, interventions to ameliorate the dysfunction in insulin dependent or non-insulin-dependent pathways were suggested (Zierath *et al.*, 2000).

A novel therapeutic intervention in the treatment of obesity and hyperglycemia might occur through the antagonism of the endocannabinoid system. Indeed, studies from animals and humans have shown that the endocannabinoids are increased in the obese state. In addition, obese animal models showed that levels of endocannabinoids were elevated in the hypothalamus and peripheral tissues (Di Marzo *et al.*, 2001; Matias *et al.*, 2006; Osei-Hyiaman *et al.*, 2005). Moreover, studies showed that circulating levels of AEA and 2-AG were raised, and 2-AG was also found to be elevated in visceral adipose tissue in obese and hyperglycaemic type 2 diabetic patients (Bluher *et al.*, 2006; Engeli *et al.*, 2005; Matias *et al.*, 2006). Furthermore, $CB_1$ knock-out mice were found to be resistant to diet-induced obesity (Osei-Hyiaman *et al.*, 2005; Ravinet Trillou *et al.*, 2004). Originally, $CB_1$ receptor antagonism was investigated as a mediator of the hypophagic effect which leads to weight loss (Di Marzo *et al.*, 2001; Vickers *et al.*, 2003). However, independent to hypophagic weight loss attributed to $CB_1$ receptor antagonism, $CB_1$ receptor antagonism was also discovered to improve metabolic parameters, such as increased glucose uptake in skeletal muscle (Liu *et al.*, 2005), increased glucose tolerance (Bermudez-Siva *et al.*, 2006; Nogueiras *et al.*, 2008) and decreased hyperinsulinemia (Doyon *et al.*, 2006) as well as effects on lipids (increased

HDL/LDL ratio and increased triglyceride) (Despres *et al.*, 2005).

As previously stated, skeletal muscle is the primary tissue for glucose uptake. $CB_1$ receptor mRNA and protein expression has been detected in skeletal muscle myotubes and tissues of rodents and humans (Cavuoto *et al.*, 2007b; Pagotto *et al.*, 2006). In addition, in mice fed a high fat diet (HFD), the expression of $CB_1$ in skeletal muscle was found to be up-regulated (Pagotto *et al.*, 2006).

From agonist and antagonist studies, both *in vitro* and *in vivo*, it seems that the endocannabinoid system plays a role in glucose transport in skeletal muscle. *In vitro*, using cell culture models (L6 mouse myotube cell line and human primary skeletal muscle cells), Esposito et al and Eckardt et al, respectively showed that $CB_1$ receptor antagonism using RIM enhanced basal and insulin-stimulated glucose transport activity (Eckardt *et al.*, 2008b; Esposito *et al.*, 2008). *In vivo*, chronic $CB_1$ receptor antagonism was found to increase insulin-stimulated glucose transport activity in obese mice (Liu *et al.*, 2005). Furthermore, chronic $CB_1$ receptor antagonism during euglycemic hyperinsulinemic clamp increased glucose uptake in diet-induced obese rats by several skeletal muscle groups (Nogueiras *et al.*, 2008). These data suggest that the endocannabinoid system can play a role regarding glucose transport in skeletal muscle.

The glucose transport into the skeletal muscle is facilitated mainly by the GLUT4 isoform. The mechanism, through which $CB_1$ antagonists affects glucose levels is unknown. AKT, GSK3, AMPK, and P38 are proteins associated with insulin-stimulated and non-insulin-stimulated signalling involved in glucose transport activity. From the literature, many researchers showed that $CB_1$ receptor might affect these proteins. Regarding P38 and AMPK, treatment of myotubes with a $CB_1$ receptor agonist

increased the phosphorylation of P38 (Eckardt *et al.*, 2008b). Even though it was shown that $CB_1$ receptor modulation did not affect AMPK in skeletal muscle in Zucker rats (Lindborg *et al.*, 2011), another group showed that chronic $CB_1$ receptor antagonism in obese mice increased AMPK phosphorylation in the liver (Watanabe *et al.*, 2009). Indeed, it was shown that RIM activated AMPK in HepG2 cells (Wu *et al.*, 2011). $CB_1$ receptor antagonism was additionally suggested to have an effect on key signaling proteins related to energy status, such as increased phospho-AMPK in cultured white adipose cells (Tedesco *et al.*, 2008). $CB_1$ receptor antagonism was also shown to increase mRNA expression of AMPK in human primary myotubes (Cavuoto *et al.*, 2007a). Regarding AKT and GSK3, there are controversial data about the phosphorylation of AKT in L6 cells, primary skeletal muscle cells and tissues. Addition of the cannabinoid HU-210 was associated with increased phosphorylation of AKT as well as GSK3β in granule cell precursors during early cerebellar development (Trazzi *et al.*, 2010). Furthermore, it was shown that THC was associated with increased phosphorylation of AKT as well as GSK3β in the central nervous system, but not with low dose-treatment of RIM (Ozaita *et al.*, 2007). However, another study showed that HU-210 induced a reduction in whole-body glucose disposal and impaired insulin-stimulated AKT phosphorylation in skeletal muscle (Song *et al.*, 2011).

The effects of $CB_1$ cannabinoid receptor agonism and antagonism in terms of glucose uptake, metabolism and insulin signalling on peripheral targets, particularly skeletal muscle are unclear (Eckardt *et al.*, 2009; Lindborg *et al.*, 2011; Lipina *et al.*, 2010). In an attempt to address this issue, the signalling events underlying the activation and inhibition of the $CB_1$ receptor in rat primary skeletal muscle cells were investigated. Furthermore, the effects of pharmacological activation or blockade of $CB_1$ receptor on insulin signalling were investigated. The effect of RIM and ACEA on gene expression

was also investigated in rat primary skeletal muscle cells.

## 5.2 Aims

### 5.2.1 General aim

The main aim of this series of experiments was to investigate the impact of $CB_1$ activation and inhibition upon insulin signaling and to characterize the molecular mechanisms that mediate the direct effects of ACEA and/or RIM on skeletal muscle.

### 5.2.2 Specific aims

-To assess whether activation of $CB_1$ receptor with both physiological and pharmacological cannabinoids (AEA and ACEA) affects ERK, P38 and AMPK phosphorylation.

-To assess whether activation of $CB_1$ receptor with ACEA and AEA and their inhibition with RIM and AM251 affects insulin-induced phosphorylation of AKT, GSK, ERK, and P38.

-To compare gene expression in rat primary skeletal muscle cells in response to the following treatments: ACEA, ACEA+RIM, RIM alone and ACEA + U0126 (MEK inhibitor). The comparison of the effects of U0126 versus vehicle and RIM versus vehicle will provide information about the direct effects of U0126 and RIM on gene expression. The independent and combined effects of ACEA and RIM will be examined by comparison of the following conditions:

- Comparison of condition (ACEA versus vehicle) and (ACEA+RIM versus RIM) wil provide information about the effect of ACEA in the presence and absence of RIM.

- Comparison of condition (ACEA versus vehicle) and (ACEA+U0126 versus U0126) wil provide information about the effect of ACEA in the presence and absence of U0126.

- Comparison of condition (ACEA versus vehicle) and (ACEA+U0126 versus ACEA) will reveal to what extent the effects of ACEA on gene expression are mediated via ERK pathway.

- Comparison of condition (ACEA versus vehicle) and (ACEA+RIM versus ACEA) will reveal to what extent the effects of ACEA on gene expression are mediated via $CB_1$ receptor.

## 5.3 Experimental design and methods

### 5.3.1 Experiments for ERK and P38 phosphorylation

Primary Wistar rat vastus lateralis 90% confluent myotubes (5 weeks in culture) (n=6 wells) were serum-starved (Ham-F 10 medium alone) for 3 hours. Then, the cells were treated for 10 minutes with vehicle (0.05% ethanol), ACEA 10 nM, ACEA 100 nM, RIM 100 nM for 40 minutes, ACEA 10 nM+ RIM (cells were pretreated with RIM for 30 minutes before addition of ACEA), AEA 10 μM and AEA 10 μM + RIM (cells were pretreated with RIM for 30 minutes before addition of AEA). After treatment, cells were washed with ice-cold PBS, and then were lysed with Trizol (800 μl per well). P-ERK/ERK and P-P38/P38 ratios were used to compare the activation of ERK and p38 between conditions.

### 5.3.2 Experiments for AMPK phosphorylation

Primary Wistar rat vastus lateralis 90% confluent myotubes (5 weeks old) in 25 $cm^2$ flasks were incubated with charcoal stripped fetal bovine serum 6% for 24 hours before treated for 1 or 2 hours with either AICAR 1 mM, vehicle (ethanol 0.01%), ACEA 10 nM, RIM 100 nM, ACEA+AICAR (cells were preincubated with ACEA for 30 minutes prior to treatment with AICAR). After treatment, cells were washed with ice-cold PBS, and then were lysed with Trizol (2 ml per 25 $cm^2$ flask). P-AMPK/cyclophilin ratio was used to compare the activation of AMPK among various conditions.

### 5.3.3 Experiments for the effect of ACEA, RIM, AM251 and insulin

Primary Wistar rat vastus lateralis 90% confluent myotubes (5 weeks old) (grown in 6% delipidated serum) were treated for 22 hours with vehicle (ethanol 0.01%), ACEA 100 nM, RIM 100 nM, AM251 100 nM and AEA 10 μM. Then, the cells were serum-starved for 2 hours, and this was followed by the cells being treated with insulin 100 nM for 10 minutes. After treatment, the cells were washed with ice-cold PBS, and then were lysed with Trizol. P-AKT/AKT, P-ERK/ERK, P-P38/P38 and P-GSK/GSK ratios were used to compare the activation of AKT, ERK1 and 2, P38 and GSK3 among various conditions.

### 5.3.4 Glucose uptake assay

Myotubes, differentiated as detailed in Chapter 2, Section 2.10, were serum-starved for 2 hours and then were treated with 2.5 nM, 5 nM, 10 nM, 50 nM and 100 nM insulin for

10 minutes, followed by addition of 27.8 KBq 3H 2-DOG and 1.5 mM cold 2-DOG for 10 minutes. Glucose uptake was carried out as described in Chapter 2.

**Calculation:**

Uptake percentage = total amount of disintegrations per minute (DPM) measured per well (absorbed) /total amount of DPM added per well * 100%

(pmoles of glucose multiply by uptake percentage)/incubation time=pmole/minutes

### 5.3.5 Microarray

#### 5.3.5.1 Experimental design

Myotubes were cultured in 25 $cm^2$ flasks and incubated with ACEA 10 nM, RIM 100 nM and U0126 10 μM for 24 hours (four flasks/condition). Ethanol 0.01% was used as a vehicle control. Fresh charcoal stripped fetal bovine serum 6% was replaced for four hours before performing the treatment. RIM and U0126 were used for 30 minutes before the relevant treatments.

#### 5.3.5.2 Procedure for the microarray

The treated myotubes were lysed using Trizol and stored at -80°C, then total RNA was extracted and cleaned up with the Qiagen Rneasy kit according to the manufacturer's instructions.

All RNA samples were examined using Agilent Bioanalyzer. Samples that had a RIN

greater than 8 were included in the analysis. These values indicated that RNA degradation did not occur. Distinct bands of 28S and 18S RNA were visualized in all RNA samples isolated from the vehicle, ACEA, RIM and U0126-treated myotubes to confirm that the RNA was suitable for microarray procedure (Table 5-1).

Table 5-1: Quality of RNA isolated from myotubes.

| Samples | RIN | Samples | RIN |
|---|---|---|---|
| Vehicle1 | 9.8 | RIM1 | 9.5 |
| Vehicle2 | 9.5 | RIM2 | 9.7 |
| Vehicle3 | 9.8 | RIM3 | 9.8 |
| Vehicle4 | 10 | RIM4 | 10 |
| ACEA1 | 8.7 | ACEA+U0126 1 | 9.8 |
| ACEA2 | 9.3 | ACEA+U0126 2 | 9.6 |
| ACEA3 | 9.8 | ACEA+U0126 3 | 9.7 |
| ACEA4 | 9.5 | ACEA+U0126 4 | 9.9 |
| ACEA+RIM1 | 9.5 | U0126 1 | 9.6 |
| ACEA+RIM2 | 9.9 | U0126 2 | 9.6 |
| ACEA+RIM3 | 9.8 | U0126 3 | 9.5 |
| ACEA+RIM4 | 8.1 | U0126 4 | 8.9 |

Briefly, synthesis of labelled cRNA, hybridization, and scanning of microarrays were carried out as described (Schafer *et al.*; Voss *et al.*, 2005) according to established methods in the manufacturer's protocols (Affymetrix, Santa Clara, CA) by staff at the Nottingham Arabidopsis Stock Centre (NASC).

### 5.3.5.3 Gene expression profiling, data processing and analysis

Global changes in gene expression induced by ACEA, RIM and U0126 were determined using Affymetrix Rat Genome 230 PM Array.

### 5.3.5.4 Pre-analysis data treatment

Before analysis took place, the raw microarray (Cel files) data was pre-processed through RMA (Robust Multichip Averaging) algorithm. RMA has the following components; background correction, normalization and probe summarization.

A) Background correction was based on the distribution of perfect match (PM) values amongst probes on an Affymetrix array. Plate and exon (PM only) arrays contain a set of antigenomic background probes that are not matched to any putative transcript region. By default, the Affymetrix software estimates probe background signal by the median response of all background probes with matching GC content to the probe in question. This background signal is then subtracted from the probe intensity to yield a background-corrected intensity.

B) Quantile normalization was performed within all arrays based on the raw intensities (Raymond *et al.*, 2010). Normalization was performed to remove nonbiological effect among all arrays. This makes all arrays comparable. The RMA used quantile normalization. In this normalization, 1) probe intensities were ranked for each array, 2) the average across all arrays was taken and 3) the corresponding values of probe intensities were all set to the average. Consequently, these steps force the distribution of measurements on all arrays to be equal.

C) Probe summarization was performed through observing probe behavior [i.e., log transformed (PM) after background correction; any values attributed to background were eliminated] on the log scale as the sum of the actual expression value on the log scale (a probe specific term).

The summary of the final steps of data transformation were:

1) Log2 transformation of the intensities.

2) Tukey's median polish was used to summarize the intensity values of individual probes into a single measurement for the corresponding gene.

After raw data was normalized, genespring GX 11 software was used to identify differentially expressed genes.

### 5.3.5.5 Initial characterisation of microarray gene expression data

The microarray data were summarized using Principal Components Analysis (PCA) based on gene expression patterns for each of the experimental conditions (Figure 5-1). All four replicates treated with ACEA, RIM and U0126 were grouped in the scatter plot.

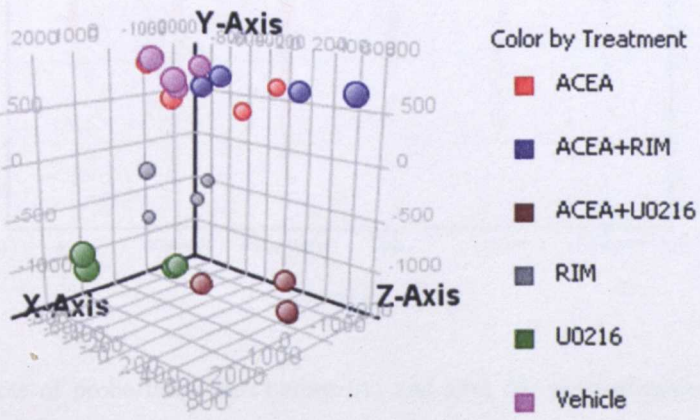


Figure 5-1: Three-dimensional scatter plot view of technical replicates of myotubes. Myotubes (four flasks, n=1 rat) were cultured and treated with 10 nM ACEA, 100 nM RIM or 10 μM U0126 for 24 hours. The Whole-Transcript Expression Analysis was performed by hybridizing RNA to the Affymetrix Rat Genome 230 PM Array. The dataset was visualized using Principal Components Analysis (PCA). Samples were displayed in respect to the first three components and coloured by the treatment parameter.

As shown in Figure 5-2; normalized intensity values (y-position) shows reasonable variability across the conditions. All boxes had relatively similar interquartile range and median of the distribution.

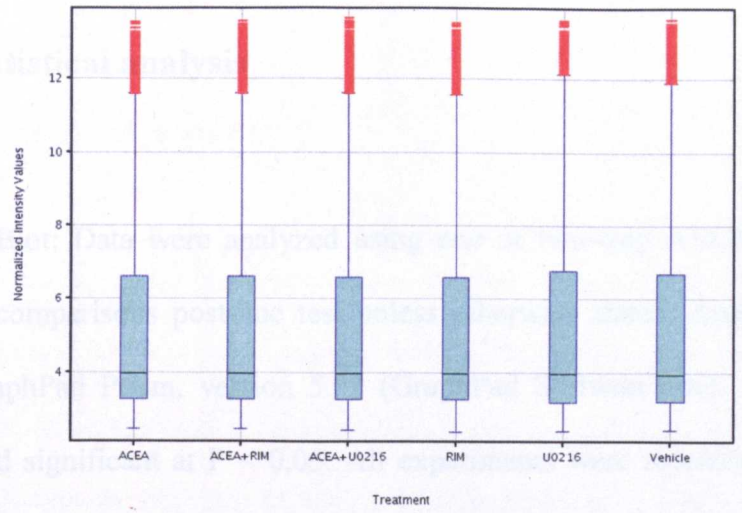


**(A)**

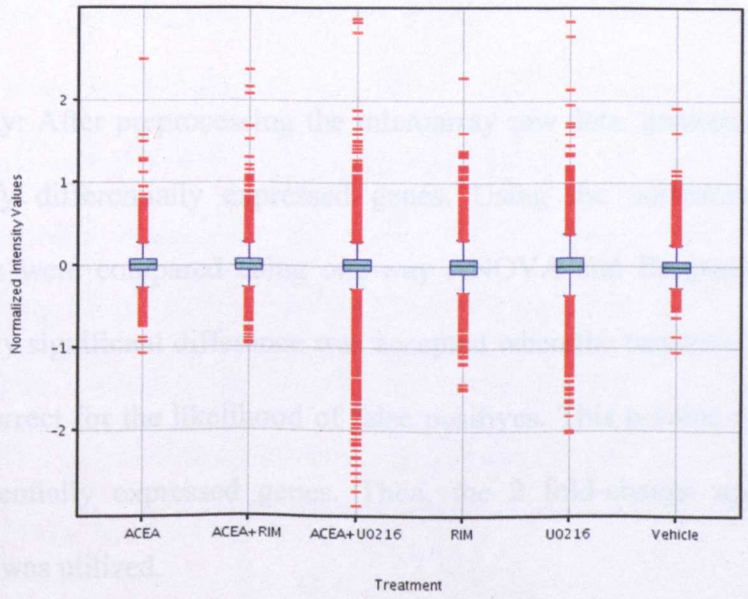


**(B)**

Figure 5-2: Box-plots of probe intensities before (A) and after (B) normalization. The raw intensity values were background-corrected, quantile-normalized and log (base 2)-transformed at the probe level using the Robust Multi-array Average (RMA).

Correlation was performed between pairs of conditions using Affymetrix IDs common to all microarrays. In order to test the reproducibility of these data, the correlation coefficient of technical replicates were calculated between conditions on the normalized data. All correlation coefficients were found to be higher than 0.98 across all conditions. The normalized data (not transformed to the median of all samples) was used in all subsequent analyses.

## 5.4 Statistical analysis

Western Blot: Data were analyzed using one or two-way ANOVA and Bonferroni's multiple comparisons post-hoc test unless otherwise stated. Analysis was performed using GraphPad Prism, version 5.03 (GraphPad Software Inc). The difference was considered significant at $P < 0.05$. All experiments were repeated at least twice from two different animals.

Microarray: After preprocessing the microarray raw data, genespring GX 11 was used to identify differentially expressed genes. Using the normalized microarray data, conditions were compared using one-way ANOVA and Benjamini-Hochberg test. A statistically significant difference was accepted when the treatment effect yielded a $P < 0.05$ to correct for the likelihood of false positives. This p-value was used as a cut off for differentially expressed genes. Then, the 2 fold-change approach (increase or decrease) was utilized.

Data were further analysed using Ingenuity Pathways Analysis (IPA) **http://www.ingenuity.com**. The list of differentially regulated genes identified by the microarray analysis using genespring GX 11 was exported into IPA, which predicted biological functions of genes that are associated with particular biological processes.

Statistics was performed from low number of repeats (n=2 rats) (no statistical difference was observed among the replicates within the same treatment) for western blot and glucose uptake experiments and (n=1 rat (4 flasks)) for microarray experiment in this chapter due to cost implications. Indeed, it is recommended to perform more repeats to support the results deduced in this chapter, in particular it is hard to depend on statistical

analysis from 1 or 2 repeats due to variations in species or technical work. More repeats will solidate the data statistically.

Due to the limitations of time and cost, a complete concentration response curve or time response curve were not performed for every drug. Instead, a single concentration and a single time point were used based on the previous literature. Different concentrations and time points are required to have a clear comprehensive image about the nature of the response. Depending on a single time point and a single ligand concentration is not sufficient to completely exclude a potential cross-talk between insulin and cannbinoids or a potential effect for RIM or ACEA in these primary skeletal muscle cells. Regarding the experimental designs for the microarray or western blot, the use of 24 hours treatment may miss potential changes in insulin sensitivity or the effects of ACEA and RIM. Indeed, repeating the microarray experiment and western blot is required at different time points such as 3 minutes, 5 minutes, 10 mintues, 30 minutes, one hour, 6 hours, 12 hours, 18 hours and 24 hours.

## 5.5 Results

### 5.5.1 Effect of ACEA, AEA, and RIM on ERK phophorylation

In order to assess the signalling of the $CB_1$ receptor, ERK phosphorylation was investigated (Figure 5-3).

Cells treated with ACEA (10 nM and 100 nM) and AEA (10 μM) for 10 minutes showed a significant increase in P-ERK1/ERK1 and P-ERK2/ERK2 ratio compared to vehicle ($P<0.001$). Pretreatment of the myotubes with 100 nM RIM for 30 minutes prior the addition of either 10 nM ACEA or 10 μM AEA inhibited these effects. However, there was no significant difference between 100 nM RIM and vehicle (0.01% ethanol). It is worth mentioning that ACEA, AEA and RIM did not activate (phosphorylate) AKT. The treatment of muscle culture with 100 nM ACEA and 100 nM RIM for 24 hours did not alter the phosphorylation for ERK1/2 compared to vehicle (Figure 5-8). The molecular weight of the bands for P-ERK1/ERK1 and P-ERK2/ERK2 was detected at 44 kDa and 42 kDa, respectively, as expected.

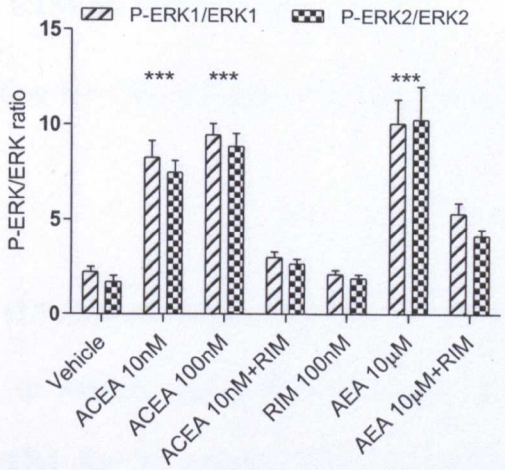


A)

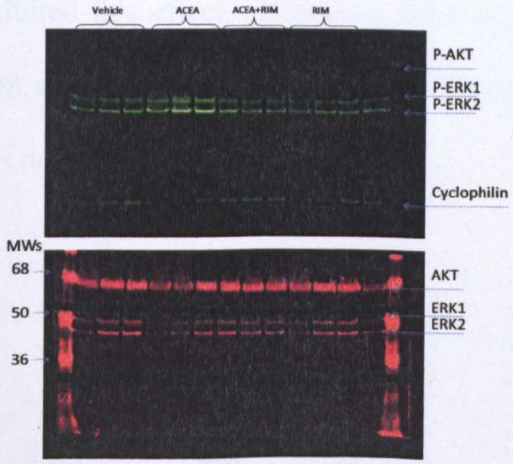


B)

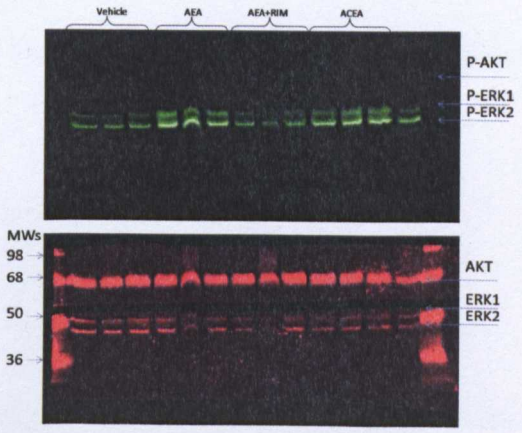


C)

Figure 5-3: Effect of ACEA, AEA and RIM on phosphorylation of ERK in rat primary muscle cells (n=2 rats). A) Myotubes were treated with vehicle (0.01% ethanol), ACEA (10 and 100 nM) or AEA (10 µM) for 10 minutes; RIM only for 40 minutes; RIM for 30 minutes before the addition of either ACEA or AEA. *** denotes P<0.001 when compared to vehicle, RIM and agonist+RIM conditions. B and C) Representative blots showing rat primary muscle cells treated with vehicle (0.01% ethanol), ACEA (10 nM) in B figure, ACEA (100 nM) in C figure, and AEA (10 µM) for 10 minutes and RIM for 30 minutes. Phospho-ERK 1/2 is shown in green bands and total ERK 1/2 in red bands. Data were analyzed using one way ANOVA test followed by Bonferroni post-hoc.

### 5.5.2 Effect of ACEA, RIM on P38 phosphorylation

In order to test the signalling for $CB_1$ receptor, P38 phosphorylation was investigated (Figure 5-4).

Cells treated with ACEA (10 nM) for 10 minutes showed a significant increase in P-P38/P38 ratio compared to vehicle ($P<0.001$). Interestingly, pretreatment of the myotubes with 100 nM RIM for 30 minutes prior the addition of 10 nM ACEA inhibited this effect. However, there was no significant difference between 100 nM RIM and vehicle (0.01% ethanol). The molecular weight of the bands for P-P38/P-38 was detected at 43 kDa as expected.

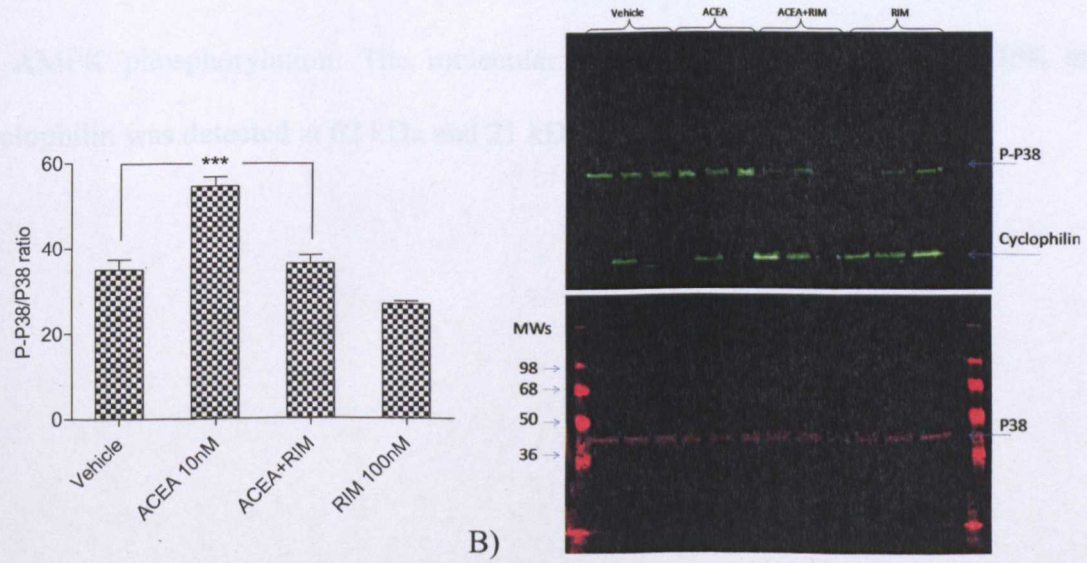


Figure 5-4: Effect of ACEA and RIM on phosphorylation of in rat primary muscle cells (n=2 rats). A) Myotubes were treated with vehicle (0.01% ethanol), ACEA (10 nM) for 10 minutes; RIM only for 40 minutes; RIM for 30 minutes before the addition of ACEA. *** denotes $P<0.001$ when compared to vehicle, RIM and ACEA+RIM conditions. B) Representative blots showing rat primary muscle cells treated with vehicle (0.01% ethanol), ACEA (10 nM) for 10 minutes and RIM for 30 minutes. Phospho-P38 is shown in green bands and total P38 in red bands. Data were analyzed using one way ANOVA test followed by Bonferroni post-hoc.

### 5.5.3 Effect of ACEA, RIM on AMPK phosphorylation

AMPK is a protein that might play a role in glucose uptake, increase cell surface GLUT4 levels and fatty acid oxidation (Aschenbach *et al.*, 2002). The effect of cannabinoids on AMPK phosphorylation was investigated (Figure 5-5).

The AMPK agonist AICAR (1 mM) produced a significant 3-6 fold stimulation of P-AMPK levels at 1 hour and 2 hours compared to vehicle ($P<0.001$), two-way ANOVA, Bonferroni *post-hoc*. However, there was no significant difference between ACEA or RIM and vehicle. Pre-treatment with ACEA did not alter the AICAR-induced increase in AMPK phosphorylation. The molecular weight of the bands for P-AMPK and cyclophilin was detected at 62 kDa and 21 kDa, respectively, as expected.

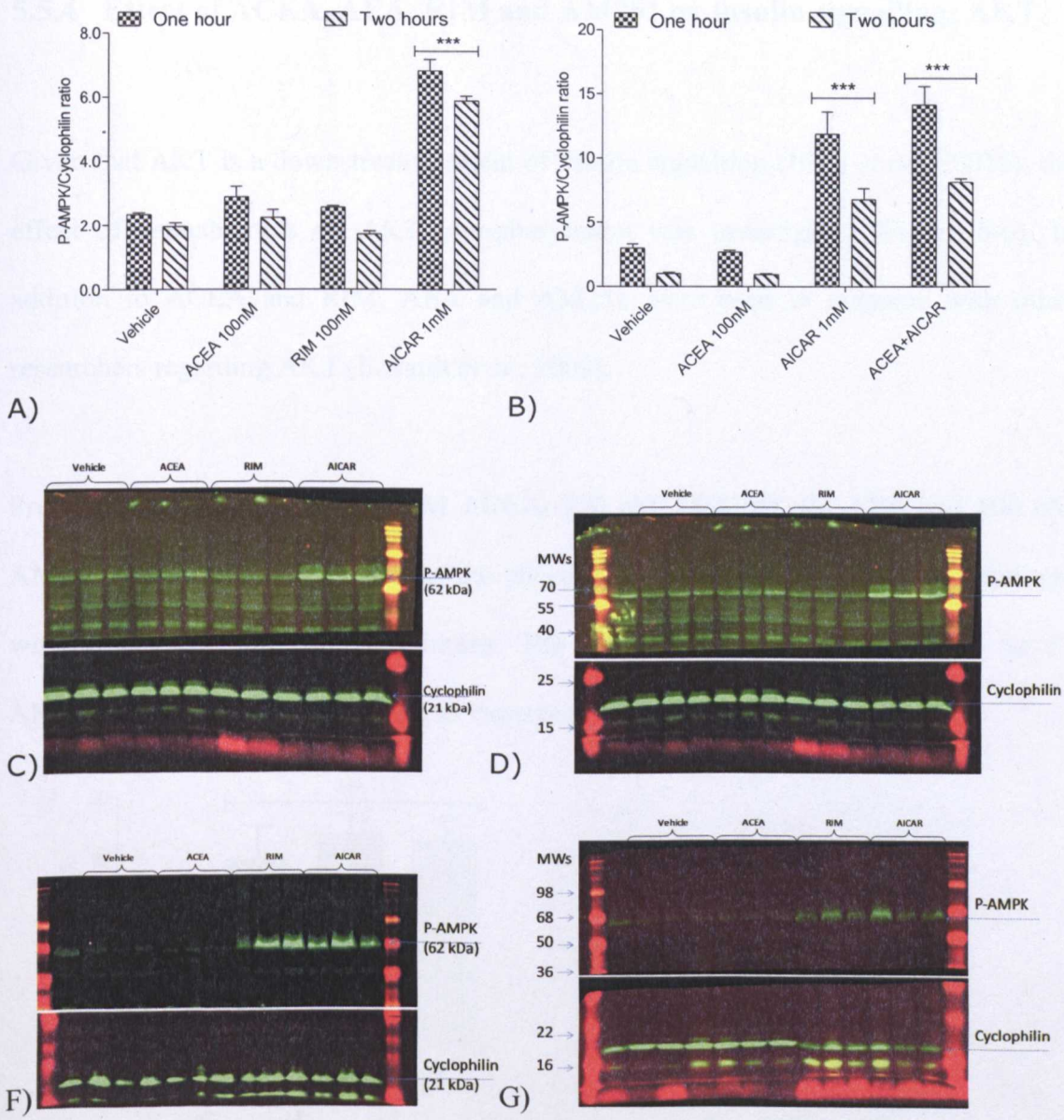


Figure 5-5: Effect of ACEA, RIM and AICAR on phosphorylation of AMPK in rat primary muscle cells (n=2 rats). A and B) Myotubes were treated with vehicle (0.01% ethanol), ACEA (100 nM), RIM (100 nM), AICAR (1 mM) and ACEA+AICAR for 1 and 2 hours. *** denotes P<0.001 when compared to vehicle, ACEA, RIM and AICAR. C and D) Representative blots showing rat primary muscle cells treated for 1 hour. F and G) Representative blots showing rat primary muscle cells treated for 2 hours. P-AMPK and cyclophilin are shown in green bands. Data were analyzed using two way ANOVA test followed by Bonferroni post-hoc.

### 5.5.4 Effect of ACEA, AEA, RIM and AM251 on insulin signalling; AKT.

Given that AKT is a downstream protein of insulin signalling (Jiang *et al.*, 2003b), the effect of cannabinoids on AKT phosphorylation was investigated (Figure 5-6). In addition to ACEA and RIM, AEA and AM251 were used to compare with other researchers regarding AKT (Eckardt *et al.*, 2009).

Pretreatment of cells with 100 nM ACEA, 100 nM RIM, 10 μM AEA and 100 nM AM251 for 24 hours did not affect the phosphorylation of AKT induced by treatment with 100 nM insulin for 10 minutes. The molecular weight of the bands for P-AKT/AKT was detected at 62 kDa as expected.

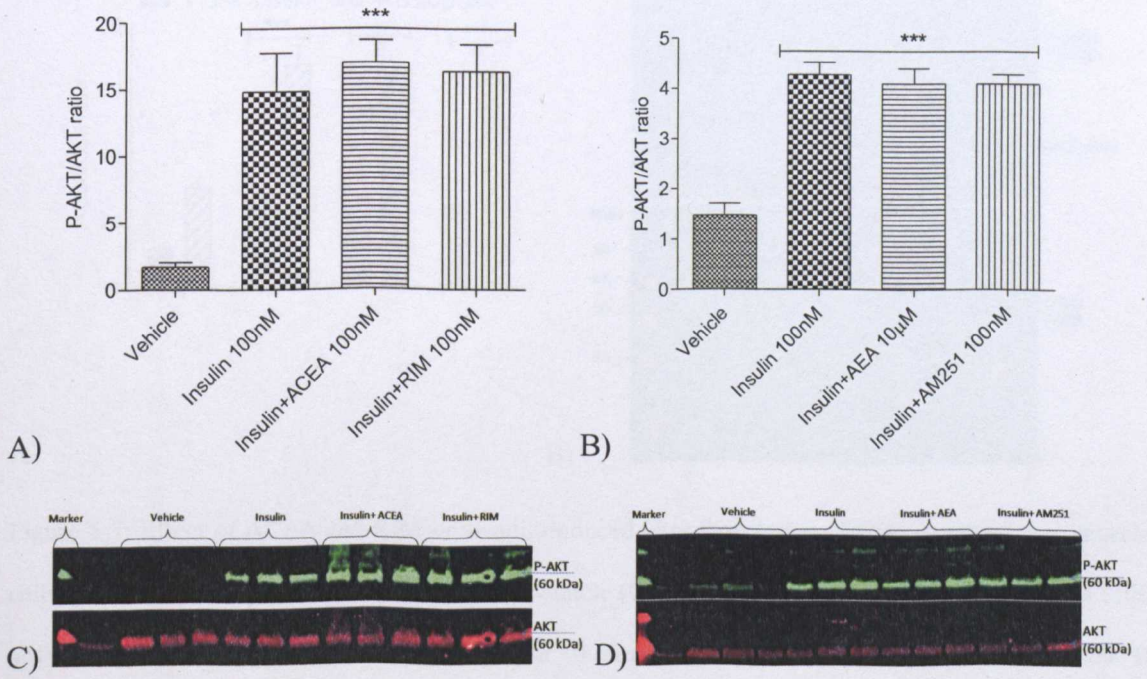


Figure 5-6: Effect of ACEA, AEA, RIM and AM251 on insulin-induced phosphorylation of AKT in rat primary muscle cells (n=2 rats). A and B) Myotubes were treated with vehicle (0.01% ethanol), ACEA (100 nM), AEA (10uM), RIM (100 nM) and AM251 (100 nM) for 24 hours before the addition of insulin for 10 minutes. *** denotes $P<0.001$ when compared to vehicle. C and D) Representative blots showing rat primary muscle cells treated with different conditions. Phospho-AKT is shown in green bands and AKT in red bands. Data were analyzed using one way ANOVA test followed by Bonferroni post-hoc.

### 5.5.5 Effect of ACEA and RIM on insulin signalling; GSK.

GSK, a downstream target for AKT, inhibits glycogen synthesis (Cross *et al.*, 1995). Therefore, the effect of cannabinoids on GSK phosphorylation was investigated (Figure 5-7). The reason behind using ACEA and RIM, not AEA and AM251, was to compare this study with what a previous study found regarding GSK in rat (Lindborg *et al.*, 2011). The pretreatment of cells with 100 nM ACEA, 100 nM RIM for 24 hours did not alter the insulin-induced phosphorylation state of GSK. The molecular weight of the bands for P-GSKα/ GSKα and P-GSKβ/GSKβ was detected at 44 kDa and 42 kDa, respectively as expected.

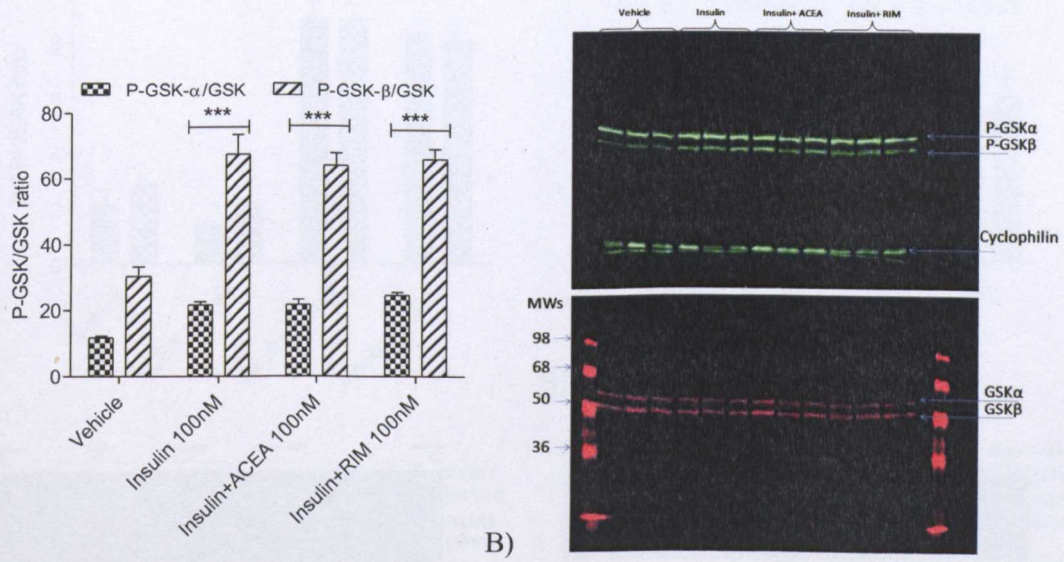


Figure 5-7: Effect of ACEA and RIM on insulin-induced phosphorylation of GSK in rat primary muscle cells (n=2 rats). A) Myotubes were treated with vehicle (0.01% ethanol), ACEA (100 nM) and RIM (100 nM) for 24 hours before the addition of insulin for 10 minutes. *** $P<0.001$ when compared to vehicle. B) Representative blots showing rat primary muscle cells treated with different conditions. Phospho-GSK is shown in green bands and GSK in red bands. Data were analyzed using one way ANOVA test followed by Bonferroni post-hoc.

### 5.5.6 Effect of ACEA and RIM on insulin signalling; ERK.

Another downstream protein of insulin signaling is ERK (Holt *et al.*, 1996). Therefore, the effect of cannabinoids on ERK phosphorylation was investigated (Figure 5-8).

The pretreatment of cells with 100 nM ACEA and 100 nM RIM for 24 hours did not alter the insulin-induced phosphorylation of ERK1/2. The molecular weight of the bands for P-ERK1/ERK1 and P-ERK2/ERK2 was detected at 44 kDa and 42 kDa, respectively, as expected.

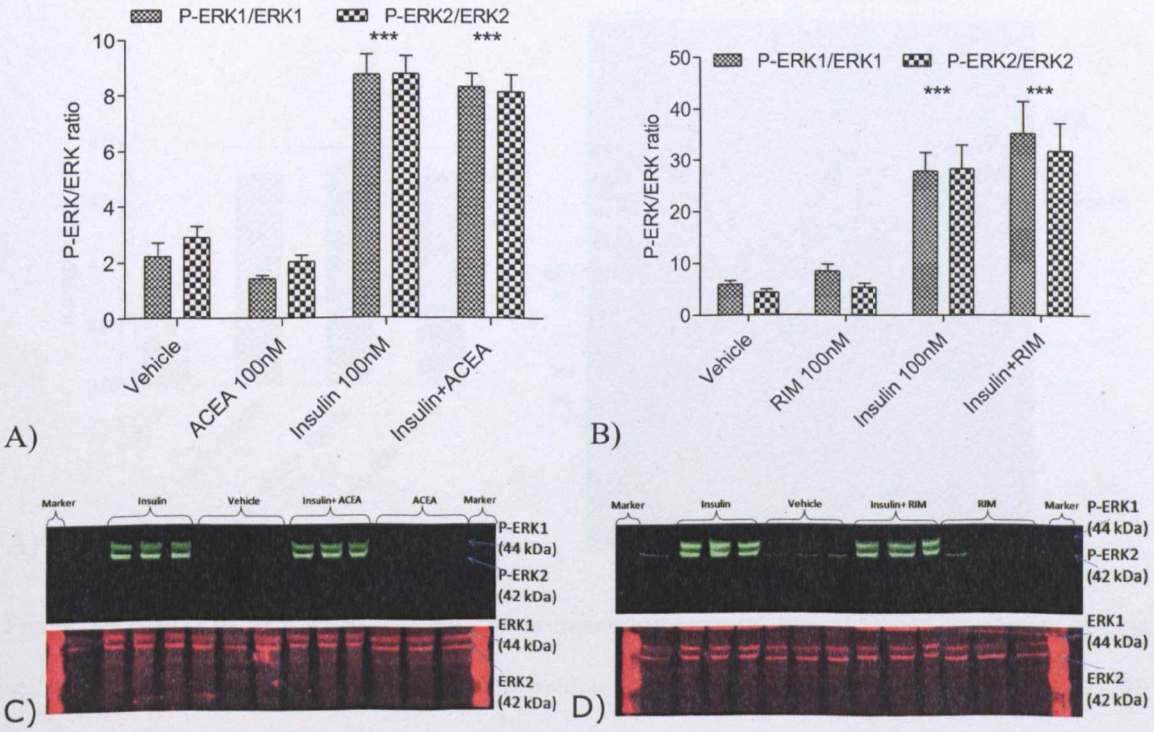


Figure 5-8: Effect of ACEA and RIM on insulin-induced phosphorylation of ERK in rat primary muscle cells (n=2 rats). A and B) Myotubes were treated with vehicle (0.01% ethanol), ACEA (100 nM) and RIM (100 nM) for 24 hours before the addition of insulin for 10 minutes. *** denotes $P<0.001$ when compared to vehicle and ACEA. C and D) Representative blots showing rat primary muscle cells treated with different conditions. Phospho-ERK is shown in green bands and total ERK in red bands. Data were analyzed using one way ANOVA test followed by Bonferroni post-hoc.

### 5.5.7 Effect of ACEA and RIM on insulin signalling; P38

Another downstream protein of insulin is P38 (Somwar *et al.*, 2000). Therefore, the effect of cannabinoids on P38 phosphorylation was investigated (Figure 5-9).

The pretreatment of cells with 100 nM ACEA or 100 nM RIM given 24 hours prior to insulin treatment did not affect the insulin-induced phosphorylation of P38. The molecular weight of the bands for P-P38/P-38 was detected at 43 kDa as expected.

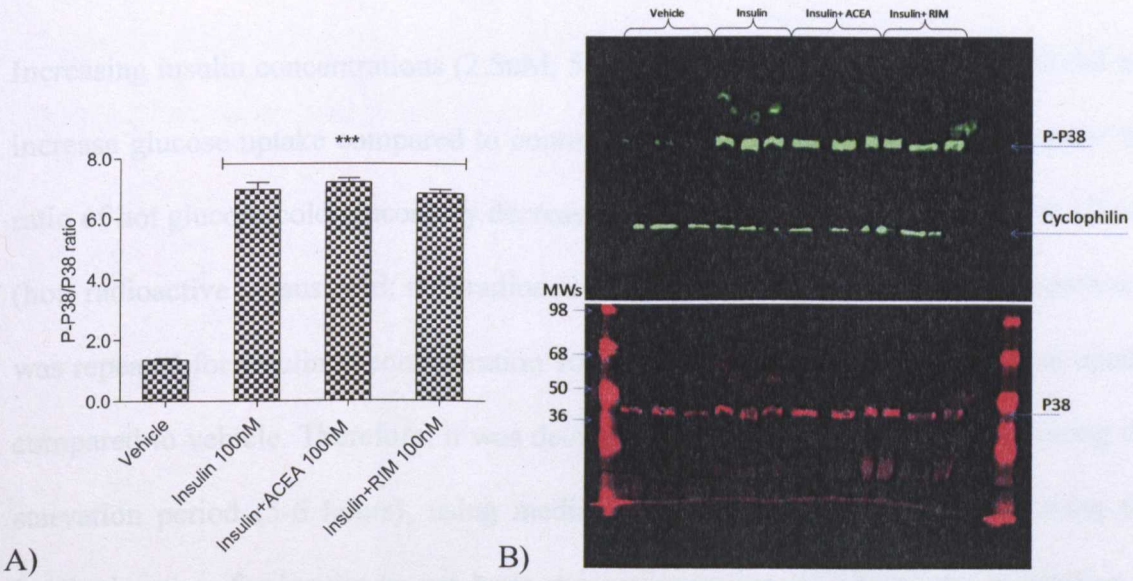


Figure 5-9: Effect of ACEA and RIM on insulin-induced phosphorylation of P38 in rat primary muscle cells (n=2 rats). A) Myotubes were treated with vehicle (0.01% ethanol), ACEA (100 nM) and RIM (100 nM) for 24 hours before the addition of insulin for 10 minutes. *** denotes $P<0.001$ when compared to vehicle. B) Representative blots showing rat primary muscle cells treated with different conditions. Phospho-P38 is shown in green bands and total P38 in red bands. Data were analyzed using one way ANOVA test followed by Bonferroni post-hoc.

### 5.5.8 The effect of cannabinoids on glucose uptake

It was shown in this study (this Chapter, Section 5.5.4) that 100 nM insulin, when incubated with skeletal muscle cell culture, resulted in an increase in AKT phosphorylation. It was also shown in previous studies that cannabinoids affect glucose uptake (Eckardt *et al.*, 2008b; Lindborg *et al.*, 2011). In order to understand the effects of cannabinoids on skeletal muscle myotubes, glucose uptake was examined in this model of skeletal muscle cell culture as an index of glucose uptake.

Increasing insulin concentrations (2.5nM, 5nM, 10nM, 50nM and 100nM) used did not increase glucose uptake compared to control. Therefore, it was decided to increase the ratio of hot glucose/cold glucose by decreasing the cold 2-DOG concentration to 10 μM (hot: radioactive versus cold: non-radioactive). At 10 μM cold glucose, the experiment was repeated for insulin at concentration 100 nM. Insulin did not induce glucose uptake compared to vehicle. Therefore, it was decided to modify the method by increasing the starvation period (5-6 hours), using media instead of reaction buffer, increasing the incubation time for insulin to one hour at a concentration of 200nM and incubation in hot glucose to 15 minutes.

In the previous conditions, insulin gave only a slight response in some wells compared to control. Unfortunately, this experiment was repeated many times, and the results were reproducible; we saw a slight but non-significant change in glucose uptake or no change. In other words, insulin did not induce glucose uptake compared to vehicle. Therefore, it was decided to modify the method of utilizing the cell culture; after collecting satellite cells (pellet), cells were plated in 75 $cm^2$ flask and grown in 25 mM glucose, 10% FBS DMEM. After they became 70% confluent, cells were trypsinized 2-

3 times with trypsin and then plated in 6 well plates. After around 3-4 days, glucose uptake assay was performed. Insulin did not induce glucose uptake compared to vehicle (Vehicle 1=19.56, Vehicle 2 = 18.74, Insulin 1 = 18.02 and Insulin 2 = 19.05 pmol/min/mg). Taking all experiments into consideration which were performed for glucose uptake in rat primary myotubes, it was decided to use 3T3-L1 adipocytes as positive control for the original and modified technique.

3T3-L1 adipocytes were serum-starved for 24 hours with 12.5mM glucose or 5 hours with 5.5 mM glucose; and then glucose uptake assay was conducted as discussed in chapter 2 section 2.11.2 and 2.11.4. 200nM insulin was shown to significantly increase glucose uptake compared to vehicle (4-6 fold) (Figure 5-10).

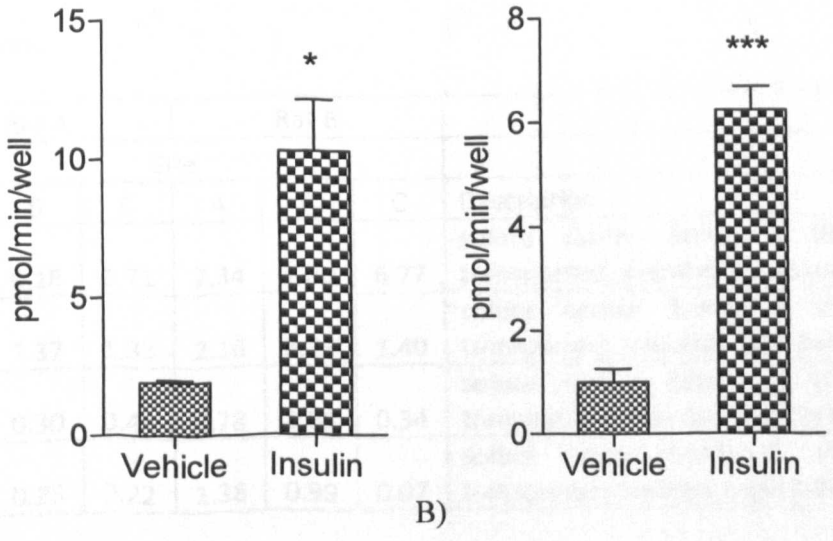


Figure 5-10: 2-DOG uptake by mature 3T3-L1 adipocytes in response to insulin (n=2 experiments). A) 2-DOG uptake, using protocol (adjusted protocol)-DMEM in 6 well plates (See Chapter 2 Section 2.11.4). 3T3-L1 adipocytes were treated with 200 nM insulin for one hour. Data was analyzed using a t-test, * $p<0.05$. B) 2-DOG uptake, using original protocol in 6 well plates (see Chapter 2, Section 2.11.2). 3T3-L1 adipocytes were treated with 200 nM insulin for 10 minutes. Data was analyzed using a t-test, *** $p<0.001$. Uptake was measured as pmol per minute per well in both figures (A+B).

The mRNA expression of GLUT4 was detected in skeletal muscles using Agilent microarray (Table 5-2). Therefore, it was decided to do the immunocytochemistry to investigate GLUT4 translocation induced by insulin in 3T3-L1 adipocytes and myotubes using the same conditions as for glucose uptake. Using immunofluorescence microscopy, the translocation and localization of the GLUT4 was visualized in 3T3-L1 adipocytes cells, upon insulin signalling (Figure 5-11). In the quiescent adipocytes, the cytoplasm vesicle was stained by anti-GLUT4 antibody (Figure 5-11-A). On the other hand, in insulin-treated adipocytes, cell membrane was stained by anti-GLUT4 antibody (Figure 5-11-B). However, no obvious cell membrane translocation of GLUT4 was observed in insulin-treated myotubes.

Table 5-2: Intensity values for mRNA expression for GLUT from skeletal muscle tissue using Agilent microarray.

| Rat A | | | Rat B | | | |
|---|---|---|---|---|---|---|
| Site | | | | | | |
| A | B | C | A | B | C | Description |
| 6.81 | 6.18 | 6.71 | 7.34 | 7.00 | 6.77 | solute carrier family 2 (facilitated glucose transporter), member 4 (Slc2a4)/GLUT4 |
| 1.58 | 1.37 | 1.33 | 2.16 | 1.65 | 1.40 | solute carrier family 2 (facilitated glucose transporter), member 4 (Slc2a4)/GLUT4 |
| 0.65 | 0.30 | 0.44 | 0.78 | 1.61 | 0.34 | solute carrier family 2 (facilitated glucose transporter), member 1 (Slc2a1)/ GLUT1 |
| 0.11 | 0.25 | 0.22 | 1.38 | 0.99 | 0.07 | solute carrier family 2, (facilitated glucose transporter) member 8 (Slc2a8)/GLUT8 |

A) 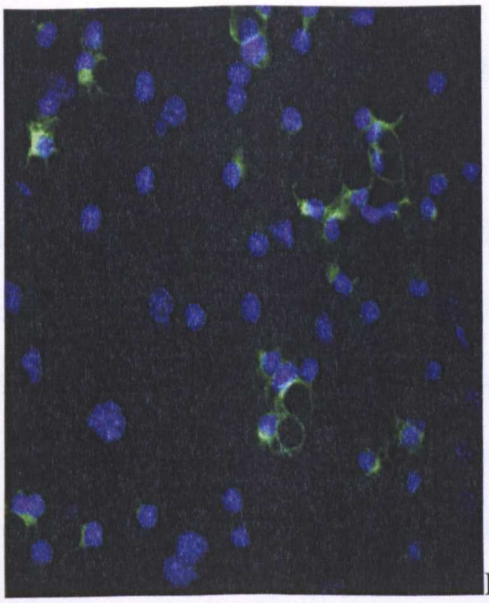 B) 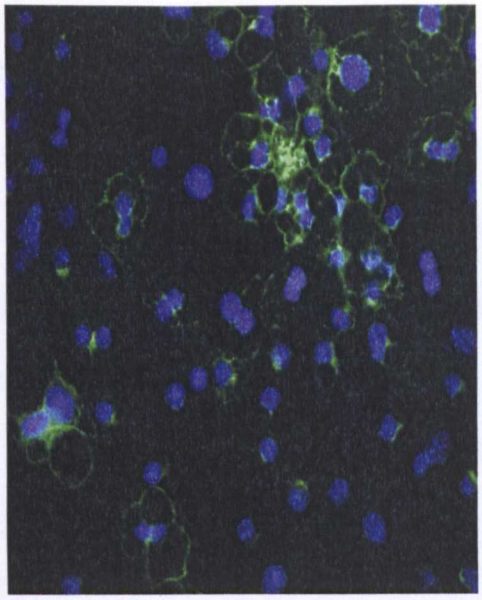

Figure 5-11: Immunofluorescence staining of GLUT4 in 3T3-L1 adipocytes using DMR fluorescent microscope (n=2 experiments). A) Microscope image of day 9 adipocytes stained with anti-GLUT4 antibody. B) Microscope image of Day 9 adipocytes were treated with 200 nM insulin for one hour. They were stained with anti-GLUT4 antibody.

### 5.5.9 The effect of the ACEA and RIM on gene expression

The phospho-ERK was activated with treatment of myotubes with ACEA. This response was inhibited by RIM. The influence of ACEA on gene expression and whether the differential genes expression affected by ACEA are $CB_1$ receptor dependent (blocked by RIM) and/or ERK dependant (blocked by U0126) was investigated using Affymetrix microarray.

Treatment with ACEA up-regulated frizzled-related protein (FRZD) mRNA gene expression and down-regulated early growth response 2 (EGR2), hyaluronan synthase 2 (HAS2), oxidized low density lipoprotein (lectin-like) receptor 1 (OLR1) and regulator of G-protein signaling 2 (RGS2) mRNA gene expression (Figure 5-12) (see (Table 9-13) in Appendix for complete data).

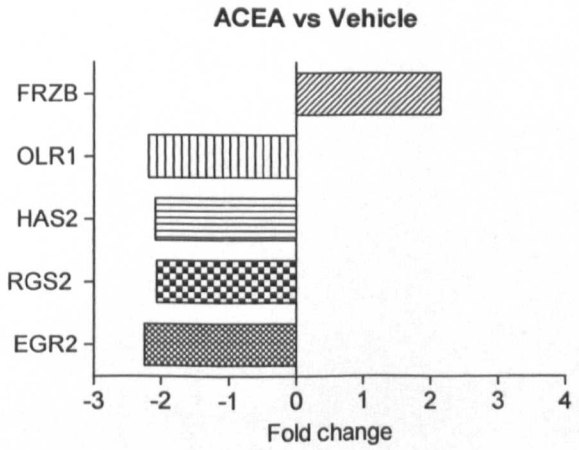


Figure 5-12. The effect of ACEA on mRNA gene expression in rat primary skeletal muscle cells (fold changes) (n=1 rat). RGS2; regulator of G-protein signaling 2, 24kDa, OLR1; oxidized low density lipoprotein (lectin-like) receptor 1, HAS2; hyaluronan synthase 2, FRZB; frizzled-related protein and EGR2; early growth response 2. Data were analyzed using one way ANOVA test followed by Benjamini-Hochberg test.

The mRNA expression of EGR2, RGS2 and HAS2 were down-regulated by ACEA; interestingly these responses were blocked by RIM (ACEA+RIM compared to ACEA). However, in the presence of RIM (ACEA+RIM vs RIM), ACEA up-regulated the mRNA expression of ERG2, RGS2 and HAS2. Interestingly, RIM alone down-regulated the expression of these genes. In other words, the influence of ACEA on ERG2, RGS2 and HAS2 are CB1 dependent. The expression of these genes was not blocked by U0126. U0126 down-regulated mRNA expression of EGR2, RGS2, HAS2 and OLR1. However, the influence of ACEA in the presence of U0126 is different to that of ACEA alone. In the presence of U0126, ACEA up-regulated the mRNA expression of RGS2 and HAS2 and down-regulated OLR1 mRNA expression (Figure 5-13).

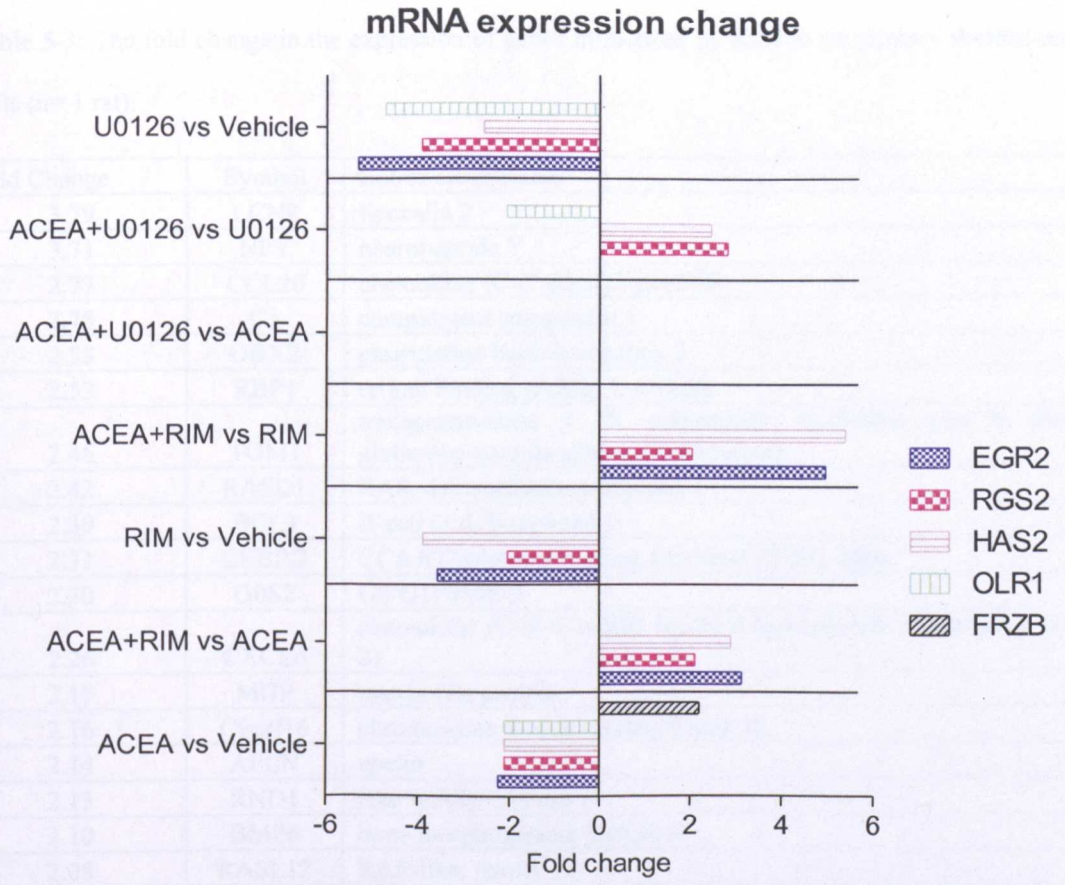


Figure 5-13: Fold changes in gene expression of EGR2, RGS2, HAS2, OLR1 and FRZB in response to different conditions in rat primary skeletal muscle cells (n=1 rat). EGR2; early growth response 2, RGS2; regulator of G-protein signaling 2, 24kDa, OLR1; oxidized low density lipoprotein (lectin-like) receptor 1, HAS2; hyaluronan synthase 2 and FRZB; frizzled-related protein. Data were analyzed using one way ANOVA test followed by Benjamini-Hochberg test.

Interestingly, treatment with RIM altered mRNA expression of a number of genes. These genes represent transcription regulators (ANKRD57, BCL3, CEBPD, EGR2, GBX2, HIVEP1, ID4, IRX3), cytokines (CCL20, CXCL6), transporters (AQP1, LCN2, RBP1, SLC16A7), peptidases (C3, PRSS35), nuclear receptors (NR4A1, NR4A2, NR4A2, NR4A3, NR4A3), GPCR (PTGER4) and growth factor (BMP6). In particular, LCN2 and NPY were up-regulated by RIM compared to vehicle while NR4A were down-regulated by RIM compared to vehicle (Table 5-3).

Table 5-3: The fold change in the expression of genes influenced by RIM in rat primary skeletal muscle cells (n= 1 rat).

| Fold Change | Symbol | Entrez Gene Name |
|---|---|---|
| 3.79 | LCN2 | lipocalin 2 |
| 3.71 | NPY | neuropeptide Y |
| 2.77 | CCL20 | chemokine (C-C motif) ligand 20 |
| 2.75 | C3 | complement component 3 |
| 2.58 | GBX2 | gastrulation brain homeobox 2 |
| 2.53 | RBP1 | retinol binding protein 1, cellular |
| 2.46 | TGM1 | transglutaminase 1 (K polypeptide epidermal type I, protein-glutamine-gamma-glutamyltransferase) |
| 2.42 | RASD1 | RAS, dexamethasone-induced 1 |
| 2.39 | BCL3 | B-cell CLL/lymphoma 3 |
| 2.31 | CEBPD | CCAAT/enhancer binding protein (C/EBP), delta |
| 2.30 | G0S2 | G0/G1switch 2 |
| 2.26 | CXCL6 | chemokine (C-X-C motif) ligand 6 (granulocyte chemotactic protein 2) |
| 2.17 | MGP | matrix Gla protein |
| 2.16 | C9orf16 | chromosome 9 open reading frame 16 |
| 2.14 | APLN | apelin |
| 2.13 | RND1 | Rho family GTPase 1 |
| 2.10 | BMP6 | bone morphogenetic protein 6 |
| 2.08 | RASL12 | RAS-like, family 12 |
| 2.08 | KRT18 | keratin 18 |
| -2.01 | ANKRD57 | ankyrin repeat domain 57 |
| -2.02 | PRSS35 | protease, serine, 35 |
| -2.03 | RGS2 | regulator of G-protein signaling 2, 24kDa |
| -2.06 | RAD51 | RAD51 homolog (S. cerevisiae) |
| -2.07 | TRIO | triple functional domain (PTPRF interacting) |
| -2.09 | NR4A2 | nuclear receptor subfamily 4, group A, member 2 |
| -2.09 | BUB1 | budding uninhibited by benzimidazoles 1 homolog (yeast) |
| -2.09 | PTGER4 | prostaglandin E receptor 4 (subtype EP4) |
| -2.10 | STARD13 | StAR-related lipid transfer (START) domain containing 13 |
| -2.11 | KIF20B | kinesin family member 20B |
| -2.12 | GNAI3 | guanine nucleotide binding protein (G protein), alpha inhibiting activity polypeptide 3 |
| -2.13 | SLC16A7 | solute carrier family 16, member 7 (monocarboxylic acid transporter 2) |
| -2.14 | EFEMP1 | EGF containing fibulin-like extracellular matrix protein 1 |
| -2.18 | LRRN4CL | LRRN4 C-terminal like |
| -2.21 | IRX3 | iroquois homeobox 3 |
| -2.21 | NR4A2 | nuclear receptor subfamily 4, group A, member 2 |
| -2.21 | ITGBL1 | integrin, beta-like 1 (with EGF-like repeat domains) |
| -2.24 | MKI67 | antigen identified by monoclonal antibody Ki-67 |
| -2.33 | HIVEP1 | human immunodeficiency virus type I enhancer binding protein 1 |
| -2.35 | KIF11 | kinesin family member 11 |
| -2.42 | ARL4C | ADP-ribosylation factor-like 4C |
| -2.56 | TRIB3 | tribbles homolog 3 (Drosophila) |
| -2.56 | AQP1 | aquaporin 1 (Colton blood group) |
| -2.58 | ECT2 | epithelial cell transforming sequence 2 oncogene |
| -2.72 | C1QTNF3 | C1q and tumor necrosis factor related protein 3 |
| -2.84 | NR4A3 | nuclear receptor subfamily 4, group A, member 3 |
| -3.23 | NR4A3 | nuclear receptor subfamily 4, group A, member 3 |

| | | |
|---|---|---|
| -3.56 | EGR2 | early growth response 2 |
| -3.88 | HAS2 | hyaluronan synthase 2 |
| -4.23 | ID4 | inhibitor of DNA binding 4, dominant negative helix-loop-helix protein |
| -5.22 | NR4A1 | nuclear receptor subfamily 4, group A, member 1 |

The treatment with RIM affected the expression of a number of genes involved in the activation of the following biological functions; adipogenesis of cells, inflammatory response, activation of phagocytes, proliferation of smooth muscle cells and impairment of tumorigenesis (Table 5-4).

Table 5-4: The biological functions ascribed to genes that were altered by treatment with RIM (n=1 rat). For the gene abbreviation, see (Table 5-3).

| Category | Functions Annotation | Predicted Activation State | Molecules |
|---|---|---|---|
| Cellular Development | adipogenesis of cells | Increased | C3,CEBPD,NPY,NR4A1,NR4A2, NR4A3 |
| Connective Tissue Development and Function | adipogenesis of cells | Increased | C3,CEBPD,NPY,NR4A1,NR4A2, NR4A3 |
| Inflammatory Response | inflammatory response | Increased | C3,CCL20,CXCL6,GNAI3,LCN2,NPY ,NR4A2,PTGER4 |
| Inflammatory Response | activation of phagocytes | Increased | C3,CXCL6,LCN2,NPY |
| Cell-To-Cell Signaling and Interaction | activation of phagocytes | Increased | C3,CXCL6,LCN2,NPY |
| Hematological System Development and Function | activation of phagocytes | Increased | C3,CXCL6,LCN2,NPY |
| Immune Cell Trafficking | activation of phagocytes | Increased | C3,CXCL6,LCN2,NPY |
| Antigen Presentation | activation of phagocytes | Increased | C3,CXCL6,LCN2,NPY |
| Cell-To-Cell Signaling and Interaction | activation of cells | Increased | BCL3,C3,CXCL6,EGR2,KRT18, LCN2,NPY |
| Cellular Growth and Proliferation | proliferation of smooth muscle cells | Increased | CEBPD,NR4A1,NR4A2,NR4A3 |
| Skeletal and | proliferation | Increased | CEBPD,NR4A1,NR4A2,NR4A3 |

| | | | |
|---|---|---|---|
| Muscular System Development and Function | of smooth muscle cells | | |
| Cancer | tumorigenesis | Decreased | AQP1,ARL4C,BCL3,BMP6,BUB1,C3, CEBPD,CXCL6,ECT2,EFEMP1,HAS2 ,ID4,ITGBL1,KIF11,KIF20B,KRT18,L CN2,MGP,MKI67,NR4A1,NR4A2,NR 4A3,PTGER4,RAD51,RASL12,RBP1, RGS2,STARD13,TRIO |

The effect of U0126 on gene expression in rat primary skeletal muscle cells is shown in Table 9-18 in Appendix. The treatment with U0126 affected the expression of a number of genes involved in the activation of tumorigenesis (Table 5-5).

Table 5-5: The biological functions ascribed to genes that were altered by treatment with U0126 (n=1 rat). For the gene abbreviation, see (Table 9-18) in Appendix.

| Category | Functions Annotation | Predicted Activation State | Molecules |
|---|---|---|---|
| Tissue Morphology | quantity of tumor cell lines | Increased | BHLHE40,BIRC5,CCNB1,IGFB P3,JUN,KIF20B,PRC1 |
| Cell Cycle | mitosis of cervical cancer cell lines | Increased | BIRC5,CCNB1,CDC20,DLGAP5 ,PLK1,PTTG1,TOP2A |
| Cell Cycle | polyploidization of cells | Increased | BIRC5,BUB1B,GPC1,TOP2A |
| Cell Death | cell death of endothelial cells | Increased | ANGPT1,BIRC5,IGFBP3,NR4A3 ,OLR1,PDGFRB,TNFRSF11B |

Treatment with U0126 alone altered the expression of 5 genes (JUN, KLF10, PDGFRB, CCNA2 and LAMA2) that have a role in the development of skeletal muscle cells (Figure 5-14).

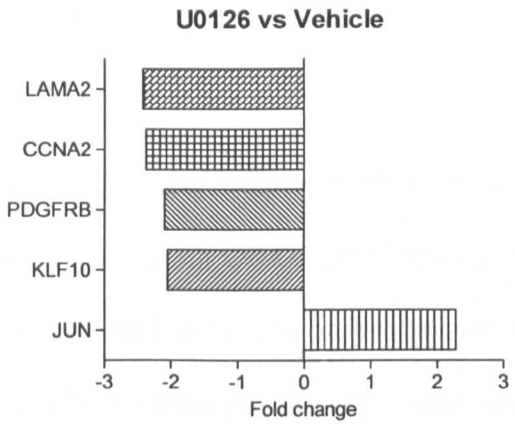


Figure 5-14: Fold changes in gene expression of JUN, KLF10, PDGFRB, CCNA2 and LAMA2 in response to U0126 in rat primary skeletal muscle cells (n=1 rat). JUN; jun proto-oncogene, KLF10; Kruppel-like factor 10, PDGFRB; platelet-derived growth factor receptor, beta polypeptide, CCNA2; cyclin A2 and LAMA2; laminin, alpha 2. Data were analyzed using one way ANOVA test followed by Benjamini-Hochberg test.

## 5.6 Discussion

In the present study, $CB_1$ receptor mRNA was detected in both skeletal muscle tissue and rat primary cells using QRT-PCR (Taqman). In previous studies, $CB_1$ receptor was found to be expressed in human and rodent skeletal muscle (Cavuoto *et al.*, 2007b). Interestingly, $CB_1$ receptor protein expression was found to be significantly decreased in soleus muscle from obese compared to lean Zucker rats (Lindborg *et al.*, 2011). However, $CB_1$ receptor mRNA expression in soleus muscle was found to be increased after high fat feeding in C56BL/6 mice (Pagotto *et al.*, 2006). In the present study, the functionality of $CB_1$ receptor was investigated by assessing the direct effect of $CB_1$ receptor agonism (ACEA and AEA) or antagonism (RIM and AM251) on the activation of key proteins involved in insulin signalling and glucose uptake in rat primary skeletal muscle cells.

The main findings from these experiments showed that treatment with ACEA (10 nM) for 10 minutes increased the activation of extracellular signal-regulated kinase 1/2 and p38 mitogen-activated protein kinase; these responses were significantly inhibited by RIM (100 nM). Insulin (100 nM) treatment of myotubes for 10 minutes increased the activation of AKT/protein kinase B, glycogen synthase kinase 3α and β, ERK1/2 and p38 MAP kinase; pre-treatment with ACEA (10 nM) and RIM (100 nM) for 24 hours failed to alter these responses. AICAR (1 mM)-stimulated AMP-activated protein kinase activity was also unaltered by ACEA.

In the present study, AEA increased ERK phosphorylation in rat primary myotubes. This activation could be due to $CB_1$ or $CB_2$ receptor activation since AEA at this concentration could work through both receptors (Lin *et al.*, 1998). Indeed, $CB_2$

receptor was found to be expressed in rodent skeletal muscle (Cavuoto *et al.*, 2007b). To differentiate which receptor mediates this effect, ACEA was also used since ACEA is more selective for $CB_1$ receptor than $CB_2$ receptor by around 2000 times (Hillard *et al.*, 1999). ACEA was found to increase ERK phosphorylation in rat primary myotubes. Interestingly, this effect induced by both AEA and ACEA was blocked by RIM, a selective $CB_1$ receptor antagonist/inverse agonist (Rinaldi-Carmona *et al.*, 1994). This finding suggests that ERK activation was mediated by activation of the $CB_1$ receptor since ACEA is a selective $CB_1$ receptor agonist at the concentration used in the present study (Hillard *et al.*, 1999). This study also provided strong evidence that $CB_1$ receptor is a functionally active receptor in skeletal muscle. This is in line with a previous study that also found that treatment of human primary myotubes with AEA (10μmol/l) for 10 minutes induces a significant phosphorylation of ERK1/2 when compared to control (Eckardt *et al.*, 2008a).

In the present study, ACEA also increased P38 phosphorylation in rat primary myotubes, which is in line with a previous study in human primary skeletal muscle cells (Eckardt *et al.*, 2008a). Interestingly, this effect induced by ACEA was blocked by RIM, a selective $CB_1$ receptor antagonist/inverse agonist (Rinaldi-Carmona *et al.*, 1994), which suggests that the cannabinoid-induced activation of P38 in skeletal muscle is mediated through activation of the $CB_1$ receptor. However, treatment of myotubes with ACEA or RIM did not phosphorylate AMPK. AICAR (1 mM)-stimulated AMP-activated protein kinase activity was also unaltered by ACEA. The time used for the treatment of myotubes with ACEA, RIM and AICAR was due fact that the phosphorlyation of AMPK in skeletal muscle was observed after one hour of AICAR administration in mice (Leick *et al.*, 2010). Futher work should be performed using different time points for the treatment.

The functionality of signalling proteins, which are involved in the regulation of insulin-dependent (AKT, GSK3β, ERK1/2 and P38) or insulin-independent (AMPKα) glucose uptake, was not altered by 24 hour $CB_1$ receptor antagonism (RIM) or agonism (ACEA). In addition, the functionality of AKT was not altered by AM251 and AEA. This is in line with a previous study that also found that insulin-induced phosphorylation of AKT, GSK3β, AMPKα and P38 was not altered by ACEA or RIM in skeletal muscle tissue from Zucker rats (Lindborg *et al.*, 2011). However, it was shown that AKT phosphorylation at Ser473 was increased in the presence of RIM in L6 myotubes (Esposito *et al.*, 2008). It was also shown that phosphorylation of AKT at Ser473 and AMPK at Thr172 were also enhanced in the liver of ob/ob mice after systemic treatment with RIM (Watanabe *et al.*, 2009). Phosphorylation of AMPK at Thr172 was increased in cultured white adipocytes in presence of RIM, as well as in epididymal fat pads from high fat-fed wild type mice compared to $CB_1$ -/- mice (Tedesco *et al.*, 2008). The mRNA expression of AMPKα was significantly increased in primary cultured human myotubes treated with RIM (Cavuoto *et al.*, 2007a). Treatment of L6 cells with RIM enhanced insulin-stimulated AKT while ACEA failed to do so (Lipina *et al.*, 2010). Moreover, treatment of L6 cells with ACEA inhibited insulin-stimulated ERK and this response was prevented by RIM (Lipina *et al.*, 2010). It has been demonstrated previously that both activation and inhibition of the $CB_1$ receptor were associated with modulation of the functionality of these signaling proteins in various tissues and cell lines. The most likely reason these results from previous studies contradict the findings from this study is that they used different model (for example, L6 cells), species or tissues.

The $CB_1$ receptor system in skeletal muscle is an emerging area of investigation for insulin-cannabinoids cross-talk. The endocannabinoid system has been shown to have a

role in the modulation of whole-body and tissue glucose regulation in several lines of investigation. Indeed, during a euglyemic-hyperinsulinemic clamp in human subjects, circulating levels of 2-AG were found to be negatively correlated with glucose infusion rates (Bluher *et al.*, 2006). During a glucose tolerance test, $CB_1$ receptor agonism (AEA 10 mg/kg or ACEA 3 mg/kg) was found to lead to elevated circulating glucose levels in rats (Bermudez-Siva *et al.*, 2006). It was shown that treatment of isolated mouse pancreatic β-cells with a $CB_1$ receptor agonist, 100 nM ACEA, inhibited glucose-induced insulin secretion (Nakata *et al.*, 2008), whereas, peripheral infusion of a $CB_1$ receptor antagonist (RIM; 10 mg/kg) in diet-induced obese rats decreased hepatic glucose production (Nogueiras *et al.*, 2008). Therefore, it appears that altering the signalling or functionality of the $CB_1$ receptor in metabolically active tissues may play a role in the endocannabinoid system's ability to modulate glucose metabolism. As skeletal muscle is the largest tissue in the body and responsible for most of insulin-stimulated glucose disposal, treatments that lead to $CB_1$ receptor antagonism might improve glucose transport in skeletal muscle. Consequently, this might make the endocannabinoid system a novel target in the treatment of insulin resistance and hyperglycemia. Therefore, glucose uptake was investigated in primary skeletal muscle cells.

This model of cells (rat primary skeletal muscle cells) did not show any significant difference for glucose uptake between vehicle and insulin. However, 3T3-L1 adipocytes showed a consistent significant difference between vehicle and insulin (5-6 fold). In this study, the explanations behind the no significant difference in glucose uptake between insulin and vehicle using the cell culture for myotubes might be explained by many suggested aspects; A) Glucose uptake in this model can occur not only through GLUT4 but also might occur through GLUT1 or another transporter of which we do not yet

know. B) Myotubes might reach the saturation level for glucose uptake in both vehicle and insulin, or that GLUT4 was not coupled to insulin in these cells. D) Glucose uptake might happen by sodium/glucose co-transporters (SGLT) (Castaneda *et al.*, 2006). However, the mechanism beyond this in skeletal muscle is unclear. Indeed, in this study, mRNA expression of SGLT2 and SGLT3 was detected in skeletal muscle using microarray (ranking out of 41,090 are 14944, 15445, respectively).

It is worth mentioning that it was shown a response to insulin regarding glucose uptake in human primary muscle cells (Sarabia *et al.*, 1990). However, the reason behind why other researchers succeeded regarding glucose uptake assay might be due to the fact that the difference in physiology between human and rat or differences in model used (such as mouse C2C12 cells or rat L6 cells). Therefore, further investigation should be recommended to examine glucose uptake in other conditions using electrode and/or hypoxic conditions. Furthermore, it is recommended to examine another GLUT4 antibody to investigate the GLUT4 translocation in skeletal muscle cells as 3T3-L1 did in response to insulin.

In a previous study investigating the effect of RIM in overweight or obese patients with type 2 diabetes, RIM was found to reduce bodyweight and cause a clinically significant reduction in $HbA_{1c}$ levels (Scheen *et al.*, 2006). However, in this study, neither RIM nor ACEA affected AKT phosphorylation in rat primary skeletal muscle cells. Indeed, RIM blocked the stimulatory effect of ACEA on ERK and P38 phosphorylation. Gene expression changes were studied in peripheral tissues such as liver and adipose from diet-induced obese mice treated with AM251 (Zhao *et al.*, 2010). They found down-regulation of genes within fatty acid and cholesterol synthetic pathways such as sterol regulatory element binding proteins 1 and 2 in both liver and adipose tissues. However,

these gene expression changes have not been studied in skeletal muscle. Therefore, in the present study a comprehensive analysis of differential gene expression in response to ACEA, RIM and U0126 treatments in rat primary skeletal muscle cells was achieved using Affymetrix Rat Genome 230 PM Array. The four technical replicates used for this analysis were found to be reproducible since the Pearson correlations for normalized intensity data for all replicates were above 0.98.

Treatment of myotubes with ACEA for 24 hours up-regulated the mRNA content of FRZB and down-regulated the expression of OLR1. On the other hand, ACEA down-regulated the expression of the RGS2, EGR2 and HAS2 genes in a $CB_1$ receptor dependent manner. Indeed, the mRNA expression of RGS2, EGR2 and HAS2 genes was blocked by RIM. Pertinent to the role of Wnt signalling in modulating the developmental myogenic differentiation of fibre-type (Anakwe *et al.*, 2003), this study has demonstrated increased rat primary skeletal muscle mRNA content of FRZB in response to ACEA. FRZB is considered as a Wnt-binding protein. ACEA decreases the mRNA expression of these genes (RGS2, EGR2 and HAS2). RGS2 was shown to be highly expressed in proliferating compared to differentiated MYOP7 (myogenic cell line) (Zacchigna *et al.*, 2008). However, another study found that RGS2 was highly up-regulated in quiescent satellite cells compared to activated satellite cells (Fukada *et al.*, 2007). Overexpression of RGS2 in early xenopus embryos revealed histologically reduced skeletal muscle tissue and inhibited trunk development (Wu *et al.*, 2000). Moreover, EGR2 was found to be highly expressed in rat soleus muscle after 3 hours of mechanical overload-induced hypertrophy (Carson *et al.*, 2002). Regarding HAS2, hyaluronan synthase is an enzyme involved in synthesis of hyaluronan molecules (an anionic, nonsulfated glycosaminoglycan). The synthesis of hyaluronan was shown in myoblasts and myotubes (Ahrens *et al.*, 1977; Angello *et al.*, 1979). One study showed

that differentiated multinucleated myotubes from chick embryo exhibit a specific decrease of hyaluronic acid in their cell layer-associated fraction of the total synthesized glycosaminoglycans (Carrino *et al.*, 1999; Pacifici *et al.*, 1980). Another study showed that down-regulating of mRNA expression of OLR1 was consistent with the commitment of C2C12 to myogenic differentiation (Janot *et al.*, 2009). There is little information in the literature about the roles of these genes in skeletal muscle. Overall, ACEA might have a role in skeletal myogenesis through regulating the expression of those genes (FRZB, RGS2, EGR2, HAS2 and OLR1). Therefore, further research is needed to address this issue.

ACEA, however, produced a different response in the presence of RIM. It is possible that ACEA might give a response in a $CB_1$ independent manner (on other receptors) when possibly almost all $CB_1$ receptors expressed in myotube was blocked by RIM. There is also a suggestion that RIM might give a response as an agonist through other receptors such as GPR55 (Godlewski *et al.*, 2009). Therefore, the overall signalling in response to ACEA and RIM compared to RIM alone was to down-regulate the mRNA expression of the FRZB, RGS2 and HAS2. It is also worth noting that the serum used in this experiment might also contain low endocannabinoid level that might interact with signalling of ACEA, RIM or U0126. Therefore, it is very hard to explain the response of ACEA in the presence of RIM (ACEA+RIM versus RIM). From this data, no conclusion can also be made as to whether the ACEA effects depend on the activation of the ERK pathway, in particular this experiment was performed from only one animal due to cost and time implications. Further work should be performed to get a clear comprehensive image in these issues, such as repeating this experiment from different animals using either microarray or QRT-PCR (Taqman) or using delipidated serum instead of charcoal stripped serum. Further work is also required to understand these

responses such as using siRNA for $CB_1$ receptor or using GPR55 antagonist.

In this study, RIM up-regulated the mRNA content of NPY, APLN and LCN2, and down-regulated GNAI3 and NR4A1. These genes were suggested to be related to insulin resistance although the exact mechanisms are not known. There are limited studies on these genes in skeletal muscle; acute administration of apelin in chow-fed mice was associated with enhanced utilization of glucose in skeletal muscle (Dray *et al.*, 2008). Similarly, administration of NPY to rats was associated with increased glucose utilization in skeletal muscle (Vettor *et al.*, 1998). Although the cross-talk between cannabinoids and GNAI3 has not been studied in skeletal muscle, $CB_1$ receptor activation was suggested to hinder insulin-stimulated IR autophosphorylation dependent on the association between GNAI3 and IR in pancreatic beta-cells (Kim *et al.*, 2011). It is worth noting that GNAI2 in skeletal muscle was suggested to have a role in insulin sensitivity through the suppression of protein-tyrosine phosphatase 1B (PTP1B) (Tao *et al.*, 2001).

LCN2 knockout mice exhibit significant decrease in fasting glucose levels and insulin sensitivity (Law *et al.*, 2010). In addition, LCN2 concentrations correlated with hyperglycemia and insulin resistance in humans (Wang *et al.*, 2007), whereas mRNA content of LCN2 was increased in liver and adipose tissue of diabetic/obese mice. Moreover, it was reported that cAMP can affect the mRNA content of NR4A1 in skeletal muscle (Kawasaki *et al.*, 2011; Pearen *et al.*, 2008; Pearen *et al.*, 2006). NR4A1 might modulate fat and glucose metabolism through regulating the expression of genes related to oxidative metabolism in skeletal muscle (Pearen *et al.*, 2008). It is worth mentioning that all of the above genes (NR4A1, NPY, APLN, LCN2 and GNAI3) were detected in rat skeletal muscle tissue using Agilent microarray at the following ranking

(506, 12597, 1827, 12118 and 15033) out of 41000. However, more research is needed to investigate the role of RIM in skeletal muscle metabolism. Moreover, measurement of NPY and apelin in response to RIM should be recommended to be investigated in skeletal muscle cells.

In this study, U0126 exerted an influence on gene expression in rat primary skeletal muscle. Indeed, U0126 up-regulated CCNA2, LAMA2, PDGFRB and KLF10 mRNA expression and down-regulated JUN mRNA expression. CCNA2 is involved in cell cycle control and C2C12 differentiation (Moran *et al.*, 2002). There is some evidence that PDGFRB is involved in skeletal and cardiac muscle development, however, its role is not yet defined (Betsholtz *et al.*, 2001; Kudla *et al.*, 1998). LAMA2 may play a role in muscle regeneration and the muscular dystrophy (Kamiguchi *et al.*, 1998; Kuang *et al.*, 1999). JUN mRNA is expressed in the satellite cells, myoblasts and myotubes post-trauma (Kami *et al.*, 1995). KLF10 mRNA expression was up-regulated during myogenic differentiation (Miyake *et al.*, 2011). It is worth noting that all of the above genes (CCNA2, LAMA2, JUN, KLF10 and PDGFRB) were detected in rat skeletal muscle tissue using Agilent microarray at the following ranking (17108, 3101, 2054, 2278 and 3198) out of 41090. Little is known about the roles of these genes (CCNA2, LAMA2, JUN, KLF10 and PDGFRB) in skeletal muscle metabolsim. However, more research is needed to examine U0126 in the proliferation and differentiation of skeletal muscle cells.

In summary, the $CB_1$ receptor was found to be functional in rat skeletal muscle. However, $CB_1$ receptor modulation for 24 hours did not alter the activation (phosphorylation) of key insulin signalling proteins such as AKT, GSK-3β, AMPKα, P38MAPK and ERK. The microarray findings revealed that ACEA might have a role in

skeletal muscle proliferation and differentiation through altering the gene expression of RGS2, EGR2, OLR1, HAS2 and FRZB. Moreover, treatment with RIM influenced the mRNA content of genes (NPY, APLN, LCN2, NR4A1 and GNAI3) related to insulin resistance, glucose and fat metabolism. It is worth noting that the ERK1/2 pathway might have a role in proliferation and differentiation in skeletal muscle cells by regulating the expression of CCNA2, LAMA2, JUN, KLF10 and PDGFRB genes (Table 5-6). Further research is warranted to establish the precise role of endocannabinnoids in the regulation of gene expression in skeletal muscle and the importance of this role in the development of insulin resisatnce and obesity.

Table 5-6: Summary of findings for Chapter 5.

| Conditions | Findings |
|---|---|
| Treatment of myotubes with ACEA and AEA for 10 minutes | ERK-phosphorylation in response to ACEA and AEA; blocked by RIM. |
| Treatment of myotubes with ACEA or RIM for one or two hours. | No AMPK phosphorylation. |
| Treatment of myotubes with ACEA or RIM for 24 hours | No alteration in insulin signalling (AKT, GSK, ERK and P38 phosphorylation) |
| Treatment of myotubes with ACEA for 24 hours. | ACEA up-regulated frizzled-related protein (FRZD) mRNA gene expression and down-regulated early growth response 2 (EGR2), hyaluronan synthase 2 (HAS2), oxidized low density lipoprotein (lectin-like) receptor 1 (OLR1) and regulator of G-protein signaling 2 (RGS2) mRNA gene expression. |
| Treatment of myotubes with RIM for 24 hours. | RIM up-regulated the mRNA content of neuropeptide Y (NPY), apelin (APLN) and lipocalin 2 (LCN2), and down-regulated guanine nucleotide binding protein (G protein), alpha inhibiting activity polypeptide 3 (GNAI3) and nuclear receptor subfamily 4, group A (NR4A). |

# Chapter 6

# General Discussions

# 6 Chapter Six: General Discussion

Skeletal muscle is a main site of fatty acid and glucose metabolism and involved in energy balance (Zurlo *et al.*, 1990). Skeletal muscle also produces skeletal movement through its contraction and maintains body glucose homeostasis, and so pharmacological tools that target the molecular mechanisms controlling skeletal muscle metabolism, functions and physiological roles may be therapeutically useful for metabolically related disorders.

Over the last few decades, significant advances in the understanding of GPCRs have been made with deorphanization of generally orphan receptors. Therefore, investigation of the functional role of GPCRs provides a promise of new targets in peripheral tissues, especially skeletal muscle. The principal aims in the present thesis were to characterize the mRNA expression of GPCRs and their partners' genes, and investigate their signalling in skeletal muscle. Indeed, investigation of the GPCRs mRNA expressed in skeletal muscle will aid in understanding the primary targets of many endogenous and exogenous compounds affecting skeletal muscle metabolism and functions. Understanding the signalling of GPCRs might help to determine their functionality and possible roles in skeletal muscle tissue. Finally, understanding the direct effects of $CB_1$ receptor agonists/antagonists will elucidate the possible roles of $CB_1$ receptor in skeletal muscle and how RIM improves metabolic parameters such as glycaemia seen in both rodent models (Cota *et al.*, 2009) and human subjects (Pi-Sunyer *et al.*, 2006).

These aims were illustrated and hopefully accomplished by using techniques such as gene expression microarray and QRT-PCR (Taqman) to detect the relative levels of

mRNA content of GPCRs, cAMP assay, calcium imaging and immunoblotting to explicitly characterize the GPCRs signalling within myotubes, especially the $CB_1$ receptors, $\alpha_{2A}$-adrenoceptors, $A_{2B}$ adenosine receptors and $P2Y_1$, $P2Y_2$ and $P2Y_6$ receptors.

As discussed in Chapter 3, GPCRs were detected in skeletal muscle tissues using QRT-PCR (Taqman) and Agilent microarray. These GPCRs include $LPA_1$ lysophosphatidic acid receptors, CXCR4, glucagon receptors, platelet-activating factors receptors, $GABA_{B1}$ receptors, $S1P_2$ sphingosine-1-phosphate receptors, parathyroid hormone receptors, mGlu2 and mGlu3 metabotropic glutamate receptors, dopamine $D_5$ receptors, neurotensin receptors 2, opioid receptors delta 1, calcitonin receptors, arginine vasopression receptors 1A, bradykinin $B_2$ receptors, $C5a_1$ complement peptide receptors, $CB_1$ receptor, GPR119, $\alpha_2$-adrenoceptor, $\beta_2$-adrenoceptor, $A_1$ and $A_{2A}$ adenosine receptors, NPY Y1 receptor, $P2Y_1$, $P2Y_2$ and $P2Y_6$ receptors genes mRNA. To date, virtually no information is reported in the literature about the physiological functions, pathophysiological roles, and regulation and gene expression patterns of such GPCRs in skeletal muscle tissues. However, these receptors (see Chapter 3) might affect a wide range of biological functions in skeletal muscle including glucose uptake and metabolism, myogenesis, regeneration, growth and contraction. These findings have identified targets which might be vital for many diseases or important to improve many parameters in disease states. Further investigation is required to investigate these receptors as potentially pharmacological targets to treat diabetes and skeletal muscle regeneration disorders.

Moreover, as discussed in Chapter 3, mRNA expressions of various isoforms of GPCR partners were also detected in skeletal muscle using Agilent microarray. These include

G protein α, β and γ subunits ($G_{\alpha s}$, $G_{\beta 1}$, $G_{\beta 2}$, $G_{\beta 5}$, $G_{\gamma 10}$ and $G_{\gamma 12}$), regulators of G protein signalling (RGS2, RGS5 and Axin1), adenylyl cyclase isoforms (AC2 and AC6), phosphodiesterase (PDE4A and PDE4D), regulatory subunits of PKA (RIα), phospholipase C isozymes (PLCδ4 and PLCδ1), diacylglycerol lipase and kinase (DAGIβ, DGKζ and DGKα), protein kinase C (PKCδ and PKCθ), low molecular weight G protein (RhoA and RhoQ) and Rho-kinase 1 (ROCK1) gene mRNA expression. These genes might be involved in a number of biological functions including skeletal muscle fibre phenotypes, hypertrophy, contraction, fat and glucose metabolism, hyperglycemia and weight gain. Interestingly, these targets might also be associated with many diseases, and identify a large research area for GPCR partners in skeletal muscle. Further investigation should also investigate these gene products as potential therapeutic options to treat diabetes and skeletal muscle regeneration disorders such as muscular dystrophy.

In the light of the data in this study, further investigations are needed to ultimately understand GPCR expression and their signalling partners in individual elements of muscle: fast and slow fibres and satellites, myoblasts, myotubes and tissues, as well as investigating models of obesity in rats (for example, comparing Wistar, Zucker obese and Zucker lean animals) and human disease (for example, comparing diabetic, obese and normal conditions). Moreover, knockout mice model or siRNA for these targets should also be investigated in skeletal muscle to understand the specific roles of these GPCRs and their partners.

A limitation to the present study was employing the Wistar rat animal model to mimic human. Even though the Wistar rat is widely used in the scientific research, it does not exactly mimic the physiology in humans (Kotokorpi *et al.*, 2007). Although several

skeletal muscle myogenic cell lines are commercially available, including rat L6 and mouse C2C12 cells, and they are easy to grow in culture compared to primary culture, rat primary skeletal muscle cells were chosen in these studies due to the fact that primary cells are more representative of the cells *in situ* than the cell lines. Indeed, cultured primary myotubes were widely used by many researchers to study the effects of various factors such as pharmacological agents on muscle physiology, metabolism and functions. This is due to the fact that cultured myotubes express protein and possess functional characteristics of skeletal muscle (Pimenta *et al.*, 2008; Stern-Straeter *et al.*, 2011). However, primary myotubes may have several limitations. First, primary myotubes lose their capacity for proliferation (Renault *et al.*, 2000). Satellite cells also proliferate for a certain period of time and then lose their ability for proliferation (Renault *et al.*, 2000). Second, cells in culture gradually lose their capacity to preserve the phenotype (Thompson, 1994). Third, contamination with fibroblasts may affect the specificity of the myotube response (Thompson, 1994; Yaffe, 1968). Fourth, the fibre composition of the muscle is not preserved in myotube culture. For example, myotubes cultured from humans co-expressed both fast and slow myosin heavy chains regardless of the fibre type of donor muscle (Bonavaud *et al.*, 2001). Fifth, primary skeletal muscle cell culture is not able to completely mimic the *in vivo* model including cross-talk between other tissues such as adipose tissue and skeletal muscle. Therefore, using primary skeletal muscle cell culture is of restricted physiological relevance. Regardless of these limitations, the primary skeletal muscle cell cultures were required to determine the direct effect of the GPCRs ligands, in particular $CB_1$ receptor agonists/antagonists, on the skeletal muscle cells in controlled settings. Moreover, it is crucial to consider that skeletal muscle tissue contains other cells including macrophages, epithelial and fibroblasts in particular, in the literature, serotonin (5-hydroxytryptamine (5-HT)) was shown to cause a rapid stimulation in glucose uptake after 30 minutes exposure via the

5-$HT_{2A}$ receptor in isolated rat skeletal muscle (Hajduch *et al.*, 1999). Therefore, the primary skeletal muscle cell cultures were used in this study.

As discussed in Chapter 4, $A_{2B}$ adenosine receptor, $\alpha_2$-adrenoceptor and P2Y receptor were found to be functional using cAMP assay, immunoblotting and calcium imaging. Consistent with a previous report showing a functional role of $A_{2B}$ adenosine receptors in skeletal muscle (Lynge *et al.*, 2003), the present study found that NECA, a non-selective adenosine receptor agonist (Castanon *et al.*, 1994; Klotz *et al.*, 1998), enhanced cAMP production in rat primary skeletal muscle cells through $A_{2B}$ adenosine receptors. However, CGS21680, an $A_{2A}$ adenosine receptor-selective agonist (Ongini *et al.*, 1999), and S-ENBA, an $A_1$ receptor-selective agonist (Haynes *et al.*, 1998; Hussain *et al.*, 1995), failed to affect cAMP production in rat primary skeletal muscle cells in the present study. Since $A_{2B}$ adenosine receptor was found to increase NR4A expression in smooth muscle, which was blocked by an antagonist (Mayer *et al.*, 2011), it is possible that $A_{2B}$ adenosine receptors affect NR4A through cAMP in skeletal muscle. Consequently, $A_{2B}$ adenosine receptors might improve fat and glucose metabolism in skeletal muscle tissue through NR4A. This is supported by the fact that 1) NR4A mRNA was found to be expressed in skeletal muscle using microarray in this study. 2) cAMP was found to be involved in increase of expression of NR4A in skeletal muscle (Kawasaki *et al.*, 2011; Pearen *et al.*, 2008; Pearen *et al.*, 2006). 3) NR4A was shown to be reduced in skeletal muscle of diabetic animals (Fu *et al.*, 2007). 4) NR4A was associated with genes related to glucose and fatty acid utilization through up-regulating the mRNA expression of PDK4, FOXO1, PGC-1α and lipin-1α (Pearen *et al.*, 2008). 5) NR4A null mice after high-fat feeding compared with wild-type animals were shown to exhibit decreased mRNA expression of GLUT4 and PDK4 and Lipin 1α and impaired insulin receptor substrate 1 (IRS-1) phosphorylation and insulin resistance in skeletal

muscle, and slower blood glucose clearance and increased body weight and decreased energy usage (Chao *et al.*, 2009). 6) In C2C12 cells, C2C12 siRNA-NR4A cells were shown to decrease mRNA expression of fatty acid translocase (CD36/fat), uncoupling protein-3 (UCP3) and GLUT4 compared to wild type native C2C12 cells (Maxwell *et al.*, 2005). 7) In C2C12 cells transfected with adenovirus-mediated NR4A expression, non-insulin glucose uptake was shown to be increased significantly compared to normal C2C12 cells (Chao *et al.*, 2007). Taken together, modulation of $A_{2B}$ adenosine receptor by ligands might affect glucose and fatty acid utilization in skeletal muscle. The implication of this finding is that $A_{2B}$ adenosine receptor agonists may be a therapeutic target for diabetes or obesity. However, NECA (0.3 mg/kg) was shown to increase fasting glucose level in C57BL/6 mice which was not observed in $A_{2B}$ receptor knockout mice (Figler *et al.*, 2011). Moreover, NECA gavage in wild-type fasted mice was shown to delay glucose disposal during an oral glucose tolerance test (GTT) which was abolished in $A_{2B}$ receptor knockout mice (Figler *et al.*, 2011). As discussed above, $A_{2B}$ adenosine receptor agonists may be a therapeutic target for diabetes. The discrepancy between the theory regarding NR4A and $A_{2B}$ receptor described above and studies in rodents published in the literature regarding NECA (Figler *et al.*, 2011) might be explained by the fact that NECA mediated the $A_1$ adenosine receptor expressed in pancreas and $A_2$ adenosine receptor expressed in liver (Arias *et al.*, 2001). Therefore, the effect of NECA in skeletal muscle through $A_{2B}$ receptor might improve glucose uptake. Further work is required to assess the level of protein and mRNA expression of NR4A in skeletal muscle and the exact molecular mechanism underlying the induction of NR4A in response to activation of the $A_{2B}$ adenosine receptors. There is no commercially selective $A_{2B}$ adenosine receptor agonist. However, Adenocard I.M. (Adenosine) might be developed to examine the glucose tolerance despite the side effects of this drug which include facial flushing, lightheadedness and diaphoresis due

to its vasodilatory effects.

There are controversial data regarding the effect of $A_{2B}$ adenosine receptor activation regarding the cellular proliferation. Although $A_{2B}$ adenosine receptor activation was shown to inhibit the proliferation of murine vascular smooth muscle cells (Dubey *et al.*, 2000), its activation was shown to stimulate MAP kinase activity in human embryonic kidney cells (Gao *et al.*, 1999) and stimulate human endothelial cells growth (Grant *et al.*, 1999). Employing $A_{2B}$ adenosine receptor knockout mice was used for investigation of vascular injury (Yang *et al.*, 2008), and $A_{2B}$ adenosine receptor si-RNA was also used for investigation of hepatocellular carcinoma (Xiang *et al.*, 2011). However, nothing is reported regarding skeletal muscle. Therefore, knockout mice or si-RNA for $A_{2B}$ adenosine receptors is required to understand potential roles of these receptors in skeletal muscle at both normal and diabetic/muscle atrophy states.

Surprisingly, the functionality of $\alpha_2$-adrenoceptor and P2Y receptors has not been studied in skeletal muscle. In the present study, the functionality of the $\alpha_2$-adrenoceptor was shown through the inhibition of UK14304, an $\alpha_2$-adrenenoceptor agonist (Jasper *et al.*, 1998), stimulation of ERK phosphorylation by rauwolscine, the selective $\alpha_2$-adrenoceptor antagonist (Convents *et al.*, 1989; Uhlen *et al.*, 1994) (see Chapter 4). As activation of ERK signal transduction was suggested to induce differentiation of skeletal muscle and growth-related processes (Bennett *et al.*, 1997; Jones *et al.*, 2001; Lopez-Ilasaca, 1998), it is possible that $\alpha_2$-adrenoceptors have a role in skeletal muscle myogenesis and growth. This result might hopefully open a question about what is the effect of $\alpha_2$-adrenoceptor in skeletal muscle. Moreover, there is a growing number of reports suggesting $\alpha_2$-adrenoceptor may represent a novel therapeutic target through regulation of insulin secretion by noradrenaline in pancreatic islets by reducing cAMP

formation (Ahren, 2000; Nakaki *et al.*, 1981). Since $\alpha_{2A}$-adrenoceptor knockout mice were shown to have lower blood glucose level compared to control mice (Savontaus *et al.*, 2008), further work including knockout mice or si-RNA for $\alpha_{2A}$-adrenoceptors in skeletal muscle should be performed to understand potential physiological and pathophysiological roles of this receptor in skeletal muscle in terms of glucose uptake, oxidation and myogenesis.

Previous reports have identified $P2Y_1$, $P2Y_2$ and $P2Y_6$ receptor mRNA expression in mouse C2C12 cells (Banachewicz *et al.*, 2005). The present study revealed that mRNA encoding $P2Y_1$, $P2Y_2$ and $P2Y_6$ receptors are detected in skeletal muscle tissue and the possibility of activation of these receptors coupled to calcium ion elevations was assessed in primary skeletal muscle cells. Intracellular calcium concentration was increased by UTP and ATP in this study, which was mainly attributed to activation of the P2Y receptors, since UTP is a selective agonist for $P2Y_2$ receptors (El-Tayeb *et al.*, 2006) and the profile of the response is typical for $G_q$-GPCRs (James *et al.*, 2001). ATP, localized at the nerve terminal, may be released after stimulation of the prejunctional neurones, leading to activation of P2Y receptors. Moreover, ATP and UTP may also be released from many cell types including endothelium, fibroblasts, epithelium, blood borne cells (RBC and platelets), smooth muscle cells and damaged tissues (Burnstock, 2008; Lazarowski *et al.*, 2003; Schwiebert *et al.*, 2003). Once ATP is released, it can be hydrolyzed by ectonucleotidases, cell surface-located enzymes, into ADP, AMP and adenosine (Huang *et al.*, 1998; Zimmermann, 2006). Furthermore, ATP can be used to produce UTP via a transphosphorlyation reaction catalyzed by extracellular nucleoside diphosphokinase (NDPK) (Lazarowski *et al.*, 2003) which was detected in this study in skeletal muscle tissue using gene expression microarray (ranking 3894 out of 41090). Indeed, ATP is considered as the source of cellular energy, and UTP is considered as an

activator of substrates. For example, once UTP activates glucose-1-phosphate, UDP-glucose is formed by UDP-glucose pyrophosphorylase, and then UDP-glucose is involved in the synthesis of glycogen (Lazarowski *et al.*, 2003).

The P2Y receptors may play a role in modulating skeletal muscle functions. Indeed, UTP was shown to activate ERK in mouse C2C12 cells in a calcium dependent manner (Banachewicz *et al.*, 2005), and ATP was shown to stimulate the proliferation of astrocyes via P2Y (Neary *et al.*, 2009) and to stimulate the proliferation of cancer cells (Deli *et al.*, 2008). As ERK was shown to have a role in myoblast proliferation (Bennett *et al.*, 1997; Jones *et al.*, 2001), it is possible that the P2Y receptors play a role in skeletal muscle growth. Indeed, skeletal muscle P2Y receptors may present new opportunities in the treatment of muscle growth disorders including muscle atrophy. The P2Y receptors may also play a role in muscle contraction through calcium modulation. Calcium might improve contraction-stimulated glucose uptake through activating GLUT4 translocation, calmodulin-dependent protein kinases, calmodulin and protein kinase Cs (Ihlemann *et al.*, 1999; Jessen *et al.*, 2005; Wright *et al.*, 2004; Youn *et al.*, 1991). However, the mechanism behind this issue is unclear. Since muscle contraction enhances glucose uptake, and ATP was also shown to activate glucose uptake in mouse C2C12 skeletal muscle cells through P2 receptors (Kim *et al.*, 2002); P2Y receptor agonists might be a therapeutic option to treat diabetes through increasing the calcium level in skeletal muscle. Further work is required to determine the P2Y receptor subtypes which are possibly responsible for these effects. There are no clinical drugs available to specifically target the activation of $P2Y_1$, $P2Y_2$ or $P2Y_6$ receptors. However, ATP and its breakdown products have been reported to mediate the pathophysiology of pulmonary hypertension, hypertension and atherosclerosis (Burnstock, 2008; Sprague *et al.*, 2003).

As discussed in Chapter 5, investigation of $CB_1$ receptor signalling and insulin signalling in skeletal muscle has produced controversial findings. One study (Lindborg *et al.*, 2011) showed no modulation of phosphorylation of AKT, GSK and ERK induced by insulin in response to ACEA and RIM, while other studies (Esposito *et al.*, 2008; Lipina *et al.*, 2010) showed that treatment with either ACEA or RIM altered the phosphorylation of these proteins induced by insulin. Long-term incubation studies, where myotubes were co-incubated with cannabinoids, were thought to be feasible means to assess the effects of prolonged $CB_1$ receptor signalling on myotubes. However, the functionality of signalling proteins that might be involved in the regulation of either insulin-dependent (AKT, GSK3β, ERK1/2 and p38) or insulin-independent (AMPKα) glucose uptake, was not altered by direct $CB_1$ receptor antagonism (RIM) or agonism (ACEA) in the present study. As discussed in Chapter 5, the difference between previous studies and the findings from the present study could have been due to physiological difference between rat and human, different representative model (L6 and C2C12 cells) employed and previously uncharacterized activities of the ligands at non-CB receptors and/or a reduced specificity at the concentrations used. Assuming the results are physiologically-relevant, the findings from this thesis suggest that cannabinoid signalling does not play a major role in insulin signalling in myotubes. Indeed, the present study demonstrated that ACEA and RIM failed to alter AKT, p38, GSK and ERK phosphorylation induced by insulin. Nevertheless, ACEA was able to induce ERK and p38 phosphorylation. This effect was only observed acutely at 10 minutes while it was not observed at extended time periods (24 hours).

As discussed in Chapter 5, the ERK phosphorylation in response to AEA was assumed to be acting in a $CB_1$ receptor selective manner. As published in the literature, AEA displays a higher affinity for recombinant $CB_1$ receptors over $CB_2$ receptors (Alexander

*et al.*, 2007; Lin *et al.*, 1998). ACEA, used at $CB_1$ receptor-selective concentrations (Hillard *et al.*, 1999), was also found to increase ERK phosphorylation in rat primary myotubes. Interestingly, this effect induced by both AEA and ACEA was blocked by the selective $CB_1$ receptor antagonist/inverse agonist, RIM (Rinaldi-Carmona *et al.*, 1994). Given that $CB_1$ mRNA expression in skeletal muscle cells and tissue was detected using QRT-PCR in the present study, these findings suggests that ERK activation was mediated via activation of the $CB_1$ receptor.

The present study also revealed that the effects of the cannabinoids were limited to ERK/p38 phosphorylation. Therefore, a comprehensive analysis of the effect of ACEA and RIM on gene expression was performed. The findings indicate, for the first time, that ACEA, synthetic compound, might affect skeletal muscle proliferation and differentiation through altering the gene expression of regulator of G-protein signaling 2 (RGS2), early growth response 2 (EGR2), hyaluronan synthase 2 (HAS2), oxidized low density lipoprotein (lectin-like) receptor 1 (OLR1) and frizzled-related protein (FRZB) (see Chapter 5). The mRNA expression of RGS2, EGR2 and HAS2 was reversed by RIM, suggesting that $CB_1$ receptors might be responsible for this effect. With several reports showing that $CB_1$ receptors are expressed throughout central and peripheral tissues where they mediate a wide range of therapeutic effects, it is possible that the $CB_1$ receptors in skeletal muscle might provide a target for the development of pharmacological strategies to modify skeletal muscle growth.

The findings from the present study indicate, for the first time, that RIM up-regulates the mRNA content of neuropeptide Y (NPY), apelin (APLN) and lipocalin 2 (LCN2), and down-regulate the mRNA content of G protein α subunit (GNAI3) and nuclear receptor subfamily 4, group A (NR4A) (see Chapter 5). As discussed in Chapter 5,

these genes were suggested to be related to insulin resistance although their exact roles are not known. The investigation in this thesis has showed that cannabinoid signalling might be more sophisticated than previously thought; indeed, the findings from the present study showed that $CB_1$ receptor is functionally expressed, although they did not fully characterize the cannabinoid machinery.

Further work is required to investigate the effect of cannabinoid signalling on skeletal muscle metabolism such as glucose uptake and oxidation and beta-oxidation in both *in vivo* and *in vitro*. Further work is also required to assess the ability of skeletal muscle cells to synthesize endogenous cannabinoids based on that NAPE-PLD, DAGL, FAAH and MAGL gene mRNA expression was classified as "present" (ranking out of 41090; 16632, 7018, 16568 and 8139, respectively) in skeletal muscle tissue in this study using gene expression microarray. Furthermore, the potential interaction between $CB_1$ receptor ligands and glucose uptake could facilitate future research aiming to develop a novel class of drugs to increase glucose and fat metabolism in skeletal muscle. Future efforts will have to be concentrated on understanding the exact mechanisms that mediate $CB_1$ receptor modulation in skeletal muscle under normal and, of likely more interest, under pathological conditions. Moreover, investigation of calcium level in response to the modulation of $CB_1$ receptors might be useful in skeletal muscle to examine the signalling pathway which might be involved in regulation of glucose uptake activation.

Furthermore, molecular protein expression and functional approaches, such as proliferation and differentiation assays and glucose uptake and oxidation and beta-oxidation assays *in vivo* and *in vitro*, are required to confirm the suggested interactions and relationships between the genes (NPY, APLN, LCN2, GNAI3, NR4A, RGS2,

EGR2, OLR1, HAS2 and FRZB) that were differentially expressed by RIM/ACEA. As RIM might give a response through mediating central and peripheral targets, and RIM diffuses across blood brain barrier (BBB) and induces side effects such as depression (Oliviero *et al.*, 2011), novel $CB_1$ receptor antagonists (Fulp *et al.*, 2012) which do not cross BBB should also be evaluated regarding their effects on skeletal muscle.

The incidence of obesity and its complications, such as hyperglycemia, is increasing globally. Indeed, pre-diabetes and type 2 diabetes have become more prevalent with obese people. Type 2 diabetes causes many complications including blindness, kidney disease and neuropathies. As discussed earlier in this thesis, many risk factors in obesity can be improved by $CB_1$ receptor antagonists acting either centrally or peripherally. The endocannabinoid system itself appears to be activated in obesity. Skeletal muscle is the principal tissue responsible for glucose uptake after food intake or during exercise. Therefore, if skeletal muscle becomes insulin resistant, this might predispose towards diabetes. Indeed, $CB_1$ receptor antagonists may become therapeutic agents for type II diabetes since they have shown to improve glucose tolerance and reduce body weight in clinical studies (Fulp *et al.*, 2012; Nam *et al.*, 2012; Scheen *et al.*, 2008). However, severe adverse effects, such as depression and high probable risk of suicide, limit and prevent them from being used. Finding alternative pharmacological ways to reduce insulin resistance in skeletal muscle is important for the prevention and treatment of diabetes. A better understanding of the metabolic effects of the $CB_1$ receptor modulation and the mechanism of this action in skeletal muscle in disease and normal states may lead to reliable therapeutic solutions. Keeping this in mind, there has been considerable interest in further understanding of the mechanisms of $CB_1$ receptor modulation in skeletal muscle as a primary target for glucose uptake and insulin signalling. Therefore, more research work is required to understand the cannabinoid

signallings in peripheral tissue such as skeletal muscle. Even though the information obtained from this thesis did not provide a direct and valid alternative way to improve skeletal muscle insulin resistance, it is anticipated that the information will help future investigators in this field to gain a more comprehensive understanding of the role of cannabinoid signalling.

Finally, it is worth mentioning that modulation of skeletal muscle function with GPCR ligands might be a possible therapeutic strategy for improving glucose uptake, skeletal muscle growth and skeletal muscle fat metabolism.

# 7 Future Work

In the present study, the effect of cannabinoid on glucose uptake in skeletal muscle and the molecular signalling pathway through which the $CB_1$ receptor modulation might affect glucose uptake activity in rat and human skeletal muscle cells were not determined. Therefore, in the light of this thesis, further work is required to examine the effects of $CB_1$ receptor agonists/antagonists in the presence of insulin to investigate any potential unknown interaction between $CB_1$ receptor and insulin signalling and to examine any potential unknown pathway for glucose uptake using gene expression microarray *in vivo* and *in vitro* in both normal and diabetic/obese state.

Moreover, further work is needed to examine how $A_{2B}$ adenosine receptor and $\alpha_{2A}$-adrenoceptor and P2Y receptors modulation might affect skeletal muscle myogenesis using proliferation and differentiation assays and gene expression microarray. Furthermore, selective agonists for $\alpha_{2A}$-adrenoceptor and $A_{2B}$ adenosine receptor are required to be synthesized in order to examine the direct effect of these receptors *in vivo* and *in vitro*, in particular skeletal muscle. Then, the response of these ligands should be investigated to understand the potential roles of these receptors in skeletal muscle.

As $CB_1$ receptor is expressed in adipose tissue, and $CB_1$ receptor activation might affect proliferation in skeletal muscle as discussed in this thesis, further work is required to examine how $CB_1$ receptor modulation might affect the adipogenesis in adipose tissue which might be useful for obesity.

The functionality of GPCRs detected in skeletal muscle in this study, in particular

bradykinin $B_2$ receptors and CXCR4, is required to be investigated in skeletal muscle using proliferation and differentiation assays, glucose uptake, oxidation and fat oxidation assays, *in vivo* and *in vitro*, in normal and diabetic and muscle atrophy state to understand the potential roles of these receptors in skeletal muscle.

Further work is also required to investigate the cross-talk between other tissues such as adipose tissue and skeletal muscle using bioconductor apparatus. Using bioconductor apparatus under electric electrode stimulation for skeletal muscle is required to be done for primary myotubes to become more representative of cells *in situ*. Using this apparatus, these GPCRs are required to be investigated in skeletal muscle under these conditions to examine the direct effect of these receptors in skeletal muscle myogenesis, glucose uptake, oxidation and fat oxidation. Moreover, examining the fibre phenotype change in response to modulation of these receptors will be potentially useful for diabetic patients.

# 8 References


Abou Mrad, J, Yakubu, F, Lin, D, Peters, JC, Atkinson, JB, Hill, JO (1992) Skeletal muscle composition in dietary obesity-susceptible and dietary obesity-resistant rats. *Am J Physiol* **262**(4 Pt 2): R684-688.

Adams, KF, Schatzkin, A, Harris, TB, Kipnis, V, Mouw, T, Ballard-Barbash, R, Hollenbeck, A, Leitzmann, MF (2006) Overweight, obesity, and mortality in a large prospective cohort of persons 50 to 71 years old. *N Engl J Med* **355**(8): 763-778.

Ahren, B (2000) Autonomic regulation of islet hormone secretion--implications for health and disease. *Diabetologia* **43**(4): 393-410.

Ahrens, PB, Solursh, M, Meier, S (1977) The synthesis and localization of glycosaminoglycans in striated muscle differentiating in cell culture. *J Exp Zool* **202**(3): 375-388.

Alexander, SP (2012) So what do we call GPR18 now? *Br J Pharmacol* **165**(8): 2411-2413.

Alexander, SP, Kendall, DA (2007) The complications of promiscuity: endocannabinoid action and metabolism. *Br J Pharmacol* **152**(5): 602-623.

Alexander, SP, Mathie, A, Peters, JA (2012) Guide to Receptors and Channels (GRAC), 5th edition. *Br J Pharmacol* **164 Suppl 1**: S1-324.

Allen, DG (2004) Skeletal muscle function: role of ionic changes in fatigue, damage and disease. *Clin Exp Pharmacol Physiol* **31**(8): 485-493.

Allison, DB, Zannolli, R, Narayan, KM (1999) The direct health care costs of obesity in the United States. *Am J Public Health* **89**(8): 1194-1199.

Alvisi, M, De Arcangelis, V, Ciccone, L, Palombi, V, Alessandrini, M, Nemoz, G, Molinaro, M, Adamo, S, Naro, F (2008) V1a vasopressin receptor expression is modulated during myogenic differentiation. *Differentiation* **76**(4): 371-380.

Amano, M, Fukata, Y, Shimokawa, H, Kaibuchi, K (2000) Purification and in vitro activity of Rho-associated kinase. *Methods Enzymol* **325**: 149-155.

An, S, Bleu, T, Hallmark, OG, Goetzl, EJ (1998) Characterization of a novel subtype of human G protein-coupled receptor for lysophosphatidic acid. *The Journal of biological chemistry* **273**(14): 7906-7910.

Anakwe, K, Robson, L, Hadley, J, Buxton, P, Church, V, Allen, S, Hartmann, C, Harfe, B, Nohno, T, Brown, AM, Evans, DJ, Francis-West, P (2003) Wnt signalling regulates myogenic differentiation in the developing avian wing. *Development* **130**(15): 3503-3514.

Andersson, A, Sjodin, A, Hedman, A, Olsson, R, Vessby, B (2000) Fatty acid profile of skeletal muscle phospholipids in trained and untrained young men. *Am J Physiol*

*Endocrinol Metab* **279**(4): E744-751.

Angello, JC, Hauschka, SD (1979) Hyaluronic acid synthesis and turnover by myotubes in culture. *Dev Biol* **73**(2): 322-337.

Arias, AM, Bisschop, PH, Ackermans, MT, Nijpels, G, Endert, E, Romijn, JA, Sauerwein, HP (2001) Aminophylline stimulates insulin secretion in patients with type 2 diabetes mellitus. *Metabolism: clinical and experimental* **50**(9): 1030-1035.

Aschenbach, WG, Hirshman, MF, Fujii, N, Sakamoto, K, Howlett, KF, Goodyear, LJ (2002) Effect of AICAR treatment on glycogen metabolism in skeletal muscle. *Diabetes* **51**(3): 567-573.

Astrup, A, Buemann, B, Western, P, Toubro, S, Raben, A, Christensen, NJ (1994) Obesity as an adaptation to a high-fat diet: evidence from a cross-sectional study. *Am J Clin Nutr* **59**(2): 350-355.

Astrup, A, O'Hill, J, Rossner, S (2004) The cause of obesity: are we barking up the wrong tree? *Obes Rev* **5**(3): 125-127.

Baker, D, Pryce, G, Giovannoni, G, Thompson, AJ (2003) The therapeutic potential of cannabis. *Lancet Neurol* **2**(5): 291-298.

Banachewicz, W, Suplat, D, Krzeminski, P, Pomorski, P, Baranska, J (2005) P2 nucleotide receptors on C2C12 satellite cells. *Purinergic Signal* **1**(3): 249-257.

Baron, AD, Brechtel, G, Wallace, P, Edelman, SV (1988) Rates and tissue sites of non-insulin- and insulin-mediated glucose uptake in humans. *Am J Physiol* **255**(6 Pt 1): E769-774.

Barton, PJ, Cullen, ME, Townsend, PJ, Brand, NJ, Mullen, AJ, Norman, DA, Bhavsar, PK, Yacoub, MH (1999) Close physical linkage of human troponin genes: organization, sequence, and expression of the locus encoding cardiac troponin I and slow skeletal troponin T. *Genomics* **57**(1): 102-109.

Baumgartner, RN, Heymsfield, SB, Roche, AF (1995) Human body composition and the epidemiology of chronic disease. *Obes Res* **3**(1): 73-95.

Bellocchio, L, Cervino, C, Pasquali, R, Pagotto, U (2008) The endocannabinoid system and energy metabolism. *J Neuroendocrinol* **20**(6): 850-857.

Bennett, AM, Tonks, NK (1997) Regulation of distinct stages of skeletal muscle differentiation by mitogen-activated protein kinases. *Science (New York, N.Y* **278**(5341): 1288-1291.

Bensaid, M, Gary-Bobo, M, Esclangon, A, Maffrand, JP, Le Fur, G, Oury-Donat, F, Soubrie, P (2003) The cannabinoid CB1 receptor antagonist SR141716 increases Acrp30 mRNA expression in adipose tissue of obese fa/fa rats and in cultured adipocyte cells. *Mol Pharmacol* **63**(4): 908-914.

Berchtold, MW, Brinkmeier, H, Muntener, M (2000) Calcium ion in skeletal muscle: its crucial role for muscle function, plasticity, and disease. *Physiol Rev* **80**(3): 1215-1265.

Berggren, JR, Boyle, KE, Chapman, WH, Houmard, JA (2008) Skeletal muscle lipid oxidation and obesity: influence of weight loss and exercise. *Am J Physiol Endocrinol Metab* **294**(4): E726-732.

Bermudez-Silva, FJ, Suarez, J, Baixeras, E, Cobo, N, Bautista, D, Cuesta-Munoz, AL, Fuentes, E, Juan-Pico, P, Castro, MJ, Milman, G, Mechoulam, R, Nadal, A, Rodriguez de Fonseca, F (2008) Presence of functional cannabinoid receptors in human endocrine pancreas. *Diabetologia* **51**(3): 476-487.

Bermudez-Siva, FJ, Serrano, A, Diaz-Molina, FJ, Sanchez Vera, I, Juan-Pico, P, Nadal, A, Fuentes, E, Rodriguez de Fonseca, F (2006) Activation of cannabinoid CB1 receptors induces glucose intolerance in rats. *Eur J Pharmacol* **531**(1-3): 282-284.

Berridge, MJ (1997) Elementary and global aspects of calcium signalling. *J Physiol* **499 ( Pt 2)**: 291-306.

Berthele, A, Platzer, S, Weis, S, Conrad, B, Tolle, TR (2001) Expression of GABA(B1) and GABA(B2) mRNA in the human brain. *Neuroreport* **12**(15): 3269-3275.

Betsholtz, C, Karlsson, L, Lindahl, P (2001) Developmental roles of platelet-derived growth factors. *Bioessays* **23**(6): 494-507.

Betty, M, Harnish, SW, Rhodes, KJ, Cockett, MI (1998) Distribution of heterotrimeric G-protein beta and gamma subunits in the rat brain. *Neuroscience* **85**(2): 475-486.

Bialek, P, Morris, C, Parkington, J, St Andre, M, Owens, J, Yaworsky, P, Seeherman, H, Jelinsky, SA (2011) Distinct protein degradation profiles are induced by different disuse models of skeletal muscle atrophy. *Physiol Genomics* **43**(19): 1075-1086.

Bidaut-Russell, M, Devane, WA, Howlett, AC (1990) Cannabinoid receptors and modulation of cyclic AMP accumulation in the rat brain. *J Neurochem* **55**(1): 21-26.

Bilski, AJ, Halliday, SE, Fitzgerald, JD, Wale, JL (1983) The pharmacology of a beta 2-selective adrenoceptor antagonist (ICI 118,551). *J Cardiovasc Pharmacol* **5**(3): 430-437.

Bindewald, K, Gunduz, D, Hartel, F, Peters, SC, Rodewald, C, Nau, S, Schafer, M, Neumann, J, Piper, HM, Noll, T (2004) Opposite effect of cAMP signaling in endothelial barriers of different origin. *Am J Physiol Cell Physiol* **287**(5): C1246-1255.

Bingham, J, Sudarsanam, S, Srinivasan, S (2006) Profiling human phosphodiesterase genes and splice isoforms. *Biochem Biophys Res Commun* **350**(1): 25-32.

Bischoff, S, Leonhard, S, Reymann, N, Schuler, V, Shigemoto, R, Kaupmann, K, Bettler, B (1999) Spatial distribution of GABA(B)R1 receptor mRNA and binding sites in the rat brain. *J Comp Neurol* **412**(1): 1-16.

Bisogno, T, Howell, F, Williams, G, Minassi, A, Cascio, MG, Ligresti, A, Matias, I, Schiano-Moriello, A, Paul, P, Williams, EJ, Gangadharan, U, Hobbs, C, Di Marzo, V, Doherty, P (2003) Cloning of the first sn1-DAG lipases points to the spatial and temporal regulation of endocannabinoid signaling in the brain. *J Cell Biol* **163**(3): 463-

468.

Bisogno, T, Sepe, N, Melck, D, Maurelli, S, De Petrocellis, L, Di Marzo, V (1997) Biosynthesis, release and degradation of the novel endogenous cannabimimetic metabolite 2-arachidonoylglycerol in mouse neuroblastoma cells. *Biochem J* **322 ( Pt 2)**: 671-677.

Blau, HM, Webster, C (1981) Isolation and characterization of human muscle cells. *Proceedings of the National Academy of Sciences of the United States of America* **78**(9): 5623-5627.

Bloom, TJ (2005) Age-related alterations in cyclic nucleotide phosphodiesterase activity in dystrophic mouse leg muscle. *Can J Physiol Pharmacol* **83**(11): 1055-1060.

Bloom, TJ (2002) Cyclic nucleotide phosphodiesterase isozymes expressed in mouse skeletal muscle. *Can J Physiol Pharmacol* **80**(12): 1132-1135.

Bluher, M, Engeli, S, Kloting, N, Berndt, J, Fasshauer, M, Batkai, S, Pacher, P, Schon, MR, Jordan, J, Stumvoll, M (2006) Dysregulation of the peripheral and adipose tissue endocannabinoid system in human abdominal obesity. *Diabetes* **55**(11): 3053-3060.

Bonavaud, S, Agbulut, O, Nizard, R, D'Honneur, G, Mouly, V, Butler-Browne, G (2001) A discrepancy resolved: human satellite cells are not preprogrammed to fast and slow lineages. *Neuromuscul Disord* **11**(8): 747-752.

Borno, A, Ploug, T, Bune, LT, Rosenmeier, JB, Thaning, P (2011) Purinergic receptors expressed in human skeletal muscle fibres. *Purinergic Signal.*

Borrmann, T, Hinz, S, Bertarelli, DC, Li, W, Florin, NC, Scheiff, AB, Muller, CE (2009) 1-alkyl-8-(piperazine-1-sulfonyl)phenylxanthines: development and characterization of adenosine A2B receptor antagonists and a new radioligand with subnanomolar affinity and subtype specificity. *J Med Chem* **52**(13): 3994-4006.

Bosier, B, Muccioli, GG, Hermans, E, Lambert, DM (2010) Functionally selective cannabinoid receptor signalling: therapeutic implications and opportunities. *Biochemical pharmacology* **80**(1): 1-12.

Boyer, JL, Mohanram, A, Camaioni, E, Jacobson, KA, Harden, TK (1998) Competitive and selective antagonism of P2Y1 receptors by N6-methyl 2'-deoxyadenosine 3',5'-bisphosphate. *Br J Pharmacol* **124**(1): 1-3.

Braissant, O, Foufelle, F, Scotto, C, Dauca, M, Wahli, W (1996) Differential expression of peroxisome proliferator-activated receptors (PPARs): tissue distribution of PPAR-alpha, -beta, and -gamma in the adult rat. *Endocrinology* **137**(1): 354-366.

Brandon, EP, Idzerda, RL, McKnight, GS (1997) PKA isoforms, neural pathways, and behaviour: making the connection. *Curr Opin Neurobiol* **7**(3): 397-403.

Briley, EM, Lolait, SJ, Axelrod, J, Felder, CC (1994) The cloned vasopressin V1a receptor stimulates phospholipase A2, phospholipase C, and phospholipase D through activation of receptor-operated calcium channels. *Neuropeptides* **27**(1): 63-74.

Brown, AJ (2007) Novel cannabinoid receptors. *Br J Pharmacol* **152**(5): 567-575.

Brown, SM, Wager-Miller, J, Mackie, K (2002) Cloning and molecular characterization of the rat CB2 cannabinoid receptor. *Biochim Biophys Acta* **1576**(3): 255-264.

Brozinick, JT, Jr., Roberts, BR, Dohm, GL (2003) Defective signaling through Akt-2 and -3 but not Akt-1 in insulin-resistant human skeletal muscle: potential role in insulin resistance. *Diabetes* **52**(4): 935-941.

Burdyga, G, Lal, S, Varro, A, Dimaline, R, Thompson, DG, Dockray, GJ (2004) Expression of cannabinoid CB1 receptors by vagal afferent neurons is inhibited by cholecystokinin. *J Neurosci* **24**(11): 2708-2715.

Burnstock, G (2008) Dual control of vascular tone and remodelling by ATP released from nerves and endothelial cells. *Pharmacol Rep* **60**(1): 12-20.

Burt, AR, Carr, IC, Mullaney, I, Anderson, NG, Milligan, G (1996) Agonist activation of p42 and p44 mitogen-activated protein kinases following expression of the mouse delta opioid receptor in Rat-1 fibroblasts: effects of receptor expression levels and comparisons with G-protein activation. *Biochem J* **320 ( Pt 1)**: 227-235.

Burton, KA, Johnson, BD, Hausken, ZE, Westenbroek, RE, Idzerda, RL, Scheuer, T, Scott, JD, Catterall, WA, McKnight, GS (1997) Type II regulatory subunits are not required for the anchoring-dependent modulation of Ca2+ channel activity by cAMP-dependent protein kinase. *Proceedings of the National Academy of Sciences of the United States of America* **94**(20): 11067-11072.

Bylund, DB, Eikenberg, DC, Hieble, JP, Langer, SZ, Lefkowitz, RJ, Minneman, KP, Molinoff, PB, Ruffolo, RR, Jr., Trendelenburg, U (1994) International Union of Pharmacology nomenclature of adrenoceptors. *Pharmacol Rev* **46**(2): 121-136.

Cable, JC, Tan, GD, Alexander, SP, O'Sullivan, SE (2011) The activity of the endocannabinoid metabolising enzyme fatty acid amide hydrolase in subcutaneous adipocytes correlates with BMI in metabolically healthy humans. *Lipids Health Dis* **10**: 129.

Cadas, H, Gaillet, S, Beltramo, M, Venance, L, Piomelli, D (1996) Biosynthesis of an endogenous cannabinoid precursor in neurons and its control by calcium and cAMP. *J Neurosci* **16**(12): 3934-3942.

Cahova, M, Vavrinkova, H, Kazdova, L (2007) Glucose-fatty acid interaction in skeletal muscle and adipose tissue in insulin resistance. *Physiol Res* **56**(1): 1-15.

Calera, MR, Martinez, C, Liu, H, Jack, AK, Birnbaum, MJ, Pilch, PF (1998) Insulin increases the association of Akt-2 with Glut4-containing vesicles. *J Biol Chem* **273**(13): 7201-7204.

Calle, EE, Kaaks, R (2004a) Overweight, obesity and cancer: epidemiological evidence and proposed mechanisms. *Nat Rev Cancer* **4**(8): 579-591.

Calle, EE, Rodriguez, C, Walker-Thurmond, K, Thun, MJ (2003) Overweight, obesity, and mortality from cancer in a prospectively studied cohort of U.S. adults. *N Engl J*

*Med* **348**(17): 1625-1638.

Calle, EE, Thun, MJ (2004b) Obesity and cancer. *Oncogene* **23**(38): 6365-6378.

Carai, MA, Colombo, G, Gessa, GL (2005) Rimonabant: the first therapeutically relevant cannabinoid antagonist. *Life Sci* **77**(19): 2339-2350.

Carr, DB, Bullen, BA, Skrinar, GS, Arnold, MA, Rosenblatt, M, Beitins, IZ, Martin, JB, McArthur, JW (1981) Physical conditioning facilitates the exercise-induced secretion of beta-endorphin and beta-lipotropin in women. *N Engl J Med* **305**(10): 560-563.

Carrino, DA, Sorrell, JM, Caplan, AI (1999) Dynamic expression of proteoglycans during chicken skeletal muscle development and maturation. *Poult Sci* **78**(5): 769-777.

Carson, JA, Nettleton, D, Reecy, JM (2002) Differential gene expression in the rat soleus muscle during early work overload-induced hypertrophy. *Faseb J* **16**(2): 207-209.

Castaneda, F, Layne, JE, Castaneda, C (2006) Skeletal muscle sodium glucose co-transporters in older adults with type 2 diabetes undergoing resistance training. *Int J Med Sci* **3**(3): 84-91.

Castanon, MJ, Spevak, W (1994) Functional coupling of human adenosine receptors to a ligand-dependent reporter gene system. *Biochem Biophys Res Commun* **198**(2): 626-631.

Castelli, MP, Ingianni, A, Stefanini, E, Gessa, GL (1999) Distribution of GABA(B) receptor mRNAs in the rat brain and peripheral organs. *Life Sci* **64**(15): 1321-1328.

Cattaneo, M, Lecchi, A, Ohno, M, Joshi, BV, Besada, P, Tchilibon, S, Lombardi, R, Bischofberger, N, Harden, TK, Jacobson, KA (2004) Antiaggregatory activity in human platelets of potent antagonists of the P2Y 1 receptor. *Biochemical pharmacology* **68**(10): 1995-2002.

Caulfield, MP, Brown, DA (1992) Cannabinoid receptor agonists inhibit Ca current in NG108-15 neuroblastoma cells via a pertussis toxin-sensitive mechanism. *Br J Pharmacol* **106**(2): 231-232.

Cavuoto, P, McAinch, AJ, Hatzinikolas, G, Cameron-Smith, D, Wittert, GA (2007a) Effects of cannabinoid receptors on skeletal muscle oxidative pathways. *Mol Cell Endocrinol* **267**(1-2): 63-69.

Cavuoto, P, McAinch, AJ, Hatzinikolas, G, Janovska, A, Game, P, Wittert, GA (2007b) The expression of receptors for endocannabinoids in human and rodent skeletal muscle. *Biochem Biophys Res Commun* **364**(1): 105-110.

Chakrabarti, A, Onaivi, ES, Chaudhuri, G (1995) Cloning and sequencing of a cDNA encoding the mouse brain-type cannabinoid receptor protein. *DNA Seq* **5**(6): 385-388.

Chalon, P, Vita, N, Kaghad, M, Guillemot, M, Bonnin, J, Delpech, B, Le Fur, G, Ferrara, P, Caput, D (1996) Molecular cloning of a levocabastine-sensitive neurotensin binding site. *FEBS letters* **386**(2-3): 91-94.

Cham, BE, Knowles, BR (1976) A solvent system for delipidation of plasma or serum without protein precipitation. *J Lipid Res* **17**(2): 176-181.

Chao, LC, Wroblewski, K, Zhang, Z, Pei, L, Vergnes, L, Ilkayeva, OR, Ding, SY, Reue, K, Watt, MJ, Newgard, CB, Pilch, PF, Hevener, AL, Tontonoz, P (2009) Insulin resistance and altered systemic glucose metabolism in mice lacking Nur77. *Diabetes* **58**(12): 2788-2796.

Chao, LC, Zhang, Z, Pei, L, Saito, T, Tontonoz, P, Pilch, PF (2007) Nur77 coordinately regulates expression of genes linked to glucose metabolism in skeletal muscle. *Mol Endocrinol* **21**(9): 2152-2163.

Chen, C, Zheng, B, Han, J, Lin, SC (1997a) Characterization of a novel mammalian RGS protein that binds to Galpha proteins and inhibits pheromone signaling in yeast. *The Journal of biological chemistry* **272**(13): 8679-8685.

Chen, CA, Manning, DR (2001) Regulation of G proteins by covalent modification. *Oncogene* **20**(13): 1643-1652.

Chen, J, Dinger, B, Fidone, SJ (1997b) cAMP production in rabbit carotid body: role of adenosine. *J Appl Physiol* **82**(6): 1771-1775.

Chen, M, Feng, HZ, Gupta, D, Kelleher, J, Dickerson, KE, Wang, J, Hunt, D, Jou, W, Gavrilova, O, Jin, JP, Weinstein, LS (2009) G(s)alpha deficiency in skeletal muscle leads to reduced muscle mass, fiber-type switching, and glucose intolerance without insulin resistance or deficiency. *Am J Physiol Cell Physiol* **296**(4): C930-940.

Chen, M, Liang, X, Bao, XJ, Wang, H, Sun, HQ, Lu, SH (2004) [Investigation of the expression of calcitonin receptor mRNA in human osteoclasts on deciduous teeth]. *Hua Xi Kou Qiang Yi Xue Za Zhi* **22**(3): 235-237.

Chen, Y, Harry, A, Li, J, Smit, MJ, Bai, X, Magnusson, R, Pieroni, JP, Weng, G, Iyengar, R (1997c) Adenylyl cyclase 6 is selectively regulated by protein kinase A phosphorylation in a region involved in Galphas stimulation. *Proceedings of the National Academy of Sciences of the United States of America* **94**(25): 14100-14104.

Chen, Y, Shyu, JF, Santhanagopal, A, Inoue, D, David, JP, Dixon, SJ, Horne, WC, Baron, R (1998) The calcitonin receptor stimulates Shc tyrosine phosphorylation and Erk1/2 activation. Involvement of Gi, protein kinase C, and calcium. *The Journal of biological chemistry* **273**(31): 19809-19816.

Cheng, HF, Jiang, MJ, Chen, CL, Liu, SM, Wong, LP, Lomasney, JW, King, K (1995) Cloning and identification of amino acid residues of human phospholipase C delta 1 essential for catalysis. *The Journal of biological chemistry* **270**(10): 5495-5505.

Chiavegatti, T, Costa, VL, Jr., Araujo, MS, Godinho, RO (2008) Skeletal muscle expresses the extracellular cyclic AMP-adenosine pathway. *Br J Pharmacol* **153**(6): 1331-1340.

Chibalin, AV, Leng, Y, Vieira, E, Krook, A, Bjornholm, M, Long, YC, Kotova, O, Zhong, Z, Sakane, F, Steiler, T, Nylen, C, Wang, J, Laakso, M, Topham, MK, Gilbert, M, Wallberg-Henriksson, H, Zierath, JR (2008) Downregulation of diacylglycerol

kinase delta contributes to hyperglycemia-induced insulin resistance. *Cell* **132**(3): 375-386.

Choi, JW, Herr, DR, Noguchi, K, Yung, YC, Lee, CW, Mutoh, T, Lin, ME, Teo, ST, Park, KE, Mosley, AN, Chun, J (2010) LPA receptors: subtypes and biological actions. *Annu Rev Pharmacol Toxicol* **50**: 157-186.

Christie, MJ, Vaughan, CW (2001) Neurobiology Cannabinoids act backwards. *Nature* **410**(6828): 527-530.

Christopoulou, FD, Kiortsis, DN (2011) An overview of the metabolic effects of rimonabant in randomized controlled trials: potential for other cannabinoid 1 receptor blockers in obesity. *J Clin Pharm Ther* **36**(1): 10-18.

Ciaraldi, TP, Nikoulina, SE, Bandukwala, RA, Carter, L, Henry, RR (2007) Role of glycogen synthase kinase-3 alpha in insulin action in cultured human skeletal muscle cells. *Endocrinology* **148**(9): 4393-4399.

Cleasby, ME, Reinten, TA, Cooney, GJ, James, DE, Kraegen, EW (2007) Functional studies of Akt isoform specificity in skeletal muscle in vivo; maintained insulin sensitivity despite reduced insulin receptor substrate-1 expression. *Mol Endocrinol* **21**(1): 215-228.

Close, RI (1972) Dynamic properties of mammalian skeletal muscles. *Physiol Rev* **52**(1): 129-197.

Colditz, GA, Willett, WC, Rotnitzky, A, Manson, JE (1995) Weight gain as a risk factor for clinical diabetes mellitus in women. *Ann Intern Med* **122**(7): 481-486.

Conklin, BR, Bourne, HR (1993) Structural elements of G alpha subunits that interact with G beta gamma, receptors, and effectors. *Cell* **73**(4): 631-641.

Convents, A, De Keyser, J, De Backer, JP, Vauquelin, G (1989) [3H]rauwolscine labels alpha 2-adrenoceptors and 5-HT1A receptors in human cerebral cortex. *Eur J Pharmacol* **159**(3): 307-310.

Coppock, HA, Owji, AA, Bloom, SR, Smith, DM (1996) A rat skeletal muscle cell line (L6) expresses specific adrenomedullin binding sites but activates adenylate cyclase via calcitonin gene-related peptide receptors. *Biochem J* **318 ( Pt 1)**: 241-245.

Coronado, R, Morrissette, J, Sukhareva, M, Vaughan, DM (1994) Structure and function of ryanodine receptors. *Am J Physiol* **266**(6 Pt 1): C1485-1504.

Corton, JM, Gillespie, JG, Hawley, SA, Hardie, DG (1995) 5-aminoimidazole-4-carboxamide ribonucleoside. A specific method for activating AMP-activated protein kinase in intact cells? *Eur J Biochem* **229**(2): 558-565.

Cota, D, Marsicano, G, Tschop, M, Grubler, Y, Flachskamm, C, Schubert, M, Auer, D, Yassouridis, A, Thone-Reineke, C, Ortmann, S, Tomassoni, F, Cervino, C, Nisoli, E, Linthorst, AC, Pasquali, R, Lutz, B, Stalla, GK, Pagotto, U (2003) The endogenous cannabinoid system affects energy balance via central orexigenic drive and peripheral lipogenesis. *J Clin Invest* **112**(3): 423-431.

Cota, D, Sandoval, DA, Olivieri, M, Prodi, E, D'Alessio, DA, Woods, SC, Seeley, RJ, Obici, S (2009) Food intake-independent effects of CB1 antagonism on glucose and lipid metabolism. *Obesity (Silver Spring)* **17**(8): 1641-1645.

Cote, M, Mauriege, P, Bergeron, J, Almeras, N, Tremblay, A, Lemieux, I, Despres, JP (2005) Adiponectinemia in visceral obesity: impact on glucose tolerance and plasma lipoprotein and lipid levels in men. *J Clin Endocrinol Metab* **90**(3): 1434-1439.

Coutts, AA, Pertwee, RG (1998) Evidence that cannabinoid-induced inhibition of electrically evoked contractions of the myenteric plexus--longitudinal muscle preparation of guinea-pig small intestine can be modulated by Ca2+ and cAMP. *Can J Physiol Pharmacol* **76**(3): 340-346.

Cross, DA, Alessi, DR, Cohen, P, Andjelkovich, M, Hemmings, BA (1995) Inhibition of glycogen synthase kinase-3 by insulin mediated by protein kinase B. *Nature* **378**(6559): 785-789.

Daugaard, JR, Nielsen, JN, Kristiansen, S, Andersen, JL, Hargreaves, M, Richter, EA (2000) Fiber type-specific expression of GLUT4 in human skeletal muscle: influence of exercise training. *Diabetes* **49**(7): 1092-1095.

de Castro, BM, De Jaeger, X, Martins-Silva, C, Lima, RD, Amaral, E, Menezes, C, Lima, P, Neves, CM, Pires, RG, Gould, TW, Welch, I, Kushmerick, C, Guatimosim, C, Izquierdo, I, Cammarota, M, Rylett, RJ, Gomez, MV, Caron, MG, Oppenheim, RW, Prado, MA, Prado, VF (2009) The vesicular acetylcholine transporter is required for neuromuscular development and function. *Mol Cell Biol* **29**(19): 5238-5250.

De Vries, L, Zheng, B, Fischer, T, Elenko, E, Farquhar, MG (2000) The regulator of G protein signaling family. *Annu Rev Pharmacol Toxicol* **40**: 235-271.

De Waard, M, Liu, H, Walker, D, Scott, VE, Gurnett, CA, Campbell, KP (1997) Direct binding of G-protein betagamma complex to voltage-dependent calcium channels. *Nature* **385**(6615): 446-450.

Del Prato, S, Marchetti, P, Bonadonna, RC (2002) Phasic insulin release and metabolic regulation in type 2 diabetes. *Diabetes* **51 Suppl 1**: S109-116.

Delbono, O, Xia, J, Treves, S, Wang, ZM, Jimenez-Moreno, R, Payne, AM, Messi, ML, Briguet, A, Schaerer, F, Nishi, M, Takeshima, H, Zorzato, F (2007) Loss of skeletal muscle strength by ablation of the sarcoplasmic reticulum protein JP45. *Proceedings of the National Academy of Sciences of the United States of America* **104**(50): 20108-20113.

Deli, T, Csernoch, L (2008) Extracellular ATP and cancer: an overview with special reference to P2 purinergic receptors. *Pathol Oncol Res* **14**(3): 219-231.

Demuth, DG, Molleman, A (2006) Cannabinoid signalling. *Life Sci* **78**(6): 549-563.

Deo, DD, Bazan, NG, Hunt, JD (2004) Activation of platelet-activating factor receptor-coupled G alpha q leads to stimulation of Src and focal adhesion kinase via two separate pathways in human umbilical vein endothelial cells. *The Journal of biological chemistry*

279(5): 3497-3508.

Despres, JP, Golay, A, Sjostrom, L (2005) Effects of rimonabant on metabolic risk factors in overweight patients with dyslipidemia. *N Engl J Med* **353**(20): 2121-2134.

Despres, JP, Lemieux, I (2006) Abdominal obesity and metabolic syndrome. *Nature* **444**(7121): 881-887.

Devane, WA, Dysarz, FA, 3rd, Johnson, MR, Melvin, LS, Howlett, AC (1988) Determination and characterization of a cannabinoid receptor in rat brain. *Mol Pharmacol* **34**(5): 605-613.

Di Castro, MA, Chuquet, J, Liaudet, N, Bhaukaurally, K, Santello, M, Bouvier, D, Tiret, P, Volterra, A (2011) Local Ca2+ detection and modulation of synaptic release by astrocytes. *Nat Neurosci* **14**(10): 1276-1284.

Di Marzo, V, Capasso, R, Matias, I, Aviello, G, Petrosino, S, Borrelli, F, Romano, B, Orlando, P, Capasso, F, Izzo, AA (2008) The role of endocannabinoids in the regulation of gastric emptying: alterations in mice fed a high-fat diet. *Br J Pharmacol* **153**(6): 1272-1280.

Di Marzo, V, De Petrocellis, L, Sugiura, T, Waku, K (1996) Potential biosynthetic connections between the two cannabimimetic eicosanoids, anandamide and 2-arachidonoyl-glycerol, in mouse neuroblastoma cells. *Biochem Biophys Res Commun* **227**(1): 281-288.

Di Marzo, V, Fontana, A, Cadas, H, Schinelli, S, Cimino, G, Schwartz, JC, Piomelli, D (1994) Formation and inactivation of endogenous cannabinoid anandamide in central neurons. *Nature* **372**(6507): 686-691.

Di Marzo, V, Goparaju, SK, Wang, L, Liu, J, Batkai, S, Jarai, Z, Fezza, F, Miura, GI, Palmiter, RD, Sugiura, T, Kunos, G (2001) Leptin-regulated endocannabinoids are involved in maintaining food intake. *Nature* **410**(6830): 822-825.

Di Marzo, V, Matias, I (2005) Endocannabinoid control of food intake and energy balance. *Nat Neurosci* **8**(5): 585-589.

Di Marzo, V, Petrocellis, LD (2006) Plant, synthetic, and endogenous cannabinoids in medicine. *Annu Rev Med* **57**: 553-574.

Donati, C, Meacci, E, Nuti, F, Becciolini, L, Farnararo, M, Bruni, P (2005) Sphingosine 1-phosphate regulates myogenic differentiation: a major role for S1P2 receptor. *Faseb J* **19**(3): 449-451.

Donnelly, R, Reed, MJ, Azhar, S, Reaven, GM (1994) Expression of the major isoenzyme of protein kinase-C in skeletal muscle, nPKC theta, varies with muscle type and in response to fructose-induced insulin resistance. *Endocrinology* **135**(6): 2369-2374.

Downes, GB, Gautam, N (1999) The G protein subunit gene families. *Genomics* **62**(3): 544-552.

Doyon, C, Denis, RG, Baraboi, ED, Samson, P, Lalonde, J, Deshaies, Y, Richard, D (2006) Effects of rimonabant (SR141716) on fasting-induced hypothalamic-pituitary-adrenal axis and neuronal activation in lean and obese Zucker rats. *Diabetes* **55**(12): 3403-3410.

Dray, A, Perkins, M (1993) Bradykinin and inflammatory pain. *Trends Neurosci* **16**(3): 99-104.

Dray, C, Knauf, C, Daviaud, D, Waget, A, Boucher, J, Buleon, M, Cani, PD, Attane, C, Guigne, C, Carpene, C, Burcelin, R, Castan-Laurell, I, Valet, P (2008) Apelin stimulates glucose utilization in normal and obese insulin-resistant mice. *Cell Metab* **8**(5): 437-445.

Droge, W, Hack, V, Breitkreutz, R, Holm, E, Shubinsky, G, Schmid, E, Galter, D (1998) Role of cysteine and glutathione in signal transduction, immunopathology and cachexia. *Biofactors* **8**(1-2): 97-102.

Dubey, RK, Gillespie, DG, Shue, H, Jackson, EK (2000) A(2B) receptors mediate antimitogenesis in vascular smooth muscle cells. *Hypertension* **35**(1 Pt 2): 267-272.

Duka, I, Shenouda, S, Johns, C, Kintsurashvili, E, Gavras, I, Gavras, H (2001) Role of the B(2) receptor of bradykinin in insulin sensitivity. *Hypertension* **38**(6): 1355-1360.

Eckardt, K, Sell, H, Eckel, J (2008a) Novel aspects of adipocyte-induced skeletal muscle insulin resistance. *Arch Physiol Biochem* **114**(4): 287-298.

Eckardt, K, Sell, H, Taube, A, Koenen, M, Platzbecker, B, Cramer, A, Horrighs, A, Lehtonen, M, Tennagels, N, Eckel, J (2008b) Cannabinoid type 1 receptors in human skeletal muscle cells participate in the negative crosstalk between fat and muscle. *Diabetologia.*

Eckardt, K, Sell, H, Taube, A, Koenen, M, Platzbecker, B, Cramer, A, Horrighs, A, Lehtonen, M, Tennagels, N, Eckel, J (2009) Cannabinoid type 1 receptors in human skeletal muscle cells participate in the negative crosstalk between fat and muscle. *Diabetologia* **52**(4): 664-674.

Eilon, G, Mundy, GR (1983) Association of increased cyclic adenosine 3':5'-monophosphate content in cultured human breast cancer cells and release of hydrolytic enzymes and bone-resorbing activity. *Cancer Res* **43**(12 Pt 1): 5792-5794.

El-Tayeb, A, Qi, A, Muller, CE (2006) Synthesis and structure-activity relationships of uracil nucleotide derivatives and analogues as agonists at human P2Y2, P2Y4, and P2Y6 receptors. *J Med Chem* **49**(24): 7076-7087.

Eldar-Finkelman, H (2002) Glycogen synthase kinase 3: an emerging therapeutic target. *Trends Mol Med* **8**(3): 126-132.

Endo, M (2009) Calcium-induced calcium release in skeletal muscle. *Physiol Rev* **89**(4): 1153-1176.

Engeli, S (2008) Dysregulation of the endocannabinoid system in obesity. *J Neuroendocrinol* **20 Suppl 1**: 110-115.

Engeli, S, Bohnke, J, Feldpausch, M, Gorzelniak, K, Janke, J, Batkai, S, Pacher, P, Harvey-White, J, Luft, FC, Sharma, AM, Jordan, J (2005) Activation of the peripheral endocannabinoid system in human obesity. *Diabetes* **54**(10): 2838-2843.

Enserink, JM, Price, LS, Methi, T, Mahic, M, Sonnenberg, A, Bos, JL, Tasken, K (2004) The cAMP-Epac-Rap1 pathway regulates cell spreading and cell adhesion to laminin-5 through the alpha3beta1 integrin but not the alpha6beta4 integrin. *The Journal of biological chemistry* **279**(43): 44889-44896.

Esfandyari, T, Camilleri, M, Ferber, I, Burton, D, Baxter, K, Zinsmeister, AR (2006) Effect of a cannabinoid agonist on gastrointestinal transit and postprandial satiation in healthy human subjects: a randomized, placebo-controlled study. *Neurogastroenterol Motil* **18**(9): 831-838.

Esposito, I, Proto, MC, Gazzerro, P, Laezza, C, Miele, C, Alberobello, AT, D'Esposito, V, Beguinot, F, Formisano, P, Bifulco, M (2008) The cannabinoid CB1 receptor antagonist rimonabant stimulates 2-deoxyglucose uptake in skeletal muscle cells by regulating the expression of phosphatidylinositol-3-kinase. *Mol Pharmacol* **74**(6): 1678-1686.

Evangelisti, C, Riccio, M, Faenza, I, Zini, N, Hozumi, Y, Goto, K, Cocco, L, Martelli, AM (2006) Subnuclear localization and differentiation-dependent increased expression of DGK-zeta in C2C12 mouse myoblasts. *J Cell Physiol* **209**(2): 370-378.

Evans, AA, Hughes, S, Smith, ME (1995) Delta-opioid peptide receptors in muscles from obese diabetic and normal mice. *Peptides* **16**(2): 361-364.

Evans, AA, Khan, S, Smith, ME (1997) Evidence for a hormonal action of beta-endorphin to increase glucose uptake in resting and contracting skeletal muscle. *J Endocrinol* **155**(2): 387-392.

Evans, AA, Smith, ME (1996) Distribution of opioid peptide receptors in muscles of lean and obese-diabetic mice. *Peptides* **17**(4): 629-634.

Evans, AA, Tunnicliffe, G, Knights, P, Bailey, CJ, Smith, ME (2001) Delta opioid receptors mediate glucose uptake in skeletal muscles of lean and obese-diabetic (ob/ob) mice. *Metabolism: clinical and experimental* **50**(12): 1402-1408.

Felder, CC, Dickason-Chesterfield, AK, Moore, SA (2006) Cannabinoids biology: the search for new therapeutic targets. *Mol Interv* **6**(3): 149-161.

Felder, CC, Joyce, KE, Briley, EM, Glass, M, Mackie, KP, Fahey, KJ, Cullinan, GJ, Hunden, DC, Johnson, DW, Chaney, MO, Koppel, GA, Brownstein, M (1998) LY320135, a novel cannabinoid CB1 receptor antagonist, unmasks coupling of the CB1 receptor to stimulation of cAMP accumulation. *J Pharmacol Exp Ther* **284**(1): 291-297.

Ferrannini, E (1998) Insulin resistance versus insulin deficiency in non-insulin-dependent diabetes mellitus: problems and prospects. *Endocr Rev* **19**(4): 477-490.

Ferrannini, E, Barrett, EJ, Bevilacqua, S, DeFronzo, RA (1983) Effect of fatty acids on glucose production and utilization in man. *J Clin Invest* **72**(5): 1737-1747.

Ferrannini, E, Haffner, SM, Mitchell, BD, Stern, MP (1991) Hyperinsulinaemia: the key feature of a cardiovascular and metabolic syndrome. *Diabetologia* **34**(6): 416-422.

Ferre, P (2004) The biology of peroxisome proliferator-activated receptors: relationship with lipid metabolism and insulin sensitivity. *Diabetes* **53 Suppl 1:** S43-50.

Figler, RA, Wang, G, Srinivasan, S, Jung, DY, Zhang, Z, Pankow, JS, Ravid, K, Fredholm, B, Hedrick, CC, Rich, SS, Kim, JK, LaNoue, KF, Linden, J (2011) Links between insulin resistance, adenosine A2B receptors, and inflammatory markers in mice and humans. *Diabetes* **60**(2): 669-679.

Figueroa, CD, Dietze, G, Muller-Esterl, W (1996) Immunolocalization of bradykinin B2 receptors on skeletal muscle cells. *Diabetes* **45 Suppl 1:** S24-28.

Fill, M, Copello, JA (2002) Ryanodine receptor calcium release channels. *Physiol Rev* **82**(4): 893-922.

Fogarty, S, Hardie, DG (2010) Development of protein kinase activators: AMPK as a target in metabolic disorders and cancer. *Biochim Biophys Acta* **1804**(3): 581-591.

Force, T, Bonventre, JV (1998) Growth factors and mitogen-activated protein kinases. *Hypertension* **31**(1 Pt 2): 152-161.

Fowler, CJ, Jacobsson, SO (2002) Cellular transport of anandamide, 2-arachidonoylglycerol and palmitoylethanolamide--targets for drug development? *Prostaglandins Leukot Essent Fatty Acids* **66**(2-3): 193-200.

Fox, MA, Sanes, JR (2007) Synaptotagmin I and II are present in distinct subsets of central synapses. *J Comp Neurol* **503**(2): 280-296.

Francis, H, LeSage, G, DeMorrow, S, Alvaro, D, Ueno, Y, Venter, J, Glaser, S, Mancino, MG, Marucci, L, Benedetti, A, Alpini, G (2007) The alpha2-adrenergic receptor agonist UK 14,304 inhibits secretin-stimulated ductal secretion by downregulation of the cAMP system in bile duct-ligated rats. *Am J Physiol Cell Physiol* **293**(4): C1252-1262.

Fredriksson, R, Lagerstrom, MC, Lundin, LG, Schioth, HB (2003) The G-protein-coupled receptors in the human genome form five main families. Phylogenetic analysis, paralogon groups, and fingerprints. *Mol Pharmacol* **63**(6): 1256-1272.

Fruen, BR, Mickelson, JR, Shomer, NH, Roghair, TJ, Louis, CF (1994) Regulation of the sarcoplasmic reticulum ryanodine receptor by inorganic phosphate. *The Journal of biological chemistry* **269**(1): 192-198.

Fu, Y, Luo, L, Luo, N, Zhu, X, Garvey, WT (2007) NR4A orphan nuclear receptors modulate insulin action and the glucose transport system: potential role in insulin resistance. *The Journal of biological chemistry* **282**(43): 31525-31533.

Fuchs, GH, Burger, G (1972) [Newer aspects of bacterial genetics. I. Molecular genetic principles and genetic regulation mechanism of intracellular information transmission]. *Dtsch Gesundheitsw* **27**(36): 1686-1689.

Fuentes, I, Cobos, AR, Segade, LA (1998) Muscle fibre types and their distribution in the biceps and triceps brachii of the rat and rabbit. *J Anat* **192 ( Pt 2):** 203-210.

Fuhlendorff, J, Gether, U, Aakerlund, L, Langeland-Johansen, N, Thogersen, H, Melberg, SG, Olsen, UB, Thastrup, O, Schwartz, TW (1990) [Leu31, Pro34]neuropeptide Y: a specific Y1 receptor agonist. *Proceedings of the National Academy of Sciences of the United States of America* **87**(1): 182-186.

Fujii, M, Ohtsubo, M, Ogawa, T, Kamata, H, Hirata, H, Yagisawa, H (1999) Real-time visualization of PH domain-dependent translocation of phospholipase C-delta1 in renal epithelial cells (MDCK): response to hypo-osmotic stress. *Biochem Biophys Res Commun* **254**(2): 284-291.

Fukada, S, Uezumi, A, Ikemoto, M, Masuda, S, Segawa, M, Tanimura, N, Yamamoto, H, Miyagoe-Suzuki, Y, Takeda, S (2007) Molecular signature of quiescent satellite cells in adult skeletal muscle. *Stem Cells* **25**(10): 2448-2459.

Fukushima, N, Kimura, Y, Chun, J (1998) A single receptor encoded by vzg-1/lpA1/edg-2 couples to G proteins and mediates multiple cellular responses to lysophosphatidic acid. *Proceedings of the National Academy of Sciences of the United States of America* **95**(11): 6151-6156.

Fulp, A, Bortoff, K, Seltzman, H, Zhang, Y, Mathews, J, Snyder, R, Fennell, T, Maitra, R (2012) Design and Synthesis of Cannabinoid Receptor 1 Antagonists for Peripheral Selectivity. *J Med Chem.*

Furman, B, Ong, WK, Pyne, NJ (2010) Cyclic AMP signaling in pancreatic islets. *Adv Exp Med Biol* **654:** 281-304.

Fuxe, K, Harfstrand, A, Agnati, LF, Kalia, M, Fredholm, B, Svensson, T, Gustafsson, JA, Lang, R, Ganten, D (1987) Central catecholamine-neuropeptide Y interactions at the pre- and postsynaptic level in cardiovascular centers. *J Cardiovasc Pharmacol* **10 Suppl 12:** S1-13.

Gahlmann, R, Wade, R, Gunning, P, Kedes, L (1988) Differential expression of slow and fast skeletal muscle troponin C. Slow skeletal muscle troponin C is expressed in human fibroblasts. *J Mol Biol* **201**(2): 379-391.

Gailly, P, Gong, MC, Somlyo, AV, Somlyo, AP (1997) Possible role of atypical protein kinase C activated by arachidonic acid in Ca2+ sensitization of rabbit smooth muscle. *J Physiol* **500 ( Pt 1):** 95-109.

Gantz, I, Muraoka, A, Yang, YK, Samuelson, LC, Zimmerman, EM, Cook, H, Yamada, T (1997) Cloning and chromosomal localization of a gene (GPR18) encoding a novel seven transmembrane receptor highly expressed in spleen and testis. *Genomics* **42**(3): 462-466.

Gao, Z, Chen, T, Weber, MJ, Linden, J (1999) A2B adenosine and P2Y2 receptors stimulate mitogen-activated protein kinase in human embryonic kidney-293 cells. cross-talk between cyclic AMP and protein kinase c pathways. *The Journal of biological chemistry* **274**(9): 5972-5980.

Gaoni Y, MR (1964) Isolation, structure, and partial synthesis of an active constituent of hashish. *J Am Chem Soc.*

Gary-Bobo, M, Elachouri, G, Gallas, JF, Janiak, P, Marini, P, Ravinet-Trillou, C, Chabbert, M, Cruccioli, N, Pfersdorff, C, Roque, C, Arnone, M, Croci, T, Soubrie, P, Oury-Donat, F, Maffrand, JP, Scatton, B, Lacheretz, F, Le Fur, G, Herbert, JM, Bensaid, M (2007) Rimonabant reduces obesity-associated hepatic steatosis and features of metabolic syndrome in obese Zucker fa/fa rats. *Hepatology* **46**(1): 122-129.

Gebremedhin, D, Lange, AR, Campbell, WB, Hillard, CJ, Harder, DR (1999) Cannabinoid CB1 receptor of cat cerebral arterial muscle functions to inhibit L-type Ca2+ channel current. *Am J Physiol* **276**(6 Pt 2): H2085-2093.

Gendron, L, Perron, A, Payet, MD, Gallo-Payet, N, Sarret, P, Beaudet, A (2004) Low-affinity neurotensin receptor (NTS2) signaling: internalization-dependent activation of extracellular signal-regulated kinases 1/2. *Mol Pharmacol* **66**(6): 1421-1430.

Gerald, C, Walker, MW, Criscione, L, Gustafson, EL, Batzl-Hartmann, C, Smith, KE, Vaysse, P, Durkin, MM, Laz, TM, Linemeyer, DL, Schaffhauser, AO, Whitebread, S, Hofbauer, KG, Taber, RI, Branchek, TA, Weinshank, RL (1996) A receptor subtype involved in neuropeptide-Y-induced food intake. *Nature* **382**(6587): 168-171.

Giannini, G, Conti, A, Mammarella, S, Scrobogna, M, Sorrentino, V (1995) The ryanodine receptor/calcium channel genes are widely and differentially expressed in murine brain and peripheral tissues. *J Cell Biol* **128**(5): 893-904.

Gillis, JM (1977) [Excitation-contraction coupling in skeletal and cardiac muscle fibers]. *J Physiol (Paris)* **73**(6): 863-876.

Glund, S, Deshmukh, A, Long, YC, Moller, T, Koistinen, HA, Caidahl, K, Zierath, JR, Krook, A (2007) Interleukin-6 directly increases glucose metabolism in resting human skeletal muscle. *Diabetes* **56**(6): 1630-1637.

Gnocchi, VF, White, RB, Ono, Y, Ellis, JA, Zammit, PS (2009) Further characterisation of the molecular signature of quiescent and activated mouse muscle satellite cells. *PLoS One* **4**(4): e5205.

Godlewski, G, Offertaler, L, Wagner, JA, Kunos, G (2009) Receptors for acylethanolamides-GPR55 and GPR119. *Prostaglandins Other Lipid Mediat* **89**(3-4): 105-111.

Goldfarb, AH, Jamurtas, AZ (1997) Beta-endorphin response to exercise. An update. *Sports Med* **24**(1): 8-16.

Gomez-Ambrosi, J, Catalan, V, Diez-Caballero, A, Martinez-Cruz, LA, Gil, MJ, Garcia-Foncillas, J, Cienfuegos, JA, Salvador, J, Mato, JM, Fruhbeck, G (2004) Gene expression profile of omental adipose tissue in human obesity. *Faseb J* **18**(1): 215-217.

Gonsiorek, W, Lunn, C, Fan, X, Narula, S, Lundell, D, Hipkin, RW (2000) Endocannabinoid 2-arachidonyl glycerol is a full agonist through human type 2 cannabinoid receptor: antagonism by anandamide. *Mol Pharmacol* **57**(5): 1045-1050.

Grant, MB, Tarnuzzer, RW, Caballero, S, Ozeck, MJ, Davis, MI, Spoerri, PE, Feoktistov, I, Biaggioni, I, Shryock, JC, Belardinelli, L (1999) Adenosine receptor activation induces vascular endothelial growth factor in human retinal endothelial cells. *Circ Res* **85**(8): 699-706.

Greco, JA, 3rd, Pollins, AC, Boone, BE, Levy, SE, Nanney, LB (2010) A microarray analysis of temporal gene expression profiles in thermally injured human skin. *Burns* **36**(2): 192-204.

Greenhaff, RMMGPL (1997) *Biochemistry of Exercise and Training.*

Griffin, G, Tao, Q, Abood, ME (2000) Cloning and pharmacological characterization of the rat CB(2) cannabinoid receptor. *J Pharmacol Exp Ther* **292**(3): 886-894.

Gruzman, A, Babai, G, Sasson, S (2009) Adenosine Monophosphate-Activated Protein Kinase (AMPK) as a New Target for Antidiabetic Drugs: A Review on Metabolic, Pharmacological and Chemical Considerations. *Rev Diabet Stud* **6**(1): 13-36.

Grynkiewicz, G, Poenie, M, Tsien, RY (1985) A new generation of Ca2+ indicators with greatly improved fluorescence properties. *The Journal of biological chemistry* **260**(6): 3440-3450.

Hajduch, E, Rencurel, F, Balendran, A, Batty, IH, Downes, CP, Hundal, HS (1999) Serotonin (5-Hydroxytryptamine), a novel regulator of glucose transport in rat skeletal muscle. *The Journal of biological chemistry* **274**(19): 13563-13568.

Ham, M, Mizumori, M, Watanabe, C, Wang, JH, Inoue, T, Nakano, T, Guth, PH, Engel, E, Kaunitz, JD, Akiba, Y (2010) Endogenous luminal surface adenosine signaling regulates duodenal bicarbonate secretion in rats. *J Pharmacol Exp Ther* **335**(3): 607-613.

Hamalainen, N, Pette, D (1995) Patterns of myosin isoforms in mammalian skeletal muscle fibres. *Microsc Res Tech* **30**(5): 381-389.

Hannon, K (2010) Peripheral endocannabinoids regulate skeletal muscle development and maintenance. *European Journal Translational Myology.*

Hansen, LH, Abrahamsen, N, Nishimura, E (1995) Glucagon receptor mRNA distribution in rat tissues. *Peptides* **16**(6): 1163-1166.

Hansen, LH, Gromada, J, Bouchelouche, P, Whitmore, T, Jelinek, L, Kindsvogel, W, Nishimura, E (1998) Glucagon-mediated Ca2+ signaling in BHK cells expressing cloned human glucagon receptors. *Am J Physiol* **274**(6 Pt 1): C1552-1562.

Hardie, DG (2004) The AMP-activated protein kinase pathway--new players upstream and downstream. *J Cell Sci* **117**(Pt 23): 5479-5487.

Hardie, DG, Carling, D (1997a) The AMP-activated protein kinase--fuel gauge of the mammalian cell? *Eur J Biochem* **246**(2): 259-273.

Hardie, DG, Corton, J, Ching, YP, Davies, SP, Hawley, S (1997b) Regulation of lipid

metabolism by the AMP-activated protein kinase. *Biochem Soc Trans* **25**(4): 1229-1231.

Harfstrand, A, Fredholm, B, Fuxe, K (1987) Inhibitory effects of neuropeptide Y on cyclic AMP accumulation in slices of the nucleus tractus solitarius region of the rat. *Neurosci Lett* **76**(2): 185-190.

Hashimoto, T, Kuriyama, K (1997) In vivo evidence that GABA(B) receptors are negatively coupled to adenylate cyclase in rat striatum. *J Neurochem* **69**(1): 365-370.

Hashimotodani, Y, Ohno-Shosaku, T, Kano, M (2007) Endocannabinoids and synaptic function in the CNS. *Neuroscientist* **13**(2): 127-137.

Haviland, DL, McCoy, RL, Whitehead, WT, Akama, H, Molmenti, EP, Brown, A, Haviland, JC, Parks, WC, Perlmutter, DH, Wetsel, RA (1995) Cellular expression of the C5a anaphylatoxin receptor (C5aR): demonstration of C5aR on nonmyeloid cells of the liver and lung. *J Immunol* **154**(4): 1861-1869.

Hayes, C, Kriska, A (2008) Role of physical activity in diabetes management and prevention. *J Am Diet Assoc* **108**(4 Suppl 1): S19-23.

Haynes, JM, Alexander, SP, Hill, SJ (1998) A1 and A2 adenosine receptor modulation of contractility in the cauda epididymis of the guinea-pig. *Br J Pharmacol* **125**(3): 570-576.

He, J, Watkins, S, Kelley, DE (2001) Skeletal muscle lipid content and oxidative enzyme activity in relation to muscle fiber type in type 2 diabetes and obesity. *Diabetes* **50**(4): 817-823.

Hechler, B, Nonne, C, Roh, EJ, Cattaneo, M, Cazenave, JP, Lanza, F, Jacobson, KA, Gachet, C (2006) MRS2500 [2-iodo-N6-methyl-(N)-methanocarba-2'-deoxyadenosine-3',5'-bisphosphate], a potent, selective, and stable antagonist of the platelet P2Y1 receptor with strong antithrombotic activity in mice. *J Pharmacol Exp Ther* **316**(2): 556-563.

Henriksen, EJ, Bourey, RE, Rodnick, KJ, Koranyi, L, Permutt, MA, Holloszy, JO (1990) Glucose transporter protein content and glucose transport capacity in rat skeletal muscles. *Am J Physiol* **259**(4 Pt 1): E593-598.

Henriksen, EJ, Jacob, S, Fogt, DL, Dietze, GJ (1998) Effect of chronic bradykinin administration on insulin action in an animal model of insulin resistance. *Am J Physiol* **275**(1 Pt 2): R40-45.

Henry, RR, Abrams, L, Nikoulina, S, Ciaraldi, TP (1995) Insulin action and glucose metabolism in nondiabetic control and NIDDM subjects. Comparison using human skeletal muscle cell cultures. *Diabetes* **44**(8): 936-946.

Herlitze, S, Garcia, DE, Mackie, K, Hille, B, Scheuer, T, Catterall, WA (1996) Modulation of Ca2+ channels by G-protein beta gamma subunits. *Nature* **380**(6571): 258-262.

Herman, RK, Kari, CK (1985) Muscle-specific expression of a gene affecting acetylcholinesterase in the nematode caenorhabditis elegans. *Cell* **40**(3): 509-514.

Herve, D, Levi-Strauss, M, Marey-Semper, I, Verney, C, Tassin, JP, Glowinski, J, Girault, JA (1993) G(olf) and Gs in rat basal ganglia: possible involvement of G(olf) in the coupling of dopamine D1 receptor with adenylyl cyclase. *J Neurosci* **13**(5): 2237-2248.

Heuckeroth, RO, Birkenmeier, EH, Levin, MS, Gordon, JI (1987) Analysis of the tissue-specific expression, developmental regulation, and linkage relationships of a rodent gene encoding heart fatty acid binding protein. *The Journal of biological chemistry* **262**(20): 9709-9717.

Hildebrandt, AL, Kelly-Sullivan, DM, Black, SC (2003) Antiobesity effects of chronic cannabinoid CB1 receptor antagonist treatment in diet-induced obese mice. *Eur J Pharmacol* **462**(1-3): 125-132.

Hillard, CJ, Manna, S, Greenberg, MJ, DiCamelli, R, Ross, RA, Stevenson, LA, Murphy, V, Pertwee, RG, Campbell, WB (1999) Synthesis and characterization of potent and selective agonists of the neuronal cannabinoid receptor (CB1). *J Pharmacol Exp Ther* **289**(3): 1427-1433.

Hinkle, RT, Dolan, E, Cody, DB, Bauer, MB, Isfort, RJ (2005) Phosphodiesterase 4 inhibition reduces skeletal muscle atrophy. *Muscle Nerve* **32**(6): 775-781.

Hinkle, RT, Hodge, KM, Cody, DB, Sheldon, RJ, Kobilka, BK, Isfort, RJ (2002) Skeletal muscle hypertrophy and anti-atrophy effects of clenbuterol are mediated by the beta2-adrenergic receptor. *Muscle Nerve* **25**(5): 729-734.

Hoffman, PN, Cleveland, DW, Griffin, JW, Landes, PW, Cowan, NJ, Price, DL (1987) Neurofilament gene expression: a major determinant of axonal caliber. *Proceedings of the National Academy of Sciences of the United States of America* **84**(10): 3472-3476.

Hoffmann, R, Wilkinson, IR, McCallum, JF, Engels, P, Houslay, MD (1998) cAMP-specific phosphodiesterase HSPDE4D3 mutants which mimic activation and changes in rolipram inhibition triggered by protein kinase A phosphorylation of Ser-54: generation of a molecular model. *Biochem J* **333 ( Pt 1)**: 139-149.

Holmes, BF, Kurth-Kraczek, EJ, Winder, WW (1999) Chronic activation of 5'-AMP-activated protein kinase increases GLUT-4, hexokinase, and glycogen in muscle. *J Appl Physiol* **87**(5): 1990-1995.

Holt, KH, Kasson, BG, Pessin, JE (1996) Insulin stimulation of a MEK-dependent but ERK-independent SOS protein kinase. *Mol Cell Biol* **16**(2): 577-583.

Homma, Y, Takenawa, T, Emori, Y, Sorimachi, H, Suzuki, K (1989) Tissue- and cell type-specific expression of mRNAs for four types of inositol phospholipid-specific phospholipase C. *Biochem Biophys Res Commun* **164**(1): 406-412.

Honda, Z, Takano, T, Gotoh, Y, Nishida, E, Ito, K, Shimizu, T (1994) Transfected platelet-activating factor receptor activates mitogen-activated protein (MAP) kinase and MAP kinase kinase in Chinese hamster ovary cells. *The Journal of biological chemistry* **269**(3): 2307-2315.

Hoover, F, Mathiesen, I, Skalhegg, BS, Lomo, T, Tasken, K (2001) Differential expression and regulation of the PKA signalling pathway in fast and slow skeletal muscle. *Anat Embryol (Berl)* **203**(3): 193-201.

Horovitz-Fried, M, Cooper, DR, Patel, NA, Cipok, M, Brand, C, Bak, A, Inbar, A, Jacob, AI, Sampson, SR (2006) Insulin rapidly upregulates protein kinase Cdelta gene expression in skeletal muscle. *Cell Signal* **18**(2): 183-193.

Houslay, MD, Adams, DR (2003) PDE4 cAMP phosphodiesterases: modular enzymes that orchestrate signalling cross-talk, desensitization and compartmentalization. *Biochem J* **370**(Pt 1): 1-18.

Howlett, AC, Barth, F, Bonner, TI, Cabral, G, Casellas, P, Devane, WA, Felder, CC, Herkenham, M, Mackie, K, Martin, BR, Mechoulam, R, Pertwee, RG (2002) International Union of Pharmacology. XXVII. Classification of cannabinoid receptors. *Pharmacol Rev* **54**(2): 161-202.

Hsieh, GC, Pai, M, Chandran, P, Hooker, BA, Zhu, CZ, Salyers, AK, Wensink, EJ, Zhan, C, Carroll, WA, Dart, MJ, Yao, BB, Honore, P, Meyer, MD (2011) Central and peripheral sites of action for CB receptor mediated analgesic activity in chronic inflammatory and neuropathic pain models in rats. *Br J Pharmacol* **162**(2): 428-440.

Huang, YH, Weng, XH, Zhou, ZQ (1998) [Extracellular ATP: effects, sources and fate]. *Sheng Li Ke Xue Jin Zhan* **29**(2): 115-119.

Hubbard, KB, Hepler, JR (2006) Cell signalling diversity of the Gqalpha family of heterotrimeric G proteins. *Cell Signal* **18**(2): 135-150.

Hussain, T, Mustafa, SJ (1995) Binding of A1 adenosine receptor ligand [3H]8-cyclopentyl-1,3-dipropylxanthine in coronary smooth muscle. *Circ Res* **77**(1): 194-198.

Hutchinson, DS, Bengtsson, T (2006) AMP-activated protein kinase activation by adrenoceptors in L6 skeletal muscle cells: mediation by alpha1-adrenoceptors causing glucose uptake. *Diabetes* **55**(3): 682-690.

Ihlemann, J, Galbo, H, Ploug, T (1999) Calphostin C is an inhibitor of contraction, but not insulin-stimulated glucose transport, in skeletal muscle. *Acta Physiol Scand* **167**(1): 69-75.

Ikeda, SR, Dunlap, K (1999) Voltage-dependent modulation of N-type calcium channels: role of G protein subunits. *Adv Second Messenger Phosphoprotein Res* **33**: 131-151.

Ikemoto, T, Komazaki, S, Takeshima, H, Nishi, M, Noda, T, Iino, M, Endo, M (1997) Functional and morphological features of skeletal muscle from mutant mice lacking both type 1 and type 3 ryanodine receptors. *J Physiol* **501 ( Pt 2)**: 305-312.

Imaizumi-Scherrer, T, Faust, DM, Benichou, JC, Hellio, R, Weiss, MC (1996) Accumulation in fetal muscle and localization to the neuromuscular junction of cAMP-dependent protein kinase A regulatory and catalytic subunits RI alpha and C alpha. *J Cell Biol* **134**(5): 1241-1254.

Ingi, T, Krumins, AM, Chidiac, P, Brothers, GM, Chung, S, Snow, BE, Barnes, CA, Lanahan, AA, Siderovski, DP, Ross, EM, Gilman, AG, Worley, PF (1998) Dynamic regulation of RGS2 suggests a novel mechanism in G-protein signaling and neuronal plasticity. *J Neurosci* **18**(18): 7178-7188.

Ishii, I, Contos, JJ, Fukushima, N, Chun, J (2000) Functional comparisons of the lysophosphatidic acid receptors, LP(A1)/VZG-1/EDG-2, LP(A2)/EDG-4, and LP(A3)/EDG-7 in neuronal cell lines using a retrovirus expression system. *Mol Pharmacol* **58**(5): 895-902.

Ishizaki, T, Maekawa, M, Fujisawa, K, Okawa, K, Iwamatsu, A, Fujita, A, Watanabe, N, Saito, Y, Kakizuka, A, Morii, N, Narumiya, S (1996) The small GTP-binding protein Rho binds to and activates a 160 kDa Ser/Thr protein kinase homologous to myotonic dystrophy kinase. *EMBO J* **15**(8): 1885-1893.

Izumi, T, Shimizu, T (1995) Platelet-activating factor receptor: gene expression and signal transduction. *Biochim Biophys Acta* **1259**(3): 317-333.

Izzo, AA, Mascolo, N, Pinto, L, Capasso, R, Capasso, F (1999) The role of cannabinoid receptors in intestinal motility, defaecation and diarrhoea in rats. *Eur J Pharmacol* **384**(1): 37-42.

Izzo, AA, Sharkey, KA (2010) Cannabinoids and the gut: new developments and emerging concepts. *Pharmacology & therapeutics* **126**(1): 21-38.

Jacoby, E, Bouhelal, R, Gerspacher, M, Seuwen, K (2006) The 7 TM G-protein-coupled receptor target family. *ChemMedChem* **1**(8): 761-782.

Jager, S, Handschin, C, St-Pierre, J, Spiegelman, BM (2007) AMP-activated protein kinase (AMPK) action in skeletal muscle via direct phosphorylation of PGC-1alpha. *Proceedings of the National Academy of Sciences of the United States of America* **104**(29): 12017-12022.

James, DE, Jenkins, AB, Kraegen, EW (1985) Heterogeneity of insulin action in individual muscles in vivo: euglycemic clamp studies in rats. *Am J Physiol* **248**(5 Pt 1): E567-574.

James, DE, Strube, M, Mueckler, M (1989) Molecular cloning and characterization of an insulin-regulatable glucose transporter. *Nature* **338**(6210): 83-87.

James, G, Butt, AM (2001) P2X and P2Y purinoreceptors mediate ATP-evoked calcium signalling in optic nerve glia in situ. *Cell Calcium* **30**(4): 251-259.

James, PT (2004) Obesity: the worldwide epidemic. *Clin Dermatol* **22**(4): 276-280.

Janot, M, Audfray, A, Loriol, C, Germot, A, Maftah, A, Dupuy, F (2009) Glycogenome expression dynamics during mouse C2C12 myoblast differentiation suggests a sequential reorganization of membrane glycoconjugates. *BMC Genomics* **10**: 483.

Jasper, JR, Lesnick, JD, Chang, LK, Yamanishi, SS, Chang, TK, Hsu, SA, Daunt, DA, Bonhaus, DW, Eglen, RM (1998) Ligand efficacy and potency at recombinant alpha2 adrenergic receptors: agonist-mediated [35S]GTPgammaS binding. *Biochemical*

*pharmacology* **55**(7): 1035-1043.

Jessen, N, Goodyear, LJ (2005) Contraction signaling to glucose transport in skeletal muscle. *J Appl Physiol* **99**(1): 330-337.

Jessen, N, Pold, R, Buhl, ES, Jensen, LS, Schmitz, O, Lund, S (2003) Effects of AICAR and exercise on insulin-stimulated glucose uptake, signaling, and GLUT-4 content in rat muscles. *J Appl Physiol* **94**(4): 1373-1379.

Jeukendrup, AE (2002) Regulation of fat metabolism in skeletal muscle. *Ann N Y Acad Sci* **967**: 217-235.

Jiang, G, Zhang, BB (2003a) Glucagon and regulation of glucose metabolism. *Am J Physiol Endocrinol Metab* **284**(4): E671-678.

Jiang, LI, Collins, J, Davis, R, Lin, KM, DeCamp, D, Roach, T, Hsueh, R, Rebres, RA, Ross, EM, Taussig, R, Fraser, I, Sternweis, PC (2007) Use of a cAMP BRET sensor to characterize a novel regulation of cAMP by the sphingosine 1-phosphate/G13 pathway. *The Journal of biological chemistry* **282**(14): 10576-10584.

Jiang, Y, Cypess, AM, Muse, ED, Wu, CR, Unson, CG, Merrifield, RB, Sakmar, TP (2001) Glucagon receptor activates extracellular signal-regulated protein kinase 1/2 via cAMP-dependent protein kinase. *Proceedings of the National Academy of Sciences of the United States of America* **98**(18): 10102-10107.

Jiang, ZY, Zhou, QL, Coleman, KA, Chouinard, M, Boese, Q, Czech, MP (2003b) Insulin signaling through Akt/protein kinase B analyzed by small interfering RNA-mediated gene silencing. *Proceedings of the National Academy of Sciences of the United States of America* **100**(13): 7569-7574.

Jin, W, Lee, NM, Loh, HH, Thayer, SA (1992) Dual excitatory and inhibitory effects of opioids on intracellular calcium in neuroblastoma x glioma hybrid NG108-15 cells. *Mol Pharmacol* **42**(6): 1083-1089.

Jin, X, Shepherd, RK, Duling, BR, Linden, J (1997) Inosine binds to A3 adenosine receptors and stimulates mast cell degranulation. *J Clin Invest* **100**(11): 2849-2857.

Jones, NC, Fedorov, YV, Rosenthal, RS, Olwin, BB (2001) ERK1/2 is required for myoblast proliferation but is dispensable for muscle gene expression and cell fusion. *J Cell Physiol* **186**(1): 104-115.

Ju, JS, Gitcho, MA, Casmaer, CA, Patil, PB, Han, DG, Spencer, SA, Fisher, JS (2007) Potentiation of insulin-stimulated glucose transport by the AMP-activated protein kinase. *Am J Physiol Cell Physiol* **292**(1): C564-572.

Juan-Pico, P, Fuentes, E, Bermudez-Silva, FJ, Javier Diaz-Molina, F, Ripoll, C, Rodriguez de Fonseca, F, Nadal, A (2006) Cannabinoid receptors regulate Ca(2+) signals and insulin secretion in pancreatic beta-cell. *Cell Calcium* **39**(2): 155-162.

Juzans, P, Comella, JX, Molgo, J, Faille, L, Angaut-Petit, D (1996) Nerve terminal sprouting in botulinum type-A treated mouse levator auris longus muscle. *Neuromuscul Disord* **6**(3): 177-185.

Kahn, CR (1978) Insulin resistance, insulin insensitivity, and insulin unresponsiveness: a necessary distinction. *Metabolism: clinical and experimental* **27**(12 Suppl 2): 1893-1902.

Kahn, RA, Gilman, AG (1984) ADP-ribosylation of Gs promotes the dissociation of its alpha and beta subunits. *The Journal of biological chemistry* **259**(10): 6235-6240.

Kami, K, Noguchi, K, Senba, E (1995) Localization of myogenin, c-fos, c-jun, and muscle-specific gene mRNAs in regenerating rat skeletal muscle. *Cell Tissue Res* **280**(1): 11-19.

Kamiguchi, H, Hlavin, ML, Yamasaki, M, Lemmon, V (1998) Adhesion molecules and inherited diseases of the human nervous system. *Annu Rev Neurosci* **21**: 97-125.

Kanzleiter, T, Preston, E, Wilks, D, Ho, B, Benrick, A, Reznick, J, Heilbronn, LK, Turner, N, Cooney, GJ (2010) Overexpression of the orphan receptor Nur77 alters glucose metabolism in rat muscle cells and rat muscle in vivo. *Diabetologia* **53**(6): 1174-1183.

Kapur, A, Zhao, P, Sharir, H, Bai, Y, Caron, MG, Barak, LS, Abood, ME (2009) Atypical responsiveness of the orphan receptor GPR55 to cannabinoid ligands. *The Journal of biological chemistry* **284**(43): 29817-29827.

Karl, MO, Fleischhauer, JC, Stamer, WD, Peterson-Yantorno, K, Mitchell, CH, Stone, RA, Civan, MM (2005) Differential P1-purinergic modulation of human Schlemm's canal inner-wall cells. *Am J Physiol Cell Physiol* **288**(4): C784-794.

Kassis, S, Olasmaa, M, Terenius, L, Fishman, PH (1987) Neuropeptide Y inhibits cardiac adenylate cyclase through a pertussis toxin-sensitive G protein. *The Journal of biological chemistry* **262**(8): 3429-3431.

Katz, M, Amit, I, Yarden, Y (2007) Regulation of MAPKs by growth factors and receptor tyrosine kinases. *Biochim Biophys Acta* **1773**(8): 1161-1176.

Kawasaki, E, Hokari, F, Sasaki, M, Sakai, A, Koshinaka, K, Kawanaka, K (2011) The effects of beta-adrenergic stimulation and exercise on NR4A3 protein expression in rat skeletal muscle. *J Physiol Sci* **61**(1): 1-11.

Kehrl, JH (1998) Heterotrimeric G protein signaling: roles in immune function and fine-tuning by RGS proteins. *Immunity* **8**(1): 1-10.

Kelley, DE (2005) Skeletal muscle fat oxidation: timing and flexibility are everything. *J Clin Invest* **115**(7): 1699-1702.

Kelley, DE, Goodpaster, B, Wing, RR, Simoneau, JA (1999) Skeletal muscle fatty acid metabolism in association with insulin resistance, obesity, and weight loss. *Am J Physiol* **277**(6 Pt 1): E1130-1141.

Kelley, DE, He, J, Menshikova, EV, Ritov, VB (2002) Dysfunction of mitochondria in human skeletal muscle in type 2 diabetes. *Diabetes* **51**(10): 2944-2950.

Kenakin, T (2010) Functional selectivity and biased receptor signaling. *J Pharmacol Exp Ther* **336**(2): 296-302.

Kiec-Wilk, B, Dembinska-Kiec, A, Olszanecka, A, Bodzioch, M, Kawecka-Jaszcz, K (2005) The selected pathophysiological aspects of PPARs activation. *J Physiol Pharmacol* **56**(2): 149-162.

Kiewe, P, Gueller, S, Komor, M, Stroux, A, Thiel, E, Hofmann, WK (2009) Prediction of qualitative outcome of oligonucleotide microarray hybridization by measurement of RNA integrity using the 2100 Bioanalyzer capillary electrophoresis system. *Ann Hematol* **88**(12): 1177-1183.

Kikkawa, H, Kurose, H, Isogaya, M, Sato, Y, Nagao, T (1997) Differential contribution of two serine residues of wild type and constitutively active beta2-adrenoceptors to the interaction with beta2-selective agonists. *Br J Pharmacol* **121**(6): 1059-1064.

Kim, MS, Lee, J, Ha, J, Kim, SS, Kong, Y, Cho, YH, Baik, HH, Kang, I (2002) ATP stimulates glucose transport through activation of P2 purinergic receptors in C(2)C(12) skeletal muscle cells. *Arch Biochem Biophys* **401**(2): 205-214.

Kim, W, Doyle, ME, Liu, Z, Lao, Q, Shin, YK, Carlson, OD, Kim, HS, Thomas, S, Napora, JK, Lee, EK, Moaddel, R, Wang, Y, Maudsley, S, Martin, B, Kulkarni, RN, Egan, JM (2011) Cannabinoids inhibit insulin receptor signaling in pancreatic beta-cells. *Diabetes* **60**(4): 1198-1209.

Klein, TW, Newton, C, Friedman, H (1998) Cannabinoid receptors and immunity. *Immunol Today* **19**(8): 373-381.

Klein, TW, Newton, C, Larsen, K, Lu, L, Perkins, I, Nong, L, Friedman, H (2003) The cannabinoid system and immune modulation. *J Leukoc Biol* **74**(4): 486-496.

Klotz, KN, Hessling, J, Hegler, J, Owman, C, Kull, B, Fredholm, BB, Lohse, MJ (1998) Comparative pharmacology of human adenosine receptor subtypes - characterization of stably transfected receptors in CHO cells. *Naunyn Schmiedebergs Arch Pharmacol* **357**(1): 1-9.

Kobilka, BK (2007) G protein coupled receptor structure and activation. *Biochim Biophys Acta* **1768**(4): 794-807.

Kohno, M, Hasegawa, H, Inoue, A, Muraoka, M, Miyazaki, T, Oka, K, Yasukawa, M (2006) Identification of N-arachidonylglycine as the endogenous ligand for orphan G-protein-coupled receptor GPR18. *Biochem Biophys Res Commun* **347**(3): 827-832.

Kostka, P, Sipos, SN, Kwan, CY, Niles, LP, Daniel, EE (1989) Identification and characterization of presynaptic and postsynaptic beta adrenoreceptors in the longitudinal smooth muscle/myenteric plexus of dog ileum. *J Pharmacol Exp Ther* **251**(1): 305-310.

Kotokorpi, P, Ellis, E, Parini, P, Nilsson, LM, Strom, S, Steffensen, KR, Gustafsson, JA, Mode, A (2007) Physiological differences between human and rat primary hepatocytes in response to liver X receptor activation by 3-[3-[N-(2-chloro-3-trifluoromethylbenzyl)-(2,2-diphenylethyl)amino]propyloxy]phe nylacetic acid

hydrochloride (GW3965). *Mol Pharmacol* **72**(4): 947-955.

Kriketos, AD, Pan, DA, Lillioja, S, Cooney, GJ, Baur, LA, Milner, MR, Sutton, JR, Jenkins, AB, Bogardus, C, Storlien, LH (1996) Interrelationships between muscle morphology, insulin action, and adiposity. *Am J Physiol* **270**(6 Pt 2): R1332-1339.

Kristiansen, K (2004) Molecular mechanisms of ligand binding, signaling, and regulation within the superfamily of G-protein-coupled receptors: molecular modeling and mutagenesis approaches to receptor structure and function. *Pharmacology & therapeutics* **103**(1): 21-80.

Kuang, W, Xu, H, Vilquin, JT, Engvall, E (1999) Activation of the lama2 gene in muscle regeneration: abortive regeneration in laminin alpha2-deficiency. *Lab Invest* **79**(12): 1601-1613.

Kudla, AJ, Jones, NC, Rosenthal, RS, Arthur, K, Clase, KL, Olwin, BB (1998) The FGF receptor-1 tyrosine kinase domain regulates myogenesis but is not sufficient to stimulate proliferation. *J Cell Biol* **142**(1): 241-250.

Kues, WA, Sakmann, B, Witzemann, V (1995) Differential expression patterns of five acetylcholine receptor subunit genes in rat muscle during development. *Eur J Neurosci* **7**(6): 1376-1385.

Kumar, CC, Madison, V (2005) AKT crystal structure and AKT-specific inhibitors. *Oncogene* **24**(50): 7493-7501.

Kumar, RN, Chambers, WA, Pertwee, RG (2001) Pharmacological actions and therapeutic uses of cannabis and cannabinoids. *Anaesthesia* **56**(11): 1059-1068.

Kume, K, Shimizu, T (1997) Platelet-activating factor (PAF) induces growth stimulation, inhibition, and suppression of oncogenic transformation in NRK cells overexpressing the PAF receptor. *The Journal of biological chemistry* **272**(36): 22898-22904.

Lacy, M, Jones, J, Whittemore, SR, Haviland, DL, Wetsel, RA, Barnum, SR (1995) Expression of the receptors for the C5a anaphylatoxin, interleukin-8 and FMLP by human astrocytes and microglia. *J Neuroimmunol* **61**(1): 71-78.

Lai, HL, Lin, TH, Kao, YY, Lin, WJ, Hwang, MJ, Chern, Y (1999) The N terminus domain of type VI adenylyl cyclase mediates its inhibition by protein kinase C. *Mol Pharmacol* **56**(3): 644-650.

Lamb, GD (2000) Excitation-contraction coupling in skeletal muscle: comparisons with cardiac muscle. *Clin Exp Pharmacol Physiol* **27**(3): 216-224.

Lanner, JT, Georgiou, DK, Joshi, AD, Hamilton, SL (2010) Ryanodine receptors: structure, expression, molecular details, and function in calcium release. *Cold Spring Harb Perspect Biol* **2**(11): a003996.

Larminie, C, Murdock, P, Walhin, JP, Duckworth, M, Blumer, KJ, Scheideler, MA, Garnier, M (2004) Selective expression of regulators of G-protein signaling (RGS) in the human central nervous system. *Brain Res Mol Brain Res* **122**(1): 24-34.

Larsen, PJ, Tang-Christensen, M, Stidsen, CE, Madsen, K, Smith, MS, Cameron, JL (1999) Activation of central neuropeptide Y Y1 receptors potently stimulates food intake in male rhesus monkeys. *J Clin Endocrinol Metab* **84**(10): 3781-3791.

Lauckner, JE, Jensen, JB, Chen, HY, Lu, HC, Hille, B, Mackie, K (2008) GPR55 is a cannabinoid receptor that increases intracellular calcium and inhibits M current. *Proceedings of the National Academy of Sciences of the United States of America* **105**(7): 2699-2704.

Laudanna, C, Campbell, JJ, Butcher, EC (1996) Role of Rho in chemoattractant-activated leukocyte adhesion through integrins. *Science (New York, N.Y* **271**(5251): 981-983.

Lauffer, LM, Iakoubov, R, Brubaker, PL (2009) GPR119 is essential for oleoylethanolamide-induced glucagon-like peptide-1 secretion from the intestinal enteroendocrine L-cell. *Diabetes* **58**(5): 1058-1066.

Law, IK, Xu, A, Lam, KS, Berger, T, Mak, TW, Vanhoutte, PM, Liu, JT, Sweeney, G, Zhou, M, Yang, B, Wang, Y (2010) Lipocalin-2 deficiency attenuates insulin resistance associated with aging and obesity. *Diabetes* **59**(4): 872-882.

Law, PY, Wong, YH, Loh, HH (2000) Molecular mechanisms and regulation of opioid receptor signaling. *Annu Rev Pharmacol Toxicol* **40**: 389-430.

Lazarowski, ER, Boucher, RC, Harden, TK (2003) Mechanisms of release of nucleotides and integration of their action as P2X- and P2Y-receptor activating molecules. *Mol Pharmacol* **64**(4): 785-795.

Le Marchand-Brustel, Y, Gual, P, Gremeaux, T, Gonzalez, T, Barres, R, Tanti, JF (2003) Fatty acid-induced insulin resistance: role of insulin receptor substrate 1 serine phosphorylation in the retroregulation of insulin signalling. *Biochem Soc Trans* **31**(Pt 6): 1152-1156.

Lee, DH, Shi, J, Jeoung, NH, Kim, MS, Zabolotny, JM, Lee, SW, White, MF, Wei, L, Kim, YB (2009) Targeted disruption of ROCK1 causes insulin resistance in vivo. *The Journal of biological chemistry* **284**(18): 11776-11780.

Lee, K, Brown, D, Urena, P, Ardaillou, N, Ardaillou, R, Deeds, J, Segre, GV (1996) Localization of parathyroid hormone/parathyroid hormone-related peptide receptor mRNA in kidney. *Am J Physiol* **270**(1 Pt 2): F186-191.

Lee, WK, Kim, JK, Seo, MS, Cha, JH, Lee, KJ, Rha, HK, Min, DS, Jo, YH, Lee, KH (1999) Molecular cloning and expression analysis of a mouse phospholipase C-delta1. *Biochem Biophys Res Commun* **261**(2): 393-399.

Leeb-Lundberg, LM, Marceau, F, Muller-Esterl, W, Pettibone, DJ, Zuraw, BL (2005) International union of pharmacology. XLV. Classification of the kinin receptor family: from molecular mechanisms to pathophysiological consequences. *Pharmacol Rev* **57**(1): 27-77.

Leick, L, Fentz, J, Bienso, RS, Knudsen, JG, Jeppesen, J, Kiens, B, Wojtaszewski, JF,

Pilegaard, H (2010) PGC-1{alpha} is required for AICAR-induced expression of GLUT4 and mitochondrial proteins in mouse skeletal muscle. *Am J Physiol Endocrinol Metab* **299**(3): E456-465.

Lemberger, L (1980) Potential therapeutic usefulness of marijuana. *Annu Rev Pharmacol Toxicol* **20**: 151-172.

Lemberger, T, Braissant, O, Juge-Aubry, C, Keller, H, Saladin, R, Staels, B, Auwerx, J, Burger, AG, Meier, CA, Wahli, W (1996) PPAR tissue distribution and interactions with other hormone-signaling pathways. *Ann N Y Acad Sci* **804**: 231-251.

Lessard, SJ, Rivas, DA, Chen, ZP, van Denderen, BJ, Watt, MJ, Koch, LG, Britton, SL, Kemp, BE, Hawley, JA (2009) Impaired skeletal muscle beta-adrenergic activation and lipolysis are associated with whole-body insulin resistance in rats bred for low intrinsic exercise capacity. *Endocrinology* **150**(11): 4883-4891.

Leung, DW, Tompkins, C, Brewer, J, Ball, A, Coon, M, Morris, V, Waggoner, D, Singer, JW (2004) Phospholipase C delta-4 overexpression upregulates ErbB1/2 expression, Erk signaling pathway, and proliferation in MCF-7 cells. *Mol Cancer* **3**: 15.

Lewis, GD, Semigran, MJ (2006) The emerging role for type 5 phosphodiesterase inhibition in heart failure. *Curr Heart Fail Rep* **3**(3): 123-128.

Lima, JJ, Feng, H, Duckworth, L, Wang, J, Sylvester, JE, Kissoon, N, Garg, H (2007) Association analyses of adrenergic receptor polymorphisms with obesity and metabolic alterations. *Metabolism: clinical and experimental* **56**(6): 757-765.

Lin, CH, Hudson, AJ, Strickland, KP (1976) Adenyl cyclase and cyclic nucleotide phosphodiesterase activities in murine muscular dystrophy. *Enzyme* **21**(1): 85-95.

Lin, S, Khanolkar, AD, Fan, P, Goutopoulos, A, Qin, C, Papahadjis, D, Makriyannis, A (1998) Novel analogues of arachidonylethanolamide (anandamide): affinities for the CB1 and CB2 cannabinoid receptors and metabolic stability. *J Med Chem* **41**(27): 5353-5361.

Lindborg, KA, Teachey, MK, Jacob, S, Henriksen, EJ (2011) Effects of in vitro antagonism of endocannabinoid-1 receptors on the glucose transport system in normal and insulin-resistant rat skeletal muscle. *Diabetes Obes Metab* **12**(8): 722-730.

Lipina, C, Stretton, C, Hastings, S, Hundal, JS, Mackie, K, Irving, AJ, Hundal, HS (2010) Regulation of MAP kinase-directed mitogenic and protein kinase B-mediated signaling by cannabinoid receptor type 1 in skeletal muscle cells. *Diabetes* **59**(2): 375-385.

Liu, ML, Olson, AL, Moye-Rowley, WS, Buse, JB, Bell, GI, Pessin, JE (1992) Expression and regulation of the human GLUT4/muscle-fat facilitative glucose transporter gene in transgenic mice. *The Journal of biological chemistry* **267**(17): 11673-11676.

Liu, QR, Pan, CH, Hishimoto, A, Li, CY, Xi, ZX, Llorente-Berzal, A, Viveros, MP, Ishiguro, H, Arinami, T, Onaivi, ES, Uhl, GR (2009) Species differences in cannabinoid receptor 2 (CNR2 gene): identification of novel human and rodent CB2 isoforms,

differential tissue expression and regulation by cannabinoid receptor ligands. *Genes Brain Behav* **8**(5): 519-530.

Liu, YL, Connoley, IP, Wilson, CA, Stock, MJ (2005) Effects of the cannabinoid CB1 receptor antagonist SR141716 on oxygen consumption and soleus muscle glucose uptake in Lep(ob)/Lep(ob) mice. *Int J Obes (Lond)* **29**(2): 183-187.

Lo Verme, J, Fu, J, Astarita, G, La Rana, G, Russo, R, Calignano, A, Piomelli, D (2005) The nuclear receptor peroxisome proliferator-activated receptor-alpha mediates the anti-inflammatory actions of palmitoylethanolamide. *Mol Pharmacol* **67**(1): 15-19.

Lopez-Ilasaca, M (1998) Signaling from G-protein-coupled receptors to mitogen-activated protein (MAP)-kinase cascades. *Biochemical pharmacology* **56**(3): 269-277.

Lorenz, W, Lomasney, JW, Collins, S, Regan, JW, Caron, MG, Lefkowitz, RJ (1990) Expression of three alpha 2-adrenergic receptor subtypes in rat tissues: implications for alpha 2 receptor classification. *Mol Pharmacol* **38**(5): 599-603.

Luster, AD (1998) Chemokines--chemotactic cytokines that mediate inflammation. *N Engl J Med* **338**(7): 436-445.

Lustig, KD, Conklin, BR, Herzmark, P, Taussig, R, Bourne, HR (1993) Type II adenylylcyclase integrates coincident signals from Gs, Gi, and Gq. *The Journal of biological chemistry* **268**(19): 13900-13905.

Lynge, J, Schulte, G, Nordsborg, N, Fredholm, BB, Hellsten, Y (2003) Adenosine A 2B receptors modulate cAMP levels and induce CREB but not ERK1/2 and p38 phosphorylation in rat skeletal muscle cells. *Biochem Biophys Res Commun* **307**(1): 180-187.

Mackie, K, Devane, WA, Hille, B (1993) Anandamide, an endogenous cannabinoid, inhibits calcium currents as a partial agonist in N18 neuroblastoma cells. *Mol Pharmacol* **44**(3): 498-503.

Mackie, K, Lai, Y, Westenbroek, R, Mitchell, R (1995) Cannabinoids activate an inwardly rectifying potassium conductance and inhibit Q-type calcium currents in AtT20 cells transfected with rat brain cannabinoid receptor. *J Neurosci* **15**(10): 6552-6561.

Mackie, K, Stella, N (2006) Cannabinoid receptors and endocannabinoids: evidence for new players. *AAPS J* **8**(2): E298-306.

MacNeil, DJ (2007) NPY Y1 and Y5 receptor selective antagonists as anti-obesity drugs. *Curr Top Med Chem* **7**(17): 1721-1733.

Maejima, T, Ohno-Shosaku, T, Kano, M (2001) Endogenous cannabinoid as a retrograde messenger from depolarized postsynaptic neurons to presynaptic terminals. *Neurosci Res* **40**(3): 205-210.

Mahon, MJ, Bonacci, TM, Divieti, P, Smrcka, AV (2006) A docking site for G protein betagamma subunits on the parathyroid hormone 1 receptor supports signaling through multiple pathways. *Mol Endocrinol* **20**(1): 136-146.

Majewski, N, Nogueira, V, Bhaskar, P, Coy, PE, Skeen, JE, Gottlob, K, Chandel, NS, Thompson, CB, Robey, RB, Hay, N (2004) Hexokinase-mitochondria interaction mediated by Akt is required to inhibit apoptosis in the presence or absence of Bax and Bak. *Mol Cell* **16**(5): 819-830.

Mallat, A, Teixeira-Clerc, F, Deveaux, V, Manin, S, Lotersztajn, S (2011) The endocannabinoid system as a key mediator during liver diseases: new insights and therapeutic openings. *Br J Pharmacol* **163**(7): 1432-1440.

Malosio, ML, Gilardelli, D, Paris, S, Albertinazzi, C, de Curtis, I (1997) Differential expression of distinct members of Rho family GTP-binding proteins during neuronal development: identification of Rac1B, a new neural-specific member of the family. *J Neurosci* **17**(17): 6717-6728.

Manning, BD, Cantley, LC (2007) AKT/PKB signaling: navigating downstream. *Cell* **129**(7): 1261-1274.

Markovic, TP, Jenkins, AB, Campbell, LV, Furler, SM, Kraegen, EW, Chisholm, DJ (1998) The determinants of glycemic responses to diet restriction and weight loss in obesity and NIDDM. *Diabetes Care* **21**(5): 687-694.

Marshall, JM (2000) Adenosine and muscle vasodilatation in acute systemic hypoxia. *Acta Physiol Scand* **168**(4): 561-573.

Martinez, A, Castro, A, Dorronsoro, I, Alonso, M (2002) Glycogen synthase kinase 3 (GSK-3) inhibitors as new promising drugs for diabetes, neurodegeneration, cancer, and inflammation. *Med Res Rev* **22**(4): 373-384.

Masure, S, Haefner, B, Wesselink, JJ, Hoefnagel, E, Mortier, E, Verhasselt, P, Tuytelaars, A, Gordon, R, Richardson, A (1999) Molecular cloning, expression and characterization of the human serine/threonine kinase Akt-3. *Eur J Biochem* **265**(1): 353-360.

Matias, I, Gonthier, MP, Orlando, P, Martiadis, V, De Petrocellis, L, Cervino, C, Petrosino, S, Hoareau, L, Festy, F, Pasquali, R, Roche, R, Maj, M, Pagotto, U, Monteleone, P, Di Marzo, V (2006) Regulation, function, and dysregulation of endocannabinoids in models of adipose and beta-pancreatic cells and in obesity and hyperglycemia. *J Clin Endocrinol Metab* **91**(8): 3171-3180.

Matsuda, LA, Lolait, SJ, Brownstein, MJ, Young, AC, Bonner, TI (1990) Structure of a cannabinoid receptor and functional expression of the cloned cDNA. *Nature* **346**(6284): 561-564.

Matsui, T, Amano, M, Yamamoto, T, Chihara, K, Nakafuku, M, Ito, M, Nakano, T, Okawa, K, Iwamatsu, A, Kaibuchi, K (1996) Rho-associated kinase, a novel serine/threonine kinase, as a putative target for small GTP binding protein Rho. *EMBO J* **15**(9): 2208-2216.

Matsumoto, M, Pocai, A, Rossetti, L, Depinho, RA, Accili, D (2007) Impaired regulation of hepatic glucose production in mice lacking the forkhead transcription factor Foxo1 in liver. *Cell Metab* **6**(3): 208-216.

Maxwell, MA, Cleasby, ME, Harding, A, Stark, A, Cooney, GJ, Muscat, GE (2005) Nur77 regulates lipolysis in skeletal muscle cells. Evidence for cross-talk between the beta-adrenergic and an orphan nuclear hormone receptor pathway. *The Journal of biological chemistry* **280**(13): 12573-12584.

Mayer, P, Hinze, AV, Harst, A, von Kugelgen, I (2011) AB receptors mediate the induction of early genes and inhibition of arterial smooth muscle cell proliferation via Epac. *Cardiovasc Res* **90**(1): 148-156.

Mayo, KE, Miller, LJ, Bataille, D, Dalle, S, Goke, B, Thorens, B, Drucker, DJ (2003) International Union of Pharmacology. XXXV. The glucagon receptor family. *Pharmacol Rev* **55**(1): 167-194.

McAllister, SD, Griffin, G, Satin, LS, Abood, ME (1999) Cannabinoid receptors can activate and inhibit G protein-coupled inwardly rectifying potassium channels in a xenopus oocyte expression system. *J Pharmacol Exp Ther* **291**(2): 618-626.

McHugh, D, Page, J, Dunn, E, Bradshaw, HB (2012) Delta(9) -Tetrahydrocannabinol and N-arachidonyl glycine are full agonists at GPR18 receptors and induce migration in human endometrial HEC-1B cells. *Br J Pharmacol* **165**(8): 2414-2424.

Meacci, E, Cencetti, F, Donati, C, Nuti, F, Farnararo, M, Kohno, T, Igarashi, Y, Bruni, P (2003) Down-regulation of EDG5/S1P2 during myogenic differentiation results in the specific uncoupling of sphingosine 1-phosphate signalling to phospholipase D. *Biochim Biophys Acta* **1633**(3): 133-142.

Mechoulam, R, Ben-Shabat, S, Hanus, L, Ligumsky, M, Kaminski, NE, Schatz, AR, Gopher, A, Almog, S, Martin, BR, Compton, DR, et al. (1995) Identification of an endogenous 2-monoglyceride, present in canine gut, that binds to cannabinoid receptors. *Biochemical pharmacology* **50**(1): 83-90.

Meotti, F, Campos, R, da Silva, K, Paszcuk, A, Costa, R, Calixto, J (2012) Inflammatory muscle pain is dependent on the activation of kinin B(1) and B(2) receptors and intracellular kinase pathways. *Br J Pharmacol* **166**(3): 1127-1139.

Meyer, TN, Schwesinger, C, Sampogna, RV, Vaughn, DA, Stuart, RO, Steer, DL, Bush, KT, Nigam, SK (2006) Rho kinase acts at separate steps in ureteric bud and metanephric mesenchyme morphogenesis during kidney development. *Differentiation* **74**(9-10): 638-647.

Michalik, L, Wahli, W (2006) Involvement of PPAR nuclear receptors in tissue injury and wound repair. *J Clin Invest* **116**(3): 598-606.

Miles, RR, Sluka, JP, Santerre, RF, Hale, LV, Bloem, L, Boguslawski, G, Thirunavukkarasu, K, Hock, JM, Onyia, JE (2000) Dynamic regulation of RGS2 in bone: potential new insights into parathyroid hormone signaling mechanisms. *Endocrinology* **141**(1): 28-36.

Minetti, GC, Feige, JN, Rosenstiel, A, Bombard, F, Meier, V, Werner, A, Bassilana, F, Sailer, AW, Kahle, P, Lambert, C, Glass, DJ, Fornaro, M Galphai2 signaling promotes skeletal muscle hypertrophy, myoblast differentiation, and muscle regeneration. *Sci*

*Signal* 4(201): ra80.

Miyake, M, Hayashi, S, Iwasaki, S, Uchida, T, Watanabe, K, Ohwada, S, Aso, H, Yamaguchi, T (2011) TIEG1 negatively controls the myoblast pool indispensable for fusion during myogenic differentiation of C2C12 cells. *J Cell Physiol* **226**(4): 1128-1136.

Mizuno, Y, Isotani, E, Huang, J, Ding, H, Stull, JT, Kamm, KE (2008) Myosin light chain kinase activation and calcium sensitization in smooth muscle in vivo. *Am J Physiol Cell Physiol* **295**(2): C358-364.

Moran, JL, Li, Y, Hill, AA, Mounts, WM, Miller, CP (2002) Gene expression changes during mouse skeletal myoblast differentiation revealed by transcriptional profiling. *Physiol Genomics* **10**(2): 103-111.

Morey, JS, Ryan, JC, Van Dolah, FM (2006) Microarray validation: factors influencing correlation between oligonucleotide microarrays and real-time PCR. *Biol Proced Online* **8**: 175-193.

Morita, N, Namikawa, K, Kiyama, H (1995) Up-regulation of PKA RI alpha subunit mRNA in rat skeletal muscle after nerve injury. *Neuroreport* **6**(7): 1050-1052.

Mosthaf, L, Vogt, B, Haring, HU, Ullrich, A (1991) Altered expression of insulin receptor types A and B in the skeletal muscle of non-insulin-dependent diabetes mellitus patients. *Proceedings of the National Academy of Sciences of the United States of America* **88**(11): 4728-4730.

Munro, S, Thomas, KL, Abu-Shaar, M (1993) Molecular characterization of a peripheral receptor for cannabinoids. *Nature* **365**(6441): 61-65.

Nagase, I, Yoshida, T, Saito, M (2001) Up-regulation of uncoupling proteins by beta-adrenergic stimulation in L6 myotubes. *FEBS letters* **494**(3): 175-180.

Nakaki, T, Nakadate, T, Ishii, K, Kato, R (1981) Postsynaptic alpha-2 adrenergic receptors in isolated rat islets of Langerhans: inhibition of insulin release and cyclic 3':5'-adenosine monophosphate accumulation. *J Pharmacol Exp Ther* **216**(3): 607-612.

Nakamura, M, Sakanaka, C, Aoki, Y, Ogasawara, H, Tsuji, T, Kodama, H, Matsumoto, T, Shimizu, T, Noma, M (1995) Identification of two isoforms of mouse neuropeptide Y-Y1 receptor generated by alternative splicing. Isolation, genomic structure, and functional expression of the receptors. *The Journal of biological chemistry* **270**(50): 30102-30110.

Nakata, M, Yada, T (2008) Cannabinoids inhibit insulin secretion and cytosolic Ca2+ oscillation in islet beta-cells via CB1 receptors. *Regul Pept* **145**(1-3): 49-53.

Nam, DH, Lee, MH, Kim, JE, Song, HK, Kang, YS, Lee, JE, Kim, HW, Cha, JJ, Hyun, YY, Kim, SH, Han, SY, Han, KH, Han, JY, Cha, DR (2012) Blockade of cannabinoid receptor 1 improves insulin resistance, lipid metabolism, and diabetic nephropathy in db/db mice. *Endocrinology* **153**(3): 1387-1396.

Nathan, DM (1993) Long-term complications of diabetes mellitus. *N Engl J Med*

**328**(23): 1676-1685.

Neary, JT, Zimmermann, H (2009) Trophic functions of nucleotides in the central nervous system. *Trends Neurosci* **32**(4): 189-198.

Neer, EJ (1995) Heterotrimeric G proteins: organizers of transmembrane signals. *Cell* **80**(2): 249-257.

Nervi, C, Benedetti, L, Minasi, A, Molinaro, M, Adamo, S (1995) Arginine-vasopressin induces differentiation of skeletal myogenic cells and up-regulation of myogenin and Myf-5. *Cell Growth Differ* **6**(1): 81-89.

Neubig, RR, Gantzos, RD, Thomsen, WJ (1988) Mechanism of agonist and antagonist binding to alpha 2 adrenergic receptors: evidence for a precoupled receptor-guanine nucleotide protein complex. *Biochemistry* **27**(7): 2374-2384.

Nevzorova, J, Evans, BA, Bengtsson, T, Summers, RJ (2006) Multiple signalling pathways involved in beta2-adrenoceptor-mediated glucose uptake in rat skeletal muscle cells. *Br J Pharmacol* **147**(4): 446-454.

Nicholson, GC, Moseley, JM, Sexton, PM, Mendelsohn, FA, Martin, TJ (1986) Abundant calcitonin receptors in isolated rat osteoclasts. Biochemical and autoradiographic characterization. *J Clin Invest* **78**(2): 355-360.

Ning, Y, O'Neill, K, Lan, H, Pang, L, Shan, LX, Hawes, BE, Hedrick, JA (2008) Endogenous and synthetic agonists of GPR119 differ in signalling pathways and their effects on insulin secretion in MIN6c4 insulinoma cells. *Br J Pharmacol* **155**(7): 1056-1065.

Nistala, R, Stump, CS (2006) Skeletal muscle insulin resistance is fundamental to the cardiometabolic syndrome. *J Cardiometab Syndr* **1**(1): 47-52.

Niswender, CM, Conn, PJ (2010) Metabotropic glutamate receptors: physiology, pharmacology, and disease. *Annu Rev Pharmacol Toxicol* **50**: 295-322.

Nogueiras, R, Veyrat-Durebex, C, Suchanek, PM, Klein, M, Tschop, J, Caldwell, C, Woods, SC, Wittmann, G, Watanabe, M, Liposits, Z, Fekete, C, Reizes, O, Rohner-Jeanrenaud, F, Tschop, MH (2008) Peripheral, but not central, CB1 antagonism provides food intake-independent metabolic benefits in diet-induced obese rats. *Diabetes* **57**(11): 2977-2991.

O'Sullivan, SE (2007) Cannabinoids go nuclear: evidence for activation of peroxisome proliferator-activated receptors. *Br J Pharmacol* **152**(5): 576-582.

Ochi, R, Hino, N, Okuyama, H (1986) Beta-adrenergic modulation of the slow gating process of cardiac calcium channels. *Jpn Heart J* **27 Suppl 1**: 51-55.

Odemis, V, Boosmann, K, Dieterlen, MT, Engele, J (2007) The chemokine SDF1 controls multiple steps of myogenesis through atypical PKCzeta. *J Cell Sci* **120**(Pt 22): 4050-4059.

Ogden, CL, Carroll, MD, Curtin, LR, McDowell, MA, Tabak, CJ, Flegal, KM (2006)

Prevalence of overweight and obesity in the United States, 1999-2004. *JAMA* **295**(13): 1549-1555.

Oka, S, Nakajima, K, Yamashita, A, Kishimoto, S, Sugiura, T (2007) Identification of GPR55 as a lysophosphatidylinositol receptor. *Biochem Biophys Res Commun* **362**(4): 928-934.

Oka, S, Toshida, T, Maruyama, K, Nakajima, K, Yamashita, A, Sugiura, T (2009) 2-Arachidonoyl-sn-glycero-3-phosphoinositol: a possible natural ligand for GPR55. *J Biochem* **145**(1): 13-20.

Okada, M, Ishimoto, T, Naito, Y, Hirata, H, Yagisawa, H (2005) Phospholipase Cdelta1 associates with importin beta1 and translocates into the nucleus in a Ca2+-dependent manner. *FEBS letters* **579**(22): 4949-4954.

Oliviero, A, Arevalo-Martin, A, Rotondi, M, Garcia-Ovejero, D, Mordillo-Mateos, L, Lozano-Sicilia, A, Panyavin, I, Chiovato, L, Aguilar, J, Foffani, G, Di Lazzaro, V, Molina-Holgado, E (2011) CB1 receptor antagonism/inverse agonism increases motor system excitability in humans. *Eur Neuropsychopharmacol* **22**(1): 27-35.

Ongini, E, Dionisotti, S, Gessi, S, Irenius, E, Fredholm, BB (1999) Comparison of CGS 15943, ZM 241385 and SCH 58261 as antagonists at human adenosine receptors. *Naunyn Schmiedebergs Arch Pharmacol* **359**(1): 7-10.

Osada, S, Mizuno, K, Saido, TC, Suzuki, K, Kuroki, T, Ohno, S (1992) A new member of the protein kinase C family, nPKC theta, predominantly expressed in skeletal muscle. *Mol Cell Biol* **12**(9): 3930-3938.

Osei-Hyiaman, D, DePetrillo, M, Pacher, P, Liu, J, Radaeva, S, Batkai, S, Harvey-White, J, Mackie, K, Offertaler, L, Wang, L, Kunos, G (2005) Endocannabinoid activation at hepatic CB1 receptors stimulates fatty acid synthesis and contributes to diet-induced obesity. *J Clin Invest* **115**(5): 1298-1305.

Overton, HA, Babbs, AJ, Doel, SM, Fyfe, MC, Gardner, LS, Griffin, G, Jackson, HC, Procter, MJ, Rasamison, CM, Tang-Christensen, M, Widdowson, PS, Williams, GM, Reynet, C (2006) Deorphanization of a G protein-coupled receptor for oleoylethanolamide and its use in the discovery of small-molecule hypophagic agents. *Cell Metab* **3**(3): 167-175.

Overton, HA, Fyfe, MC, Reynet, C (2008) GPR119, a novel G protein-coupled receptor target for the treatment of type 2 diabetes and obesity. *Br J Pharmacol* **153 Suppl 1**: S76-81.

Ozaita, A, Puighermanal, E, Maldonado, R (2007) Regulation of PI3K/Akt/GSK-3 pathway by cannabinoids in the brain. *J Neurochem* **102**(4): 1105-1114.

Pacher, P, Batkai, S, Kunos, G (2006) The endocannabinoid system as an emerging target of pharmacotherapy. *Pharmacol Rev* **58**(3): 389-462.

Pacifici, M, Molinaro, M (1980) Developmental changes in glycosaminoglycans during skeletal muscle cell differentiation in culture. *Exp Cell Res* **126**(1): 143-152.

Pagotto, U, Marsicano, G, Cota, D, Lutz, B, Pasquali, R (2006) The emerging role of the endocannabinoid system in endocrine regulation and energy balance. *Endocr Rev* **27**(1): 73-100.

Pan, DA, Lillioja, S, Kriketos, AD, Milner, MR, Baur, LA, Bogardus, C, Jenkins, AB, Storlien, LH (1997) Skeletal muscle triglyceride levels are inversely related to insulin action. *Diabetes* **46**(6): 983-988.

Pandey, R, Mousawy, K, Nagarkatti, M, Nagarkatti, P (2009) Endocannabinoids and immune regulation. *Pharmacol Res* **60**(2): 85-92.

Park, D, Jhon, DY, Lee, CW, Lee, KH, Rhee, SG (1993) Activation of phospholipase C isozymes by G protein beta gamma subunits. *The Journal of biological chemistry* **268**(7): 4573-4576.

Parmentier, ML, Pin, JP, Bockaert, J, Grau, Y (1996) Cloning and functional expression of a Drosophila metabotropic glutamate receptor expressed in the embryonic CNS. *J Neurosci* **16**(21): 6687-6694.

Pearen, MA, Myers, SA, Raichur, S, Ryall, JG, Lynch, GS, Muscat, GE (2008) The orphan nuclear receptor, NOR-1, a target of beta-adrenergic signaling, regulates gene expression that controls oxidative metabolism in skeletal muscle. *Endocrinology* **149**(6): 2853-2865.

Pearen, MA, Ryall, JG, Maxwell, MA, Ohkura, N, Lynch, GS, Muscat, GE (2006) The orphan nuclear receptor, NOR-1, is a target of beta-adrenergic signaling in skeletal muscle. *Endocrinology* **147**(11): 5217-5227.

Pearson, G, Robinson, F, Beers Gibson, T, Xu, BE, Karandikar, M, Berman, K, Cobb, MH (2001) Mitogen-activated protein (MAP) kinase pathways: regulation and physiological functions. *Endocr Rev* **22**(2): 153-183.

Pedersen, BK (2011) Muscles and their myokines. *J Exp Biol* **214**(Pt 2): 337-346.

Perez-Martin, A, Dumortier, M, Raynaud, E, Brun, JF, Fedou, C, Bringer, J, Mercier, J (2001) Balance of substrate oxidation during submaximal exercise in lean and obese people. *Diabetes Metab* **27**(4 Pt 1): 466-474.

Perez, DM, Karnik, SS (2005) Multiple signaling states of G-protein-coupled receptors. *Pharmacol Rev* **57**(2): 147-161.

Periasamy, M, Strehler, EE, Garfinkel, LI, Gubits, RM, Ruiz-Opazo, N, Nadal-Ginard, B (1984) Fast skeletal muscle myosin light chains 1 and 3 are produced from a single gene by a combined process of differential RNA transcription and splicing. *The Journal of biological chemistry* **259**(21): 13595-13604.

Perio, A, Rinaldi-Carmona, M, Maruani, J, Barth, F, Le Fur, G, Soubrie, P (1996) Central mediation of the cannabinoid cue: activity of a selective CB1 antagonist, SR 141716A. *Behav Pharmacol* **7**(1): 65-71.

Pessin, JE, Saltiel, AR (2000) Signaling pathways in insulin action: molecular targets of insulin resistance. *J Clin Invest* **106**(2): 165-169.

Pette, D, Staron, RS (1997) Mammalian skeletal muscle fiber type transitions. *Int Rev Cytol* **170:** 143-223.

Pi-Sunyer, FX, Aronne, LJ, Heshmati, HM, Devin, J, Rosenstock, J (2006) Effect of rimonabant, a cannabinoid-1 receptor blocker, on weight and cardiometabolic risk factors in overweight or obese patients: RIO-North America: a randomized controlled trial. *JAMA* **295**(7): 761-775.

Pieples, K, Wieczorek, DF (2000) Tropomyosin 3 increases striated muscle isoform diversity. *Biochemistry* **39**(28): 8291-8297.

Pierce, KL, Premont, RT, Lefkowitz, RJ (2002) Seven-transmembrane receptors. *Nat Rev Mol Cell Biol* **3**(9): 639-650.

Pimenta, AS, Gaidhu, MP, Habib, S, So, M, Fediuc, S, Mirpourian, M, Musheev, M, Curi, R, Ceddia, RB (2008) Prolonged exposure to palmitate impairs fatty acid oxidation despite activation of AMP-activated protein kinase in skeletal muscle cells. *J Cell Physiol* **217**(2): 478-485.

Pimienta, G, Pascual, J (2007) Canonical and alternative MAPK signaling. *Cell Cycle* **6**(21): 2628-2632.

Plati, J, Tsomaia, N, Piserchio, A, Mierke, DF (2007) Structural features of parathyroid hormone receptor coupled to Galpha(s)-protein. *Biophys J* **92**(2): 535-540.

Poyner, DR, Sexton, PM, Marshall, I, Smith, DM, Quirion, R, Born, W, Muff, R, Fischer, JA, Foord, SM (2002) International Union of Pharmacology. XXXII. The mammalian calcitonin gene-related peptides, adrenomedullin, amylin, and calcitonin receptors. *Pharmacol Rev* **54**(2): 233-246.

Qiao, J, Mei, FC, Popov, VL, Vergara, LA, Cheng, X (2002) Cell cycle-dependent subcellular localization of exchange factor directly activated by cAMP. *The Journal of biological chemistry* **277**(29): 26581-26586.

Quinn, JM, Morfis, M, Lam, MH, Elliott, J, Kartsogiannis, V, Williams, ED, Gillespie, MT, Martin, TJ, Sexton, PM (1999) Calcitonin receptor antibodies in the identification of osteoclasts. *Bone* **25**(1): 1-8.

Rabito, SF, Minshall, RD, Nakamura, F, Wang, LX (1996) Bradykinin B2 receptors on skeletal muscle are coupled to inositol 1,4,5-trisphosphate formation. *Diabetes* **45 Suppl 1:** S29-33.

Randall, MD, Alexander, SP, Bennett, T, Boyd, EA, Fry, JR, Gardiner, SM, Kemp, PA, McCulloch, AI, Kendall, DA (1996) An endogenous cannabinoid as an endothelium-derived vasorelaxant. *Biochem Biophys Res Commun* **229**(1): 114-120.

Randle, PJ, Garland, PB, Hales, CN, Newsholme, EA (1963) The glucose fatty-acid cycle. Its role in insulin sensitivity and the metabolic disturbances of diabetes mellitus. *Lancet* **1**(7285): 785-789.

Ratajczak, MZ, Majka, M, Kucia, M, Drukala, J, Pietrzkowski, Z, Peiper, S, Janowska-

Wieczorek, A (2003) Expression of functional CXCR4 by muscle satellite cells and secretion of SDF-1 by muscle-derived fibroblasts is associated with the presence of both muscle progenitors in bone marrow and hematopoietic stem/progenitor cells in muscles. *Stem Cells* **21**(3): 363-371.

Ravinet Trillou, C, Delgorge, C, Menet, C, Arnone, M, Soubrie, P (2004) CB1 cannabinoid receptor knockout in mice leads to leanness, resistance to diet-induced obesity and enhanced leptin sensitivity. *Int J Obes Relat Metab Disord* **28**(4): 640-648.

Raymond, F, Metairon, S, Kussmann, M, Colomer, J, Nascimento, A, Mormeneo, E, Garcia-Martinez, C, Gomez-Foix, AM (2010) Comparative gene expression profiling between human cultured myotubes and skeletal muscle tissue. *BMC Genomics* **11:** 125.

Rayner, DV, Thomas, ME, Trayhurn, P (1994) Glucose transporters (GLUTs 1-4) and their mRNAs in regions of the rat brain: insulin-sensitive transporter expression in the cerebellum. *Can J Physiol Pharmacol* **72**(5): 476-479.

Reaven, GM (2005) The insulin resistance syndrome: definition and dietary approaches to treatment. *Annu Rev Nutr* **25:** 391-406.

Rebola, N, Sebastiao, AM, de Mendonca, A, Oliveira, CR, Ribeiro, JA, Cunha, RA (2003) Enhanced adenosine A2A receptor facilitation of synaptic transmission in the hippocampus of aged rats. *J Neurophysiol* **90**(2): 1295-1303.

Reggio, PH (2003) Pharmacophores for ligand recognition and activation/inactivation of the cannabinoid receptors. *Curr Pharm Des* **9**(20): 1607-1633.

Reichart, DL, Hinkle, RT, Lefever, FR, Dolan, ET, Dietrich, JA, Sibley, DR, Isfort, RJ (2011) Activation of the dopamine 1 and dopamine 5 receptors increase skeletal muscle mass and force production under non-atrophying and atrophying conditions. *BMC Musculoskelet Disord* **12:** 27.

Renault, V, Piron-Hamelin, G, Forestier, C, DiDonna, S, Decary, S, Hentati, F, Saillant, G, Butler-Browne, GS, Mouly, V (2000) Skeletal muscle regeneration and the mitotic clock. *Exp Gerontol* **35**(6-7): 711-719.

Rens-Domiano, S, Hamm, HE (1995) Structural and functional relationships of heterotrimeric G-proteins. *Faseb J* **9**(11): 1059-1066.

Reuter, H (1987) Calcium channel modulation by beta-adrenergic neurotransmitters in the heart. *Experientia* **43**(11-12): 1173-1175.

Rimbault, M, Robin, S, Vaysse, A, Galibert, F (2009) RNA profiles of rat olfactory epithelia: individual and age related variations. *BMC Genomics* **10:** 572.

Rimm, EB, Stampfer, MJ, Giovannucci, E, Ascherio, A, Spiegelman, D, Colditz, GA, Willett, WC (1995) Body size and fat distribution as predictors of coronary heart disease among middle-aged and older US men. *Am J Epidemiol* **141**(12): 1117-1127.

Rinaldi-Carmona, M, Barth, F, Heaulme, M, Shire, D, Calandra, B, Congy, C, Martinez, S, Maruani, J, Neliat, G, Caput, D, et al. (1994) SR141716A, a potent and selective antagonist of the brain cannabinoid receptor. *FEBS letters* **350**(2-3): 240-244.

Roche, R, Hoareau, L, Bes-Houtmann, S, Gonthier, MP, Laborde, C, Baron, JF, Haffaf, Y, Cesari, M, Festy, F (2006) Presence of the cannabinoid receptors, CB1 and CB2, in human omental and subcutaneous adipocytes. *Histochem Cell Biol* **126**(2): 177-187.

Roscioni, SS, Elzinga, CR, Schmidt, M (2008) Epac: effectors and biological functions. *Naunyn Schmiedebergs Arch Pharmacol* **377**(4-6): 345-357.

Ross, RA (2003) Anandamide and vanilloid TRPV1 receptors. *Br J Pharmacol* **140**(5): 790-801.

Ryberg, E, Larsson, N, Sjogren, S, Hjorth, S, Hermansson, NO, Leonova, J, Elebring, T, Nilsson, K, Drmota, T, Greasley, PJ (2007) The orphan receptor GPR55 is a novel cannabinoid receptor. *Br J Pharmacol* **152**(7): 1092-1101.

Santi, P, Solimando, L, Zini, N, Santi, S, Riccio, M, Guidotti, L (2003) Inositol-specific phospholipase C in low and fast proliferating hepatoma cell lines. *Int J Oncol* **22**(5): 1147-1153.

Sarabia, V, Ramlal, T, Klip, A (1990) Glucose uptake in human and animal muscle cells in culture. *Biochem Cell Biol* **68**(2): 536-542.

Sarret, P, Beaudet, A, Vincent, JP, Mazella, J (1998) Regional and cellular distribution of low affinity neurotensin receptor mRNA in adult and developing mouse brain. *J Comp Neurol* **394**(3): 344-356.

Sarret, P, Gendron, L, Kilian, P, Nguyen, HM, Gallo-Payet, N, Payet, MD, Beaudet, A (2002) Pharmacology and functional properties of NTS2 neurotensin receptors in cerebellar granule cells. *The Journal of biological chemistry* **277**(39): 36233-36243.

Sato, S, Nomura, S, Kawano, F, Tanihata, J, Tachiyashiki, K, Imaizumi, K (2010) Adaptive effects of the beta2-agonist clenbuterol on expression of beta2-adrenoceptor mRNA in rat fast-twitch fiber-rich muscles. *J Physiol Sci* **60**(2): 119-127.

Savontaus, E, Fagerholm, V, Rahkonen, O, Scheinin, M (2008) Reduced blood glucose levels, increased insulin levels and improved glucose tolerance in alpha2A-adrenoceptor knockout mice. *Eur J Pharmacol* **578**(2-3): 359-364.

Sawzdargo, M, Nguyen, T, Lee, DK, Lynch, KR, Cheng, R, Heng, HH, George, SR, O'Dowd, BF (1999) Identification and cloning of three novel human G protein-coupled receptor genes GPR52, PsiGPR53 and GPR55: GPR55 is extensively expressed in human brain. *Brain Res Mol Brain Res* **64**(2): 193-198.

Schafer, HL, Linz, W, Falk, E, Glien, M, Glombik, H, Korn, M, Wendler, W, Herling, AW, Rutten, H AVE8134, a novel potent PPARalpha agonist, improves lipid profile and glucose metabolism in dyslipidemic mice and type 2 diabetic rats. *Acta Pharmacol Sin* **33**(1): 82-90.

Scheen, AJ, Finer, N, Hollander, P, Jensen, MD, Van Gaal, LF (2006) Efficacy and tolerability of rimonabant in overweight or obese patients with type 2 diabetes: a randomised controlled study. *Lancet* **368**(9548): 1660-1672.

Scheen, AJ, Paquot, N, Van Gaal, LF (2008) [CB1 receptor inhibition and glucose metabolism: role of rimonabant in type 2 diabetes]. *Rev Med Suisse* **4**(168): 1812-1817.

Schiaffino, S, Reggiani, C (1994) Myosin isoforms in mammalian skeletal muscle. *J Appl Physiol* **77**(2): 493-501.

Schmitz-Peiffer, C, Biden, TJ (2008) Protein kinase C function in muscle, liver, and beta-cells and its therapeutic implications for type 2 diabetes. *Diabetes* **57**(7): 1774-1783.

Schreier, T, Kedes, L, Gahlmann, R (1990) Cloning, structural analysis, and expression of the human slow twitch skeletal muscle/cardiac troponin C gene. *The Journal of biological chemistry* **265**(34): 21247-21253.

Schulz, R, Eisinger, DA, Wehmeyer, A (2004) Opioid control of MAP kinase cascade. *Eur J Pharmacol* **500**(1-3): 487-497.

Schwiebert, EM, Zsembery, A (2003) Extracellular ATP as a signaling molecule for epithelial cells. *Biochim Biophys Acta* **1615**(1-2): 7-32.

Sei, Y, Gallagher, KL, Basile, AS (1999) Skeletal muscle type ryanodine receptor is involved in calcium signaling in human B lymphocytes. *The Journal of biological chemistry* **274**(9): 5995-6002.

Seki, N, Sugano, S, Suzuki, Y, Nakagawara, A, Ohira, M, Muramatsu, M, Saito, T, Hori, T (1998) Isolation, tissue expression, and chromosomal assignment of human RGS5, a novel G-protein signaling regulator gene. *J Hum Genet* **43**(3): 202-205.

Serra, C, Federici, M, Buongiorno, A, Senni, MI, Morelli, S, Segratella, E, Pascuccio, M, Tiveron, C, Mattei, E, Tatangelo, L, Lauro, R, Molinaro, M, Giaccari, A, Bouche, M (2003) Transgenic mice with dominant negative PKC-theta in skeletal muscle: a new model of insulin resistance and obesity. *J Cell Physiol* **196**(1): 89-97.

Shapiro, MS, Wollmuth, LP, Hille, B (1994) Modulation of Ca2+ channels by PTX-sensitive G-proteins is blocked by N-ethylmaleimide in rat sympathetic neurons. *J Neurosci* **14**(11 Pt 2): 7109-7116.

Shenoy, SK, Drake, MT, Nelson, CD, Houtz, DA, Xiao, K, Madabushi, S, Reiter, E, Premont, RT, Lichtarge, O, Lefkowitz, RJ (2006) beta-arrestin-dependent, G protein-independent ERK1/2 activation by the beta2 adrenergic receptor. *The Journal of biological chemistry* **281**(2): 1261-1273.

Shenoy, SK, Lefkowitz, RJ (2003) Multifaceted roles of beta-arrestins in the regulation of seven-membrane-spanning receptor trafficking and signalling. *Biochem J* **375**(Pt 3): 503-515.

Shepherd, PR, Kahn, BB (1999) Glucose transporters and insulin action--implications for insulin resistance and diabetes mellitus. *N Engl J Med* **341**(4): 248-257.

Shepherd, PR, Withers, DJ, Siddle, K (1998) Phosphoinositide 3-kinase: the key switch mechanism in insulin signalling. *Biochem J* **333 ( Pt 3)**: 471-490.

Shida, D, Kitayama, J, Yamaguchi, H, Okaji, Y, Tsuno, NH, Watanabe, T, Takuwa, Y, Nagawa, H (2003) Lysophosphatidic acid (LPA) enhances the metastatic potential of human colon carcinoma DLD1 cells through LPA1. *Cancer Res* **63**(7): 1706-1711.

Shimizu, T, Honda, Z, Nakamura, M, Bito, H, Izumi, T (1992) Platelet-activating factor receptor and signal transduction. *Biochemical pharmacology* **44**(6): 1001-1008.

Shire, D, Calandra, B, Rinaldi-Carmona, M, Oustric, D, Pessegue, B, Bonnin-Cabanne, O, Le Fur, G, Caput, D, Ferrara, P (1996) Molecular cloning, expression and function of the murine CB2 peripheral cannabinoid receptor. *Biochim Biophys Acta* **1307**(2): 132-136.

Shivachar, AC, Eikenburg, DC (1999) Differential effects of epinephrine and norepinephrine on cAMP response and g(i3)alpha protein expression in cultured sympathetic neurons. *J Pharmacol Exp Ther* **291**(1): 258-264.

Sidossis, LS, Wolfe, RR (1996) Glucose and insulin-induced inhibition of fatty acid oxidation: the glucose-fatty acid cycle reversed. *Am J Physiol* **270**(4 Pt 1): E733-738.

Sierra, DA, Popov, S, Wilkie, TM (2000) Regulators of G-protein signaling in receptor complexes. *Trends Cardiovasc Med* **10**(6): 263-268.

Simon, MF, Daviaud, D, Pradere, JP, Gres, S, Guigne, C, Wabitsch, M, Chun, J, Valet, P, Saulnier-Blache, JS (2005) Lysophosphatidic acid inhibits adipocyte differentiation via lysophosphatidic acid 1 receptor-dependent down-regulation of peroxisome proliferator-activated receptor gamma2. *The Journal of biological chemistry* **280**(15): 14656-14662.

Singh, AT, Gilchrist, A, Voyno-Yasenetskaya, T, Radeff-Huang, JM, Stern, PH (2005) G alpha12/G alpha13 subunits of heterotrimeric G proteins mediate parathyroid hormone activation of phospholipase D in UMR-106 osteoblastic cells. *Endocrinology* **146**(5): 2171-2175.

Singh, GK, Siahpush, M, Hiatt, RA, Timsina, LR (2011) Dramatic increases in obesity and overweight prevalence and body mass index among ethnic-immigrant and social class groups in the United States, 1976-2008. *J Community Health* **36**(1): 94-110.

Sipe, JC, Waalen, J, Gerber, A, Beutler, E (2005) Overweight and obesity associated with a missense polymorphism in fatty acid amide hydrolase (FAAH). *Int J Obes (Lond)* **29**(7): 755-759.

Sjoholt, G, Gulbrandsen, AK, Lovlie, R, Berle, JO, Molven, A, Steen, VM (2000) A human myo-inositol monophosphatase gene (IMPA2) localized in a putative susceptibility region for bipolar disorder on chromosome 18p11.2: genomic structure and polymorphism screening in manic-depressive patients. *Mol Psychiatry* **5**(2): 172-180.

Smerdu, V, Karsch-Mizrachi, I, Campione, M, Leinwand, L, Schiaffino, S (1994) Type IIx myosin heavy chain transcripts are expressed in type IIb fibers of human skeletal muscle. *Am J Physiol* **267**(6 Pt 1): C1723-1728.

Smith, JL, Ju, JS, Saha, BM, Racette, BA, Fisher, JS (2004) Levodopa with carbidopa

diminishes glycogen concentration, glycogen synthase activity, and insulin-stimulated glucose transport in rat skeletal muscle. *J Appl Physiol* **97**(6): 2339-2346.

Smrcka, AV (2008) G protein betagamma subunits: central mediators of G protein-coupled receptor signaling. *Cell Mol Life Sci* **65**(14): 2191-2214.

Soga, T, Ohishi, T, Matsui, T, Saito, T, Matsumoto, M, Takasaki, J, Matsumoto, S, Kamohara, M, Hiyama, H, Yoshida, S, Momose, K, Ueda, Y, Matsushime, H, Kobori, M, Furuichi, K (2005) Lysophosphatidylcholine enhances glucose-dependent insulin secretion via an orphan G-protein-coupled receptor. *Biochem Biophys Res Commun* **326**(4): 744-751.

Somwar, R, Perreault, M, Kapur, S, Taha, C, Sweeney, G, Ramlal, T, Kim, DY, Keen, J, Cote, CH, Klip, A, Marette, A (2000) Activation of p38 mitogen-activated protein kinase alpha and beta by insulin and contraction in rat skeletal muscle: potential role in the stimulation of glucose transport. *Diabetes* **49**(11): 1794-1800.

Song, D, Bandsma, RH, Xiao, C, Xi, L, Shao, W, Jin, T, Lewis, GF (2011) Acute cannabinoid receptor type 1 (CB1R) modulation influences insulin sensitivity by an effect outside the central nervous system in mice. *Diabetologia* **54**(5): 1181-1189.

Song, XM, Kawano, Y, Krook, A, Ryder, JW, Efendic, S, Roth, RA, Wallberg-Henriksson, H, Zierath, JR (1999) Muscle fiber type-specific defects in insulin signal transduction to glucose transport in diabetic GK rats. *Diabetes* **48**(3): 664-670.

Spielman, WS, Arend, LJ (1991) Adenosine receptors and signaling in the kidney. *Hypertension* **17**(2): 117-130.

Spoto, B, Fezza, F, Parlongo, G, Battista, N, Sgro, E, Gasperi, V, Zoccali, C, Maccarrone, M (2006) Human adipose tissue binds and metabolizes the endocannabinoids anandamide and 2-arachidonoylglycerol. *Biochimie* **88**(12): 1889-1897.

Sprague, RS, Olearczyk, JJ, Spence, DM, Stephenson, AH, Sprung, RW, Lonigro, AJ (2003) Extracellular ATP signaling in the rabbit lung: erythrocytes as determinants of vascular resistance. *Am J Physiol Heart Circ Physiol* **285**(2): H693-700.

Staron, RS, Kraemer, WJ, Hikida, RS, Fry, AC, Murray, JD, Campos, GE (1999) Fiber type composition of four hindlimb muscles of adult Fisher 344 rats. *Histochem Cell Biol* **111**(2): 117-123.

Starowicz, KM, Cristino, L, Matias, I, Capasso, R, Racioppi, A, Izzo, AA, Di Marzo, V (2008) Endocannabinoid dysregulation in the pancreas and adipose tissue of mice fed with a high-fat diet. *Obesity (Silver Spring)* **16**(3): 553-565.

Stein, EA, Fuller, SA, Edgemond, WS, Campbell, WB (1996) Physiological and behavioural effects of the endogenous cannabinoid, arachidonylethanolamide (anandamide), in the rat. *Br J Pharmacol* **119**(1): 107-114.

Stern-Straeter, J, Bonaterra, GA, Kassner, SS, Zugel, S, Hormann, K, Kinscherf, R, Goessler, UR (2011) Characterization of human myoblast differentiation for tissue-engineering purposes by quantitative gene expression analysis. *J Tissue Eng Regen Med*

5(8): e197-206.

Storlien, LH, Pan, DA, Kriketos, AD, O'Connor, J, Caterson, ID, Cooney, GJ, Jenkins, AB, Baur, LA (1996) Skeletal muscle membrane lipids and insulin resistance. *Lipids* **31 Suppl:** S261-265.

Straiker, A, Mackie, K (2006) Cannabinoids, electrophysiology, and retrograde messengers: challenges for the next 5 years. *AAPS J* **8**(2): E272-276.

Strange, PG (1993) Dopamine receptors: structure and function. *Prog Brain Res* **99:** 167-179.

Suarez, J, Llorente, R, Romero-Zerbo, SY, Mateos, B, Bermudez-Silva, FJ, de Fonseca, FR, Viveros, MP (2009) Early maternal deprivation induces gender-dependent changes on the expression of hippocampal CB(1) and CB(2) cannabinoid receptors of neonatal rats. *Hippocampus* **19**(7): 623-632.

Sugiura, T, Kondo, S, Sukagawa, A, Nakane, S, Shinoda, A, Itoh, K, Yamashita, A, Waku, K (1995) 2-Arachidonoylglycerol: a possible endogenous cannabinoid receptor ligand in brain. *Biochem Biophys Res Commun* **215**(1): 89-97.

Sun, Y, Alexander, SP, Garle, MJ, Gibson, CL, Hewitt, K, Murphy, SP, Kendall, DA, Bennett, AJ (2007) Cannabinoid activation of PPAR alpha; a novel neuroprotective mechanism. *Br J Pharmacol* **152**(5): 734-743.

Suzuki, Y, Shen, T, Poyard, M, Best-Belpomme, M, Hanoune, J, Defer, N (1998) Expression of adenylyl cyclase mRNAs in the denervated and in the developing mouse skeletal muscle. *Am J Physiol* **274**(6 Pt 1): C1674-1685.

Swaminath, G (2008) Fatty acid binding receptors and their physiological role in type 2 diabetes. *Arch Pharm (Weinheim)* **341**(12): 753-761.

Tajsharghi, H (2008) Thick and thin filament gene mutations in striated muscle diseases. *Int J Mol Sci* **9**(7): 1259-1275.

Tanabe, Y, Masu, M, Ishii, T, Shigemoto, R, Nakanishi, S (1992) A family of metabotropic glutamate receptors. *Neuron* **8**(1): 169-179.

Tanabe, Y, Nomura, A, Masu, M, Shigemoto, R, Mizuno, N, Nakanishi, S (1993) Signal transduction, pharmacological properties, and expression patterns of two rat metabotropic glutamate receptors, mGluR3 and mGluR4. *J Neurosci* **13**(4): 1372-1378.

Tang, T, Gao, MH, Lai, NC, Firth, AL, Takahashi, T, Guo, T, Yuan, JX, Roth, DM, Hammond, HK (2008) Adenylyl cyclase type 6 deletion decreases left ventricular function via impaired calcium handling. *Circulation* **117**(1): 61-69.

Tang, WJ, Gilman, AG (1991) Type-specific regulation of adenylyl cyclase by G protein beta gamma subunits. *Science (New York, N.Y* **254**(5037): 1500-1503.

Tao, J, Malbon, CC, Wang, HY (2001) Galpha(i2) enhances insulin signaling via suppression of protein-tyrosine phosphatase 1B. *The Journal of biological chemistry* **276**(43): 39705-39712.

Taussig, R, Quarmby, LM, Gilman, AG (1993) Regulation of purified type I and type II adenylylcyclases by G protein beta gamma subunits. *The Journal of biological chemistry* **268**(1): 9-12.

Taussig, R, Tang, WJ, Hepler, JR, Gilman, AG (1994) Distinct patterns of bidirectional regulation of mammalian adenylyl cyclases. *The Journal of biological chemistry* **269**(8): 6093-6100.

Taylor, CW, Laude, AJ (2002) IP3 receptors and their regulation by calmodulin and cytosolic Ca2+. *Cell Calcium* **32**(5-6): 321-334.

Tedesco, L, Valerio, A, Cervino, C, Cardile, A, Pagano, C, Vettor, R, Pasquali, R, Carruba, MO, Marsicano, G, Lutz, B, Pagotto, U, Nisoli, E (2008) Cannabinoid type 1 receptor blockade promotes mitochondrial biogenesis through endothelial nitric oxide synthase expression in white adipocytes. *Diabetes* **57**(8): 2028-2036.

Tharp, WG, Lee, YH, Maple, RL, Pratley, RE (2008) The cannabinoid CB1 receptor is expressed in pancreatic delta-cells. *Biochem Biophys Res Commun* **372**(4): 595-600.

Thibonnier, M, Graves, MK, Wagner, MS, Auzan, C, Clauser, E, Willard, HF (1996) Structure, sequence, expression, and chromosomal localization of the human V1a vasopressin receptor gene. *Genomics* **31**(3): 327-334.

Thomas, DE, Elliott, EJ, Naughton, GA (2006) Exercise for type 2 diabetes mellitus. *Cochrane Database Syst Rev* **3**: CD002968.

Thompson, LV (1994) Effects of age and training on skeletal muscle physiology and performance. *Phys Ther* **74**(1): 71-81.

Tian, J, Smogorzewski, M, Kedes, L, Massry, SG (1993) Parathyroid hormone-parathyroid hormone related protein receptor messenger RNA is present in many tissues besides the kidney. *Am J Nephrol* **13**(3): 210-213.

Tilakaratne, N, Sexton, PM (2005) G-Protein-coupled receptor-protein interactions: basis for new concepts on receptor structure and function. *Clin Exp Pharmacol Physiol* **32**(11): 979-987.

Tobin, AB (2008) G-protein-coupled receptor phosphorylation: where, when and by whom. *Br J Pharmacol* **153 Suppl 1**: S167-176.

Tofovic, SP, Branch, KR, Oliver, RD, Magee, WD, Jackson, EK (1991) Caffeine potentiates vasodilator-induced renin release. *J Pharmacol Exp Ther* **256**(3): 850-860.

Toft, I, Bonaa, KH, Lindal, S, Jenssen, T (1998) Insulin kinetics, insulin action, and muscle morphology in lean or slightly overweight persons with impaired glucose tolerance. *Metabolism: clinical and experimental* **47**(7): 848-854.

Toschi, A, Severi, A, Coletti, D, Catizone, A, Musaro, A, Molinaro, M, Nervi, C, Adamo, S, Scicchitano, BM (2011) Skeletal muscle regeneration in mice is stimulated by local overexpression of V1a-vasopressin receptor. *Mol Endocrinol* **25**(9): 1661-1673.

Traini, C, Pedata, F, Cipriani, S, Mello, T, Galli, A, Giovannini, MG, Cerbai, F, Volpini, R, Cristalli, G, Pugliese, AM (2011) P2 receptor antagonists prevent synaptic failure and extracellular signal-regulated kinase 1/2 activation induced by oxygen and glucose deprivation in rat CA1 hippocampus in vitro. *Eur J Neurosci* **33**(12): 2203-2215.

Trazzi, S, Steger, M, Mitrugno, VM, Bartesaghi, R, Ciani, E (2010) CB1 cannabinoid receptors increase neuronal precursor proliferation through AKT/glycogen synthase kinase-3beta/beta-catenin signaling. *The Journal of biological chemistry* **285**(13): 10098-10109.

Tso, PH, Yung, LY, Wong, YH (2000) Regulation of adenylyl cyclase, ERK1/2, and CREB by Gz following acute and chronic activation of the delta-opioid receptor. *J Neurochem* **74**(4): 1685-1693.

Tsou, K, Brown, S, Sanudo-Pena, MC, Mackie, K, Walker, JM (1998) Immunohistochemical distribution of cannabinoid CB1 receptors in the rat central nervous system. *Neuroscience* **83**(2): 393-411.

Turu, G, Hunyady, L Signal transduction of the CB1 cannabinoid receptor. *J Mol Endocrinol* **44**(2): 75-85.

Uhlen, S, Porter, AC, Neubig, RR (1994) The novel alpha-2 adrenergic radioligand [3H]-MK912 is alpha-2C selective among human alpha-2A, alpha-2B and alpha-2C adrenoceptors. *J Pharmacol Exp Ther* **271**(3): 1558-1565.

Ulloa-Aguirre, A, Stanislaus, D, Janovick, JA, Conn, PM (1999) Structure-activity relationships of G protein-coupled receptors. *Arch Med Res* **30**(6): 420-435.

Urban, JD, Clarke, WP, von Zastrow, M, Nichols, DE, Kobilka, B, Weinstein, H, Javitch, JA, Roth, BL, Christopoulos, A, Sexton, PM, Miller, KJ, Spedding, M, Mailman, RB (2007) Functional selectivity and classical concepts of quantitative pharmacology. *J Pharmacol Exp Ther* **320**(1): 1-13.

Urena, P, Kong, XF, Abou-Samra, AB, Juppner, H, Kronenberg, HM, Potts, JT, Jr., Segre, GV (1993) Parathyroid hormone (PTH)/PTH-related peptide receptor messenger ribonucleic acids are widely distributed in rat tissues. *Endocrinology* **133**(2): 617-623.

van Biesen, T, Hawes, BE, Luttrell, DK, Krueger, KM, Touhara, K, Porfiri, E, Sakaue, M, Luttrell, LM, Lefkowitz, RJ (1995) Receptor-tyrosine-kinase- and G beta gamma-mediated MAP kinase activation by a common signalling pathway. *Nature* **376**(6543): 781-784.

van Blitterswijk, WJ, Houssa, B (2000) Properties and functions of diacylglycerol kinases. *Cell Signal* **12**(9-10): 595-605.

Vasyutina, E, Stebler, J, Brand-Saberi, B, Schulz, S, Raz, E, Birchmeier, C (2005) CXCR4 and Gab1 cooperate to control the development of migrating muscle progenitor cells. *Genes Dev* **19**(18): 2187-2198.

Vettor, R, Pagano, C, Granzotto, M, Englaro, P, Angeli, P, Blum, WF, Federspil, G, Rohner-Jeanrenaud, F, Jeanrenaud, B (1998) Effects of intravenous neuropeptide Y on insulin secretion and insulin sensitivity in skeletal muscle in normal rats. *Diabetologia*

41(11): 1361-1367.

Vickers, SP, Webster, LJ, Wyatt, A, Dourish, CT, Kennett, GA (2003) Preferential effects of the cannabinoid CB1 receptor antagonist, SR 141716, on food intake and body weight gain of obese (fa/fa) compared to lean Zucker rats. *Psychopharmacology (Berl)* **167**(1): 103-111.

Vidal-Puig, AJ, Considine, RV, Jimenez-Linan, M, Werman, A, Pories, WJ, Caro, JF, Flier, JS (1997) Peroxisome proliferator-activated receptor gene expression in human tissues. Effects of obesity, weight loss, and regulation by insulin and glucocorticoids. *J Clin Invest* **99**(10): 2416-2422.

Vita, N, Oury-Donat, F, Chalon, P, Guillemot, M, Kaghad, M, Bachy, A, Thurneyssen, O, Garcia, S, Poinot-Chazel, C, Casellas, P, Keane, P, Le Fur, G, Maffrand, JP, Soubrie, P, Caput, D, Ferrara, P (1998) Neurotensin is an antagonist of the human neurotensin NT2 receptor expressed in Chinese hamster ovary cells. *Eur J Pharmacol* **360**(2-3): 265-272.

Voss, MD, Beha, A, Tennagels, N, Tschank, G, Herling, AW, Quint, M, Gerl, M, Metz-Weidmann, C, Haun, G, Korn, M (2005) Gene expression profiling in skeletal muscle of Zucker diabetic fatty rats: implications for a role of stearoyl-CoA desaturase 1 in insulin resistance. *Diabetologia* **48**(12): 2622-2630.

Wadden, TA, Butryn, ML, Wilson, C (2007) Lifestyle modification for the management of obesity. *Gastroenterology* **132**(6): 2226-2238.

Wade, SM, Lan, K, Moore, DJ, Neubig, RR (2001) Inverse agonist activity at the alpha(2A)-adrenergic receptor. *Mol Pharmacol* **59**(3): 532-542.

Wainscott, DB, Sasso, DA, Kursar, JD, Baez, M, Lucaites, VL, Nelson, DL (1998) [3H]Rauwolscine: an antagonist radioligand for the cloned human 5-hydroxytryptamine2b (5-HT2B) receptor. *Naunyn Schmiedebergs Arch Pharmacol* **357**(1): 17-24.

Wakai, A, Winter, DC, Street, JT, O'Sullivan, RG, Wang, JH, Redmond, HP (2001) Inosine attenuates tourniquet-induced skeletal muscle reperfusion injury. *J Surg Res* **99**(2): 311-315.

Waldeck-Weiermair, M, Zoratti, C, Osibow, K, Balenga, N, Goessnitzer, E, Waldhoer, M, Malli, R, Graier, WF (2008) Integrin clustering enables anandamide-induced Ca2+ signaling in endothelial cells via GPR55 by protection against CB1-receptor-triggered repression. *J Cell Sci* **121**(Pt 10): 1704-1717.

Waldo, GL, Corbitt, J, Boyer, JL, Ravi, G, Kim, HS, Ji, XD, Lacy, J, Jacobson, KA, Harden, TK (2002) Quantitation of the P2Y(1) receptor with a high affinity radiolabeled antagonist. *Mol Pharmacol* **62**(5): 1249-1257.

Walker, N, Lepee-Lorgeoux, I, Fournier, J, Betancur, C, Rostene, W, Ferrara, P, Caput, D (1998) Tissue distribution and cellular localization of the levocabastine-sensitive neurotensin receptor mRNA in adult rat brain. *Brain Res Mol Brain Res* **57**(2): 193-200.

Walter, U, Waldmann, R, Nieberding, M (1988) Intracellular mechanism of action of

vasodilators. *Eur Heart J* **9 Suppl H:** 1-6.

Wang, P, Myers, JG, Wu, P, Cheewatrakoolpong, B, Egan, RW, Billah, MM (1997) Expression, purification, and characterization of human cAMP-specific phosphodiesterase (PDE4) subtypes A, B, C, and D. *Biochem Biophys Res Commun* **234**(2): 320-324.

Wang, Y, Lam, KS, Kraegen, EW, Sweeney, G, Zhang, J, Tso, AW, Chow, WS, Wat, NM, Xu, JY, Hoo, RL, Xu, A (2007) Lipocalin-2 is an inflammatory marker closely associated with obesity, insulin resistance, and hyperglycemia in humans. *Clin Chem* **53**(1): 34-41.

Waraich, RS, Weigert, C, Kalbacher, H, Hennige, AM, Lutz, SZ, Haring, HU, Schleicher, ED, Voelter, W, Lehmann, R (2008) Phosphorylation of Ser357 of rat insulin receptor substrate-1 mediates adverse effects of protein kinase C-delta on insulin action in skeletal muscle cells. *The Journal of biological chemistry* **283**(17): 11226-11233.

Warmington, SA, Tolan, R, McBennett, S (2000) Functional and histological characteristics of skeletal muscle and the effects of leptin in the genetically obese (ob/ob) mouse. *Int J Obes Relat Metab Disord* **24**(8): 1040-1050.

Watanabe, T, Kubota, N, Ohsugi, M, Kubota, T, Takamoto, I, Iwabu, M, Awazawa, M, Katsuyama, H, Hasegawa, C, Tokuyama, K, Moroi, M, Sugi, K, Yamauchi, T, Noda, T, Nagai, R, Terauchi, Y, Tobe, K, Ueki, K, Kadowaki, T (2009) Rimonabant ameliorates insulin resistance via both adiponectin-dependent and adiponectin-independent pathways. *The Journal of biological chemistry* **284**(3): 1803-1812.

Watt, MJ (2009) Adipose tissue-skeletal muscle crosstalk: are endocannabinoids an unwanted caller? *Diabetologia* **52**(4): 571-573.

Webb, TE, Feolde, E, Vigne, P, Neary, JT, Runberg, A, Frelin, C, Barnard, EA (1996) The P2Y purinoceptor in rat brain microvascular endothelial cells couple to inhibition of adenylate cyclase. *Br J Pharmacol* **119**(7): 1385-1392.

Wedegaertner, PB, Wilson, PT, Bourne, HR (1995) Lipid modifications of trimeric G proteins. *The Journal of biological chemistry* **270**(2): 503-506.

Whyte, LS, Ryberg, E, Sims, NA, Ridge, SA, Mackie, K, Greasley, PJ, Ross, RA, Rogers, MJ (2009) The putative cannabinoid receptor GPR55 affects osteoclast function in vitro and bone mass in vivo. *Proceedings of the National Academy of Sciences of the United States of America* **106**(38): 16511-16516.

Williams, CM, Kirkham, TC (1999) Anandamide induces overeating: mediation by central cannabinoid (CB1) receptors. *Psychopharmacology (Berl)* **143**(3): 315-317.

Willis, BS, Niswender, CM, Su, T, Amieux, PS, McKnight, GS (2011) Cell-type specific expression of a dominant negative PKA mutation in mice. *PLoS One* **6**(4): e18772.

Willsky, GR, Chi, LH, Liang, Y, Gaile, DP, Hu, Z, Crans, DC (2006) Diabetes-altered gene expression in rat skeletal muscle corrected by oral administration of vanadyl

sulfate. *Physiol Genomics* **26**(3): 192-201.

Wilson, RI, Nicoll, RA (2002) Endocannabinoid signaling in the brain. *Science (New York, N.Y* **296**(5568): 678-682.

Witteman, JC, Willett, WC, Stampfer, MJ, Colditz, GA, Sacks, FM, Speizer, FE, Rosner, B, Hennekens, CH (1989) A prospective study of nutritional factors and hypertension among US women. *Circulation* **80**(5): 1320-1327.

Woodgett, JR (1990) Molecular cloning and expression of glycogen synthase kinase-3/factor A. *EMBO J* **9**(8): 2431-2438.

Wright, DC, Geiger, PC, Holloszy, JO, Han, DH (2005) Contraction- and hypoxia-stimulated glucose transport is mediated by a Ca2+-dependent mechanism in slow-twitch rat soleus muscle. *Am J Physiol Endocrinol Metab* **288**(6): E1062-1066.

Wright, DC, Hucker, KA, Holloszy, JO, Han, DH (2004) Ca2+ and AMPK both mediate stimulation of glucose transport by muscle contractions. *Diabetes* **53**(2): 330-335.

Wu, C, Zeng, Q, Blumer, KJ, Muslin, AJ (2000) RGS proteins inhibit Xwnt-8 signaling in Xenopus embryonic development. *Development* **127**(13): 2773-2784.

Wu, HM, Yang, YM, Kim, SG (2011) Rimonabant, a Cannabinoid Receptor Type 1 Inverse Agonist, Inhibits Hepatocyte Lipogenesis by Activating Liver Kinase B1 and AMP-Activated Protein Kinase Axis Downstream of G{alpha}i/o Inhibition. *Mol Pharmacol* **80**(5): 859-869.

Xiang, HJ, Chai, FL, Wang, DS, Dou, KF (2011) Downregulation of the adenosine a2b receptor by RNA interference inhibits hepatocellular carcinoma cell growth. *ISRN Oncol* **2011**: 875684.

Yaffe, D (1968) Retention of differentiation potentialities during prolonged cultivation of myogenic cells. *Proceedings of the National Academy of Sciences of the United States of America* **61**(2): 477-483.

Yagisawa, H (2006) Nucleocytoplasmic shuttling of phospholipase C-delta1: a link to Ca2+. *J Cell Biochem* **97**(2): 233-243.

Yamaguchi, M, Ogawa, R, Watanabe, Y, Uezumi, A, Miyagoe-Suzuki, Y, Tsujikawa, K, Yamamoto, H, Takeda, S, Fukada, SI (2012) Calcitonin receptor and Odz4 are differently expressed in Pax7-positive cells during skeletal muscle regeneration. *J Mol Histol.*

Yamaguchi, N, Xu, L, Pasek, DA, Evans, KE, Meissner, G (2003) Molecular basis of calmodulin binding to cardiac muscle Ca(2+) release channel (ryanodine receptor). *The Journal of biological chemistry* **278**(26): 23480-23486.

Yan, ZC, Liu, DY, Zhang, LL, Shen, CY, Ma, QL, Cao, TB, Wang, LJ, Nie, H, Zidek, W, Tepel, M, Zhu, ZM (2007) Exercise reduces adipose tissue via cannabinoid receptor type 1 which is regulated by peroxisome proliferator-activated receptor-delta. *Biochem Biophys Res Commun* **354**(2): 427-433.

Yang, D, Koupenova, M, McCrann, DJ, Kopeikina, KJ, Kagan, HM, Schreiber, BM, Ravid, K (2008) The A2b adenosine receptor protects against vascular injury. *Proceedings of the National Academy of Sciences of the United States of America* **105**(2): 792-796.

Yang, E, Maguire, T, Yarmush, ML, Berthiaume, F, Androulakis, IP (2007) Bioinformatics analysis of the early inflammatory response in a rat thermal injury model. *BMC Bioinformatics* **8**: 10.

Ye, X (2008) Lysophospholipid signaling in the function and pathology of the reproductive system. *Hum Reprod Update* **14**(5): 519-536.

Yea, K, Kim, J, Lim, S, Park, HS, Park, KS, Suh, PG, Ryu, SH (2008) Lysophosphatidic acid regulates blood glucose by stimulating myotube and adipocyte glucose uptake. *J Mol Med (Berl)* **86**(2): 211-220.

Yin, H, Chu, A, Li, W, Wang, B, Shelton, F, Otero, F, Nguyen, DG, Caldwell, JS, Chen, YA (2009) Lipid G protein-coupled receptor ligand identification using beta-arrestin PathHunter assay. *The Journal of biological chemistry* **284**(18): 12328-12338.

Youn, JH, Gulve, EA, Holloszy, JO (1991) Calcium stimulates glucose transport in skeletal muscle by a pathway independent of contraction. *Am J Physiol* **260**(3 Pt 1): C555-561.

Yuzbasioglu, A, Onbasilar, I, Kocaefe, C, Ozguc, M (2010) Assessment of housekeeping genes for use in normalization of real time PCR in skeletal muscle with chronic degenerative changes. *Exp Mol Pathol* **88**(2): 326-329.

Zacchigna, S, Ostli, EK, Arsic, N, Pattarini, L, Giacca, M, Djurovic, S (2008) A novel myogenic cell line with phenotypic properties of muscle progenitors. *J Mol Med (Berl)* **86**(1): 105-115.

Zeng, L, Fagotto, F, Zhang, T, Hsu, W, Vasicek, TJ, Perry, WL, 3rd, Lee, JJ, Tilghman, SM, Gumbiner, BM, Costantini, F (1997) The mouse Fused locus encodes Axin, an inhibitor of the Wnt signaling pathway that regulates embryonic axis formation. *Cell* **90**(1): 181-192.

Zhang, F, Strand, A, Robbins, D, Cobb, MH, Goldsmith, EJ (1994) Atomic structure of the MAP kinase ERK2 at 2.3 A resolution. *Nature* **367**(6465): 704-711.

Zhang, J, Phillips, DI, Wang, C, Byrne, CD (2004) Human skeletal muscle PPARalpha expression correlates with fat metabolism gene expression but not BMI or insulin sensitivity. *Am J Physiol Endocrinol Metab* **286**(2): E168-175.

Zhao, W, Fong, O, Muise, ES, Thompson, JR, Weingarth, D, Qian, S, Fong, TM (2010) Genome-wide expression profiling revealed peripheral effects of cannabinoid receptor 1 inverse agonists in improving insulin sensitivity and metabolic parameters. *Mol Pharmacol* **78**(3): 350-359.

Zhou, G, Myers, R, Li, Y, Chen, Y, Shen, X, Fenyk-Melody, J, Wu, M, Ventre, J, Doebber, T, Fujii, N, Musi, N, Hirshman, MF, Goodyear, LJ, Moller, DE (2001) Role

of AMP-activated protein kinase in mechanism of metformin action. *J Clin Invest* **108**(8): 1167-1174.

Zhou, G, Sebhat, IK, Zhang, BB (2009) AMPK activators--potential therapeutics for metabolic and other diseases. *Acta Physiol (Oxf)* **196**(1): 175-190.

Zierath, JR, Krook, A, Wallberg-Henriksson, H (2000) Insulin action and insulin resistance in human skeletal muscle. *Diabetologia* **43**(7): 821-835.

Zimmermann, H (1992) 5'-Nucleotidase: molecular structure and functional aspects. *Biochem J* **285 ( Pt 2)**: 345-365.

Zimmermann, H (2006) Ectonucleotidases in the nervous system. *Novartis Found Symp* **276**: 113-128; discussion 128-130, 233-117, 275-181.

Zimmet, P, Turner, R, McCarty, D, Rowley, M, Mackay, I (1999) Crucial points at diagnosis. Type 2 diabetes or slow type 1 diabetes. *Diabetes Care* **22 Suppl 2**: B59-64.

Zurlo, F, Larson, K, Bogardus, C, Ravussin, E (1990) Skeletal muscle metabolism is a major determinant of resting energy expenditure. *J Clin Invest* **86**(5): 1423-1427.

# 9 Appendix

## 9.1 Agilent microarray

### 9.1.1 Agilent bioanalyzer

The tables below represent RIN values for the samples (Table 9-1) and (Table 9-2).

Table 9-1: Characterizations of samples taken from rat A.

| | Samples | | | | |
|---|---|---|---|---|---|
| Rat A | Skeletal 1 | Skeletal 2 | Skeletal 3 | Liver 1 | Adipose 1 |
| | RNA extraction | | | | |
| RIN (Agilent bioanalyzer) | 7.7 | 7.7 | 7.7 | 9.3 | 9.7 |
| **Nanodrop** | | | | | |
| A260/280 ratio | 2 | 1.9 | 1.9 | 2 | 1.9 |
| A260/230 ratio | 2.1 | 2.1 | 1.8 | 2.1 | 2.1 |
| Conc (ng/µl) | 358.3 | 265.5 | 435.1 | 1243 | 194.7 |

Table 9-2: Characterizations of samples taken from rat B.

| | Samples | | | | |
|---|---|---|---|---|---|
| Rat B | Skeletal 4 | Skeletal 5 | Skeletal 6 | Liver 2 | Adipose 2 |
| | RNA extraction | | | | |
| RIN (Agilent bioanalyzer) | 7.6 | 8.4 | 8.6 | 9 | 8.9 |
| **Nanodrop** | | | | | |
| A260/280 ratio | 1.9 | 1.9 | 2.1 | 2 | 2 |
| A260/230 ratio | 2.1 | 2.1 | 2.3 | 2 | 2 |
| Conc (ng/µl) | 1405.6 | 607.6 | 669.32 | 343.79 | 1336.7 |

### 9.1.2 Sample preparation and labeling

Sample preparation includes four steps: Preparing One-Color Spike-Mix; preparing labeling reaction; purifying the labelled/amplified RNA and quantifying the cRNA.

One-Color Spike-Mix was prepared according to the protocol on Agilent One-Color RNA Spike-In Kit. Agilent One-Color Spike-Mix was thawed and mixed. The thawed Agilent One-Color Spike-Mix was heated at 37 C° for 5 minutes and vortexed again. 1:10 dilution was then prepared as illustrated in the (Table 9-3).

Table 9-3: Dilutions of Agilent One-Color Spike-Mix for cyanine 3-labelling.

| Starting amount of RNA | | Serial dilution | | | Spike-mix volume to be used in each labeling reaction (µL). |
|---|---|---|---|---|---|
| Total RNA (ng) | Maximum volume of RNA (µL) | First | Second | Third | |
| 500 | 5.3 | 1:20 | 1:25 | 1:10 | 5 |

Labelling was performed using the Agilent Gene Expression system according to protocol in Agilent Quick Amp Kit, One-Color. For the synthesis of cDNA, the low RNA input linear amplification kit (Agilent) was used to produce an initial RNA amplification of at least 100 fold. This strategy utilizes an adapter T7 primer for first-strand cDNA synthesis with MMLV reverse transcriptase, followed by in vitro transcription using T7 RNA Polymerase to simultaneously amplify target material and incorporate Cy3 labelled CTP (Perkin Elmer).

Template and T7 Promoter Primer Mix was prepared as illustrated in the (Table 9-4). RNA sample, dilution Spike-Mix, T7 promoter primer and water were mixed. The primer and the template were denatured by incubating the reaction at 65 C° for 10 minutes, and then placed on ice for 5 minutes.

Table 9-4: Template and T7 promoter primer mix.

| Total RNA input (ng) | Max RNA volume (µL) | Third dilution of spike-mix volume (µL) | T7 promoter primer (µL) | Total volume (µL) |
|---|---|---|---|---|
| 500 | 5.3 | 5 | 1.2 | 11.5 |

cDNA master mix was prepared by mixing the reagents in order as illustrated in the (Table 9-5). cDNA master mix was then added and mixed to each sample tube. Samples were incubated at 40 C° in a circulating water bath for 2 hours, then incubated at 65 C° circulating water bath for 15 minutes, placed on ice for 5 minutes.

Table 9-5: cDNA master mix.

| Component | Volume (µL) per reaction |
|---|---|
| 5X First Strand Buffer | 4 |
| 0.1 M DTT | 2 |
| 10 mM dNTP mix | 1 |
| MMLV-RT | 1 |
| RNaseOut | 0.5 |
| Total Volume | 8.5 |

Transcription Master Mix was prepared by mixing the reagents in order as illustrated in the (Table 9-6). Transcription Master Mix was then added and mixed to each sample tube. Foiled samples were incubated at 40 C° in a circulating water bath for 2 hours.

Table 9-6: Transcription master mix.

| Component | Volume (µL) per reaction |
|---|---|
| Nuclease-free water | 15.3 |
| 4X Transcription Buffer | 20 |
| 0.1 M DTT | 6 |
| NTP mix | 8 |
| 50% PEG | 6.4 |
| RNaseOUT | 0.5 |
| Inorganic pyrophosphatase | 0.6 |
| T7 RNA Polymerase | 0.8 |
| Cyanine 3-CTP | 2.4 |
| Total Volume | 60 |

The labelled/amplified RNA was then purified using Qiagen's RNeasy mini spin columns.

The concentrations of cRNA (ng/µL) and cyanine 3 (pmol/µL) were measured using the NanoDrop ND-1000 Spectrophotometer, labelling efficiency was determined using the yield and specific activity of each reaction. The yield and specific activity were determined as follows:

The yield (µg cRNA) was calculated from the concentration of cRNA (ng/µL):

(Concentration of cRNA) * 30 µL (elution volume) / 1000 = µg of cRNA.

The specific activity was calculated from the concentrations of cRNA (ng/µL) and cyanine 3 (pmol/µL) as follows:

(Concentration of Cy3) / (Concentration of cRNA) * 1000 = pmol Cy3 per µg cRNA.

cRNA preparation will be repeated if the yield is less than 1.65 µg and the specific activity is less than 9.0 pmol Cy3 per µg cRNA, as illustrated in the (Table 9-7) and (Table 9-8).

Table 9-7: Yield and specific activity for the samples taken from rat A.

| Samples | | | | | |
|---|---|---|---|---|---|
| Rat A | Skeletal 1 | Skeletal 2 | Skeletal 3 | Liver 1 | Adipose 1 |
| **Labelling** | | | | | |
| Yield (ug) | 6.8 | 1.7 | 8.3 | 5.15 | 5.17 |
| Specific activity (pmol Cy-3/ug) | 9.1 | 9.3 | 18.6 | 9.9 | 9.5 |

Table 9-8: Yield and specific activity for the samples taken from rat B.

| | Samples | | | | |
|---|---|---|---|---|---|
| Rat B | Skeletal 4 | Skeletal 5 | Skeletal 6 | Liver 2 | Adipose 2 |
| **Labelling** | | | | | |
| Yield (ug) | 9.8 | 6.01 | 7.4 | 13.9 | 2.89 |
| Specific activity (pmol Cy-3/ug) | 13.4 | 15.3 | 13.8 | 17.6 | 16.2 |

Labelling was examined by the yield and specific activity of the reaction. None of the samples yielded less than 1.65 μg and specific activity less than 9.0 pmol Cy3 per μg cRNA.

### 9.1.3 Hybridization

Of each sample, 1.65 μg labelled cRNA was fragmented and hybridized on the Whole Rat Genome Expression Array (4x44K, Agilent). Fragmentation mix was prepared by mixing the reagents shown in the (Table 9-9).

Table 9-9: Fragmentation mix for 4x44K microarrays.

| Component | Volume/Mass |
|---|---|
| Labelled, linearly amplified cRNA | 1.65µg |
| Agilent Blocking Agent (10x) | 11µl |
| Nuclease free water | Bring volume to 52.8µl |
| Fragmentation Buffer (25x) | 2.2µl |

The samples were incubated at 60 C° for exactly 30 minutes in order to fragment RNA. Afterwards the fragmentation was stopped by adding of 2x Hybridization buffer. The final hybridization mixture for the 4x44k (4 array/slide; total volume 110µl each) Whole Rat Genome microarrays was prepared by adding cRNA from fragmentation mix to Agilent hybridization buffer (2x), (2xGE, HI-RPM) as shown in the (Table 9-10).

Table 9-10: Hybridization mix for 4x44K microarrays.

| Component | Volume |
|---|---|
| cRNA from Fragmentation Mix | 55µl |
| Agilent Hybridization Buffer (2x), (2xGE, HI-RPM) | 55µl |

The sample was spun down for one minute at room temperature and kept on ice until loading onto the array, which was performed immediately. The (Table 9-11) below shows the hybridization sample volume.

Table 9-11: Hybridization sample.

| Component | Volume |
|---|---|
| Volume prepared | 110 µL |
| Hybridization sample volume | 100 µL |

Hybridization on microarray slides (Agilent) was then carried out at 65 C° for 17 hours using an Agilent sureHyb chamber and an Agilent hybridization oven.

### 9.1.4 Microarray wash

Slides were washed in Gene Expression Wash Buffer I (Agilent) at room temperature for one minute and in Gene Expression Wash Buffer II (Agilent, prewarmed to 37 C°) for an additional minute. Afterwards slides were dried; they were assembled into an appropriate slide holder for scanning.

### 9.1.5 Scanning

TIFF (Tagged Image File Format) images were immediately generated by the Agilent scanner. Scans were made with a pixel resolution of 5µm and sixteen-bit TIFF image. The TIFF images were processed with feature extraction software 9.5.3 (Agilent) using default parameters (protocol One-Color_GE_5.7) to obtain background subtracted processed signal intensities. Feature extraction software converted these digital TIFF images of hybridization intensity to the numerical measures of the hybridization intensity of each feature that quantified gene expression (Figure 9-1).

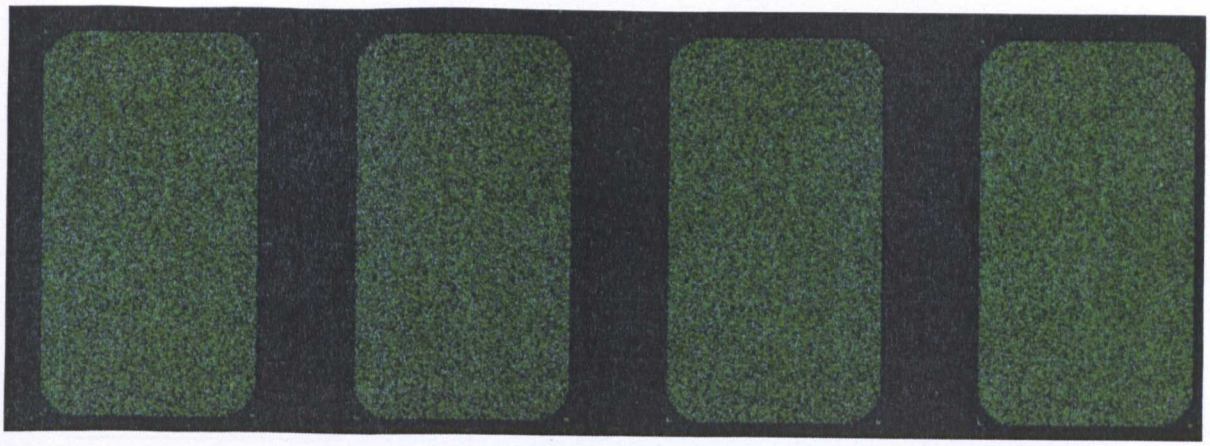

Figure 9-1: Representative TIFF image from the microarray.

## 9.1.6 Agilent QC

Figure 9-2: The quality control from the feature extraction software after scanning.

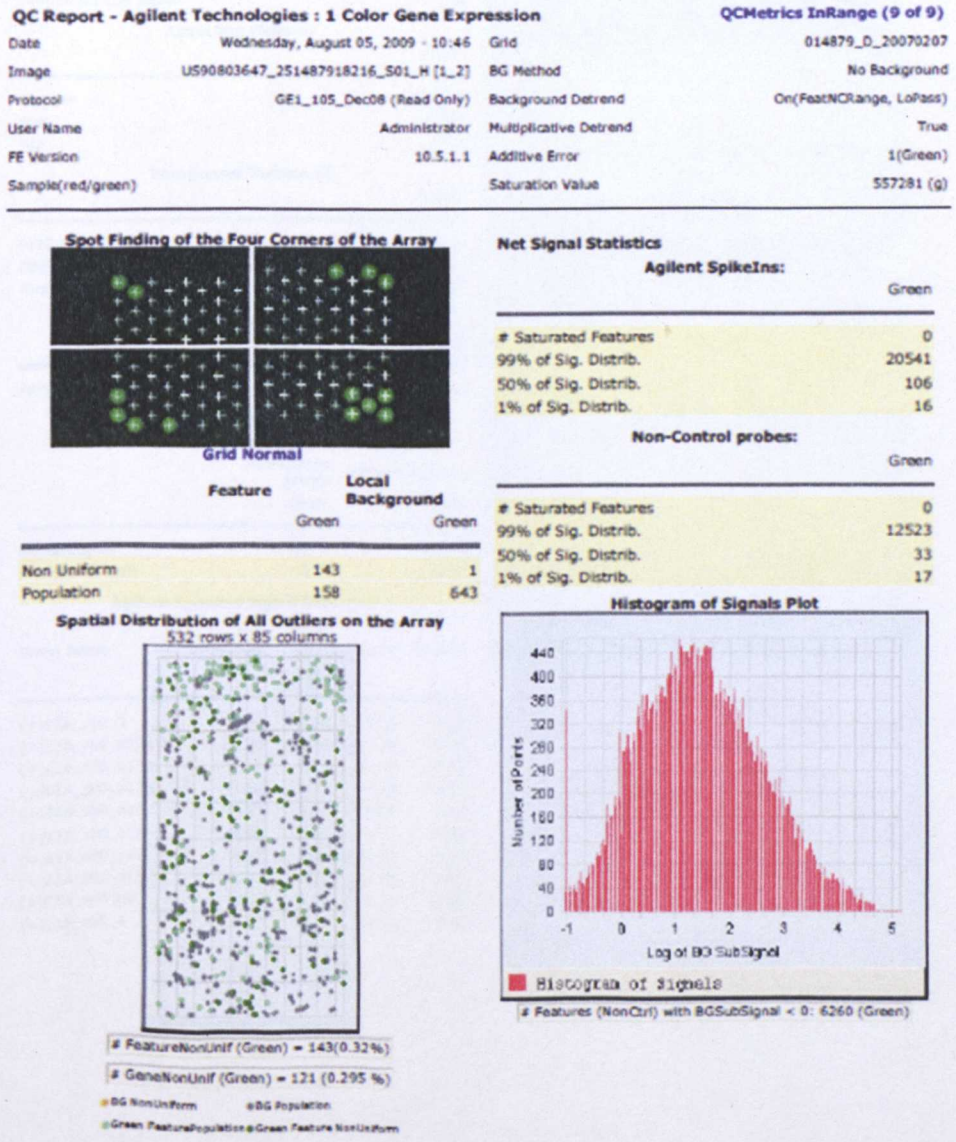

**QC Report - Agilent Technologies : 1 Color Gene Expression**

| | | | |
|---|---|---|---|
| Date | Wednesday, August 05, 2009 - 10:46 | Grid | 014879_D_20070207 |
| Image | US90803647_251487918216_S01_H [1_2] | BG Method | No Background |
| Protocol | GE1_105_Dec08 (Read Only) | Background Detrend | On(FeatNCRange, LoPass) |
| User Name | Administrator | Multiplicative Detrend | True |
| FE Version | 10.5.1.1 | Additive Error | 1(Green) |
| Sample(red/green) | | Saturation Value | 557281 (g) |

**QCMetrics InRange (9 of 9)**

**Spot Finding of the Four Corners of the Array**

Grid Normal

| | Feature | Local Background |
|---|---|---|
| | Green | Green |
| Non Uniform | 143 | 1 |
| Population | 158 | 643 |

**Spatial Distribution of All Outliers on the Array**

532 rows x 85 columns

# FeatureNonUnif (Green) = 143(0.32%)

# GeneNonUnif (Green) = 121 (0.295 %)

BG NonUniform BG Population

Green FeaturePopulation Green Feature NonUniform

**Net Signal Statistics**

**Agilent SpikeIns:**

| | Green |
|---|---|
| # Saturated Features | 0 |
| 99% of Sig. Distrib. | 20541 |
| 50% of Sig. Distrib. | 106 |
| 1% of Sig. Distrib. | 16 |

**Non-Control probes:**

| | Green |
|---|---|
| # Saturated Features | 0 |
| 99% of Sig. Distrib. | 12523 |
| 50% of Sig. Distrib. | 33 |
| 1% of Sig. Distrib. | 17 |

**Histogram of Signals Plot**

Number of Ports

440 400 360 320 280 240 200 160 120 80 40 0

-1 0 1 2 3 4 5

Log of BG SubSignal

Histogram of Signals

# Features (NonCtrl) with BGSubSignal < 0: 6260 (Green)

**Negative Control Stats**

| | Green |
|---|---|
| Average Net Signals | 18.69 |
| StdDev Net Signals | 1.34 |
| Average BG Sub Signal | -1.32 |
| StdDev BG Sub Signal | 1.02 |

**Local Bkg (inliers)**

| | Green |
|---|---|
| Number | 44375 |
| Avg | 21.94 |
| SD | 1.26 |

**Foreground Surface Fit**

| | Green |
|---|---|
| RMS_Fit | 0.95 |
| RMS_Resid | 1.14 |
| Avg_Fit | 27.30 |

**Multiplicative Surface Fit**

| | Green |
|---|---|
| RMS_Fit | 0.14 |

**Reproducibility: %CV for Replicated Probes**

| | Median %CV Signal (inliers) | |
|---|---|---|
| | Non-Control probes | Agilent SpikeIns |
| | Green | Green |
| BGSubSignal | 15.71 | 15.50 |
| ProcessedSignal | 6.96 | 6.89 |

**Agilent SpikeIns Signal Statistics**

| Probe Name | Log (Relative Conc.) | Median (Log Proc. Sig.) | % CV | StdDev |
|---|---|---|---|---|
| (+)E1A_r60_3 | 0.30 | 0.06 | 45.33 | 0.12 |
| (+)E1A_r60_a104 | 1.30 | 0.06 | 181.55 | 0.23 |
| (+)E1A_r60_a107 | 2.30 | 0.20 | 80.03 | 0.21 |
| (+)E1A_r60_a135 | 3.30 | 1.27 | 13.86 | 0.07 |
| (+)E1A_r60_a20 | 3.83 | 1.86 | 6.89 | 0.03 |
| (+)E1A_r60_a22 | 4.30 | 2.18 | 6.37 | 0.03 |
| (+)E1A_r60_a97 | 4.82 | 2.69 | 15.95 | 0.10 |
| (+)E1A_r60_n11 | 5.30 | 3.37 | 6.66 | 0.03 |
| (+)E1A_r60_n9 | 5.82 | 3.56 | 11.46 | 0.06 |
| (+)E1A_r60_1 | 6.30 | 4.25 | 6.54 | 0.03 |

**Spatial Distribution of Median Signals for each Row**

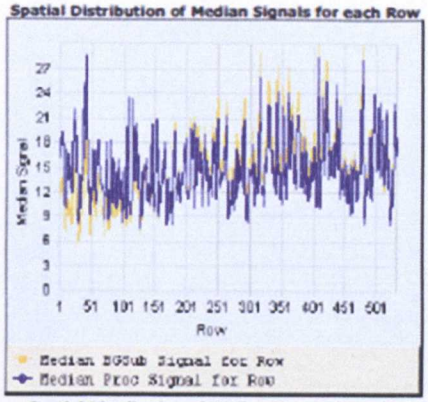


**Spatial Distribution of Median Signals for each Column**

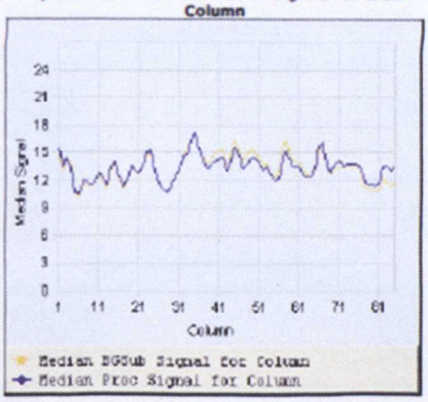

**Agilent SpikeIns: %CV of Avg. Processed Signal Plot**

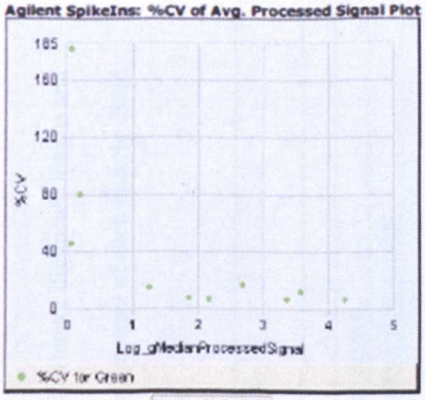


Median %CV: 6.89

**Agilent SpikeIns: Log(Signal) vs. Log(Relative concentration) Plot**

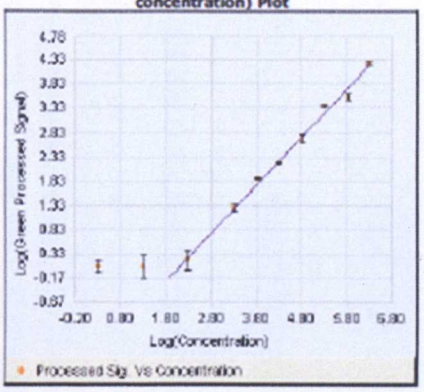


**Evaluation Metrics for GE1_QCMT_Dec08**

| Metric Name | Value | UpLim | LowLim | IsMandatory |
|---|---|---|---|---|
| AnyColorPrcntFeatNonUnif... | 0.32 | 1.00 | NA | False |
| DetectionLimit | 0.59 | 2.00 | 0.01 | False |
| absGE1E1aSlope | 0.99 | 1.20 | 0.90 | False |
| gE1aMedCVProcSignal | 6.89 | 8.00 | NA | False |
| gNegCtrlAveBGSubSig | -1.32 | 5.00 | -10.00 | False |
| gNegCtrlAveNetSig | 18.69 | 40.00 | NA | False |
| gNegCtrlSDevBGSubSig | 1.02 | 10.00 | NA | False |
| gNonCntrlMedCVProcSignal | 6.96 | 8.00 | NA | False |
| gSpatialDetrendRMSFilter... | 1.14 | 15.00 | NA | False |

♦ In Normal Range ♦ Evaluate

**Agilent Spike-In Concentration-Response Statistics**

**Linear Range Statistics:**

| | |
|---|---|
| Low Signal | -0.31 |
| High Signal | 5.87 |
| Low Relative Concentration | 1.73 |
| High Relative Concentration | 7.99 |
| Slope | 0.99 |
| R^2 Value | 0.99 |

**Signal Detection Limit Statistics**

| | |
|---|---|
| Saturation Point | 5.75 |
| Low Threshold | -0.35 |
| Low Threshold Error | 0.33 |
| Spike-In Detection Limit | 0.59 |

## 9.2 GPCRs

Table 9-12: Relative intensity values for GPCRs classified as "present" in all skeletal muscle samples from two rats. Site A is a mixture of extensor digitorum longus and tibialis anterior, site B is a mixture of soleus and plantaris, and site C is a mixture of red and white gastronemius muscle with roughly equal amount of each muscle. Bold text indicated 38 GPCR entities detected in skeletal muscle.

| Rat A | | | Rat B | | | GPCRs |
|---|---|---|---|---|---|---|
| Site | | | | | | |
| A | B | C | A | B | C | |
| 4.6 | 4.2 | 4.5 | 4.4 | 4.1 | 4.8 | **Rattus norvegicus EGF, latrophilin and seven transmembrane domain containing 1 (Eltd1), mRNA [NM_022294]** |
| 3.5 | 3.8 | 3.4 | 4.4 | 3.8 | 4.0 | **PREDICTED: Rattus norvegicus G protein-coupled receptor, family C, group 5, member C (Gprc5c), mRNA [XM_213518]** |
| 3.9 | 3.5 | 4.3 | 3.5 | 3.6 | 3.6 | **Rattus norvegicus latrophilin 1 (Lphn1), mRNA [NM_022962]** |
| 2.9 | 2.1 | 2.2 | 2.8 | 4.1 | 4.0 | **Rattus norvegicus endothelial differentiation, lysophosphatidic acid G-protein-coupled receptor, 2 (Edg2), mRNA [NM_053936]** |
| 2.3 | 2.1 | 1.8 | 2.4 | 2.2 | 2.1 | **Rattus norvegicus G protein-coupled receptor 116 (Gpr116), mRNA [NM_139110]** |
| 1.8 | 1.6 | 2.4 | 2.3 | 2.0 | 2.1 | **Rattus norvegicus chemokine (C-X-C motif) receptor 4 (Cxcr4), mRNA [NM_022205]** |
| 1.8 | 1.6 | 2.3 | 2.2 | 2.1 | 2.1 | **Rattus norvegicus chemokine (C-X-C motif) receptor 4 (Cxcr4), mRNA [NM_022205]** |
| 1.7 | 1.2 | 0.9 | 1.4 | 1.6 | 1.7 | **Rattus norvegicus purinergic receptor P2Y, G-protein coupled 2 (P2ry2), mRNA [NM_017255]** |
| 1.0 | 1.7 | 1.4 | 1.1 | 1.2 | 0.7 | **PREDICTED: Rattus norvegicus G protein-coupled receptor, family C, group 5, member B (predicted) (Gprc5b_predicted), mRNA [XM_215095]** |
| 1.0 | 1.2 | 0.9 | 1.2 | 1.0 | 1.2 | **Rattus norvegicus leucine-rich repeat-containing G protein-coupled receptor 4 (Lgr4), mRNA [NM_173328]** |
| 0.9 | 1.1 | -0.2 | 1.3 | 1.6 | 1.8 | **Rattus norvegicus chemokine orphan receptor 1 (Cmkor1), mRNA [NM_053352]** |
| 0.1 | 1.9 | 2.6 | 0.8 | 0.3 | 0.6 | **PREDICTED: Rattus norvegicus brain-specific angiogenesis inhibitor 2 (predicted) (Bai2_predicted), mRNA [XM_232778]** |
| 1.2 | 0.8 | 1.2 | 1.1 | 1.1 | 0.9 | **Rattus norvegicus adrenergic receptor, beta 2 (Adrb2), mRNA [NM_012492]** |
| 0.6 | 1.1 | 1.2 | 1.4 | 1.1 | 0.2 | **Rattus norvegicus angiotensin receptor-like 1 (Agtrl1), mRNA [NM_031349]** |
| 1.0 | 1.3 | 0.6 | 0.7 | 0.8 | 0.6 | **PREDICTED: Rattus norvegicus G protein-coupled receptor 125 (predicted) (Gpr125_predicted), mRNA [XM_223485]** |
| 0.2 | 0.0 | 0.4 | 0.8 | 1.2 | 0.8 | **PREDICTED: Rattus norvegicus G protein-coupled receptor 68 (predicted) (Gpr68_predicted), mRNA [XM_001065526]** |
| 1.0 | 1.6 | 0.8 | 0.4 | -1.4 | 0.4 | **Rattus norvegicus glucagon receptor (Gcgr), transcript variant 2, mRNA [NM_172091]** |
| 0.3 | 0.2 | 0.3 | 0.2 | 1.1 | 0.6 | **Rattus norvegicus platelet-activating factor receptor (Ptafr), mRNA [NM_053321]** |
| 0.0 | -0.2 | 0.5 | 0.7 | 0.5 | 0.3 | **Rattus norvegicus adenosine A2a receptor (Adora2a), mRNA [NM_053294]** |
| -0.7 | -1.1 | 0.2 | 0.9 | 0.6 | 0.8 | **Rattus norvegicus adrenergic receptor, alpha 1d (Adra1d), mRNA [NM_024483]** |
| -0.3 | -0.7 | 0.1 | 0.0 | 1.0 | 0.0 | **Rattus norvegicus pyrimidinergic receptor P2Y, G-protein coupled, 6 (P2ry6), mRNA [NM_057124]** |

| | | | | | | |
|---|---|---|---|---|---|---|
| -0.1 | 0.3 | 0.4 | -0.3 | -0.2 | -0.6 | Rattus norvegicus gamma-aminobutyric acid (GABA) B receptor 1 (Gabbr1), mRNA [NM_031028] |
| -0.3 | -0.7 | -0.6 | 0.4 | 0.0 | 0.0 | Rattus norvegicus G protein-coupled receptor 4 (Gpr4), mRNA [NM_001025680] |
| -0.4 | 0.1 | -0.6 | 0.6 | 0.1 | -1.4 | Rattus norvegicus G protein-coupled receptor 56 (Gpr56), mRNA [NM_152242] |
| -0.4 | -0.7 | -0.4 | -0.9 | 0.2 | -0.1 | Rattus norvegicus endothelial differentiation, sphingolipid G-protein-coupled receptor, 5 (Edg5), mRNA [NM_017192] |
| -0.2 | -0.3 | -0.3 | -0.5 | -0.4 | -0.5 | Rattus norvegicus latrophilin 2 (Lphn2), mRNA [NM_134408] |
| -0.1 | -0.6 | -0.7 | -0.6 | 0.1 | -0.6 | Rattus norvegicus parathyroid hormone receptor 1 (Pthr1), mRNA [NM_020073] |
| -1.0 | -0.6 | 0.4 | -0.6 | -1.2 | -0.1 | Rat metabotropic glutamate receptor 2 mRNA, primary transcript. [M92075] |
| -0.3 | -0.2 | -1.1 | -0.9 | -0.8 | -0.1 | Rattus norvegicus similar to purinergic receptor P2Y, G-protein coupled, 5 (MGC112684), mRNA [NM_001045843] |
| -0.1 | -0.4 | -0.5 | -0.5 | -1.2 | -0.9 | Rat metabotropic glutamate receptor 3 mRNA, primary transcript. [M92076] |
| -1.1 | -1.1 | -1.0 | -1.1 | 0.4 | 0.0 | Rattus norvegicus endothelial differentiation, lysophosphatidic acid G-protein-coupled receptor, 2 (Edg2), mRNA [NM_053936] |
| -1.4 | -0.7 | 0.2 | -0.3 | -1.1 | -0.8 | Cadherin EGF LAG seven-pass G-type receptor 2 (Multiple epidermal growth factor-like domains 3) (Fragment). [Source:Uniprot/SWISSPROT;Acc:Q9QYP2] [ENSRNOT00000027263] |
| -0.6 | -1.3 | -0.7 | -0.5 | -0.4 | -0.6 | Adenosine A1 receptor. [Source:Uniprot/SWISSPROT;Acc:P25099] [ENSRNOT00000004602] |
| 0.2 | 0.1 | -1.2 | -0.5 | -1.2 | -1.5 | Rattus norvegicus adrenergic receptor, alpha 2a (Adra2a), mRNA [NM_012739] |
| -0.5 | -0.4 | -3.0 | -0.9 | 0.5 | 0.1 | Rattus norvegicus endothelial differentiation, lysophosphatidic acid G-protein-coupled receptor, 2 (Edg2), mRNA [NM_053936] |
| -1.4 | -1.0 | -0.5 | -0.8 | -1.8 | -0.7 | Rattus norvegicus dopamine receptor D5 (Drd5), mRNA [NM_012768] |
| -1.1 | -1.0 | -1.0 | -0.6 | -1.0 | -1.8 | Rattus norvegicus neurotensin receptor 2 (Ntsr2), mRNA [NM_022695] |
| -1.1 | -1.7 | -0.1 | -0.9 | -1.8 | -1.0 | Rattus norvegicus opioid receptor, delta 1 (Oprd1), mRNA [NM_012617] |
| -1.8 | -1.5 | -1.3 | -1.3 | -0.1 | -1.2 | Rattus norvegicus EGF-like module containing, mucin-like, hormone receptor-like sequence 1 (Emr1), mRNA [NM_001007557] |
| -0.5 | -0.9 | -0.9 | -1.8 | -1.4 | -1.7 | Rattus norvegicus calcitonin receptor (Calcr), transcript variant 1, mRNA [NM_053816] |
| -0.6 | -0.8 | -1.4 | -0.8 | -1.5 | -2.1 | Cardiac sphingosine-1-phosphate specific receptor (Fragment). [Source:Uniprot/SPTREMBL;Acc:Q9QZG4] [ENSRNOT00000019473] |
| -2.2 | -2.0 | -1.3 | -1.2 | -1.0 | -0.2 | Rattus norvegicus arginine vasopressin receptor 1A (Avpr1a), mRNA [NM_053019] |
| -1.2 | -1.4 | -1.7 | -1.4 | -0.6 | -1.8 | Rattus norvegicus MAS-related GPR, member F (Mrgprf), mRNA [NM_153722] |
| -0.6 | -0.6 | -0.8 | -3.1 | -2.2 | -1.1 | PREDICTED: Rattus norvegicus G protein-coupled receptor 114 (predicted) (Gpr114_predicted), mRNA [XM_240979] |
| -1.6 | -2.2 | -1.2 | -1.4 | -1.3 | -1.0 | PREDICTED: Rattus norvegicus chemokine (C-C motif) receptor-like 2 (predicted) (Ccrl2_predicted), mRNA [XM_236658] |
| -1.2 | -1.2 | -1.9 | -1.8 | -1.7 | -0.9 | Rattus norvegicus purinergic receptor P2Y, G-protein coupled 1 (P2ry1), mRNA [NM_012800] |
| 0.3 | -0.9 | -2.1 | -2.1 | -2.2 | -2.0 | Rattus norvegicus bradykinin receptor, beta 2 (Bdkrb2), mRNA [NM_173100] |
| -2.0 | -2.6 | -2.7 | -1.7 | -0.1 | -0.5 | Rattus norvegicus complement component 5, receptor 1 (C5r1), mRNA [NM_053619] |
| -1.2 | -1.1 | -2.8 | -1.8 | -1.0 | -1.7 | Rattus norvegicus neuropeptide Y receptor Y1 (Npy1r), mRNA [NM_001013032] |
| -1.6 | -2.1 | -2.0 | -2.1 | -0.4 | -1.2 | Rattus norvegicus purinergic receptor P2Y, G-protein coupled 12 (P2ry12), mRNA [NM_022800] |
| -1.9 | -1.2 | -1.5 | -1.9 | -2.6 | -1.6 | Rattus norvegicus adrenergic receptor, alpha 2b (Adra2b), mRNA [NM_138505] |
| -1.2 | -1.2 | -2.2 | -1.2 | -1.4 | -4.1 | Rattus norvegicus corticotropin releasing hormone receptor 2 (Crhr2), mRNA [NM_022714] |
| -2.6 | -2.6 | -1.0 | -1.9 | -1.7 | -1.3 | Rattus norvegicus cholinergic receptor, muscarinic 3 (Chrm3), mRNA [NM_012527] |
| -1.4 | -1.3 | -3.0 | -1.8 | -1.9 | -2.0 | Rattus norvegicus adrenomedullin receptor (Admr), mRNA [NM_053302] |

| | | | | | | |
|---|---|---|---|---|---|---|
| -1.9 | -2.1 | -1.7 | -1.8 | -1.9 | -2.1 | Rattus norvegicus G protein-coupled receptor 19 (Gpr19), mRNA [NM_080579] |
| -1.6 | -2.3 | -2.1 | -2.0 | -1.6 | -2.2 | Rattus norvegicus G protein-coupled receptor 153 (Gpr153), mRNA [NM_001034855] |
| -2.0 | -2.0 | -1.8 | -2.1 | -2.3 | -2.4 | Rattus norvegicus thromboxane A2 receptor (Tbxa2r), mRNA [NM_017054] |
| -2.3 | -2.7 | -2.5 | -2.4 | -1.2 | -1.7 | Rattus norvegicus G protein-coupled receptor 153 (Gpr153), mRNA [NM_001034855] |
| -2.0 | -2.0 | -1.3 | -3.1 | -3.2 | -1.7 | Rattus norvegicus mRNA for GABAB receptor 1d, complete cds. [AB016161] |
| -2.9 | -3.3 | -2.4 | -2.1 | -1.0 | -2.4 | Rattus norvegicus purinergic receptor P2Y, G-protein coupled, 14 (P2ry14), mRNA [NM_133577] |
| -2.1 | -2.6 | -2.8 | -2.5 | -1.9 | -2.0 | Rattus norvegicus 5-hydroxytryptamine (serotonin) receptor 2B (Htr2b), mRNA [NM_017250] |
| -2.3 | -1.5 | -2.9 | -2.3 | -2.7 | -2.3 | PREDICTED: Rattus norvegicus endothelial differentiation, lysophosphatidic acid G-protein-coupled receptor 6 (predicted) (Edg6_predicted), mRNA [XM_234930] |
| -2.0 | -2.0 | -2.0 | -2.5 | -3.0 | -2.7 | Rattus norvegicus MAS-related GPR, member D (Mrgprd), mRNA [NM_001001506] |
| -2.2 | -2.4 | -1.6 | -2.4 | -3.0 | -3.0 | Rattus norvegicus G protein-coupled receptor 157 (Gpr157), mRNA [NM_001012107] |
| -2.3 | -2.5 | -3.0 | -2.5 | -1.5 | -2.7 | Rattus norvegicus vasoactive intestinal peptide receptor 2 (Vipr2), mRNA [NM_017238] |
| -2.2 | -2.9 | -3.5 | -2.4 | -1.6 | -2.1 | Rattus norvegicus adenosine A2B receptor (Adora2b), mRNA [NM_017161] |
| -2.8 | -3.4 | -3.6 | -2.3 | -2.1 | -1.7 | Rattus norvegicus endothelin receptor type B (Ednrb), mRNA [NM_017333] |
| -2.6 | -2.4 | -1.7 | -2.8 | -3.9 | -2.8 | Rattus norvegicus tachykinin receptor 2 (Tacr2), mRNA [NM_080768] |
| -1.8 | -2.2 | -3.5 | -2.7 | -2.5 | -3.6 | Rattus norvegicus G protein-coupled receptor 20 (Gpr20), mRNA [NM_022216] |
| -3.1 | -3.2 | -3.0 | -2.6 | -2.3 | -2.8 | Rattus norvegicus galanin receptor 2 (Galr2), mRNA [NM_019172] |
| -3.5 | -2.7 | -3.2 | -3.5 | -1.8 | -2.2 | Rattus norvegicus chemokine (C-C motif) receptor 1 (Ccr1), mRNA [NM_020542] |
| -2.2 | -2.4 | -2.2 | -3.0 | -3.4 | -3.7 | Rattus norvegicus neuropeptides B/W receptor 1 (Nbpwr1), mRNA [NM_001014784] |
| -4.2 | -2.1 | -1.8 | -2.8 | -3.2 | -3.0 | PREDICTED: Rattus norvegicus G protein-coupled receptor 45 (predicted) (Gpr45_predicted), mRNA [XM_237112] |
| -2.3 | -2.3 | -2.4 | -3.2 | -3.7 | -3.3 | Rattus norvegicus somatostatin receptor 5 (Sstr5), mRNA [NM_012882] |
| -2.7 | -3.0 | -3.2 | -3.4 | -2.7 | -2.5 | Rattus norvegicus gamma-aminobutyric acid (GABA) B receptor 2 (Gabbr2), mRNA [NM_031802] |
| -3.2 | -3.5 | -3.1 | -3.3 | -2.8 | -2.5 | PREDICTED: Rattus norvegicus G protein-coupled receptor 126 (predicted) (Gpr126_predicted), mRNA [XM_218313] |
| -2.8 | -3.5 | -3.0 | -2.7 | -3.8 | -2.8 | Rattus norvegicus G protein-coupled receptor 3 (Gpr3), mRNA [NM_153727] |
| -3.0 | -4.2 | -3.4 | -2.8 | -3.6 | -1.9 | Rattus norvegicus G protein-coupled receptor 149 (Gpr149), mRNA [NM_138891] |
| -2.5 | -2.1 | -3.6 | -3.0 | -4.3 | -3.4 | Rattus norvegicus relaxin 3 receptor 1 (Rln3r1), mRNA [NM_001008310] |
| -2.6 | -3.4 | -3.3 | -3.8 | -3.0 | -3.2 | Rattus norvegicus somatostatin receptor 3 (Sstr3), mRNA [NM_133522] |
| -3.6 | -2.9 | -3.6 | -2.9 | -3.3 | -3.0 | Rattus norvegicus 5-hydroxytryptamine (serotonin) receptor 7 (Htr7), mRNA [NM_022938] |
| -2.6 | -2.8 | -2.7 | -3.7 | -4.2 | -3.3 | Rattus norvegicus cadherin EGF LAG seven-pass G-type receptor 3 (Celsr3), mRNA [NM_031320] |
| -3.2 | -2.9 | -2.6 | -3.3 | -4.0 | -3.5 | Cadherin EGF LAG seven-pass G-type receptor 2 (Multiple epidermal growth factor-like domains 3) (Fragment). [Source:Uniprot/SWISSPROT;Acc:Q9QYP2] [ENSRNOT00000027263] |
| -3.5 | -3.9 | -3.2 | -2.7 | -2.6 | -3.6 | Rattus norvegicus adrenergic receptor, alpha 2c (Adra2c), mRNA [NM_138506] |
| -3.1 | -2.8 | -2.8 | -3.7 | -4.1 | -3.6 | Rattus norvegicus histamine H4 receptor (Hrh4), mRNA [NM_131909] |
| -3.6 | -3.0 | -2.5 | -3.5 | -4.0 | -3.8 | Rattus norvegicus arginine vasopressin receptor 2 (Avpr2), mRNA [NM_019136] |
| -3.7 | -3.2 | -2.5 | -3.6 | -3.8 | -3.7 | Rattus norvegicus adrenergic receptor, beta 1 (Adrb1), mRNA [NM_012701] |

| | | | | | | |
|---|---|---|---|---|---|---|
| -3.4 | -3.1 | -3.1 | -3.5 | -3.4 | -4.1 | Rattus norvegicus B2 bradykinin receptor mRNA, complete cds. [M59967] |
| -3.8 | -3.7 | -3.8 | -3.3 | -3.5 | -3.3 | Rattus norvegicus adenosine A2a receptor (Adora2a), mRNA [NM_053294] |
| -3.9 | -3.3 | -3.5 | -3.9 | -3.3 | -4.3 | PREDICTED: Rattus norvegicus G protein-coupled receptor 162 (predicted) (Gpr162_predicted), mRNA [XM_342757] |
| -4.2 | -4.2 | -2.7 | -3.7 | -3.9 | -4.2 | Rattus norvegicus prostaglandin E receptor 1 (Ptger1), mRNA [NM_013100] |
| -3.8 | -4.3 | -3.0 | -3.5 | -4.8 | -4.0 | Cadherin EGF LAG seven-pass G-type receptor 2 (Multiple epidermal growth factor-like domains 3) (Fragment). [Source:Uniprot/SWISSPROT;Acc:Q9QYP2] [ENSRNOT00000027263] |
| -3.9 | -4.1 | -4.1 | -3.8 | -4.1 | -3.4 | Rattus norvegicus dopamine receptor D3 (Drd3), mRNA [NM_017140] |
| -4.2 | -4.2 | -4.0 | -4.0 | -3.8 | -4.3 | Rattus norvegicus adenosine A1 receptor (Adora1), mRNA [NM_017155] |

## 9.3 Affymetrix results

Table 9-13: Fold changes in the expression of genes influenced by ACEA in rat primary skeletal muscle cells.

| Fold Change | Symbol | Entrez Gene Name |
|---|---|---|
| 2.1 | FRZB | frizzled-related protein |
| -2.1 | RGS2 | regulator of G-protein signaling 2, 24kDa |
| -2.1 | HAS2 | hyaluronan synthase 2 |
| -2.2 | OLR1 | oxidized low density lipoprotein (lectin-like) receptor 1 |
| -2.2 | EGR2 | early growth response 2 |

Table 9-14: Fold changes in the expression of genes influenced by ACEA+RIM vs ACEA in rat primary skeletal muscle cells.

| Fold Change | Symbol | Entrez Gene Name |
|---|---|---|
| 4.0 | EGR1 | early growth response 1 |
| 4.0 | IL6 | interleukin 6 (interferon, beta 2) |
| 3.1 | EGR2 | early growth response 2 |
| 2.9 | HAS2 | hyaluronan synthase 2 |
| 2.5 | DUSP6 | dual specificity phosphatase 6 |
| 2.5 | FOS | FBJ murine osteosarcoma viral oncogene homolog |
| 2.4 | HES1 | hairy and enhancer of split 1, (Drosophila) |
| 2.3 | DUSP6 | dual specificity phosphatase 6 |
| 2.2 | ID1 | inhibitor of DNA binding 1, dominant negative helix-loop-helix protein |
| 2.2 | NR4A1 | nuclear receptor subfamily 4, group A, member 1 |
| 2.1 | RGS2 | regulator of G-protein signaling 2, 24kDa |
| 2.0 | BHLHE40 | basic helix-loop-helix family, member e40 |
| 2.0 | DUSP6 | dual specificity phosphatase 6 |

Table 9-15: Fold changes in the expression of genes influenced by ACEA+RIM vs RIM in rat primary skeletal muscle cells.

| Fold Change | Symbol | Entrez Gene Name |
|---|---|---|
| 6.1 | NR4A1 | nuclear receptor subfamily 4, group A, member 1 |
| 5.4 | HAS2 | hyaluronan synthase 2 |
| 5.0 | EGR2 | early growth response 2 |
| 3.2 | CHAC1 | ChaC, cation transport regulator homolog 1 (E. coli) |
| 3.1 | ARL4C | ADP-ribosylation factor-like 4C |
| 3.0 | ID4 | inhibitor of DNA binding 4, dominant negative helix-loop-helix protein |
| 2.9 | LOC257642 | rRNA promoter binding protein |
| 2.7 | EGR1 | early growth response 1 |
| 2.7 | HES1 | hairy and enhancer of split 1, (Drosophila) |

| | | |
|---|---|---|
| 2.5 | DPT | dermatopontin |
| 2.4 | DUSP6 | dual specificity phosphatase 6 |
| 2.4 | KLF10 | Kruppel-like factor 10 |
| 2.3 | OBFC2A | oligonucleotide/oligosaccharide-binding fold containing 2A |
| 2.2 | BHLHE40 | basic helix-loop-helix family, member e40 |
| 2.2 | DUSP6 | dual specificity phosphatase 6 |
| 2.2 | BHLHE40 | basic helix-loop-helix family, member e40 |
| 2.2 | EFEMP1 | EGF containing fibulin-like extracellular matrix protein 1 |
| 2.2 | LRRN4CL | LRRN4 C-terminal like |
| 2.1 | KIF11 | kinesin family member 11 |
| 2.1 | PTGER4 | prostaglandin E receptor 4 (subtype EP4) |
| 2.1 | ITGBL1 | integrin, beta-like 1 (with EGF-like repeat domains) |
| 2.1 | PLAU | plasminogen activator, urokinase |
| 2.1 | ECT2 | epithelial cell transforming sequence 2 oncogene |
| 2.1 | ERRFI1 | ERBB receptor feedback inhibitor 1 |
| 2.0 | RGS2 | regulator of G-protein signaling 2, 24kDa |
| 2.0 | GEM | GTP binding protein overexpressed in skeletal muscle |
| 2.0 | AKR1CL1 | aldo-keto reductase family 1, member C-like 1 |
| -2.0 | LOC100363014 | REST corepressor 1-like |
| -2.0 | HMGXB4 | HMG box domain containing 4 |
| -2.0 | CCNG2 | cyclin G2 |
| -2.0 | HP | haptoglobin |
| -2.0 | DMRT2 | doublesex and mab-3 related transcription factor 2 |
| -2.1 | ANKRD37 | ankyrin repeat domain 37 |
| -2.1 | Gm12253 | predicted gene 12253 |
| -2.1 | MSL1 | male-specific lethal 1 homolog (Drosophila) |
| -2.2 | RBP1 | retinol binding protein 1, cellular |
| -2.2 | RASL12 | RAS-like, family 12 |
| -2.2 | C9orf16 | chromosome 9 open reading frame 16 |
| -2.2 | Fam60a (rat) | family with sequence similarity 60, member A |
| -2.4 | Cd24a | CD24a antigen |
| -2.4 | ANGPTL4 | angiopoietin-like 4 |
| -2.4 | BMP6 | bone morphogenetic protein 6 |
| -2.5 | CXCL6 | chemokine (C-X-C motif) ligand 6 (granulocyte chemotactic protein 2) |
| -2.6 | MGP | matrix Gla protein |
| -2.8 | GBX2 | gastrulation brain homeobox 2 |
| -3.3 | DPYSL3 | dihydropyrimidinase-like 3 |
| -4.6 | C3 | complement component 3 |
| -4.7 | NPY | neuropeptide Y |
| -4.7 | CCL20 | chemokine (C-C motif) ligand 20 |
| -4.8 | LCN2 | lipocalin 2 |

Table 9-16: Fold changes in the expression of genes influenced by ACEA+U0126 vs ACEA in rat primary skeletal muscle cells.

| Fold Change | Symbol | Entrez Gene Name |
|---|---|---|
| 9.4 | ALDH3A1 | aldehyde dehydrogenase 3 family, member A1 |
| 7.2 | AHRR | aryl-hydrocarbon receptor repressor |
| 3.1 | ASPN | asporin |
| 2.5 | BAMBI | BMP and activin membrane-bound inhibitor homolog (Xenopus laevis) |
| 2.5 | BMP6 | bone morphogenetic protein 6 |
| 2.4 | C8orf42 | chromosome 8 open reading frame 42 |
| 2.3 | BDKRB1 | bradykinin receptor B1 |
| 2.2 | CCNL1 | cyclin L1 |
| 2.2 | CA4 | carbonic anhydrase IV |
| 2.1 | C1QTNF3 | C1q and tumor necrosis factor related protein 3 |
| 2.1 | ASPN | asporin |
| -2.0 | CCND1 | cyclin D1 |
| -2.1 | CCND1 | cyclin D1 |
| -2.1 | C15orf23 | chromosome 15 open reading frame 23 |
| -2.1 | ANXA3 | annexin A3 |
| -2.1 | CDCA2 | cell division cycle associated 2 |
| -2.2 | BMPER | BMP binding endothelial regulator |
| -2.2 | CDKN2C | cyclin-dependent kinase inhibitor 2C (p18, inhibits CDK4) |
| -2.2 | BUB1 | budding uninhibited by benzimidazoles 1 homolog (yeast) |
| -2.2 | ARHGEF3 | Rho guanine nucleotide exchange factor (GEF) 3 |
| -2.2 | C13orf33 | chromosome 13 open reading frame 33 |
| -2.2 | CD200 | CD200 molecule |
| -2.3 | AFAP1L2 | actin filament associated protein 1-like 2 |
| -2.4 | AURKB | aurora kinase B |
| -2.4 | ALDH1A2 | aldehyde dehydrogenase 1 family, member A2 |
| -2.4 | CDKN1C | cyclin-dependent kinase inhibitor 1C (p57, Kip2) |
| -2.4 | AURKA | aurora kinase A |
| -2.4 | ANXA8/ANXA8L1 | annexin A8 |
| -2.5 | C15orf48 | chromosome 15 open reading frame 48 |
| -2.6 | AMPD3 | adenosine monophosphate deaminase 3 |
| -2.6 | ARHGAP11A | Rho GTPase activating protein 11A |
| -2.6 | ASF1B | ASF1 anti-silencing function 1 homolog B (S. cerevisiae) |
| -3.0 | C13orf33 | chromosome 13 open reading frame 33 |
| -3.1 | BIRC5 | baculoviral IAP repeat containing 5 |
| -3.1 | CDC20 | cell division cycle 20 homolog (S. cerevisiae) |
| -3.1 | BMP3 | bone morphogenetic protein 3 |
| -3.2 | AKAP12 | A kinase (PRKA) anchor protein 12 |
| -3.3 | CDCA8 | cell division cycle associated 8 |
| -3.4 | ARG2 | arginase, type II |
| -3.5 | C15orf23 | chromosome 15 open reading frame 23 |
| -3.6 | AQP1 | aquaporin 1 (Colton blood group) |
| -3.8 | CDK1 | cyclin-dependent kinase 1 |
| -3.9 | BUB1B | budding uninhibited by benzimidazoles 1 homolog beta (yeast) |

| | | |
|---|---|---|
| -4.1 | CDCA3 | cell division cycle associated 3 |
| -4.6 | AGTR2 | angiotensin II receptor, type 2 |
| -4.9 | CCNB1 | cyclin B1 |
| -5.4 | CCNA2 | cyclin A2 |
| -5.6 | CDC20 | cell division cycle 20 homolog (S. cerevisiae) |
| -7.2 | CCNB1 | cyclin B1 |
| -7.6 | CCNB2 | cyclin B2 |

Table 9-17: Fold changes in the expression of genes influenced by ACEA+U0126 vs U0126 in rat primary skeletal muscle cells.

| Fold Change | Symbol | Entrez Gene Name |
|---|---|---|
| 4.4 | NR4A1 | nuclear receptor subfamily 4, group A, member 1 |
| 3.1 | IL6 | interleukin 6 (interferon, beta 2) |
| 2.9 | RGS2 | regulator of G-protein signaling 2, 24kDa |
| 2.7 | RGS2 | regulator of G-protein signaling 2, 24kDa |
| 2.5 | ID1 | inhibitor of DNA binding 1, dominant negative helix-loop-helix protein |
| 2.4 | HAS2 | hyaluronan synthase 2 |
| 2.1 | HMGCR | 3-hydroxy-3-methylglutaryl-CoA reductase |
| 2.1 | EGR1 | early growth response 1 |
| 2.0 | ALDH3A1 | aldehyde dehydrogenase 3 family, member A1 |
| -2.0 | CCNG2 | cyclin G2 |
| -2.0 | KIAA0101 | KIAA0101 |
| -2.0 | CCNB1 | cyclin B1 |
| -2.0 | OLR1 | oxidized low density lipoprotein (lectin-like) receptor 1 |
| -2.0 | TRIM59 | tripartite motif containing 59 |
| -2.1 | KRT18 | keratin 18 |
| -2.1 | ADH7 | alcohol dehydrogenase 7 (class IV), mu or sigma polypeptide |
| -2.1 | C430048L16Rik/ Rbm12b | RIKEN cDNA C430048L16 gene |
| -2.1 | LARP4B | La ribonucleoprotein domain family, member 4B |
| -2.1 | NAA40 | N(alpha)-acetyltransferase 40, NatD catalytic subunit, homolog (S. cerevisiae) |
| -2.1 | BUB1 | budding uninhibited by benzimidazoles 1 homolog (yeast) |
| -2.1 | GRAMD3 | GRAM domain containing 3 |
| -2.1 | CCNB1 | cyclin B1 |
| -2.1 | CKAP2 | cytoskeleton associated protein 2 |
| -2.2 | CYP1A1 | cytochrome P450, family 1, subfamily A, polypeptide 1 |
| -2.2 | TBX5 | T-box 5 |
| -2.3 | CCNB2 | cyclin B2 |
| -2.3 | MAGEH1 | melanoma antigen family H, 1 |
| -2.4 | ECT2 | epithelial cell transforming sequence 2 oncogene |
| -2.5 | KIF23 | kinesin family member 23 |
| -2.5 | TXNIP | thioredoxin interacting protein |
| -2.6 | RACGAP1 | Rac GTPase activating protein 1 |
| -2.7 | SIX4 | SIX homeobox 4 |
| -3.1 | CCNA2 | cyclin A2 |

Table 9-18: Fold changes in the expression of genes influenced by U0126 in rat primary skeletal muscle cells.

| Fold Change | Symbol | Entrez Gene Name |
|---|---|---|
| 9.04 | GSTA5 | glutathione S-transferase alpha 5 |
| 8.53 | AHRR | aryl-hydrocarbon receptor repressor |
| 7.11 | CYP1A1 | cytochrome P450, family 1, subfamily A, polypeptide 1 |
| 6.24 | RASD1 | RAS, dexamethasone-induced 1 |
| 4.10 | SLC7A11 | solute carrier family 7 (anionic amino acid transporter light chain, xc- system), member 11 |
| 3.94 | ALDH3A1 | aldehyde dehydrogenase 3 family, member A1 |
| 3.73 | RBP4 | retinol binding protein 4, plasma |
| 3.17 | D4S234E | DNA segment on chromosome 4 (unique) 234 expressed sequence |
| 3.09 | WNT4 | wingless-type MMTV integration site family, member 4 |
| 3.05 | TIPARP | TCDD-inducible poly(ADP-ribose) polymerase |
| 2.92 | EEPD1 | endonuclease/exonuclease/phosphatase family domain containing 1 |
| 2.86 | LBP | lipopolysaccharide binding protein |
| 2.83 | CSRP2 | cysteine and glycine-rich protein 2 |
| 2.80 | ZNF423 | zinc finger protein 423 |
| 2.67 | BMP6 | bone morphogenetic protein 6 |
| 2.59 | ZBTB41 | zinc finger and BTB domain containing 41 |
| 2.56 | G0S2 | G0/G1switch 2 |
| 2.56 | ASPN | asporin |
| 2.48 | BAMBI | BMP and activin membrane-bound inhibitor homolog (Xenopus laevis) |
| 2.43 | NQO1 | NAD(P)H dehydrogenase, quinone 1 |
| 2.43 | GPC1 | glypican 1 |
| 2.39 | C8orf42 | chromosome 8 open reading frame 42 |
| 2.36 | ADH7 | alcohol dehydrogenase 7 (class IV), mu or sigma polypeptide |
| 2.29 | JUN | jun proto-oncogene |
| 2.26 | NOG | noggin |
| 2.23 | C1QTNF3 | C1q and tumor necrosis factor related protein 3 |
| 2.22 | ASPN | asporin |
| 2.21 | LOC100359945 | rCG41562-like |
| 2.20 | CYP1B1 | cytochrome P450, family 1, subfamily B, polypeptide 1 |
| 2.18 | TMEM100 | transmembrane protein 100 |
| 2.17 | RCAN2 | regulator of calcineurin 2 |
| 2.15 | ZNF385A | zinc finger protein 385A |
| 2.13 | TMEM140 | transmembrane protein 140 |
| 2.13 | JUN | jun proto-oncogene |
| 2.12 | DMRT2 | doublesex and mab-3 related transcription factor 2 |
| 2.10 | PTGES | prostaglandin E synthase |
| 2.09 | KRT18 | keratin 18 |
| 2.08 | CTHRC1 | collagen triple helix repeat containing 1 |
| 2.08 | TGFBI | transforming growth factor, beta-induced, 68kDa |
| 2.06 | RBM5 | RNA binding motif protein 5 |
| 2.05 | Gsta4 | glutathione S-transferase, alpha 4 |
| 2.04 | C13orf15 | chromosome 13 open reading frame 15 |
| 2.01 | MRGPRF | MAS-related GPR, member F |

| | | |
|---|---|---|
| -2.02 | C13orf33 | chromosome 13 open reading frame 33 |
| -2.02 | TK1 | thymidine kinase 1, soluble |
| -2.03 | AKAP12 | A kinase (PRKA) anchor protein 12 |
| -2.03 | DLGAP5 | discs, large (Drosophila) homolog-associated protein 5 |
| -2.03 | LOC257642 | rRNA promoter binding protein |
| -2.04 | CXCL6 | chemokine (C-X-C motif) ligand 6 (granulocyte chemotactic protein 2) |
| -2.04 | MTMR10 | myotubularin related protein 10 |
| -2.04 | ECM1 | extracellular matrix protein 1 |
| -2.04 | ENPP1 | ectonucleotide pyrophosphatase/phosphodiesterase 1 |
| -2.04 | LTBP1 | latent transforming growth factor beta binding protein 1 |
| -2.05 | THY1 | Thy-1 cell surface antigen |
| -2.05 | C13orf33 | chromosome 13 open reading frame 33 |
| -2.05 | KLF10 | Kruppel-like factor 10 |
| -2.05 | THY1 | Thy-1 cell surface antigen |
| -2.06 | EFEMP1 | EGF containing fibulin-like extracellular matrix protein 1 |
| -2.06 | C13orf33 | chromosome 13 open reading frame 33 |
| -2.07 | NR4A2 | nuclear receptor subfamily 4, group A, member 2 |
| -2.07 | DPYSL3 | dihydropyrimidinase-like 3 |
| -2.08 | GPR126 | G protein-coupled receptor 126 |
| -2.09 | CDCA2 | cell division cycle associated 2 |
| -2.09 | KIF4A | kinesin family member 4A |
| -2.10 | STARD13 | StAR-related lipid transfer (START) domain containing 13 |
| -2.10 | ARG2 | arginase, type II |
| -2.10 | TNFAIP6 | tumor necrosis factor, alpha-induced protein 6 |
| -2.10 | PDGFRB | platelet-derived growth factor receptor, beta polypeptide |
| -2.10 | ZDHHC2 | zinc finger, DHHC-type containing 2 |
| -2.11 | DUSP14 | dual specificity phosphatase 14 |
| -2.12 | STMN2 | stathmin-like 2 |
| -2.12 | ID4 | inhibitor of DNA binding 4, dominant negative helix-loop-helix protein |
| -2.12 | C15orf23 | chromosome 15 open reading frame 23 |
| -2.12 | CENPW | centromere protein W |
| -2.13 | TOP2A | topoisomerase (DNA) II alpha 170kDa |
| -2.15 | LOC687121 | similar to Shc SH2-domain binding protein 1 |
| -2.16 | THBS4 | thrombospondin 4 |
| -2.16 | SERPINB9 | serpin peptidase inhibitor, clade B (ovalbumin), member 9 |
| -2.17 | HMMR | hyaluronan-mediated motility receptor (RHAMM) |
| -2.17 | AFAP1L2 | actin filament associated protein 1-like 2 |
| -2.18 | KIF18B | kinesin family member 18B |
| -2.18 | ASPM | asp (abnormal spindle) homolog, microcephaly associated (Drosophila) |
| -2.18 | SERPINB1 | serpin peptidase inhibitor, clade B (ovalbumin), member 1 |
| -2.19 | SPON2 | spondin 2, extracellular matrix protein |
| -2.20 | CXCL1 | chemokine (C-X-C motif) ligand 1 (melanoma growth stimulating activity, alpha) |
| -2.20 | SOX4 | SRY (sex determining region Y)-box 4 |
| -2.22 | SKA1 | spindle and kinetochore associated complex subunit 1 |
| -2.23 | SPP1 | secreted phosphoprotein 1 |
| -2.23 | C15orf48 | chromosome 15 open reading frame 48 |
| -2.23 | PKP2 | plakophilin 2 |
| -2.23 | KIF20B | kinesin family member 20B |

| | | |
|---|---|---|
| -2.26 | C3 | complement component 3 |
| -2.26 | AKAP2/PALM 2-AKAP2 | A kinase (PRKA) anchor protein 2 |
| -2.27 | ARHGAP11A | Rho GTPase activating protein 11A |
| -2.27 | CDCA3 | cell division cycle associated 3 |
| -2.29 | UPP1 | uridine phosphorylase 1 |
| -2.31 | TNFRSF11B | tumor necrosis factor receptor superfamily, member 11b |
| -2.31 | CXCL1 | chemokine (C-X-C motif) ligand 1 (melanoma growth stimulating activity, alpha) |
| -2.33 | IL1RL1 | interleukin 1 receptor-like 1 |
| -2.33 | TOP2A | topoisomerase (DNA) II alpha 170kDa |
| -2.34 | ARHGEF3 | Rho guanine nucleotide exchange factor (GEF) 3 |
| -2.34 | KIFC1 | kinesin family member C1 |
| -2.36 | CD200 | CD200 molecule |
| -2.36 | RRM2 | ribonucleotide reductase M2 |
| -2.37 | LAMC2 | laminin, gamma 2 |
| -2.37 | SOX4 | SRY (sex determining region Y)-box 4 |
| -2.38 | SFRP4 | secreted frizzled-related protein 4 |
| -2.38 | CCNA2 | cyclin A2 |
| -2.38 | CKS2 | CDC28 protein kinase regulatory subunit 2 |
| -2.40 | CXCL1 | chemokine (C-X-C motif) ligand 1 (melanoma growth stimulating activity, alpha) |
| -2.41 | NUSAP1 | nucleolar and spindle associated protein 1 |
| -2.41 | SLC16A7 | solute carrier family 16, member 7 (monocarboxylic acid transporter 2) |
| -2.42 | BIRC5 | baculoviral IAP repeat containing 5 |
| -2.42 | LAMA2 | laminin, alpha 2 |
| -2.44 | PLK1 | polo-like kinase 1 |
| -2.44 | PLSCR1 | phospholipid scramblase 1 |
| -2.44 | FOSL1 | FOS-like antigen 1 |
| -2.44 | ANGPT1 | angiopoietin 1 |
| -2.48 | MTMR10 | myotubularin related protein 10 |
| -2.50 | IFITM1 | interferon induced transmembrane protein 1 (9-27) |
| -2.51 | COL8A1 | collagen, type VIII, alpha 1 |
| -2.52 | CRABP1 | cellular retinoic acid binding protein 1 |
| -2.52 | COL15A1 | collagen, type XV, alpha 1 |
| -2.54 | HAS2 | hyaluronan synthase 2 |
| -2.54 | KIF11 | kinesin family member 11 |
| -2.56 | SLC2A3 | solute carrier family 2 (facilitated glucose transporter), member 3 |
| -2.56 | COL15A1 | collagen, type XV, alpha 1 |
| -2.57 | KIF2C | kinesin family member 2C |
| -2.57 | TACC3 | transforming, acidic coiled-coil containing protein 3 |
| -2.58 | IRS2 | insulin receptor substrate 2 |
| -2.61 | IL1RL1 | interleukin 1 receptor-like 1 |
| -2.62 | BHLHE40 | basic helix-loop-helix family, member e40 |
| -2.62 | NUF2 | NUF2, NDC80 kinetochore complex component, homolog (S. cerevisiae) |
| -2.62 | C15orf23 | chromosome 15 open reading frame 23 |
| -2.68 | RACGAP1 | Rac GTPase activating protein 1 |
| -2.72 | CDC20 | cell division cycle 20 homolog (S. cerevisiae) |
| -2.73 | AKAP2/PALM 2-AKAP2 | A kinase (PRKA) anchor protein 2 |
| -2.74 | CKAP2 | cytoskeleton associated protein 2 |

| | | |
|---|---|---|
| -2.75 | DIO3 | deiodinase, iodothyronine, type III |
| -2.78 | BHLHE40 | basic helix-loop-helix family, member e40 |
| -2.79 | CCNB1 | cyclin B1 |
| -2.79 | CENPF | centromere protein F, 350/400kDa (mitosin) |
| -2.80 | RAMP3 | receptor (G protein-coupled) activity modifying protein 3 |
| -2.82 | UBE2C | ubiquitin-conjugating enzyme E2C |
| -2.83 | KIF23 | kinesin family member 23 |
| -2.85 | ECT2 | epithelial cell transforming sequence 2 oncogene |
| -2.85 | CDK1 | cyclin-dependent kinase 1 |
| -2.89 | PRC1 | protein regulator of cytokinesis 1 |
| -2.89 | BMP3 | bone morphogenetic protein 3 |
| -2.89 | IGFBP3 | insulin-like growth factor binding protein 3 |
| -2.90 | TTK | TTK protein kinase |
| -2.92 | BUB1B | budding uninhibited by benzimidazoles 1 homolog beta (yeast) |
| -3.04 | CDKN3 | cyclin-dependent kinase inhibitor 3 |
| -3.06 | MKI67 | antigen identified by monoclonal antibody Ki-67 |
| -3.09 | HMMR | hyaluronan-mediated motility receptor (RHAMM) |
| -3.21 | PTTG1 | pituitary tumor-transforming 1 |
| -3.23 | AQP1 | aquaporin 1 (Colton blood group) |
| -3.29 | KRT7 | keratin 7 |
| -3.33 | FAM64A | family with sequence similarity 64, member A |
| -3.38 | NUSAP1 | nucleolar and spindle associated protein 1 |
| -3.41 | IGFBP3 | insulin-like growth factor binding protein 3 |
| -3.42 | EGR1 | early growth response 1 |
| -3.52 | PRSS35 | protease, serine, 35 |
| -3.55 | GPR83 | G protein-coupled receptor 83 |
| -3.70 | CDC20 | cell division cycle 20 homolog (S. cerevisiae) |
| -3.72 | Gm12253 | predicted gene 12253 |
| -3.80 | RGS2 | regulator of G-protein signaling 2, 24kDa |
| -3.83 | CCNB1 | cyclin B1 |
| -3.87 | ERRFI1 | ERBB receptor feedback inhibitor 1 |
| -3.96 | CCNB2 | cyclin B2 |
| -3.96 | KIF20A | kinesin family member 20A |
| -3.98 | AGTR2 | angiotensin II receptor, type 2 |
| -4.10 | ID4 | inhibitor of DNA binding 4, dominant negative helix-loop-helix protein |
| -4.10 | RGS2 | regulator of G-protein signaling 2, 24kDa |
| -4.60 | ESM1 | endothelial cell-specific molecule 1 |
| -4.71 | OLR1 | oxidized low density lipoprotein (lectin-like) receptor 1 |
| -4.76 | AKAP12 | A kinase (PRKA) anchor protein 12 |
| -5.30 | EGR2 | early growth response 2 |
| -5.32 | NR4A3 | nuclear receptor subfamily 4, group A, member 3 |
| -6.15 | NR4A3 | nuclear receptor subfamily 4, group A, member 3 |
| -6.25 | Prl8a9 | prolactin family8, subfamily a, member 9 |
| -7.29 | NR4A1 | nuclear receptor subfamily 4, group A, member 1 |